

**The utility of the Liverpool Uveal Melanoma Prognostication Online
'LUMPO' as a prognostication algorithm in determining metastatic risk in uveal
melanoma**



Thesis submitted in accordance with the requirements of the University of Liverpool for the
degree of Doctor in Philosophy

Dr Alda Cunha, MBBS, FAPGCMSphth

March 2022

Supervisors:

Prof. Sarah Coupland - Consultant Histopathologist/George Holt Chair of Pathology,

University of Liverpool

Prof. Azzam Taktak - Clinical Scientist, Liverpool University Hospitals NHS Foundation Trust

Dr Joseph Sacco - Medical Oncologist, Clatterbridge Cancer Centre

Prof. Dyfrig Hughes - Health Economist, Bangor University

DEDICATION

For all those who have supported me for the past four years, writing this thesis would have been impossible without them.

“Who doesn’t thank for the little things doesn’t thank enough”

- Angolan Proverb -

Acknowledgements

Firstly, I would like to express my sincere gratitude to my P.I. Prof. Sarah Coupland for her continued support of my Ph.D. study and related research, especially her patience, motivation, and immense knowledge. I am also deeply grateful to Prof. Azzam Taktak for his guidance and support, essentially for his experience in statistics, above all for his ability to convey this knowledge to me in a way that I could understand. My sincere thanks also to Dr Helen Kalirai for her limitless assistance, wisdom, and support in so many ways along this long journey. I would also like to express my gratitude to Dr Joseph Sacco and Prof. Dyfrig Hughes for their guidance and constructive criticism during this research. I could not have had a better team of mentors and advisors to supervise this thesis.

I gratefully acknowledge the Instituto Nacional de Gestão de Bolsas de Estudo de Angola – INAGBE, for the generous funding of my project. My sincere thanks to Dr Maria Madalena Chimpolo, for recommending and encouraging me to complete my PhD, and essentially for her friendship and support throughout this journey.

I would like to express my gratitude to Dr Antonio Eleuteri for his enormous contribution to this research. He and his team developed LUMPO, and its new version that was used to validate LUMPO externally, as well as its new feature, which was used to perform a liver screening cost analysis on UM patients for this thesis. I would also like to express my gratitude to Prof. Heinrich Heimann and Dr Rumana Hussein for their clinical research support, and I also thank the rest of the clinical team at the LOOC. I would also like to express my sincere thanks to all uveal melanoma patients who kindly gave their consent to the LOORG Biobank to use their clinical data for investigation, making this study possible. I would also like to thank the collaborating members of the European Ocular Oncology Group for their invaluable contributions, time, and efforts in participating in the multi-centre study of this thesis.

My sincere thanks to the excellent research group, LOORG, and its present and past members: Karen, Sophie, Luna, Carlos, Jodi, Jo, Gemma, Simon, Amelia, Jakub, Debbie, Dawn, Jenna, Max, Yamini, Sam, Natalie, Graham, Hayley, Luisa, Martina, Hongrun. Mainly for having been a family present in multiple ways, where laughter, fun, tears, encouraging hugs, and the warm “tea time” were never lacking.

I thank my colleagues at the medical school, we are a friendly and close-knit group of over 30 years, thank you Drs; Ana Paula, Euridice, Ana Ruth, Filipa, Joana, Manuela Clementina, Kuku Elizabeth, Luzia, Sandra, Elsa, Vanda Marina, Marilinda, Aláide, Ana Teresa, Dulce, and so many other colleagues throughout my career.

I also thank my colleagues at the Instituto Nacional de Oftalmologia de Angola (IONA) for their friendship and companionship throughout my training and career as an ophthalmologist; thank you Drs Luisa, Carmen, Rosa, Alcina, Amelia, Sara, David, Walter, and all the other former and current new colleagues, as well as all the members of the IONA.

I am also grateful to the INAGBE fellows for all their support and friendship throughout this long way of study in the UK. Thank you Lúdia, José, Arsénio, Paulo, Gabriel, Arlete, Abreu.

I am grateful to all my close friends and family "and I have so many". They have always been there and are very precious to me, I have always had prayers, kind words and encouragement from all of them. A special thanks to my friends, Ana Paula Pereira and Eurídice dos Santos, we walked a long journey together from high school, Medical School, and through so many stages of our lives, you are always present even from a distance. I also thank my friend Carlos Figueiredo for his friendship and encouragement throughout this thesis.

Finally, I would like to thank my family. Thank you, Paulo Jorge Manuel, for being on my corner, minimizing my daily thousand tasks. Thank you for having surprised me in so many ways and for bringing me so much wisdom and joy. You are my safe harbour. My dear siblings, Fernando Cunha, Jorge Cunha, and Ana Paula Cunha Cruz, who would I be without you. You looked after me in so many ways. I thank my children Fabio Cunha Rola, Daniel Cunha Rola, Ruben Cunha Rola, Joel Cunha Rola and Miriam Cunha Rola, for their understanding, encouragement, and support along the way. You have always been and continue to be my inspiration! Thank you, my lovely children.

To my parents, Henrique Cunha, and Maria Cunha, I am eternally grateful. Your unconditional support, inspiration and Blessings have been my encouragement. Thank you for teaching me habits of hard work and persistence and for believing in me.

Abstract

Uveal melanoma (UM) is the most common primary intraocular malignancy in adults. Approximately 50% of patients with UM develop metastatic disease, usually occurring in the liver. Patient survival is directly related to the presence of hepatic metastases and how they affect liver function. After the identification of metastases, most patients die within a year, and the differing forms of existing treatment rarely extend life considerably. It has been proposed that prognostication can improve the quality of life, even when the probability of survival is reduced. Certain prognostic factors have been identified in UM that are associated with an increased risk of metastatic disease: these are clinical parameters as well as the histomorphological and genetic features of the primary UM. A team from Liverpool designed in 2011 a multiparameter algorithm called the “Liverpool Uveal Melanoma Prognostication Online” (LUMPO), to establish the prognosis for UM patients, stratifying them according to their relative risk of metastatic death. This was based on data collected over 20 years, and was validated externally by other ocular oncology centres. It was later updated to LUMPO3, and included new parameters and functions. The objective of this thesis was to perform a retrospective study, analysing the liver scan reports of patients with UM; examining whether LUMPO3 is able to predict the appearance of metastases in patients in Liverpool, and to determine the cost analysis of liver screening for the detection of metastases in patients with UM; and also to validate LUMPO3 externally.

Following the Introductory chapter, the characteristics of the scan reports of 615 patients diagnosed with UM were analysed in Chapter 2. The data were collected over an eleven-year period (2008-2018). Data of the characteristics of liver scanning and the metastases detected were analysed, and later combined with the demographic, histological, genetic and patient outcome data. It was estimated that 37% of UM patients treated in Liverpool developed metastases at different stages of the disease. The analysis of the characteristics of the primary UM demonstrated that increasing tumour size and hence TNM staging category of the UM, was associated with an increasing risk of metastatic disease and reduced survival. Most metastatic UM were associated with monosomy 3 and gain of chromosome 8q. Many previous studies have identified different risk groups (low, intermediate and high) for UM patients to develop metastases: in this study, I identified 3 groups of patients that were divided according to when and whether they developed metastatic disease. Liver surveillance was most frequent in patients who ultimately developed metastases and the most frequent modality employed was magnetic resonance imaging (MRI).

In chapter 3, the same cohort of 615 UM patients were analysed, here focussing on the estimated costs for all scans performed for which both the minimum and maximum costs were calculated using the NICE costing for clinical imaging. A feature of LUMPO3 called “linear predictor of death due to metastases” (lpm�) was extracted to predict the onset of liver metastases and to determine the hypothetical costs of liver surveillance in UM patients. Model performance was determined in terms of discrimination and calibration. Results showed consistent discrimination performances over a 5-year time period from date of initial treatment. Calibration performance was determined visually with good agreement between observed and predicted onset of UM metastases up to 10 years following initial treatment. The results suggested that unnecessary radiological examinations could be avoided in the UM patients with low metastatic risk, without any adverse effects to patient management. These results suggested that this lpm� could save costs by minimizing the number of examinations for metastases screening, and likely decrease the patient angst associated with liver screening.

Chapter 4 study was a multicentre project that allowed the recruitment of a sufficient number of patients from 7 external collaborative centres, using the existing clinical network within the Ocular Oncology Group and the USA. Data were collected from patients diagnosed and / or treated for UM at these collaborating centres. The results showed that LUMPO3 is a reasonably accurate and valuable tool for predicting all-cause mortality in UM patients, despite the differences in the recording of clinical, histopathological and genetic data between the centres and hence the various cohorts studied. The calibration graphs presenting the expected probabilities of actuarial survival showed a good agreement between the observed and the predicted probabilities. In conclusion, I examined in detail “real world” data of UM patients treated in various ocular oncology centres that allowed the construction of the LUMPO3 model, and its validation in Liverpool. These data are valuable when considering the costs of surveillance programs, as well as potential modifications and revisions to the predictive algorithms for UM.

Table of Contents

	Page
Dedication.....	2
Acknowledgments.....	3
Abstract.....	5
Table of contents.....	6
List of Figures.....	15
List of Tables.....	20
List of abbreviations.....	23
List of thesis-related peer-reviewed publications to date.....	26
List of oral presentations.....	27
Declaration.....	28

Chapter 1:

General Introduction

1.1 Definition and Incidence.....	31
1.1.1. Age and sex specific incidence.....	32
1.1.2 Etiological factors.....	32
1.1.3. Host factors.....	32
1.1.3.1 Ethnicity.....	32
1.1.3.2 Choroidal Naevi.....	33
1.1.3.3 Genetic predisposition.....	34
1.1.4 Environmental factors.....	35

1.1.4.1 Sunlight exposure.....	35
1.1.4.2 Occupation.....	36
1.2 Clinical features of UM.....	37
1.2.1 Choroidal melanoma.....	37
1.2.2 Ciliary body melanoma.....	40
1.2.3 Iris melanoma.....	42
1.3 Histopathological features of UM.....	42
1.4 Genetic alterations in UM.....	46
1.4.1 Chromosome 3.....	46
1.4.2 Chromosome 8q.....	47
1.4.3 Chromosome 1.....	47
1.4.4 Chromosome 6.....	47
1.4.5 Genetic mutations in UM.....	48
1.4.5.1 <i>GNAQ</i> and <i>GNA11</i>	48
1.4.5.2. <i>SF3B1</i>	48
1.4.5.3 <i>EIF1AX</i>	48
1.4.5.4 <i>BAP1</i>	49
1.4.6 Next generation sequencing panels for prognostication.....	49
1.4.7 Most commonly genetic methods used for prognostication in UM.....	50
1.4.7.1 Gene expressing profiling.....	51
1.5 Diagnosis and treatment of UM.....	51
1.5.1 Diagnosis.....	51
1.5.1 UM treatment options.....	55
1.6 Metastatic Disease in UM.....	57
1.6.1 Metastatic dissemination and incidence.....	57
1.6.2 Sites of metastases.....	58

1.6.3 Early diagnosis and conventional screening tools for metastatic UM.....	59
1.6.3.1 Follow-up strategies in UM.....	60
1.6.3.1.1 Liver Function Tests.....	60
1.6.3.1.2 Imaging.....	61
1.6.3.1.2.1 Hepatic ultrasonography.....	62
1.6.3.1.2.2 Computer tomography.....	63
1.6.3.1.2.3 Magnetic Resonance Image.....	64
1.6.3.1.2.4 Positron Emission Tomography.....	65
1.6.4 Signs and symptoms in metastatic UM.....	67
1.6.5 Determination of risk of metastases.....	67
1.6.6 Treatment for metastatic disease.....	67
1.6.6.1 Systemic therapy.....	68
1.6.6.2. Loco regional Therapy.....	70
1.6.6.3 Adjuvant Therapy.....	73
1.6.7 Prognostic for metastatic disease in UM.....	73
1.7. Prognostication in UM.....	74
1.7.1. Identifying risk factors.....	74
1.7.2 Accurate prognostication.....	74
1.7.3 Benefits of prognostication.....	75
1.7.4 Survival predictors.....	75
1.7.4.1 Clinical Prognostic Factors.....	76
1.7.4.1.1 Age and gender.....	78
1.7.4.1.2 Tumour size.....	78
1.7.4.1.3 Extraocular extension.....	78
1.7.4.1.4 Ciliary body involvement.....	80
1.7.4.1.5 Histopathological Prognostic Factors.....	80
1.7.4.1.6 Cytogenetic Prognostic Factors.....	80
1.7.5 Risks of prognostication.....	81

1.7.6 Alternative prognostication.....	81
1.7.7 Elaboration of a clinical risk-assessment tool.....	83
1.8 The Liverpool Uveal Melanoma Prognosticator Online (LUMPO).....	84
1.9 Outline of the thesis.....	91

Chapter 2:

Liver-screening analysis to identify uveal melanoma metastases in patients treated at the Liverpool Ocular Oncology Centre between the years 2008-2018

2.1 Introduction.....	94
2.1.1 Risk stratification.....	95
2.1.2 Surveillance protocols.....	95
2.1.3 Surveillance modality.....	97
2.2 Patients and Methods.....	99
2.2.1 Study design.....	99
2.2.2 Data Collection.....	103
2.2.3 Data for analyses.....	104
2.2.3.1 Statistical analysis.....	105
2.3 Results.....	106
2.3.1 Baseline characteristics of the patients.....	106
2.3.1.2 Demographic and clinical analysis.....	106
2.3.1.3 Histological analysis.....	106
2.3.1.4 Genetic analysis.....	107
2.3.1.5 Follow-up and outcome analysis.....	107
2.3.2 Type of primary treatment performed.....	111
2.3.3 Survival.....	112

2.3.3.1 Gender.....	112
2.3.3.2 Primary tumour size	113
2.3.3.3 Primary tumour histopathological features	115
2.3.3.4 Primary tumour clinical features.....	118
2.3.3.5 Primary tumour chromosomal status	120
2.3.4 Liver screening analysis.....	127
2.3.4.1 Frequency and modality of the scans	127
2.3.4.2 Regularity of liver surveillance	128
2.3.4.3 Detection of metastases at time of the primary treatment.....	133
2.3.5 Management of metastatic disease.....	133
2.3.5.1 Characteristic of detected hepatic metastases through liver surveillance	135
2.3.5.2 Metastases-related mortality	137
2.3.6 Categorizing 615 patients into 3 groups according to when and whether patients had metastases.....	138
2.3.7 Survival for the 3 categorized groups of patients: 1) developed metastases within 2 years 2) after 2 years 3) never demonstrated metastases.....	148
2.4 Discussion.....	149
2.4.1 Frequency of UM metastases.....	152
2.4.2 Primary UM size and risk of metastases.....	152
2.4.3 Primary UM genetics and risk of metastases.....	155
2.4.4 Liverpool liver surveillance – detected metastases, number and type of scans.....	156
2.4.5 UM metastases characteristics in the Liverpool liver surveillance programme.....	159
2.4.6 Outcome of patients with UM metastases in the Liverpool liver surveillance programme.....	160
2.4.7 Three groups of patients stratified according to when and whether developed metastases.....	161
2.4.8 Regularity of liver surveillance in the real world.....	164

Chapter 3:

Analysis of costs of liver screening for metastases in patients treated at the Liverpool Ocular Oncology Centre between the years 2008 and 2018 using the LUMPO3

3.1 Introduction	167
3.1.1 Factors associated with follow-up liver screening.....	167
3.1.2 Cost-effectiveness of liver surveillance.....	167
3.1.3 Clinical prediction models.....	169
3.2 Material and Methods	171
3.2.1 Data Collection.....	171
3.2.1.1 Data from scan reports.....	171
3.2.1.2 Occurrence of metastases.....	172
3.2.1.3 Costs-utility analysis of imaging.....	172
3.2.2 Model Validation.....	175
3.3 Results	177
3.3.1 Overall imaging utilization.....	177
3.3.2 Imaging modality.....	178
3.3.3 Factors associated with follow-up imaging.....	179
3.3.3.1 Time and number of scans until the detection of metastases in 150 patients whose metastases were detected through liver surveillance.....	179
3.3.3.2 Time and number of scans until the detection of metastases in 79 patients whose metastases were detected by autopsy.....	183
3.3.3.3 Time and number of scans in 386 patients who never demonstrated metastases during the liver screening study.....	186

3.3.4 Incidence of metastases.....	189
3.3.5 Costs analysis of imaging.....	190
3.3.5.1 Costs of imaging for patients who developed metastases.....	190
3.3.5.2 Costs of imaging for patients who did not develop metastases.....	190
3.3.6 Statistical analysis results.....	191
3.3.6.1 Model validation.....	191
3.3.6.2 Discrimination and calibration.....	191
3.3.6.3 Cost analysis of liver scanning.....	194
3.4 Discussion.....	197
3.4.1 Overall imaging utilization and imaging modality.....	199
3.4.2 Time and number of scans until the detection of metastases.....	199
3.4.3 Time and number of scans in 386 patients who never demonstrated metastases during the liver screening study.....	201
3.4.4 Costs analysis of imaging.....	202
3.4.5 Discrimination and calibration, cumulative incidences of onset of metastases, and cost analysis of liver scanning for LUMPO3 validation using <i>lpmd</i>	204
3.4.5.1 Model performance	204
3.4.5.2 Cost analysis of liver scanning using the <i>lpmd</i>	206

Chapter 4:

External Validation of LUMPO3

4.1 Introduction.....	211
4.2 Methods.....	214
4.2.1 Study design.....	214
4.2.2 Patient recruitment and sample collection.....	216
4.2.3 Demographics of patients whose tumours were treated.....	216

4.2.4 Statistical analyses.....	217
4.3 Results.....	218
4.3.1 Characteristics of the patients.....	218
4.3.2 Demographic and clinical analysis.....	218
4.3.3 Histological analysis.....	219
4.3.4 Genetic analysis.....	219
4.3.5 Follow-up and outcome analysis.....	220
4.3.5 Statistical Analyses.....	224
4.3.5.1 Discrimination.....	224
4.3.5.2 Calibration.....	225
4.4 Discussion.....	227

Chapter 5: Summary

5.1 Conclusions and Future Directions.....	231
Appendices.....	238
Appendix 1 – Proposal Sample study 1 (Proforma).....	238
Appendix 2 – Demographics, clinical, histological, genetic, follow-up and outcome information from 615 patients enrolled in study 1.....	239
Appendix 3 - Inserted variables for the model for study 1, including its description and coding scheme.....	248
Appendix 4 - Correlations between genetics and primary tumour TNM stage according to AJCC 8th edition (cross tabulations).....	249
Appendix 5 - Associations between chromosomal copy numbers (cross tabulations).....	250
Appendix 6 - Proposal Sample for study 2 (Proforma).....	251

Appendix 7 – Liver scans data information from 615 patients enrolled in study 2.....	252
Appendix 8 - Proposal sample for study 3 (proforma).....	258
Appendix 9 – Inserted variables for the model of study 3, including its description and coding scheme.....	259
REFERENCES.....	260

List of Figures

Chapter 1

Figure 1.1 Anatomical location of UM.....	31
Figure 1.2 Histology of the choroid.....	37
Figure 1.3 Large dome-shaped choroidal melanoma.....	39
Figure 1.4 Large mushroom-shaped choroidal melanoma.....	39
Figure 1.5 Ciliochoroidal melanoma.....	41
Figure 1.6 Histology of the iris and ciliary body.....	41
Figure 1.7 Melanoma cells.....	41
Figure 1.8 Dome-shaped choroidal melanoma in which there is a secondary serous retinal detachment.....	52
Figure 1.9 Mushroom-shaped choroidal melanoma with a vascular congestion at its apex and covering the optic disc.....	52
Figure 1.10 Multiple liver metastases (arrow heads) of UM.....	58
Figure 1.11 Ultrasound image.....	62
Figure 1.12 CT image of the abdomen.....	63
Figure 1.13 MRI image of the abdomen.....	65
Figure 1.14 Positron emission tomography images.....	66
Figure 1.15 Vortex vein involvement in UM with EOE.....	79

Figure 1.16 Posterior choroidal melanoma extended extra-sclerally.....	79
Figure 1.17 LUMPO – Version 3. Example of a personalized survival curve representing a hypothetical 60-year-old female patient with a UM 10mm in diameter and 5mm thick.....	86
Figure 1.18 LUMPO – Version 3. The same hypothetical patient above with an initial liver scan performed 6 months after treatment as per usual practice.....	87
Figure 1.19 LUMPO – Version 3. The same hypothetical patient above but with more risk factors including the presence of closed loops, higher mitotic rate and chromosome 8q gain.....	88
 <u>Chapter 2</u>	
Figure 2.1 Flow diagram for data collection for Liver-screening analysis to identify UM metastases in patients treated at the LOOC.....	102
Figure 2.2 Overview of patients included in the Liver-screening analysis study.....	108
Figure 2.3 Kaplan-Meier survival curve and table for all primary UM stratified according to gender.....	112
Figure 2.4 Kaplan-Meier survival curve and table for all primary UM stratified according to TNM staging based on the AJCC (8th Edition) classification.....	114
Figure 2.5 Kaplan-Meier survival curve and table where patient survival was stratified according to epithelioid cells presence.....	115
Figure 2.6 Kaplan-Meier survival curve and table where patient survival was stratified according to closed loops presence	116
Figure 2.7 Kaplan-Meier survival curve and table where patient survival was stratified according to mitotic counts.....	117

Figure 2.8 Kaplan-Meier survival curve and table where patient survival was stratified according to ciliary body involvement.....	118
Figure 2.9 Kaplan-Meier survival curve and table where patient survival was stratified according to extraocular extension presence.....	119
Figure 2.10: Kaplan-Meier survival curve and table according to copy number of chromosome 1p.....	121
Figure 2.11 Kaplan-Meier survival curve and table according to copy number of chromosome3.....	122
Figure 2.12 Kaplan-Meier survival curve and table according to copy number of chromosome6p.....	123
Figure 2.13 Kaplan-Meier survival curve and table according to copy number of chromosome 6q	125
Figure 2.14 Kaplan-Meier survival curve and table according to copy number of chromosome 8p	125
Figure 2.15 Kaplan-Meier survival curve and table according to copy number of chromosome 8q	126
Figure 2.16 Kaplan-Meier survival curve and table for patients stratified according to regularity of the liver screening.....	130
Figure 2.17 Patients who had a first liver scan at time of the primary treatment.....	131
Figure 2.18 Patients' distribution scheme representing the assessment of the 615 patients initially evaluated regarding their outcome considering the detection of metastases and cause of death	134

Figure 2.19 Kaplan-Meier survival curve and table where all the UM patients were stratified according to when and whether developed metastases.....	148
--	-----

Chapter 3

Figure 3.1 Frequency of imaging scans per patient within 11 years of liver surveillance for UM patients.....	177
---	-----

Figure 3.2 Overall yearly utilisation of MRI, CT and US scanning.....	179
--	-----

Figure 3.3 Patients whose metastases were diagnosed by clinical imaging – time to the first detection of metastases.....	180
---	-----

Figure 3.4 Patients whose metastases were diagnosed by clinical imaging – total number of scans until the detection of metastases	180
--	-----

Figure 3.5 Patients whose metastases were detected at autopsy – median time until the detection of metastases.....	182
---	-----

Figure 3.6 Patients whose metastases were detected at autopsy – total number of scans until the detection of metastases.....	184
---	-----

Figure 3.7 386 patients who did not demonstrated metastases grouped according to the time to the last scan.....	187
--	-----

Figure 3.8 386 patients who did not demonstrated metastases grouped according to the total number of scans until the last scan	187
---	-----

Figure 3.9: Incidence of metastases at different time points of the development of the disease for all 229 patients diagnosed of metastases.....	189
---	-----

Figure 3.10: ROC (Receiving Operating Characteristic) graph at 5 years	192
---	-----

Figure 3.11: Comparison of observed and expected number of metastases onset events within 0.5 to 10 years since management..... 193

Chapter 4

Figure 4.1. Flow diagram for the external validation of LUMPO3.....215

Figure 4.2 Kaplan–Meier estimates of all-cause mortality for the centres involved in the study.....223

Figure 4.3 Calibration graphs showing the comparison of observed and predicted survival in each of the external data sets for 3 years after treatment.....226

List of Tables

Chapter 1

Table 1.1 Posterior Uveal Melanoma Category based on the American Joint Cancer Committee/Tumour Node Metastases (AJCC/TNM) (8th Edition) Staging system.....54

Table 1.2 Distant Metastases of Posterior Uveal Melanoma Category based on the AJCC/TNM staging system.....54

Table 1.3 Clinical prognostic factors in UM.....77

Table 1.4 Summary on previous studies on prognostic models in UM.....90

Chapter 2

Table 2.1 UM Patient Characteristics, overall data (2008-2018).....109

Table 2.2 Type of primary treatment.....111

Table 2.3 Patients grouped according to the type of scan and the frequency of scans performed.....127

Table 2.4 Patients grouped according to the number of scans per patient.....128

Table 2.5 Characteristics of 208 patients who had only one scan during the liver screening study.....131

Table 2.6 Number of liver metastases detected through liver surveillance in the 615 UM patients.....135

Table 2.7 Size, location and AJCC/TNM staging of the detected metastases.....136

Table 2.8 Extra hepatic metastases in the 150 patients in whom metastases were detected during the liver screening study.....136

Table 2.9 150 UM patients grouped according to time to first metastases detection to death.....	138
Table 2.10 Characteristics of 108 UM patients who developed metastases within 2 years of diagnosis of the ocular tumour.....	140
Table 2.11 Characteristics of 121 UM patients who developed metastases after 2 years of diagnosis of the ocular tumour.....	141
Table 2.12 Characteristics of 386 UM patients in whom metastases were not demonstrated in Liverpool throughout the liver screening study period.....	146

Chapter 3

Table 3.1 Costs of MRI, CT and US according to NICE guidelines.....	174
Table 3.2 Modality and frequency of scans performed.....	178
Table 3.3 Number of scans until the detection of metastases and number of events.....	182
Table 3.4 Frequency of scans in 79 UM patients whose metastases were detected at autopsy.....	185
Table 3.5 Frequency of scans in 386 UM patients who never developed metastases.....	188
Table 3.6 Estimated costs of liver imaging for UM patients who developed metastases based on the NICE guidelines.....	192
Table 3.7 Estimated costs of liver imaging for UM patients who did not develop metastases based on the NICE guidelines.....	191
Table 3.8 Area under the ROC	192
Table 3.9 Sensitivity, specificity, positive and negative predictive values within 5 years, for different decision thresholds.....	193

Table 3.10 Cost analysis using the linear predictor of death due to metastases (*lpmd*) for different decision threshold points regarding the number of metastases missed and avoided scans..... 195

Table 3.11 Cost analysis using the *lpmd* for different thresholds regarding cost savings for recommended scans..... 195

Table 3.12 Cost analysis using the *lpmd* for different thresholds regarding cost savings for scans not recommended 196

Chapter 4

Table 4.1 Patient characteristics. Development data (Liverpool) and external validation data (from seven ocular oncology centres—Leiden, Rotterdam, San Francisco, Rostock, Moscow, Genoa and Essen).....221

Table 4.2 Discrimination performance of LUMPO3 — per year up to 4 years of follow up.....224

List of abbreviations

ACR	Alda Cunha Rola
AJCC	American Joint Committee on Cancer
ALT	Alanine aminotransferase
AMD	Age macular degeneration
AP	Alkaline phosphatase
ASCO	The American Society of Clinical Oncology
AST	Aspartate aminotransferase
AT	Azzam Taktak
ATP	Adenosine Triphosphate
AUROC	Area under the receiving operating characteristic curve
AUHT	(The) Aintree University Hospital NHS Trust
BAP1	BRCA1 associated protein-1
BCG	Bacillus Calmette-Guerin
BCLC	Barcelona Clinic Liver Cancer
BOLD	Bleomycin, vincristine, lomustine and dacarbazine
BRAF	Human gene that encodes a protein called B-Raf
BRCA1	Breast cancer type 1 susceptibility protein
BTG	British Technology Group
CBI	Ciliary body involvement
CCC	Clatterbridge Cancer Centre
CD3	Cluster of differentiation 3
CGH	Comparative Genome Hybridization
COMS	Collaborative ocular melanoma study
CRIS	Clinical Record Interactive System
CRLM	Colorectal cancer and liver metastases
CSMD1	CUB and Sushi multiple domains 1
CT	Computer Tomography
CXR	Chest X-Ray
DM	Data manager
EIF1AX	Eukaryotic translation initiation factor 1A, X-chromosomal
EMCH	Leiden and Erasmus Medical Centre Hospital
EOE	Extraocular extension
Epi	Epithelioid cells
FAF	Fundus auto fluorescence
FFA	Fundus fluorescein angiography
FISH	Fluorescence in situ Hybridization
GDG	Guideline development group for UM
GEP	Gene expression profile
GM-CSF	Granulocyte macrophage colony-stimulating factor
GNA11	Guanine nucleotide binding protein α 1
GNAQ	Guanine nucleotide-binding protein Q polypeptide
HER2	Human epidermal growth factor receptor 2

HIED	Helmholz Institute of Eye Diseases
HLA-A*2:1	Human leukocyte antigen serotype within the HLA-A
HPF	High power field
HTA	Health technology assessment
IBM	International business machines corporation
ICGA	Indocyanine green angiography
ICI	Immune checkpoint inhibitors
ID	Identifier number
IE	Immune embolization
IMCgp100	Immunocore glycoprotein 100
ImmTAC	Immune-mobilising monoclonal TCRs against cancer
Ki-67	MKI67 (Marker of proliferation Ki-67)
KTN1	Kinectin protein
LBD	Tumour largest basal diameter
LBIH	Liverpool Bio-Innovation Hub
LDH	Lactase Dehydrogenase
LDLM	Largest diameter of the largest metastases
LFTs	Liver function tests
LJB	Laura J Bonnet
LOOC	Liverpool Ocular Oncology Clinic
Loops	Extravascular closed connective tissue loops
Lpmd	Linear predictor of death due to metastases
Lpod	Linear predictor of death due to causes other than metastases
LUHFT	(The) Liverpool University Hospitals NHS Foundation Trust
LUMC	Leiden University Medical Centre
LUMPO	Liverpool Uveal Melanoma Prognosticator Online
LUMPO3	Liverpool Uveal Melanoma Prognosticator Online – Version 3
M0	No distant metastases by clinical classification
M1	Distant Metastases identified
M1a	Largest Diameter of the largest metastases ≤ 3.0
M1b	Largest Diameter of the largest metastases 3.1 - 8.0 cm
M1c	Largest Diameter of the largest metastases ≥ 8.1 cm
MD	Medical Doctor
Mitoc	Mitotic count per 40 high powered fields
MLPA	Multiplex ligation-dependent probe amplification
MRI	Magnetic Resonance Image
mRNA	messenger Ribonucleic acid
MSA	Microsatellite analysis
Mx	Unknown whether metastases are present or not
N/A	Not available
N0	Any case without clinical or pathologic evidence of lymph nodes
N1	Evidence of regional lymph node metastases
NHS	National Health Service
NICE	National Institute for Health and Care Excellence
NNS	Number needed to scan metric
NRES	National Research Ethics Service

NX	No information about regional lymph node metastases
OCA2	Oculocutaneous albinism
OCT	Optical coherence tomography
ODM	Oculo-dermal melanocytosis
OOB	Ocular Oncology Biobank
OOG	Ophthalmic Oncology Group
PAS	Periodic Acid Schiff
PBR	Proton beam irradiation
PCR	Polymerase chain reaction
PET	Positron emission tomography
PRXT	Plaque brachytherapy
REC	Research Ethics Committee
RFA	Radiofrequency ablation
RNA	Ribonucleic acid
ROC	Receiving operating characteristic
RPE	Retinal Pigment Epithelium
SCNA	Somatic Chromosomal Number Alterations
SCOO	S.C. Oculistica Oncologica
SCSG	The Scottish Consensus Statement Group
SEER	Surveillance Epidemiology and End results
SF3B1	Splicing factor 3B subunit 1
SIRT	Selective internal radiotherapy
SNP	Single Nucleotide Polymorphism
SPSS	Statistical package for the social sciences
T0	No evidence of primary tumour
T1	TNM Tumour size category 1
T2	Tumour size category 2
T3	Tumour size category 3
T4	Tumour size category 4
TCRs	T-cell receptors
TGCA	The Cancer Genome Atlas
TILs	Tumour Infiltrating Lymphocytes
TNF	Tumour necrosis factors
TNM	Tumour, regional lymph node, distant metastases
TP53BP1	Tumour suppressor p53-binding protein 1
TTC28	Tetratricopeptide repeat domain 28
UBM	Ultrasound biomicroscopy
UCFS	University of California, San Francisco
UHE	University Hospital of Essen
UHSB	University Hospital Schleswig-Holstein
UIN	Unique study identification number
UK	United Kingdom
UoL	University of Liverpool
US	Ultrasound
UH	Ultrasound height
USA	United States of America

USG
UV

Ultrasonography
Ultraviolet

List of thesis-related peer-reviewed publications to date:

Cunha Rola, A., Taktak, A., Eleuteri, A., Kalirai, H., Heimann, H., Hussain, R., ... & Marinkovic, M. (2020). Multicentre external validation of the Liverpool uveal melanoma prognosticator online: An OOG collaborative study. *Cancers*, 12(2), 477.

Eleuteri, A., **Rola, A. C.**, Kalirai, H., Hussain, R., Sacco, J., Damato, B. E., ... & Taktak, A. F. (2021). Cost-utility analysis of a decade of liver screening for metastases using the Liverpool Uveal Melanoma Prognosticator Online (LUMPO). *Computers in Biology and Medicine*, 130, 104221.

In preparation

A. Cunha Rola, H. Kalirai, J. Sacco, R. Hussain, H. Heimann, A. Eleuteri, A.F.G. Taktak, S.E. Coupland. Ten-year retrospective analysis of liver surveillance undertaken in uveal melanoma patients treated at the Liverpool Ocular Oncology Centre.

List of oral presentations

- 06.2020 Oral presentation at World Ophthalmology Congress Virtual.
An overview of eye care delivery in Angola: A needs assessment and educational approaches.
- 05.2019 Oral presentation at North West Cancer Research Centre end-of-year talk, Liverpool.
Annual summary of the project: Validation of the Liverpool Uveal Melanoma Prognostication Online3 'LUMPO3' as a prognostication algorithm in determining metastatic risk in uveal melanoma in Liverpool, and external validation of LUMPO3.
- 03.2019 Oral presentation at National Congress of Ophthalmological Society of South Africa – in the Leadership Development Programme 3. Cape Town, South Africa.
Glaucoma in Angola: Size of the problem.
The role of telehealth in glaucoma screening.
- 06.2018 Oral presentation at North West Cancer Research Centre end-of-year talk, Liverpool.
Annual summary of the project: The utility of the Liverpool Uveal Melanoma Prognostication Online 'LUMPO' as a prognostication algorithm in determining metastatic risk in uveal melanoma.
- 03.2018 Oral presentation at the 53rd OOG Meeting. Sienna, Italy
External Validation of LUMPO3 – overview of the project.

Declaration

The work presented in this thesis, unless otherwise indicated, was done by myself and is not part of any other thesis or publication in any other way. The publications that have been peer-reviewed as a result of these experiments are listed on the previous page. The data research work was performed at the Institute of Systems, Molecular and Integrative Biology, and the hospital records of the Royal Liverpool and Broadgreen University Hospital NHS Trust.

This project was undertaken for a period of four years under the supervision of Prof. Sarah E. Coupland, Prof. Azzam Taktak, Prof. Dyfrig Hughes and Dr Joseph Sacco. The funding was generously provided by the Instituto Nacional de Gestão de Bolsas de Estudo de Angola - INAGBE.

All data from patients diagnosed with UM were identified and kindly provided by the Liverpool Ocular Oncology Biobank at the University of Liverpool. Patients have provided their consent to the use of their tissue samples and anonymised data.

This study complies with the principles of the Declaration of Helsinki and the guidelines of Good Clinical Practice. Approval for the study was obtained from the Health Research Authority (NRES REC ref 18 / NW / 0748).

Dr Alda Cunha

Date: 24/09/2021

Chapter 1

General Introduction

1.1 Definition and Incidence

Uveal melanoma (UM) is the most common primary intraocular malignant tumour in adults [1]. UM are thought to arise from the melanocytes of the uvea, which is the middle and vascularized pigmented layer of the eye, including the iris, ciliary body, and choroid. The choroid is the posterior and major part of the uveal tract and is interposed between the outer sclera and the innermost layer of the neuro-ectodermal retina. The term 'uvea' comes the Latin word 'uva' (grape) as a result of its similarity in appearance to a black-purple grape, when the sclera is stripped from its surface [2]. UM account for about 98% of all ocular melanomas with the remainder occurring in the conjunctiva and eyelids. Most UM arise in the choroid (90%), followed by the ciliary body (6-8%) with about 1-2% developing in the iris [2-6] (Figure 1.1).

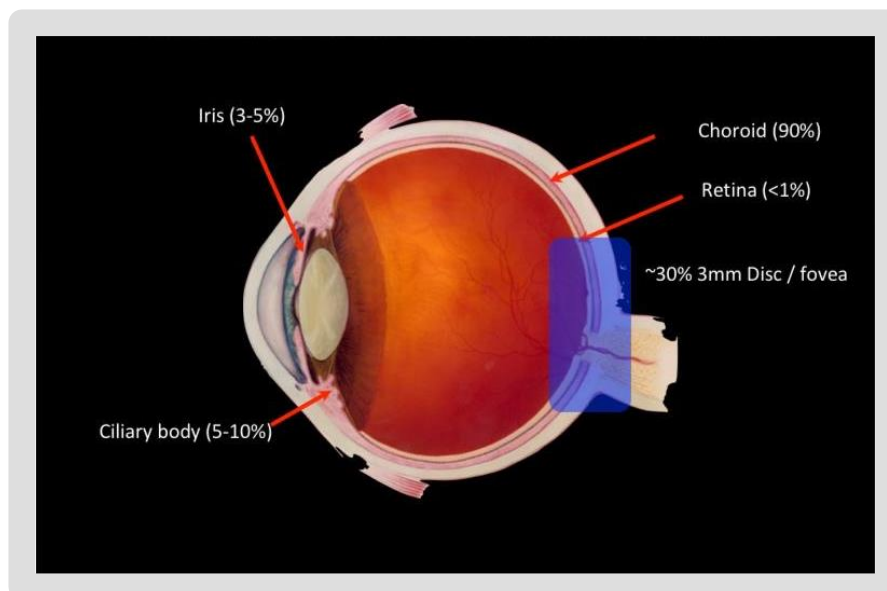


Figure 1.1 Anatomical location of UM: The uveal tract is comprised of the choroid, the ciliary body and the iris. The majority of ocular melanomas arise within the uvea (90%), followed by the ciliary body (5-10%), and iris (3-5%) (Courtesy of Prof. Heimann).

UM differ significantly from cutaneous counterparts, including in their clinical, epidemiological and prognostic features, despite the common embryological origin being melanocytes, which are thought to arise from neural crest cells. Whilst an increasing incidence of cutaneous melanoma has been observed in recent years, the incidence rates of UM have remained relatively stable over decades [7]. In one study from the United States of America (USA) [8], the incidence of UM ranges from 5.3 to 10.9 cases per million inhabitants [6], with it occurring most commonly in the Nordic countries compared to those around the Mediterranean or in Asia [9,10].

1.1.1. Age and sex specific incidence

UM is most often observed in older age groups, although it has been reported in patients at all ages. It has a specific incidence rate that increases with ageing, with a peak at age 70 years. Only about 1% of UM cases occur in young patients under eighteen years [11,12]. It affects males and females similarly, although a slight predominance is observed in males [12,13].

1.1.2 Etiological factors

The aetiology of UM remains uncertain [13,14] but various host and environmental factors have been described, and will be considered in more detail below.

1.1.3. Host factors

1.1.3.1 Ethnicity

UM predominantly affects the white fair-skinned population [12,14]. Based on data from the Surveillance, Epidemiology and End Results (SEER) [12], the relative risk of UM is 1.2 for Asians and Pacific Islanders, 5.4 for Hispanics and 19.2 for non-Hispanic white patients compared to black patients [8,13]. The fundamental basis of ethnic predisposition for UM remains unclear. However, light skin colour, blonde hair and blue eyes are also specific risk factors for the host. This is a potential link between the light colour of the eyes and the greater propensity for the development of UM. Blue or grey irises are related to pheomelanin (yellow-

brown pigment), while brown irises are related to eumelanin (black-brown pigment) [15]. Melanocytes with reduced functional OCA2 (Oculocutaneous albinism), which are likely to be involved in the synthesis of melanin by rate-limiting steps, demonstrate a defective synthesis of eumelanin while presenting a normal synthesis of pheomelanin [16]. UM can range from being amelanotic, slightly pigmented to excessively pigmented. Amelanocytic tumours are associated with catalytically inactive or less active tyrosinase [16].

1.1.3.2 Choroidal Naevi

Cutaneous naevi are a well-known risk factor for the development of cutaneous melanoma. It is believed that some (a very small proportion) UM also arise from choroidal naevi [17,18]. Choroidal naevi involve the entire thickness of the choroid, with the exception of the choriocapillaris [17]. They usually do not cause symptoms and are diagnosed mainly in routine ophthalmoscopy. They appear as a grey-brown slate lesion with minimal thickness. The margins are generally poorly defined. Similar to UM, choroidal naevi are associated with ethnicity, and increase with age, with an age-adjusted prevalence of 0.6% in the black population, 2.7% in the Hispanic population and 2.1% in the other [19]. Approximately 3% of individuals over 30 years of age present with naevi in the posterior half of the choroid, and it is estimated that 1 in 4800 choroidal naevi per year may modify into a melanoma [20]. Existing clinical and histopathological evidence suggests that choroidal melanoma may arise from a pre-existing choroidal naevi [17,18] or *de novo* [21]. However, there is a scarcity of risk estimates for malignant transformation of a choroidal naevi, due to the lack of reliable population-based data [20]. The risk of malignant transformation can be estimated at 1 in 8845, assuming that all melanoma arises from pre-existing naevi [20].

Special types of uveal naevi include the Naevus of Ota and magnocellular naevus (melanocytoma). The former is being defined as a congenital pigmentary abnormality that consists of the presence of excess melanocytes in the periocular skin, sclera, uvea, orbit, meninges, palate, or tympanic membrane. This pigmentation is, in most cases, unilateral. Melanocytic pigmentation can affect only the skin or eyes and can also occur as a combination

of both; therefore, the term ocular-dermal melanocytosis (ODM) is also used. The main concern of the ODM is the risk of developing melanoma, principally in the uvea [22,23]. ODM is a rare condition in the general population, with a prevalence estimated of 0.04%, but in those with UM ODM is found to be approximately 3% of patients [24-26].

Melanocytoma is defined as a specific variant of the melanocytic naevus, typically located at the optic disc or in the ciliary body, clinically characterized by dark brown to black colour and histopathologically composed of deeply pigmented cells round to oval with small, round and uniform nuclei. Uveal melanocytomas appear as very dark pigmented tumours of the choroid, ciliary body or iris. Although they are probably congenital lesions, the age range of presentation does not differ from UM, being useful in the differential diagnosis. Frangieh et al. [27] reported that the majority of reported cases occurred in the white population. Therefore, unlike optic nerve melanocytomas, uveal melanocytomas do not occur usually in black people. Distinguishing this benign tumour from UM can be tricky due to the slow-growing ability of melanocytomas. This slow growth can result in the tumour extension through the sclera to the epi-sclera. In addition, melanocytomas may undergo necrosis, resulting in pigment dispersion, uveitis and 'melanomalytic' glaucoma (i.e., the trabecular meshwork and drainage channels are blocked by pigment).

1.1.3.3 Genetic predisposition

Development of UM is usually considered to be a sporadic event. However, some cases of familial UM have been reported in the literature [28]. It is very rare, occurring in only 0.6% of all patients with UM [29]. Uncommon occurrences of UM that manifest characteristics indicating a hereditary predisposition have been rarely described; such as the familial UM, primary bilateral UM, those in young individuals, and primary multifocal UM [30]. As above, UM is also known in association with ODM: it is estimated that about 1 in 400 Caucasian individuals with ODM followed for life will develop UM [25]. The biological basis for the susceptibility to develop UM, could be a large number of melanocytes in the uveal tract of patients with ODM [25], particularly for bilateral [31] and multifocal UM [32]. UM usually

develops alongside ocular and dermal hyperpigmentation. Recent genetic studies have identified Guanine nucleotide-binding protein Q polypeptide (*GNAQ*) as a link between naevus of Ota and UM, thus explaining the increased risk of patients with naevus of Ota to develop UM [33,34]. UM associated with melanocytosis has a high risk of metastases: it is estimated that the risk is approximately 60% higher than UM not associated with melanocytosis [24,35].

Recently, *BAP1* [(ubiquitin carboxy-terminal hydrolase) or "protein associated with *BRACA1*"] germline mutations [36,37] have been identified in families with uveal and cutaneous melanoma [38,39], and also in patients with familial cutaneous melanoma and familial UM. The germline mutation of the *BAP1* gene has been identified to be responsible for predisposition to the "*BAP1* syndrome, comprising UM, malignant mesothelioma, meningioma, lung adenocarcinoma and other cancers, e.g. renal cell carcinoma and some skin cancers [40].

Despite the fact that germline *BRCA1* / *BRCA2* mutation has not been universally observed [41], some cases of UM in the germline *BRCA1* / *BRCA2* mutation scenario have been reported [42] [43,44]. Based on this finding, the authors Easton et al. and Wooster et al. [42,45] advocate that such mutations should be suspected in patients with a personal or family history of breast and ovarian cancer, and advise the screening of families with these mutations, even in the absence of other cancers [44].

1.1.4 Environmental factors

1.1.4.1 Sunlight exposure

Several factors of the host, such as ethnicity, association with choroidal naevi and genetic predisposition, have been investigated. Numerous environmental factors, such as occupational association and exposure to sunlight, were also investigated in case-control studies [46]. Evidence regarding the contributory role of exposure to sunlight and ultraviolet radiation (UVR) to the aetiology of posterior UM is insufficient, and contrasts that of

cutaneous melanoma [14,47]. In most of these studies, the results showed a lack of statistical significance or a weak positive correlation [48] between posterior UM and UVR. The relationship between UVR and posterior UM has been explored in various ways in several case-control studies [9]. Exposure to sunlight has been quantified taking into account the estimated time spent outdoors [49], the cumulative exposure to UV-B light throughout life [48] and the propensity to sunburn [50]. Analysis of all somatic coding and noncoding somatic single nucleotide substitutions in UM; however, shows the absence of a mutation signature induced by UV (pyrimidine dimers) [51], which are commonly seen in cutaneous and conjunctival melanomas [52,53].

The iris receives a greater amount of UV light than the posterior structures of the uvea (i.e. choroid) due to the specific filtering effects of the cornea, lens, the retinal pigment epithelium and the vitreous [47]. Iris melanomas located in front of the lens could be influenced by DNA damage induced by UV exposure [47]. Indeed iris melanomas have been suggested to demonstrate slightly different genetic alterations than the posterior UM, hinting at a role of UV in these anterior UM (see below) [54]. On the other hand, blue eyes with a decreased number of melanosomes within the melanocytes are at greater risk of developing UM, [55] [56]. The colour and melanin content of the iris generally remains constant in adult life [57]. Similar variations in the melanin content of the ciliary body and the choroid between blue eyes and brown eyes have been demonstrated [58].

1.1.4.2 Occupation

There is no consistent evidence to indicate occupational exposure to other environmental agents as a risk factor for UM development [48], although a few case-control studies have evaluated occupation as a risk factor for UM. A significant excess of cases of UM in electrical workers, technicians and other in-house workers, such as scientists, judges, teachers and managers have been pointed as a risk group for UM in studies in England and Canada [9]; yet a particular pathogenic factor has not been identified. Some carcinogenic factors have

been investigated and indicated as causative agents, including as chemicals, electromagnetic fields, endocrine disrupters, pesticides, artificial hormones and mobile phones [49,59]. However, the association of occupational exposure to external agents remains questionable.

1.2 Clinical features of UM

1.2.1 Choroidal melanoma

About 80-90% of UM arise in the choroid, as reported by numerous epidemiological and clinical studies [60]. The human choroid comprises blood vessels, melanocytes, fibroblasts, resident immunocompetent cells, and supporting collagenous and elastic connective tissue [61,62]. The choroid contains three interconnected layers of blood vessels that increase in size as they approach the sclera (**Figure 1.2**). An inner layer of leaky, fenestrated capillaries is called the choriocapillaris; a second layer of medium-sized vessels, called Sattler's layer; and a third most outermost layer called Haller's layer.

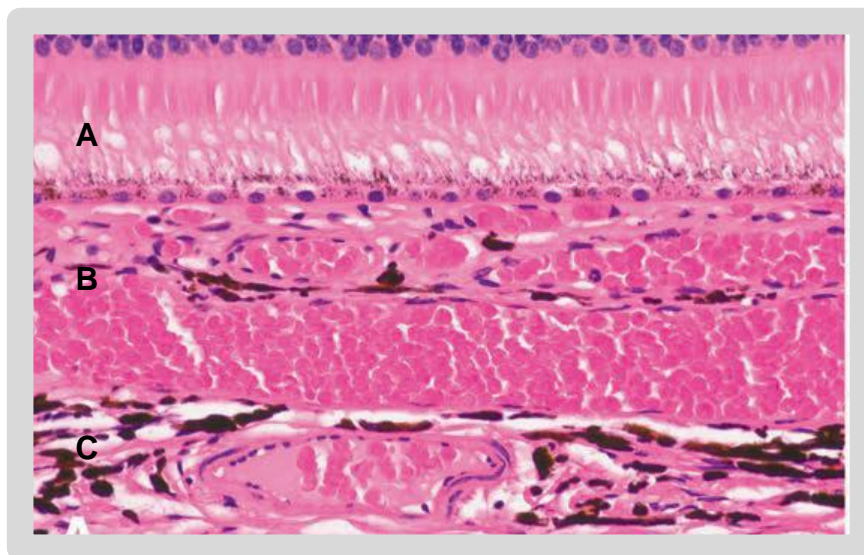


Figure 1.2 Histology of the choroid: The choroid is the posterior part of the uveal tract. A: The choriocapillaris, the inner layer containing small vessels that is located directly below the Bruch's membrane. B: The Sattler's layer, the medium-sized vessel layer. C: The large vessel layer (Haller's layer, outer layer) (Image sourced Eagle RC. *Eye pathology: an atlas and text*: Lippincott Williams & Wilkins; 2012) [2].

The choroid's highly vascularized nature reflects its main function, i.e. the supply of oxygen and nutrients to either the outer retina in species that possess a retinal vasculature or to the entire retina in species that lack a retinal blood supply. Other functions include thermoregulation, intraocular pressure modulation, and aqueous humour drainage via the uveoscleral pathway [61,63]. The numerous melanocytes present in the human choroidal stroma are distributed below the choriocapillaris and between the vascular layers of Haller and Sattler, some being closely opposed to the outer blood vessel walls. They are also present in the lamina fusca of the suprachoroid, where they take on a fusiform morphology. The choroidal melanocytes exhibit a pigment content, which varies depending on the ethnicity and the colour of the eye. An equivalent number of melanocytes are present in all ethnic backgrounds, but individuals with dark pigmentation have larger cells filled with larger melanin granules. The melanin granules found in the uveal melanocytes are easily distinguished from the large ellipsoidal melanin granules found in the apical cytoplasm of the epithelial cells of the retinal pigment epithelium (RPE), which line the inner surface of Bruch's membrane (**Figure 1.2**). Apart from providing pigmentation to absorb light, it is unclear what other functions the choroidal melanocytes perform. Just below the inner layer of the choroid lies Bruch's membrane, which is a sandwich-like structure composed of an extracellular matrix material, much of its composition is type I collagen and has a central core of elastic tissue.

In the early stage of development, when choroidal melanoma is smaller and containing an intact Bruch's membrane, the melanomas have a dome shape with a thickness equal to about half of their diameter (**Figure 1.3**). If Bruch's membrane is ruptured, the tumour morphology resembles a mushroom or collar-stud shape with 'strangulation' of the melanoma at its 'neck' by Bruch's membrane, causing engorgement of the blood vessels within the tumour 'head' (**Figure 1.4**). Should Bruch's membrane rupture at the tumour edge, the melanoma develops an irregular 'lop-sided' shape. Sporadically, the presence of multiple

ruptures of Bruch's membrane may result in various sub-retinal or intra-vitreous neoplastic hernias.

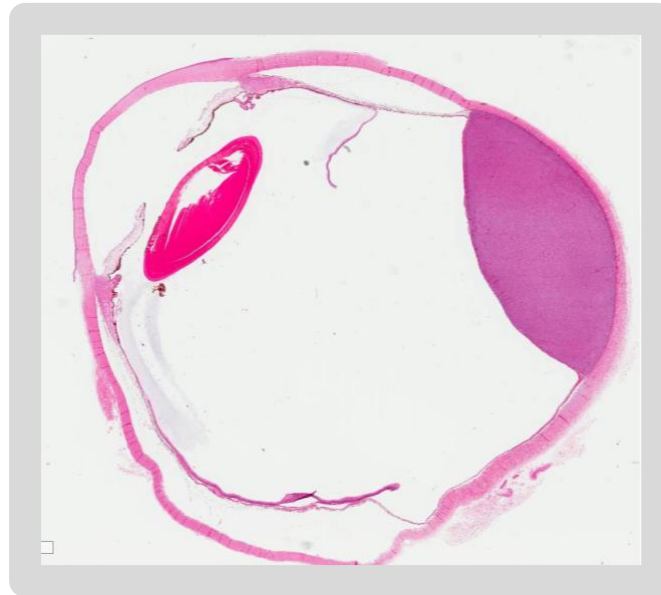


Figure 1.3 Large dome-shaped choroidal melanoma (courtesy of Prof. S. E. Coupland).

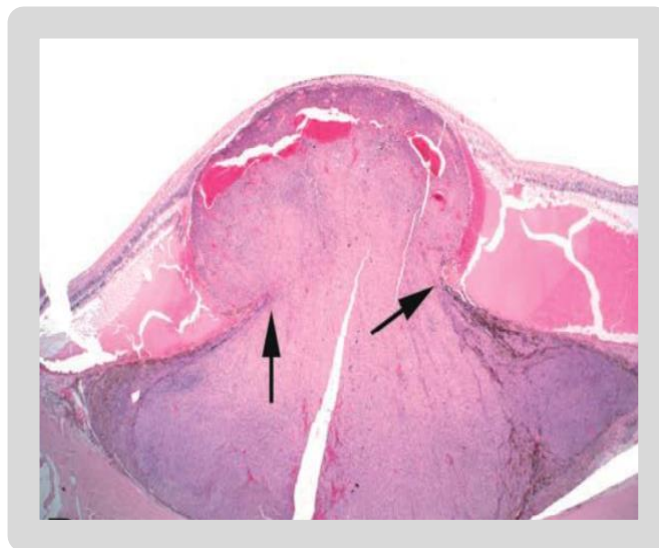


Figure 1.4 Large mushroom-shaped choroidal melanoma - The arrows point to the edge of the rupture in Bruch's membrane (Image sourced Eagle RC. Eye pathology: an atlas and text: Lippincott Williams & Wilkins; 2012)[2].

Choroidal melanomas present with a variety of clinical features and may manifest a progressive multiplicity of symptoms. Several factors may influence the clinical presentation of UM, such as its site, pigmentation, size, extent of secondary retinal detachment, haemorrhage or inflammation, or any extra-scleral extension of the tumour. About 10% of cases are asymptomatic, usually discovered on routine ocular fundus examinations [60]. In general, choroidal melanomas can cause multiple symptoms, but most patients complain of reduced visual acuity or blurred vision, and about 10-30% of patients may report symptoms such as photopsia, scotomas, vitreous floaters, metamorphosis or micropsia [64].

1.2.2 Ciliary body melanoma

The ciliary body is interposed between the iris and the choroid and has two main components, the pars plicata and the pars plana. The anterior pars plicata is composed of ciliary processes, which secrete the aqueous humour that fills the anterior chamber. The stroma of the posterior pars plana is composed of smooth muscle, whose function is the focusing of the lens (i.e. accommodation).

About 5% of UM cases affect the ciliary body [60]. Ciliary body melanomas may present as a circumscribed or annular form ("ring" of melanoma) (**Figure 1.5**). The circumscribed ciliary body melanoma at the time of diagnosis is generally larger than the iris melanoma and has a nodular shape. Initially, this tumour is confined to the ciliary body and is therefore asymptomatic. Generally, they are brown, corresponding to the colour of the ciliary pigment epithelium around it, unless the tumour, in which case the exact colour of the tumour becomes visible, has invaded it. Ciliary body melanomas usually invade the iris root and the anterior chamber, where they become visible clinically through the cornea. They can sow cells into the anterior chamber, on the surface of the iris and into the anterior chamber angle, causing elevated intraocular pressure [65]. Ultimately, they can exit via Schlemm's canal into the systemic circulation.

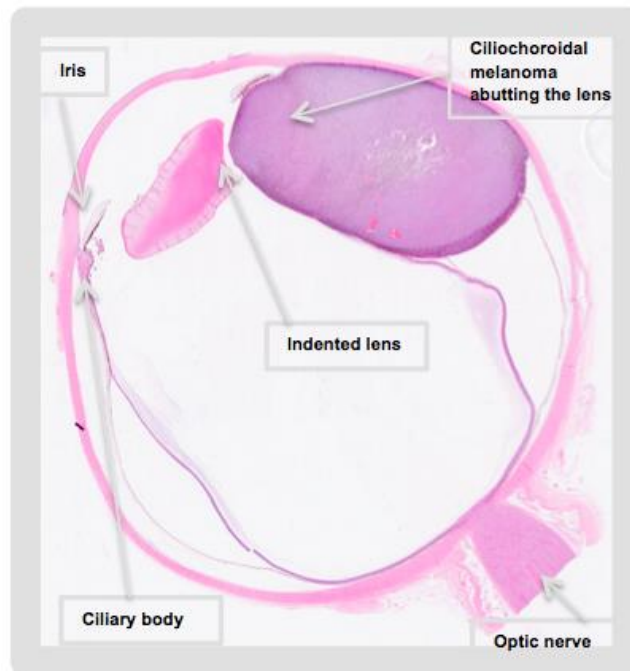


Figure 1.5 Ciliochoroidal melanoma, which has abutted the lens causing its indentation (courtesy of Prof. S. E. Coupland).

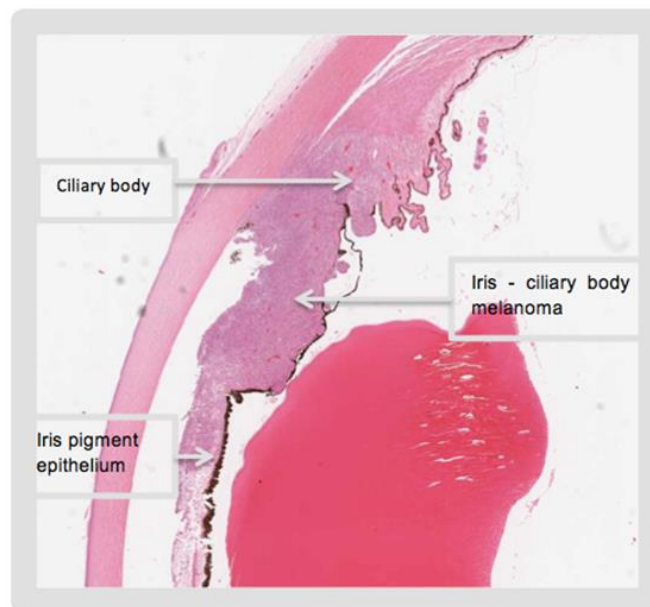


Figure 1.6 Histology of the iris and ciliary body: The iris, the most anterior part composed of three layers; the anterior layer, which is the most superficial tract, the middle layer or stroma, composed of pigmented and non-pigmented cells, and the posterior layer, composed of the dilating muscle of the iris and the pigment epithelium (courtesy of Prof. S. E. Coupland).

1.2.3 Iris melanoma

The iris is the anterior visible part of the uveal tract. It is composed of three layers; the anterior layer, which is the most superficial tract composed by an arrangement of fibroblasts, melanocytes and collagen, the middle layer, or the stroma, consisted by pigmented and non-pigmented cells, and the posterior layer, which is composed by the iris dilating muscle and the pigment epithelium (**Figure 1.6**). Iris melanomas are the least frequent of all UM.

Non-pigmented irises have a higher risk of developing iris melanoma [66]. As above, ODM is also a risk factor for iris melanoma [67]. Melanoma of the iris may arise from pre-existing nevi or *de novo*. The rate of malignant transformation of iris nevi into melanoma is estimated to be about 3% in 5 years [68]. Due to their location, iris melanomas are diagnosed and treated when they are relatively small, compared to tumours located in the ciliary body and choroid. Iris melanoma cells are usually less aggressive compared to posterior UM cells. Iris melanomas generally present as a small, pigmented, vascularized nodular lesion with an indolent clinical course and may be circumscribed or diffuse. Those located within the peripheral iris may represent an anterior extension of the ciliary body or choroidal melanoma, and therefore, it is of utmost importance to examine the posterior segment in all cases of iris melanoma. Slit lamp examination, gonioscopy and ultrasonography allow staging of the tumour to guide the most appropriate treatment [66]. Certain clinical features within a melanocytic iris tumour, such as inferior location, diffuse iris extension, episodes of hyperchromic heterochromia are often associated with glaucoma and predict a greater risk of growth [68].

1.3 Histopathological features of UM

To understand UM's biology, a range of laboratory techniques have been applied to these tumours. These have included morphological analyses, immunohistochemistry techniques and more recently genetic tools, all of which have contributed to the discovery and

description of several prognostic features in UM. These prognostic factors have helped to stratify UM patients into metastatic risk groups, which in turn enable clinical management.

A morphological classification for UM was proposed in 1931 by Callender [69,70] based on cytological and histopathological characteristics, showing the prognostic value of this classification. Callender basically divided UM cells into two main cytological types: spindle and epithelioid (**Figure 1.7**).

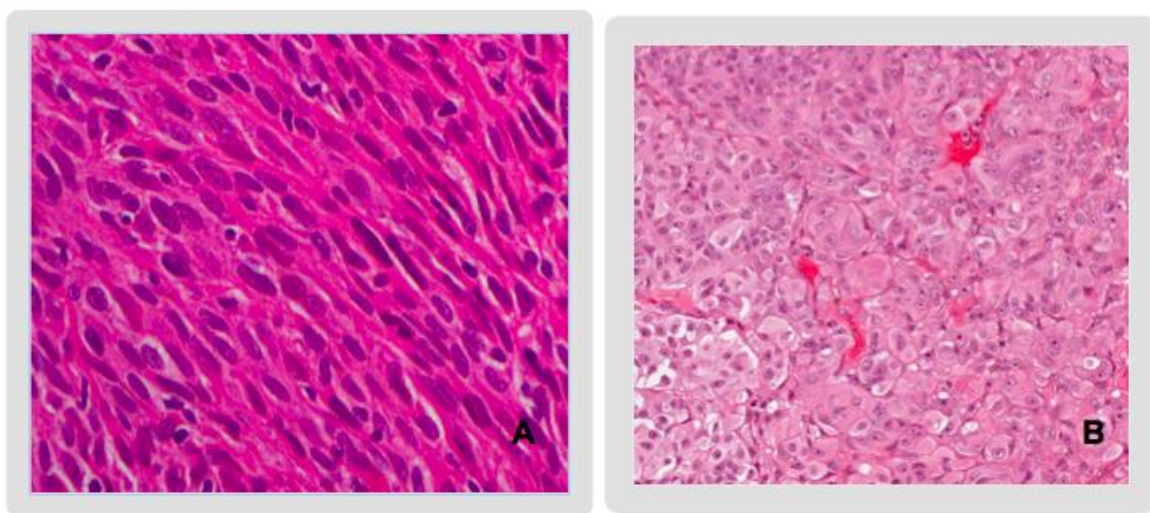


Figure 1.7 Melanoma cells: A) Spindle melanoma cells. The nuclei are thin, smooth and cigar-shaped, with finely dispersed chromatin and indistinct nucleoli. B) Melanoma epithelioid cells. The cytoplasmic margins of these large and poorly cohesive cells of epithelioid melanoma are easily discernible. Epithelioid cell nuclei are typically round and have a coherently grouped peripheral margin of chromatin (courtesy of Prof. S. E. Coupland).

Having identified two subtypes of spindle cells based on their nuclear characteristics. Subtype A cells that have a thin nucleus with fine chromatin and an indistinct nucleolus, generally they have a fold in the nuclear envelope, giving the appearance of a chromatin web. The subtype B cells have a denser nucleus, coarser chromatin and more prominent and eosinophilic nucleolus. Since this original description by Callender, it is now thought that

the Spindle A cells represent naevus cells, and so the term “Spindle-celled” UM typically means that it is composed of Spindle B cells [71].

The epithelioid cells of UM are larger and more pleomorphic than spindle-type cells, and frequently they have plentiful clear cytoplasm and a distinct cell membrane, and often exhibit an extracellular space between adjacent epithelioid-type cells. One of the characteristics that differentiate them from fusiform cells is exactly this loss of cell cohesion. UM of spindle cell type are associated with better prognosis, while tumours of epithelioid cell types are linked with a poorer prognosis [72].

Other histopathological characteristics routinely used to evaluate the malignant potential of UM are the mitotic figures, and the presence of closed connective tissue loops. The prognostic value of mitotic counts in UM was first demonstrated by McLean and associates [73]. They found that UM often contains some mitotic figures and recommended that a minimum of 40 high power fields (40x targets) be scanned. Greater numbers of mitoses are associated with a greater chance of metastatic disease; these findings have since been confirmed by others [74-76]. Vascular or connective tissue patterns have a high significance in the prognosis of UM [77,78]. The presence of Periodic Acid Schiff (PAS)-positive connective tissue loops is significantly associated with UM-related death [72]. It is worth mentioning here that both parameters - i.e. mitotic count (>5) and the presence/absence of connective tissue loops – are included in the Liverpool uveal melanoma prognosticator, described in more detail below.

Recently, features that link molecular changes in invasive and metastatic properties of cultured UM cells and the formation of microvessels have been reported [79]. To assess tumour vascularization as a histological prognostic factor for metastases of eyes removed for choroidal and ciliary body melanomas, two methods were adopted: The calculation of vascular density [80] and the detection of microcirculation patterns [81] formed by micro-remodelling circulation [82].

Vascular density is measured in histological sections, in which the number of vessels in a given unit area of the tumour is counted, which presents a positive point for an endothelial marker [83]. In addition, the measurement of vascular density between histological levels of UM is variable. Vascular density can vary within a given histological section and between different levels of the same tumour [84]. On the other hand, independent groups have confirmed the significance of the association between microcirculatory architecture and the result in several studies in other tumour systems [73,76,85]

Other histological parameters of primary UM associated with a poor prognosis, include high density of lymphocytes and macrophages [86]. In UM, the presence of a substantial number of inflammatory cells does not represent an effective anti-tumour immune response. Instead, a pronounced infiltration of UM by lymphocytes is associated with a poor prognosis. Similarly, a significant infiltration of UM by macrophages is associated with poor prognosis [87,88]. This may be related to immuno-regulation influence of the intraocular microenvironment [89]. There are two main types of macrophages, of which have been identified - 1) the classically activated macrophage, which can stimulate immune responses and has antibacterial and antiangiogenic functions, and - 2) the alternately activated macrophage, which differently, exhibits anti-inflammatory and pro-angiogenic functions. These two types of macrophages are called M1 and M2 macrophages, respectively [90]. The tumour support functions of M2 macrophages may explain the relationship between low survival and density of macrophages in UM, since M2 is the dominant non-tumorous cells in both primary and secondary UM [91], and is considered pro-angiogenic and tumour promoter.

1.4 Genetic alterations in UM

For some decades, it has been acknowledged that changes in the number of copies on certain chromosomes in the tumour cells correlate with an enhanced risk for the development of metastases in UM. The main somatic chromosomal number alterations (SCNA) identified associated with patient survival include monosomy 3, polysomy 8q, polysomy 6p and loss of 1p [92]. Loss of chromosome 3, gain in 8q, loss in chromosome 1p and loss in chromosome 6q are associated with poor prognosis [93].

1.4.1 Chromosome 3

Monosomy 3, which is the complete loss of a copy of chromosome 3, is the most common alteration and is the most important prognostic factor within most cases with chromosome 3 aberrations in UM. Partial aberrations on chromosome 3 (partial deletion of a copy of chromosome 3) and isodisomy (loss of one copy of chromosome 3 and duplication of the remaining defective copy) were also both reported as having metastatic potential. It has been proposed that there can be heterogeneity for chromosome 3 in rare UMS. For example, Schoenfield et al. described in a study of UM the presence of monosomy 3 at the base of the tumour and disomy 3 at the apex of the tumour [94,95]. The presence of monosomy 3 indicates high-risk melanoma and an increased risk of metastatic disease. Monosomy 3 is often associated with clinical and histopathological risk factors, which include increased tumour diameter, the involvement of the ciliary body, tumour location, epithelioid cell type, high mitotic rate, vascular loops, and the extraocular extension of the tumour [72,93,96]. In more recent studies, the BRCA1 tumour suppressor gene 1 (*BAP1*) has been mapped on chromosome 3p21.1. Its somatic mutation has been associated with metastatic disease in UM [97].

1.4.2 Chromosome 8q

Chromosome 8q gain is the most common alteration in most cases with aberrations on chromosome 8 and can affect about 41 to 53% of cases of UM, whereas 8p loss rarely occurs [98-100]. The most common forms of 8q gain are trisomy 8, isochromosome 8q and amplification of the c-myc gene [101]. Gain of chromosome 8q is an important prognostic factor for UM, either when presented alone or when it coexists with monosomy 3. The 8q chromosome gain commonly co-exists more with monosomy 3 and is associated with worse prognosis than the 8q gain alone or monosomy 3 alone. Damato et al. reported that in a study of 356 patients with UM, in 42% of the cases UM did not show cytogenetic abnormalities of chromosomes 3 or 8, 11% in 8q, 21% in monosomy 3 in 8%, and 27% in 8q gain and monosomy 3 combined [96]. 8q gain was associated with clinical and histopathological risk factors, which included the largest tumour diameter, ciliary body tumour location, epithelioid cell type, high mitotic rate, and vascular loops [96].

1.4.3 Chromosome 1

When loss of part or whole chromosome 1p occurs alone or coexists with monosomy 3, it is associated with poor prognosis [98,102]. Loss of chromosome 1p occurs more frequently in UM with monosomy 3 (40%) than with disomy 3 (10%) [103]. The concomitant loss of chromosomes 1p and 3 combined have a stronger association with UM metastatic disease than either one of them separately.

1.4.4 Chromosome 6

Gain of chromosome 6p is generally reciprocally exclusive with monosomy 3 [104]. For chromosome 6p gain UM, it was proposed that they represent a separate group of UM with an alternative genetic pathway in carcinogenesis compared to those with monosomy 3 [104]. The gain of chromosome 6 is a strong indicator of good prognosis of UM and has an inverse association with UM-related metastases [105]. Coexistence of 6p gain and monosomy 3 occurs in only 4% of cases of UM [106]. Loss of chromosome 6q is associated with poor prognosis.

1.4.5 Genetic mutations in UM

1.4.5.1 *GNAQ* and *GNA11*

Mutations in *GNAQ* are present in about 50% of UM and can occur in all stages of the disease [33,107]. Studies have shown that mutations in exons 4 (R183) and 5 (Q209) of GTPases *GNAQ* and guanine nucleotide binding protein α 11 (*GNA11*) are unique to UM and uveal nevi [108], and the two genes are found mutated in approximately 80- 90% of UM and are reciprocally exclusive [109]. They are believed to be an initial event in the development of UM [110]. *GNA11* mutations are seen in 30-50% of UM at different stages of tumour progression [108].

1.4.5.2. *SF3B1*

SF3B1 (Splicing factor 3B subunit 1) is one of the few genes that are commonly mutated in UM, allowing a more accurate molecular taxonomy of this cancer. Consistent with this idea, *GNAQ* or *GNA11* mutations were present in most of our *SF3B1* and *BAP1* mutants, suggesting that they appeared earlier than the *SF3B1* and *BAP1* mutations [107]. However, the *SF3B1* and *BAP1* mutations were almost mutually exclusive, indicating that they may represent alternative pathways for the progression of the tumour [33]. *SF3B1* encodes the subunit 1 of the protein complex of union factor 3b, which is a component of the small nuclear complex of U2 ribonucleoprotein (snRNP) that participates in the alteration of pre-mRNAs [111]. Splicing factor 3b is also a component of the small U129-type spliceosome [111]. Further investigations are under way to elucidate the consequences of *SF3B1* mutations on uveal melanoma progression in order to therapeutically target these effects [112].

1.4.5.3 *EIF1AX*

Mutations in *EIF1AX* (Eukaryotic translation initiation factor 1A, X-chromosomal) in UM are considered a relatively recent finding, occurring through access points in exons 1 and 2 [113]. They are associated with a more favourable prognosis, since they have only been shown to occur in cases of disomy 3 and are reciprocally exclusive of *BAP1* and *SF3B1* mutations.

Various studies have demonstrated that mutations in *EIF1Ax* play a protecting role in the prevention of metastases, even taking into account other risk factors [113,114].

1.4.5.4 *BAP1*

BAP1 or "protein associated with BARCA1" is a deubiquitinating enzyme found on the short arm of chromosome 3. The *BAP1* gene is mapped to chromosome 3p21.1 and codes for a cutting enzyme located in the cell nucleus [115]. The enzyme regulates cell growth and appears to be important in the pathogenesis of cancer. Inactivating mutations of *BAP1* are found in up to 84% of metastatic UM [97,116]. Recently, the lack of nuclear expression of the *BAP1* protein has been associated with metastatic diseases in UM and their progression [117,118]. In addition, lack of *BAP1* gene expression has also been associated with an immune profile modulation towards a regulatory and dysfunctional immune response, which favours tumour growth, metastatic dissemination and potentially immunotherapy failure [119].

1.4.6 Next generation sequencing panels for prognostication

Recently, research using whole genome sequencing has led to the discovery of several genetic changes, which correlate with a different survival pattern [120,121]. The novel custom-designed next-generation sequencing (NGS) assays for UM can be used to predict prognosis for patients with UM based on the status of the mutation and the chromosomal status of chromosomes 1, 3 and 8. The assays can be performed using newly isolated DNA or DNA obtained from formalin fixed and paraffin embedded (FFPE) tumour material.

Recent genomic studies have reported that UM could be subdivided into four main groups using unsupervised hierarchical clusters, according to genetic changes (SCNA, mutations and RNA-Sequencing), which have been associated with an increasingly poor prognosis [53,122]. Based on these findings, several efforts have been made to design the NGS specifically targeted for UM. In one of the most recent studies, Thornton et al. 2020, reported the largest cohort of UM patients to be analysed using a targeted NGS panel to date. The ability of the NGS to detect SCNA in chromosome 1, 3, 6 and 8 and mutations in *GNAQ*, *GNA11*, *BAP1*,

SF3B1, and *EIF1AX* was examined [121]. Primary UM DNA samples from 117 consenting patients treated at LOOC, Liverpool University Hospitals NHS Foundation Trust, with a median follow-up of 65 months were analysed. The study revealed, among other findings, that monosomy 3-UM that was wild-type for *BAP1*, but that had *SF3B1* mutations. New mutations were also identified in *TTC28* (Tetratricopeptide repeat domain 28), *KTN1* (Kinectin protein), *CSMD1* (CUB and Sushi multiple domains 1) and *TP53BP1* (Tumour suppressor p53-binding protein 1) [121].

1.4.7 Most commonly genetic methods used for prognostication in UM

The genetic prognosis test for UM patients is routinely performed as part of the patient management protocol, a practice used at the Liverpool Ocular Oncology Centre (LOOC), one of the three supraregional reference centres for the treatment of adult eye tumours in England [123].

As above, certain SCNA that mainly affect chromosomes 1p, 3, 6 and 8 have been identified by a variety of genetic techniques which facilitate the ability to perform genetic prognostic tests for metastatic risk stratification. These methods vary from low resolution techniques such as fluorescence in situ hybridization (FISH) and microsatellite analysis (MSA) to higher resolution methods, such as comparative genome hybridization (CGH), multiplex ligation-dependent probe amplification (MLPA) and SNP (Single Nucleotide Polymorphism) arrays [92]. As above, monosomy 3 continues to be the strongest genetic predictor for the development of the metastatic disease in UM. 8q polysomy, which is a predictive marker independent of poor prognosis, increases the predictive diagnostic when this information is associated with the presence of monosomy 3 and the clinical and histomorphological characteristics of the tumour. In contrast to monosomy 3 and polysomy 8q, the presence of 6p polysomy has been described as an indicator of a good prognosis for the UM, being associated with disomy of chromosome 3 and better patient survival.

1.4.7.1 Gene expressing profiling

Different molecular prognostic methods, such as the gene expression profile (GEP), have also been explored to overcome some of the limitations of cytogenetic techniques and provide physicians with an alternate clinical test to determine the prognosis of individual UM patients. Notably, it was found that UM could be divided into two basic categories based on their GEP, and these categories were strongly associated with prognosis. Class 1-low risk of metastases or class 2-high risk of metastases [124]. This GEP test, which has since been commercialised via Castle Biosciences, is based on the messenger RNA (mRNA) expression of 12 discriminant genes and three control genes [125] [126].

1.5 Diagnosis and treatment of UM

1.5.1 Diagnosis

The management of UM patients involves the consideration of many factors such as tumour detection, diagnosis, patient counselling and care planning, treatment of local tumour recurrence and other ocular complications, prognostication, psychological support, screening for metastatic disease, if appropriate, and treatment of metastases. A specialist multidisciplinary team best delivers these management measures. The diagnosis of UM is mainly based on clinical examination by biomicroscopy and indirect ophthalmoscopy. Auxiliary tests may be used to confirm the diagnosis and may include colour fundus photography, ultrasonography (USG), fundus fluorescein angiography (FFA), Indocyanine green angiography (ICGA), ultrasound biomicroscopy (UBM), optical coherence tomography (OCT), and fundus auto fluorescence (FAF) (**Figures 1.8 and 1.9**). When the clinical diagnosis is unclear, a fine needle biopsy of the tumour can be performed. Early detection of UM considerably enhances the chances of maintaining a functional eye, and possibly of

crucial importance in the prevention of metastatic dissemination, particularly if the tumour is small.

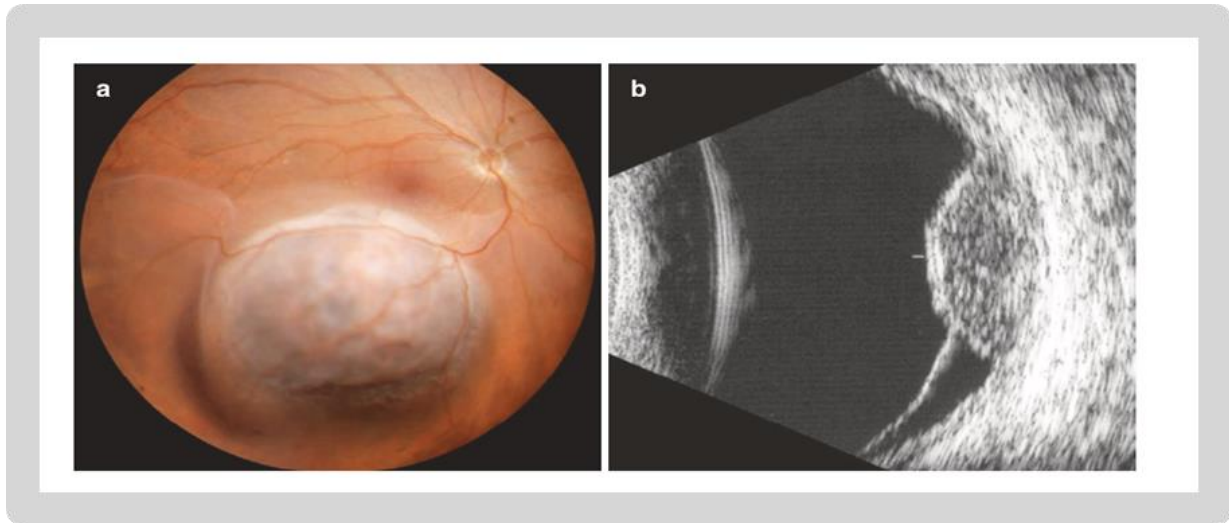


Figure 1.8 Dome-shaped choroidal melanoma in which there is a secondary serous retinal detachment. (a) Fundoscopy image. (b) Ultrasonography (image sourced from Singh, 2019) [127].

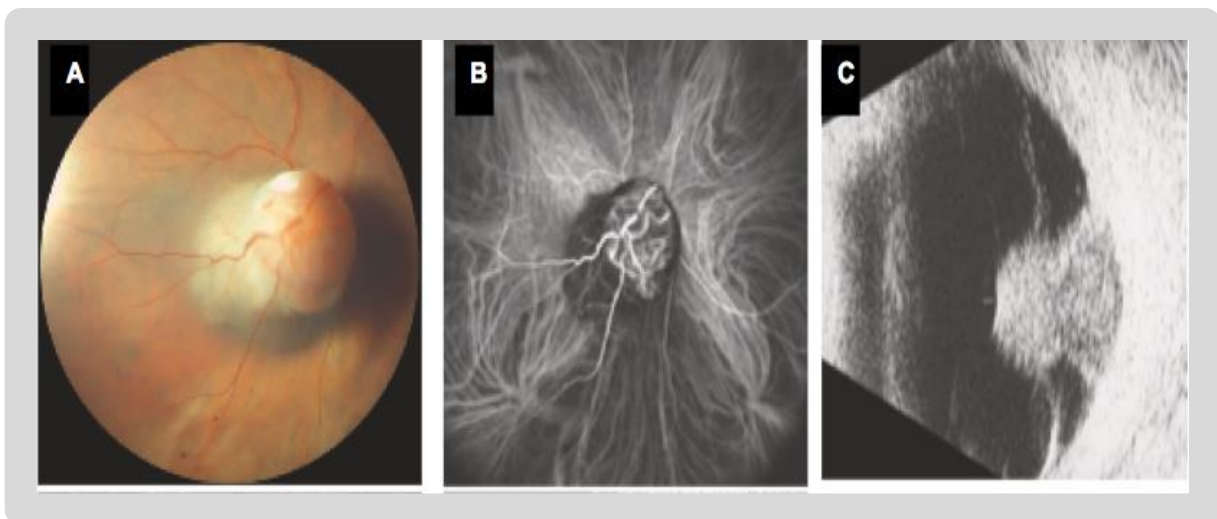


Figure 1.9 Mushroom-shaped choroidal melanoma with a vascular congestion at its apex and covering the optic disc. (a) Fundoscopy view. (b) ICG angiography. (c) 10 MHz ultrasonography (image sourced from Singh, 2019)[127].

Some studies describing delays in the diagnosis of UM have reported that about 28-37% of these lesions were not detected during the first examination [35,128]. It is of primary importance that patients exhibiting any symptoms suggestive of posterior segment pathologies, such as loss of vision, metamorphosis or photopsia, should be submitted to examination of the fundus of the eye with dilatation of the iris [128,129]. UM have been previously classified based on tumour thickness in research and clinical settings. In the Collaborative Ocular Melanoma Study (COMS) classification system: small tumours were defined as those up to 3 mm thick with a base diameter of not more than 16 mm, medium tumours range from 3.1 to 8 mm thick with a base diameter of not more than 16 mm and the large tumours are those thicker than 8 mm and have a base diameter greater than 16 mm. It was described by the COMS that the risk of metastases increases 5% with each increase of 1 mm in tumour thickness measured by ultrasonography [130].

More recently, the anatomical classification of UM has been updated to new evidence-based categories that provide a basis for UM staging as component of the American Joint Committee of Cancer (AJCC)/Tumour, Node, Metastases (TNM) staging system applied in all types of cancer (**Table 1.1 and Table 1.2**). In the classification for the tumour node metastases staging system in the AJCC/TNM staging system, tumour size is assessed and defined in the category T (1-4), involvement of lymph node in the N category (NX, N0, N1) and the existence of distant metastases in the M category (MX, M0, M1a, M1b, M1c).

For UM, T is classified based on the width and basal thickness of the tumour (T1, T2, T3, T4) and then divided into subgroups reflecting the involvement of the iris, ciliary body, choroid and the extra-scleral extension of the tumour (a, b, c, and d and e). For the staging of UM, two systems are used, one for anteriorly located iris melanomas and the other for posterior ciliary and choroidal body melanomas, since the two types differ not only in anatomical location but also regarding prognosis. Both systems are based on the parameters of evaluation of the anatomical extension of the tumour. The AJCC staging system (7th and 8th editions) proved to be a good predictor of survival in UM patients [131].

Table 1.1: Posterior Uveal Melanoma Category Based on the American Joint Cancer Committee (8th Edition) Classification

T1	Tumour base < 3-9 mm with thickness ≤ 6 mm
	Tumour base 9.1-12 mm with thickness ≤ 3 mm
T1a	T1 tumour without ciliary body involvement and extraocular extension
T1b	T1 tumour with ciliary body involvement
T1c	T1 tumour without ciliary body involvement but with extraocular extension ≤ 5mm in diameter
T1d	T1 tumour with ciliary body involvement and extraocular extension ≤ 5 mm in diameter
T2	Tumour base < 9 mm with thickness 6-9 mm
	Tumour base 9.1-12 mm with thickness 3.1-9 mm
	Tumour base 12.1-15 mm with thickness ≤ 6 mm
	Tumour base 15.1-18 mm with thickness ≤ 3 mm
T2a	T2 tumour without ciliary body involvement and extraocular extension
T2b	T2 tumour with ciliary body involvement
T2c	T2 tumour without ciliary body involvement but with extraocular extension ≤ 5mm in diameter
T2d	T2 tumour with ciliary body involvement and extraocular extension ≤ 5mm in diameter
T3	Tumour base 3.1-9 mm with thickness 9.1-12 mm
	Tumour base 9.1-12 mm with thickness 9.1-15 mm
	Tumour base 12.1-15 mm with thickness 6.1-15 mm
	Tumour base 15.1-18 mm with thickness 3.1-12 mm
T3a	T3 tumour without ciliary body involvement and extraocular extension
T3b	T3 tumour with ciliary body involvement
T3c	T3 tumour without ciliary body involvement but with extraocular extension ≤ 5mm in diameter
T3d	T3 tumour with ciliary body involvement and extraocular extension ≤ 5mm in diameter
T4	Tumour base 12.1-15 mm with thickness >15 mm
	Tumour base 15.1-18 mm with thickness >12 mm
	Tumour base >18 mm with any thickness
T4a	T4 tumour without ciliary body involvement and extraocular extension
T4b	T4 tumour with ciliary body involvement
T4c	T4 tumour without ciliary body involvement but with extraocular extension ≤ 5mm in diameter
T4d	T4 tumour with ciliary body involvement and extraocular extension ≤ 5mm in diameter
T4e	Any tumour size with extraocular extension ≤ 5mm in diameter

Table 1.2: Distant Metastases of Posterior Uveal Melanoma Category Based on American Joint Cancer Committee (8th Edition) Classification

M0	No distant metastases
M1	Distant metastases
M1a	Largest diameter of the largest metastases 3 cm or less
M1b	Largest diameter of the largest metastases 3.1–8.0 cm
M1c	Largest diameter of the largest metastases 8.1 cm or more
Mx	Unknown

As mentioned above, small UM can present as flat or dome-shaped tumours. Over time, the UM may rupture Bruch's membrane and can shape its pathognomonic form "mushroom", which can be clearly visualized on USG. If the tumour has infiltrated the retina after Bruch's membrane rupture, vitreous haemorrhage may occur. The most commonly used auxiliary method in the diagnosis of UM is the USG. Usually, the tumour presents low to medium internal reflectivity in A-mode USG that decreases toward the sclera. In B-mode, the tumour appears as an acoustically hollow dome-shaped or mushroom mass or as a hyper-echoic masse with less reflectivity than the surrounding choroid, thus giving an acoustically hollow appearance. Additionally, USG is also helpful in evaluating extraocular extension of the tumour. The areas of hyporefectivity compared to normal orbital tissue are considered an orbital extension of the tumour. For the evaluation of UM that originate in the ciliary body, UBM is a useful diagnostic tool that allows the visualization and evaluation of hyporefective plaques on the surface of the tumour, internal tumour reflectivity, specific vascularization and, if present, extraocular extension of the tumour.

UM can be simulated by a variety of lesions, among these lesions are the choroidal tumours, especially choroidal naevi, metastatic tumours, choroidal haemangioma and osteoma; haemorrhagic lesions such as AMD (Age Macular Degeneration) associated with haemorrhagic detachment of the choroid; retinal tumours such as congenital retinal pigment epithelium hypertrophy, and retinal pigment epithelial adenocarcinoma; and certain inflammatory lesions, such as posterior scleritis.

1.5.1 UM treatment options

There is range of therapeutic possibilities for primary UM treatment. These include various forms of radiotherapy, surgical resection (local tumour resection and enucleation) and phototherapy [132,133]. The local tumour control rates at five years in most specialised treatment centres exceed 90% [133]. The selection of the most appropriate treatment option

applicable is made based on the size, location, and extension of the tumour and always taking into consideration the expectations and the preferences of the patient.

In general, the treatment of the first choice for choroidal melanomas is radiotherapy, selecting some form of resection when radiation therapy is capable of causing collateral damage by a toxic syndrome or excessive collateral damage to healthy tissues. In most centres, the first choice of radiotherapy is brachytherapy, which is performed with plate-shaped applicators containing isotopes such as iodine-125 or ruthenium-106, which emit γ and β irradiation, respectively. Iodine-125 plates are more largely used in the USA, while ruthenium-106 plates are more widely used in Europe [134]. The plaque is sutured to the external surface of the sclera overlying the tumour, and removed days after the necessary dose of at least 80 Gy [135,136] has been delivered to the tumour.

Surgery – either local tumour resection or enucleation – are also commonly used operative procedures in the treatment of UM.

Despite the progress in treatment methods for the primary UM, and a growing trend of eye-saving therapies over the past 30 years, survival rates of UM patients have continued unchanged. Almost 50% of UM patients develop disseminated disease, predominantly in the liver, but also in the lungs (24%) and the bones (16%) [132,133]. Early surgical removal of metastases improved the survival of some patients [137]. However, in general, the prognosis for UM patients with metastatic disease is currently poor due to the lack of efficient therapeutic agents [133]. That being said, massive efforts are presently underway to improve patient outcomes with metastatic disease. Consequently, by identifying patients at high risk of metastases and their referral to the various clinical trials involving a range of novel therapies, may enable the breakthrough discovery, as seen in other cancers.

1.6 Metastatic Disease in UM

1.6.1 Metastatic dissemination and incidence

Metastases are the leading cause of death in patients with UM, whether in the short or long term [132]. It would appear that the ocular treatment type does not influence survival [138]; however, it has been recently been proposed that treatment of high-risk UM at a very early stage may limit tumour cell dissemination [139].

The production of metastases is a highly complex process: due to the lack of lymphatic vessels within the eye, UM metastatic dissemination occurs via the bloodstream[140]. Circulating tumour cells have indeed been detected in the peripheral blood of UM patients at all stages of the disease [141]. The cells that survive in the circulation may eventually become entrapped at the microvasculature, and extravasate out of the blood. Metastases are most commonly detected initially in the liver on screening, although at an advanced stage they involve other organs, such as skin, bones and lungs. This marked hepatotropism suggests that there must be something specific about the liver with regard to the development of the metastatic niche for UM cells ("seeds"). This concept was first described by the Austrian ophthalmologist Ernst Fuchs in 1882, who wrote about "the metastatic embolus and its relationship with the recipient tissue", later inspiring Stephen Paget, who described the concept of "seed and soil", in which "seeds" refer to certain tumour cells with metastatic capacity, and "soil" is any organ or tissue that provides an adequate environment for seed growth [142]. Finally, metastatic cells must be able to respond to the local microenvironment to proliferate in distant organs.

In only <1% of all UM patients, is it clinically evident metastatic disease at the time of its initial presentation [143]. However, studies of patients undergoing long-term follow-up revealed metastases in 31% of cases in 5 years, 45% in 15 years and almost 50% in 25 years [132]. It was proposed by these findings that subclinical metastases are present in these cases at the time of primary treatment. The association of primary and metastatic growing data for UM

suggests that metastases arise when the primary tumour is still with a small size [144]. Metastases are too small to be clinically detected by the current imaging procedures, at the time of the diagnosis of the primary UM [144] [145]. After 10 years of observation, more than 40% of patients with large UM would develop metastatic disease, while less than 20% of patients with medium or small primary tumour will develop this disease [146].

1.6.2 Sites of metastases

As mentioned above, the liver is the main target organ for metastatic dissemination of UM (**Figure 1.10**); being involved in up to 90% of UM patients with metastatic disease [147-149], while other potential sites such as lung, bone and skin, may be affected beyond the liver in almost half of the cases, with lymph nodes and the brain being less commonly involved [143], but almost exclusively after liver invasion [150]. Extremely rare are the metastases to the contralateral eye or orbit [151]. The extent of metastatic disease is greater than clinically suspected in cases submitted to autopsy. The possibility of coexistence of a second primary tumour should be considered in an atypical clinical setting.

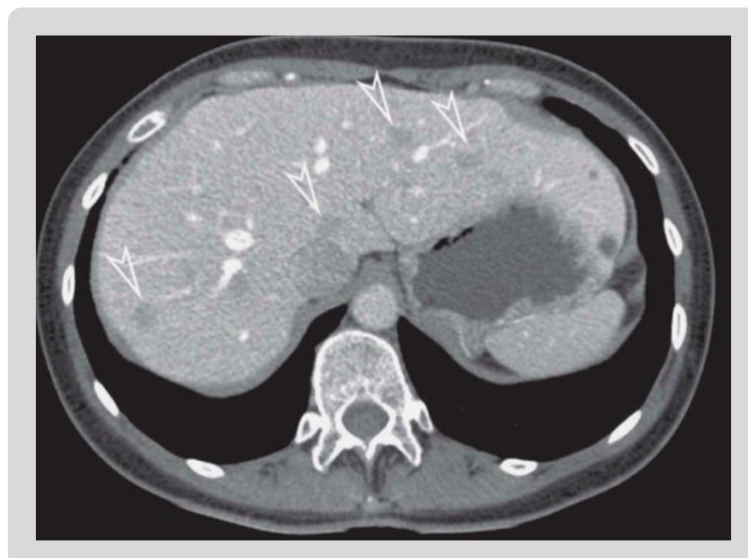


Figure 1.10 Multiple liver metastases (arrow heads) of UM. (Image sourced from Kivelä, 2013) [152].

1.6.3 Early diagnosis and conventional screening tools for metastatic UM

The hope that ocular treatment may prolong the life of patients with UM, even after the onset of metastatic dissemination, leading to the interruption of the dissemination of tumour cells to the bloodstream, thus limiting metastatic burden, is the reasoning behind the early detection and treatment of UM [153]. Detection and early treatment of UM should improve opportunities for eye and vision preservation and prolong life [64]. For example, smaller tumours require less extensive radiation in the eye and are less likely to approach the optic disc and fovea [153]. According to Damato et al. [64] in an audit in the LOOC between 1996 and 2011, these authors reported that patients who did not show symptoms had more likelihood of retaining the eye. On the other hand, symptomatic patients, in whom the tumour was initially not diagnosed, were more likely to experience further delays in treatment. They are more likely to have a reduction in vision, greater diameter of the basal tumour, the involvement of the optic disc and extraocular tumour spread [153]. For this reason, in case they are not detected more promptly, they are more likely to require primary enucleation. This audit reported that there is a likelihood of improving the detection of UM, particularly if detected early by optometrists in the community. It has also been reported that patients are not undergoing a complete eye examination. In this case, the enclosure of the use of photography of the fundus of the eye, during the primary eye care procedures, should improve this situation.

As previously mentioned, the presence of UM metastases in the liver is directly related to the patient's survival; when metastases are present, the prognosis is poor and survival is reduced to less than 6 months in the absence of treatment [154]. Improvement in survival has been demonstrated in recent series using novel therapies in some patients [155,156]; this will be discussed further below. Patients generally have 'liver failure' as their cause of death due to extensive parenchymal invasion by melanoma cells [129]. A variety of systemic therapies, immunotherapies and loco-regional treatments have shown promising results in pre-clinical settings and are currently being reviewed in clinical trials worldwide [155,157]. So far,

however, the best survival results have been observed in patients with the localized liver disease who were diagnosed early enough to be eligible for surgical removal by liver resection [158]. Similarly, early detection of metastatic disease may potentially increase the effectiveness of existing therapies. It is necessary to examine the considerations for routine surveillance for the development of metastatic disease after definitive management of UM and describe the various surveillance methodologies that are available. Given the immense predominance of hepatic implication, the liver has become the main focus in metastatic surveillance strategies.

1.6.3.1 Follow-up strategies in UM

Several screening protocols are used for the systematic screening of UM, although it is controversial because of the lack of efficient treatment for metastatic disease. For instance, in a report from the COMS, patients with medium and large size choroidal melanomas were selected annually for metastases screening through physical examination, imaging and liver function tests (LFTs) [159].

1.6.3.1.1 Liver Function Tests

LFTs include a series of liver tests, such as aspartate aminotransferase (AST), alanine aminotransferase (ALT), alkaline phosphatase (AP), and bilirubin. All high LFTs lead to a diagnostic evaluation (imaging with or without biopsy), to confirm the presence of melanoma metastases. In the COMS study, the sensitivity and specificity of the LFTs were 14.7 and 92.3%, respectively. Sensitivity improved to only 19% in large tumours [159]. The positive predictive value was 45.7% and the predicted negative value was 71.0%. Of all LFTs, alkaline phosphatase showed the highest sensitivity. These findings indicate that abnormal LFTs values accurately predict metastases in only 50% of cases. On the other hand, normal LFTs are not reliable, with a 30% false negative rate. Chest X-rays were not effective as they were positive in only 3% of the patients selected [159].

The combination of LFTs provides an indirect measurement of the liver function, presenting the benefit of being substantially less costly and largely accessible. Nevertheless, LFTs are narrowed by low sensitivity [160]. For example, increases in LFT results may not be specifically caused by UM but are the result of other conditions such as inflammations, infections, or other liver malignancies, which may be caused by alcohol or drugs. There is some disagreement about the most sensitive components of the panel comprising the LFTs; some authors may have a preference for lactate dehydrogenase and others prefer the gamma-glutamyl transpeptidase and alkaline phosphatase. Due to the low sensitivity of LFTs, studies have questioned their effectiveness as a surveillance method [160]. Consequently, it is considered important to inform patients of the chances of still having metastases, where LFTS are normal. Some suggest that the combination of LFTs with other tests (e.g. US) can increase their value [158]; however, general consensus is that LFTs add little to liver surveillance strategies.

Currently, there is no consensus on the favoured surveillance modality [161]. New blood biomarkers are being assessed to predict and measure response to therapy because of the inclination of UM for haematogenous dissemination. Growth factors, circulating tumour cells, microRNA, beta-2 microglobulin molecules and immunological markers are all among the most recently used biomarkers [162].

1.6.3.1.2 Imaging

The main purpose of systemic surveillance is based on liver imaging. Even though survival seems to be no different, even in adequately selected individuals, and despite the fact if patients are diagnosed based on the symptoms or screening methods currently used (imaging, physical examination, hepatic panel) [163,164].

1.6.3.1.2.1 Hepatic ultrasonography

Abdominal hepatic ultrasound (US) (**Figure 1.11**) is a non-invasive, inexpensive methodology that is widely available and, if performed by an experienced operator, may have high sensitivity, even in the presence of small lesions [161]. In Finland, for example, it is estimated that about 95% of cases are detected in asymptomatic patients when LFTs are combined with semi-annual ultrasound [158]. There is the ability to detect liver disease with US even in patients with normal LFTs. However, the technique depends on the operator and the assessment may be limited by the body mass index. There is evidence suggesting that screening for isolated hepatic metastases using US, which can be performed every 6-12 months, may be adequate to detect subclinical metastatic melanoma [165]. In a retrospective review of 265 patients, six-month hepatic ultrasonography was isolated and had a positive predictive value of 53% [166].

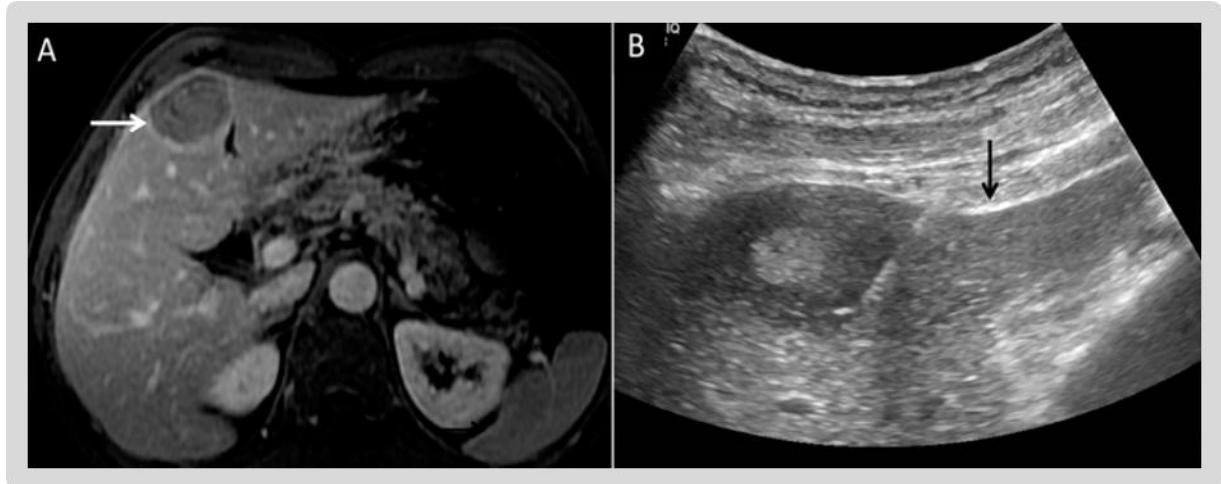


Figure 1.11 Hepatic Ultrasound image. A) Image showing metastatic lesion (arrow) in the medial segment of the left lobe of the liver. B) Ultrasound-guided core biopsy of the same lesion was performed, confirming metastases. The arrow points to the needle (Image sourced from Balasubramanya et al. 2016).

1.6.3.1.2.2 Computer tomography

Computer tomography (CT) (**Figure 1.12**) has also been used for routine radiologic surveillance in UM and is used to confirm studies after abnormal serum markers or abdominal US. It is less expensive, faster and has greater availability compared to Magnetic Resonance Image (MRI). Compared to US, it is independent of the operator, since patient images are generated using a computer algorithm. There are no published studies comparing CT and MRI for surveillance in UM, making it difficult to make an appropriate choice between these two approaches. However, there are reported cases in which only isolated lesions of metastatic disease are visualized in the liver with the CT, whereas contrast-enhanced MRI is the most specific modality for detecting small hepatic metastases [167]. CT has the disadvantage of being related to radiation exposure associated with CT.

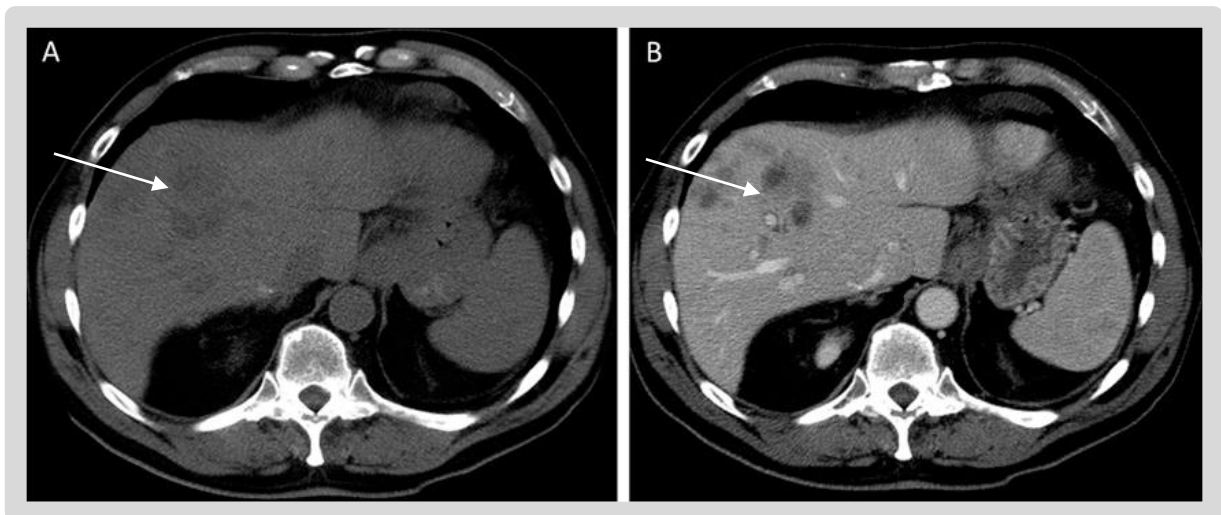


Figure 1.12 CT image of the abdomen. A) Non-contrast CT showing ill-defined lesions in the right lobe of the liver. B) Contrast-enhanced CT performed on the same patient. It appears that lesions are better assessed in the images post-contrast. (Image sourced from Balasubramanya et al. 2016).

1.6.3.1.2.3 Magnetic Resonance Image

Magnetic Resonance Image (MRI) (**Figure 1.13**) is a popular method for surveillance of UM, particularly for patients with a high risk of metastases. It is an expensive methodology and it has some limitations for its performance such as those with larger body habitus, the presence of metallic implants, and the claustrophobia. As observed in other techniques, MRI also has the disadvantage of presenting false-positive results, although it may be more sensitive in the identification of relevant lesions. It may not be adequate for the distinction between lesions of benign or malignant origin (e.g. liver haemangiomas versus metastases), and as like other imaging methodologies, this may complicate the screening process, leading to additional diagnostic evaluations, more resources, and having to subject the patients to invasive procedures [168]. Even so, MRI has advantages over other imaging devices, provides high-resolution images with relative accessibility compared to Positron Emission Tomography (PET), CT, and newer devices have some non-radiation functions, making this method a safe option for repeated testing, particularly for young women. Evidence in the literature reported by a UK group suggest that MRI can detect asymptomatic liver metastases in patients with high-risk UM [169]. MRI scans performed every six months successfully detected metastatic disease in 92% of UM patients before they had symptoms, and almost 50% of patients had fewer than five lesions measuring less than 2 cm in diameter.

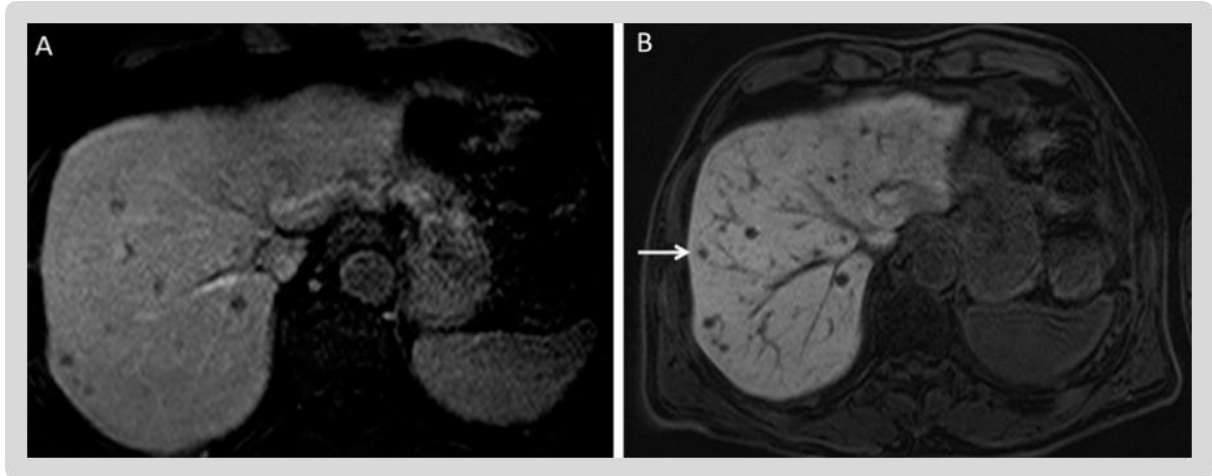


Figure 1.13 MRI image. A) Demonstration of multiple hypodense lesions concerning metastases. B) Post-contrast image demonstrating several other lesions in addition to the previously seen lesions (arrow). (Image sourced from Balasubramanya et al. 2016).

1.3.1.2.4 Positron Emission Tomography

Positron Emission Tomography (PET) (**Figure 1.14**) is also commonly used to assess melanoma metastases. The literature reports that UM metastases are avid fludeoxyglucose (FDG), similar to metastases from cutaneous melanoma [170]. However, PET is much less sensitive than MRI with regard to the assessment of liver metastases, due to the irregular FDG uptake in the liver which can obscure small, avid lesions as there is a small target to background proportion. Another limitation for locating small metastases using PET are the artefacts caused by breathing movements. Although PET is a good method of detecting metastases, there are still other disadvantages to consider including the fact that it is not universally accessible, is relatively expensive, and is insensitive to small lesions, especially those less than 1 cm. It is also important to ponder the disadvantageous fact that PET uses a substantial amount of radiation.

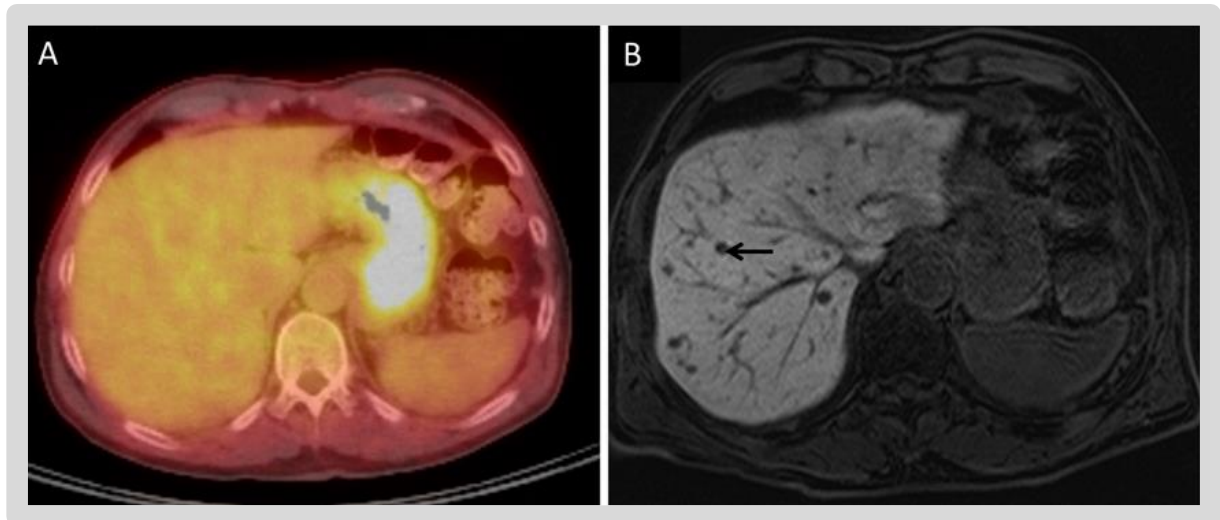


Figure 1.14 Positron emission tomography images. A) Fused images through the liver where no focal uptake of fludeoxyglucose that suggests metastases is seen. B) The post-contrast image taken on the same day shows multiple, tiny, consistent and rounded hypointense lesions compatible with metastases (arrow) (Image sourced from Balasubramanya et al. 2016).

Due to the absence of available convincing data, the decision regarding the continuation of hepatic surveillance should be made after a detailed discussion between the patient and the physician implementing the surveillance, regarding the risks, benefits and limitations of the tests that will be performed. In the case of opting for surveillance, the interval time could be adjusted in relation to the estimated recurrence risk, considering a more intensive surveillance program for those with a higher risk of recurrence. For these patients, routine imaging may be reasonable at each 6-month interval, while for those at lower risk; the image at one interval of 6 or 12 months may be appropriate. The ideal length of follow-up remains controversial so far. Despite the well-documented late recurrences of UM that occur more than 10 years after the initial diagnosis of the disease, the benefit of routine radiologic follow-up after 10 years should be evaluated in relation to the risks and costs associated with continuous imaging.

1.6.4 Signs and symptoms in metastatic UM

Patients with UM metastases may have a variety of organ involvement-based symptoms. At the time of detection of their metastases, about 60% of the patients are asymptomatic [165]. Some of the common complaints are nonspecific symptoms such as general malaise, loss of appetite and jaundice. Abnormal LFTs, hepatomegaly, and abnormal liver appearance on imaging tests are highly suspected of metastases. However, LFTs may be normal in about one third of patients with hepatic metastases [165]. To confirm the diagnosis, a needle biopsy is usually conducted.

1.6.5 Determination of risk of metastases

The risk of metastases and the period between the diagnosis of the primary tumour and its metastases is determined by various clinical, histopathological, cytogenetic and molecular genetic factors [171]. This will be discussed in greater detail below in section **1.7.4**. when describing prognostication in UM. In the management of cancer, one of the most difficult challenges is metastases - contributed by recurrent invasion of tumour cells, which eventually result in tumours at sites far from the body [172]. Regardless of the aetiology of this disease, little is known about the fundamental biology of its aggressiveness in some patients and relative quiescence in others. At the moment of the diagnosis, many patients may have subclinical metastases [173], which emphasises the crucial need to recognise prognostic markers suggestive of UM and with invasive and metastatic potential. Histologically, the UM typical cells are associated with poor prognosis [174] and metastatic behaviour.

1.6.6 Treatment for metastatic disease

Systemic metastases of UM are difficult to treat, despite advances in the diagnosis and management of primary UM [175]. Management of metastatic UM will depend on whether the metastatic disease is confined to the liver or not. Regional therapies - such as surgical resection [176,177] isolated hepatic perfusion [178], intra-arterial liver chemotherapy

[178,179] or chemoembolization of hepatic metastases [180,181] - are used for the treatment of metastatic disease confined to the liver. Systemic approaches using chemotherapy, immunotherapy, or a combination of both are used when extra hepatic metastases are present [182].

1.6.6.1 Systemic therapy

Traditionally, chemotherapy is a treatment option, although responses are infrequent (<10%) and no survival benefit has been shown in clinical trials [183]. For the treatment of metastatic UM, several chemotherapeutic agents have been investigated. The combination of bleomycin, fotemustine, dacarbazine and vincristine with interferon (BOLD) have been reported [184]. These treatments were subsequently proven and reported as overly optimistic in a substantial number of patients [185] [186]. In addition, the Eastern Cooperative Oncology Group suggested that liver metastases from UM have a 10% of response rate to combined treatment (combination of Darmouth - dacarbazine, carmustine, cisplatin and tamoxifen), compared with metastatic cutaneous melanoma, which positive response rates are 33% [187]. However, encouraging results have been obtained using combined targeted therapy in 14 patients who received treosulfan and gemcitabine, improving the survival rate survival rate to 14 months [188].

Immunotherapy is a type of cancer treatment that boosts the body's natural defences to fight cancer. Include here that Immunotherapy has been considered the state of the art of cancer treatment of most advanced metastatic solid cancers [189]. It uses cytokines or antibodies to restore the host anti-tumour immune system functions. Immunotherapy with bacillus Calmette-Guerin (BCG) extracted with methanol, interleukin 2 or with lymphokine-activated killer cells has shown low efficacy [190,191] [192]. However, immunotherapy using immune checkpoint inhibitors (ICI), have significantly improved the survival of metastatic cutaneous melanoma and many other cancer patients, whether isolated or in combination with other ICI [193]. There are limited data about the antitumor effects of the ICI ipilimumab and nivolumab in the

treatment of metastatic UM. However, the combination of both ipilimumab and nivolumab for the management of metastatic UM had shown promising results, in terms of toxicity, tolerability and survival [155,157,194].

An experimental immunotherapy drug helped to prolong lives of UM patients more than other patients who received current treatments for the disease according to the results of large clinical trials [146]. The drug, called tebentafusp, which is an ImmTAC [immune-mobilising monoclonal TCRs (T-cell receptors) against cancer], designed to recognize intracellular cancer antigens with ultra-high affinity and selectively eliminate these cancer cells through an effector function of anti-CD3 immune activation. It is a type of treatment called a bispecific fusion protein. In its mechanism of action, the ImmTAC targets a fragment of the specific lineage of melanocytes, the antigen gp100280-288 antigen presented by HLA-A * 2:1. To date, clinical trials with tebentafusp in metastatic UM have been reported [195,196] and other clinical studies are still ongoing. Sacco et al [197] published results in abstract form of a phase II multi-centre study tebentafusp (IMCgp100) in UM patients. Although the first endpoint of the overall response rate was 5%, 44% patients had a reduction in the target lesions. The overall survival rate was 12 months, being 62% in all patients and 86% of reduction in patients with target lesion. This study has very recently been published as a full paper in the New England Journal of Medicine, and represents the first breakthrough in metastatic UM treatment [156].

Adoptive transfer of autologous Tumour Infiltrating Lymphocytes (TILs) has shown promising results to mediate objective tumour regression in patients with metastatic UM [198]. Specific vaccines for UM, with specificity for Xenogeneic and human cells, are being exploited from a therapeutic and preventive point of view for the treatment of metastases [199,200].

The definition of targeted therapy indicates the interference of aimed drugs with a specific molecular pathway considered to represent a critical role in the development and progression of the tumour [201]. In contrast to cutaneous melanoma, in UM, *BRAF* (human gene that

encodes a protein called B-Raf) mutations are extremely rare (<1%), and the vast majority, more than 75%, demonstrate mutations in the *GNAQ* and *GNA11* genes [107,108]. Studies reported that these target therapies include drugs that can modify the pathways that regulate the cell cycle, which inhibits the molecules involved in invasion and metastases, and also interrupt tumour angiogenesis [201].

1.6.6.2. Loco regional Therapy

In patients with metastatic UM that are confined to the liver, treatments with a loco-regional approach may be implemented, ranging from surgical excision of lesions, radiofrequency ablation (RFA), intra-arterial chemotherapy, radioembolization and chemoembolization. All these therapeutic modalities may offer the advantage of limiting systemic side effects, but on the other hand, do not prevent the progression of extra hepatic micro-metastases. Although some results showing response to these therapies are observed, they do not generally influence the general survival rate [202].

Complete resection of solitary metastases at the liver or other sites offers a distinct survival advantage [176,177,203,204]. However, when it is feasible to perform total excision of metastases, followed by intra-arterial hepatic chemotherapy, a greater median survival is observed [205]. In patients with metastatic UM eligible for total resection of metastases that are isolated, whether in the liver or in other locations, were observed the longest average survival times [176,177,203]. Lamentably, only 10% of the patients with metastatic UM have this profile, and it is also verified that furthermore, the majority of patients end up developing hepatic or extra hepatic metastases [177]. Some studies have suggested that the RFA, a therapeutic approach in which the use of a heating probe based on changeable radiofrequency electric current, may be useful for the treatment of hepatic metastases of UM. However, only limited cases were reported [206]. A promising therapeutic approach published, based on the combination of surgery with chemotherapy (fotemustine and / or dacarbazine +

cisplatin) was tested with the aim of presenting better results, and may prolong the median survival of life for about 22 months [205].

Chemoembolization is a palliative treatment for tumours found in the liver, is used to achieve a prolonged and high concentration of local chemotherapeutic agents. Such chemotherapeutic agents are loaded into eluting drug spheres, which also obstruct the blood vessels, thereby decreasing blood flow to the tumour. The most commonly used embolic agents are polyvinyl alcohol or the gelatine sponge. It should be noted that this approach is generally confined to patients who have preserved liver function and in whom the disease is essentially concentrated in the liver. Chemoembolization until now, it has been studied only in patients who did not respond prior to chemotherapy regimens. Treatments with cisplatin, fotemustine and irinotecan have been studied in patients with hepatic metastases related to UM. Not all Centres have been able to reproduce the results of chemoembolization, but the MD Anderson Cancer Centre [148] reported objective responses in more than a third of their cases [148,207].

In the last decade, a new therapy has been developed to improve the survival of patients with metastatic UM, immune-embolization (IE), which is used to delay or suppress the growth of extra hepatic metastases, investigators have used granulocyte macrophage colony-stimulating factor (GM-CSF) for IE. IE with GM-CSF is designed to destroy hepatic metastases through the ischemic effects of embolization; these cytokines are injected directly into the arteries supplying the liver, combined with embolization of the hepatic artery. The antigen present in the cells will be stimulated with the GM-CSF and the systemic immunity against the tumour cells could be enhanced. The procedure improves the survival of patients with hepatic metastases of up to five months under conventional treatment for an average of 14.5 months [207,208].

Hepatic UM metastases may benefit from treatment from selective chemotherapy by infusion through a catheter through the hepatic artery (Intra-arterial hepatic chemotherapy), since the

blood supply to liver tumours (primary and secondary) comes from the hepatic artery, whereas portal circulation mainly supplies normal liver tissue [209,210]. This intra-arterial approach will allow a high local concentration of drugs with reduced systemic toxicity. Several drugs have been tested using various procedures, ranging from isolated hepatic perfusion, hepatic arterial infusion, and peripheral hepatic perfusion. Basically, Isolated hepatic perfusion involves the installation of an extracorporeal circuit, through which the chemotherapeutic agent will be circulating through the hepatic artery and flow only through the hepatic parenchyma, circumventing the systemic circulation. Melphalan and tumour necrosis factors (TNF) or cisplatin, have been used for this technique, but no change in survival rates has been observed [209-211]. Encouraging results have been reported by Karydis et al. [179] by utilizing percutaneous isolated hepatic perfusion with Melphalan, using a double-balloon catheter (Delcath Systems Inc., New York, US). They reported that the use of Melphalan percutaneous hepatic perfusion led to lasting control of the intrahepatic disease.

An accepted treatment modality that extended its applicability in recent years for chemosensitive and unresectable hepatic neoplasms, is the radio-embolization also known as selective internal radiotherapy (SIRT). Radio-embolization is based principally on the administration of ⁹⁰Y-loaded microspheres in the arterial vasculature of the liver, Ytrin90 [212]. Currently, two types of microspheres have been accepted and are commercially accessible from the Food and Drug Administration: resin microspheres (SIR-spheres; SirTex Medical) and glass microspheres (TheraSpheres; BTG International Ltd.). Ytrin90 has been traditionally utilised for liver malignancies. The minute size of the Y-loaded microspheres permits them to preferentially installing the tumour microcirculation, delivering radiation in a small circuit. Owing to the fact of the preferred arterial flow, the microspheres occlude small tumour arterioles, selectively irradiating the tumours. Hepatic radio-embolization is also performed for palliative purposes and is based on the same principle of chemoembolization (i.e., double blood supply, the tumour being primarily perfused by the hepatic artery). The aim

is to provide a high dose of radiation to the malignant tissue, sparing the normal parenchyma, thus limiting the lesions associated with radiation [213].

1.6.6.3 Adjuvant Therapy

The lack of survival benefit for current treatment modalities for UM and the presence of asymptomatic metastases at the time of diagnosis led to the exploration of adjuvant therapies for UM patients, whether systemic or loco regional. Such studies are currently in experimental stages and have not yet become a standard of care for high risk UM patients [186,214,215]. Adjuvant therapy in these patients is intended to prevent or delay micro-metastases from development to macro-metastases. It is often used after primary treatments, such as surgery, to decrease the chance of tumour recurrence. Even if surgery has been successful and removal of any tumour is visible, microscopic fragments of the tumour may sometimes remain and be undetectable with current methods. Adjuvant therapy administered prior to the main treatment is termed neo-adjuvant therapy. This type of adjuvant therapy can also decrease the chance of recurrence, and is often used to make primary treatment - such as surgery or radiation treatment - easier or more effective. It may cause significant side effects and these treatments do not benefit all patients. The main treatments used as adjuvant therapies are chemotherapy, hormone therapy, radiation therapy, Immunotherapy and targeted therapy. Because none of these treatments is completely harmless, it is important to determine the risks of adjuvant therapy versus the benefits. Molecular and cytogenetic studies can help to determine whether adjuvant therapy is appropriate or not, and if so, which type [216].

1.6.7 Prognostic for metastatic disease in UM

In patients with extrahepatic UM metastases, essentially at the level of the lung, skin or soft tissues in the early stages, with an age of less than 60 years, females, and a longer interval from the moment they were diagnosed to the time when the metastatic disease arose, are associated with a good prognosis [163]. As mentioned above, life expectancy in patients with metastatic UM, is generally poor [217], although recent studies have reported improved

survival using innovative treatments and so there is hope on the horizon in some subgroups of UM patients [155].

1.7. Prognostication in UM

1.7.1. Identifying risk factors

Presently, to identify patients who are likely to benefit from regular screening, there is until now no clinical risk assessment tools available to clinicians. There is a vast literature about the potential risk factors for metastatic disease in UM, which includes physical characteristics or personal and family history of specific cancers or clinical syndromes that predispose to UM. However, the evidence supporting the association of prognostic factors with UM has a considerable variation; some of which have been investigated only in single observational studies, while others have been systematically reviewed and meta-analysed. To begin a process for developing a clinical risk assessment tool, it is necessary first to identify the risk factors for UM those have already been established through a systematic review of meta-analyses. Thus, the awareness of these variables will guide future searches using additional resources that would merit consideration in a scoring system based on risk factors, and from which clinicians could already be guided in relation to the distinction of patients presenting a higher risk profile while developing and validating formal and standardized tools.

1.7.2 Accurate prognostication

It is described that almost all UM patients want to know their prognosis for survival, whether this is 'good' or 'bad' tumour, and even when they are told that prognostication is most unlikely to improve their chances of prolonging life [133]. Patients, who cannot receive a precise prognosis because genetic testing failed, are the most distressed. As with other cancers, prognostication is an important aspect of patient care, identifying high-risk patients requiring special care while allowing low-risk patients to be reassured of their good survival prospects.

The pathologist is well placed to play a valuable role in this process. This is because histological grade, and genetic type of melanoma profoundly influence prognosis.

1.7.3 Benefits of prognostication

Damato et al. [218] [219,220] first put forward the practice of providing a personalized survival curve for each UM patient, to be sent then to the oncologists allowing individualized or personalised management with respect to surveillance for metastatic disease, the modality to be used and how often this was undertaken. This enables screening to be targeted only at high-risk UM patients, avoiding expensive and stressful investigations in those who are unlikely to develop metastases. Whether such screening is cost-effective is a controversial subject, about which we will investigate within this thesis. The survival curves calculated after obtaining the predictor factors, and identified the high-risk patients, should enhance the statistical power of survival studies, thereby reducing the number of patients required, increasing the study's feasibility, and shortening recruitment time. When estimating the chances of metastatic disease and the chances of metastatic death in an individual patient, it is first necessary to determine whether or not the tumour has some metastatic potential. Prognosis can help save those with a good prognosis of unnecessary investigations, saving to themselves and to the Health Systems, unnecessary expenses. It also allows for screening tests for high-risk individuals, which can therefore be investigated more fully than would otherwise be possible. Another advantage is that it may increase the possibilities of research in innovative systemic therapies, such as adjuvant therapy, which aims to help prevent or delay the onset of metastatic disease in high-risk patients.

1.7.4 Survival predictors

The survival time is best estimated by the combination of anatomical, histological and genetic predictors [219]. Nevertheless, one difficulty with the multivariate analysis is the bias produced by the lack of data. Bias also occurs due to conflicting causes of death, regardless of UM.

Many authors have listed several risk factors such as clinical, histopathological and cytogenetic for adequate identification and subsequent management of UM, which may identify those patients who are at high risk of developing metastases and are likely to benefit from adjunctive prophylactic or therapeutic treatments. With the advent of molecular biology and cytogenetics, several biological and cytological markers have been identified, which can further predict the prognosis and assist the clinician in making decisions.

1.7.4.1 Clinical Prognostic Factors

It has been known for many years that clinic-pathological factors, such as sex, increased patient age, increased thickness and diameter of the primary tumour, involvement of the ciliary body, extraocular tumour extension and epithelioid cell type, are associated with an increased risk of metastatic UM disease [221] (**Table 1.3**). These factors are essentially useful for the development of classification systems in which patients are grouped into categories based on a similar prognosis.

Table 1.3: Clinical Prognostic factors in UM

Category	Factor	Features
Clinical	Age	Increased age
	Sex	Slight predominance in males
	Tumour dimensions	Largest basal diameter/ Greater tumour thickness
	Ciliary body involvement	Often associated extraocular invasion
	Extraocular extension	Often associated with larger tumours (but not always).
Histological	Epithelioid cells	Associated worse prognosis
	Spindle cells	Associated with better prognosis
	Extravascular matrix patterns	Closed vascular loops associated metastases and increased mortality.
	Mitotic count per specified number of high power fields	Higher numbers associated with a greater chance of metastatic death.
	Non-neoplastic cellular infiltrates	Macrophages and lymphocytes – increased mortality.
Genetic	Chromosome 3 loss	Most important prognostic factor - chromosome 3 aberrations. Correlated - metastatic death.
	Chromosome 8 gain	Increased mortality, alone or when it coexists with monosomy 3.
	Chromosome 1p loss	Chromosomes 1p and 3 combined stronger risk.
	Chromosome 6 gain	Relatively good prognosis.
Genetic Mutations	<i>GNAQ and GNA11</i>	Believed to be an initial event in UM.
	<i>SF3B1</i>	May represent alternative pathways for the progression of UM.
	<i>EIF1Ax</i>	Play a protecting role in the prevention of metastases.
	<i>BAP1</i>	Associated with metastatic diseases and their progression.

1.7.4.1.1 Age and gender

Although the influence of age on the prognosis of UM is uncertain, recent studies indicate that worse prognosis is more likely to be associated with increasing age [3]. Until now, few studies have concluded that the age of presentation does not influence the prognosis of UM [222]. In contrast, other studies indicate that the prognosis of life is more favourable in children with UM compared to adults. More recent studies have also shown no differences in death-related metastases based on gender. However, some reports suggest a better prognosis in women compared to men [3,92], with a twice as high mortality rate in men compared to women in the first 10 years of diagnosis of posterior UM [223]. Certain hormonal factors, especially oestrogen, may lead to direct or indirect inhibition of the development of metastases in women.

1.7.4.1.2 Tumour size

One of the most important clinical prognostic factors of UM is tumour size (greater basal diameter and thickness) [130,224]. Some studies on meta-analyses reported that the combined pondered estimates of 5-year mortality rates associated with UM were 16% for small tumours (<2-3 mm tumour thickness and <10-11 mm baseline diameter), 32% for mean tumours (3-8 mm tumour thickness and <15-16 mm baseline diameter) and 53% for large tumours (> 8 mm tumour thickness and > 15 mm baseline diameter) [224]. Kujala et al. reported a significant association between the largest basal diameter (LBD) of the tumour and the mortality related to UM [132].

1.7.4.1.3 Extraocular extension

The presence of tumour extraocular extension (EOE) (**Figures 1.15 and 1.16**) is a poor prognostic factor for UM, and can be found in about 8 to 15% of cases [225-227] [3]. Usually EOE results in a poor prognosis and is associated with tumours with larger diameters, anterior tumour extension, and large basal tumour diameter; diffuse UM, epithelioid cellularity, and closed vascular loops, high rate mitotic and monosomy 3. Overall survival may be more related to the characteristics of the intraocular portion of the tumour than to EOE unless the EOE is

largely extensive (> 5 mm). (58) Mortality rates are markedly higher for patients with large EOE and can be 5 years in 78% of patients [228].

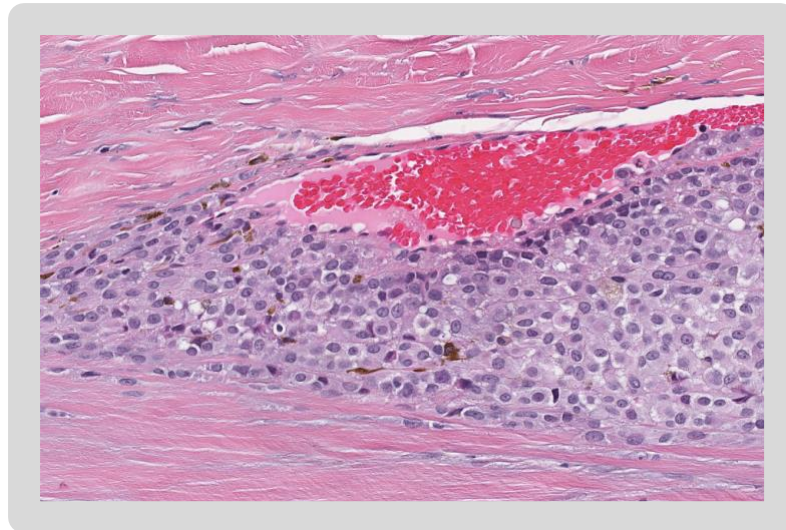


Figure 1.15: Vortex vein involvement in UM with EOE, shows melanoma in the lumen of the vessel (courtesy of Prof. S. E. Coupland).

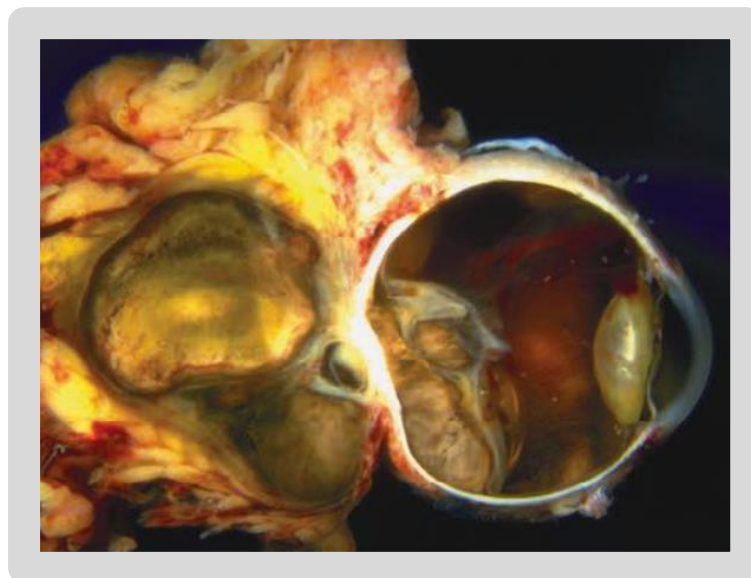


Figure 1.16: Posterior choroidal melanoma extended extra-sclerally, forming a large pigmented orbital mass, also present invasion of the optic nerve (Image sourced Eagle RC. Eye pathology: an atlas and text: Lippincott Williams & Wilkins; 2012)[2].

1.7.4.1.4 Ciliary body involvement

As above, melanomas of the ciliary body are less common than choroidal tumours. Most tumours involving the ciliary body are likely to arise in the peripheral choroid and invade the ciliary body. Tumours that initially appear in the ciliary body tend to be smaller and more spherical in shape than the choroidal tumours that invade the ciliary body. Anterior invasion involving the root of the iris, angular structures and the anterior chamber is common. Clinically, the patient can notice the anterior extension, and what is thought to be a small tumour of the iris may represent only a small part of the remaining tumour. Melanoma of the underlying ciliary body may show other clinical signs such as dilation and tortuosity of conjunctival blood vessels, called 'sentinel' vessels.

Ciliary body melanomas usually invade the posterior chamber, retreating the lens, thus creating a lenticular notch. The diffuse type of melanoma also occurs in the ciliary body, where the tumour tends to grow circumferentially in a ring configuration [70,171]. Like diffuse choroidal tumours, these tumours often have extraocular invasion.

1.7.4.1.5 Histopathological Prognostic Factors

Please read description above in the sub-section 1.3.

1.7.4.1.6 Cytogenetic Prognostic Factors

The most recent studies have highlighted the importance of cytogenetic features in the prognosis of UM. Tumour samples for genetic testing are obtained from enucleation specimens or intraoperatively by fine needle aspiration biopsy. Survival in patients with UM is determined by aberrations on chromosomes 1, 3, 6 and 8 [93,229]. Please read description above in more detail above in the sub-section 1.4.

1.7.5 Risks of prognostication

Prognostication is considered by some to be expensive, taking into account the cost of biopsy procedures and, in addition, the cost of laboratory procedures and investigations. It can sometimes be inaccurate since in some cases patients with a good prognosis may develop metastatic disease and some of those who receive a poor prognosis may survive longer than expected [230].

One limitation of prognostic tools is the reliance on 'black-box' methods, such as artificial neural networks. Such methods contribute little to the understanding the underlying mechanisms. However, in the context of a clinically useful tool, good correlation with the Kaplan-Meier analysis in different risk groups is reassuring. Other risks include complications, which may occur during procedures, or biopsy techniques. Such complications include intraocular bleeding, infections, intraocular seeding and dissemination of the tumour to extraocular tissues.

1.7.6 Alternative prognostication

The alternative approach is to screen all patients for metastatic disease before treatment of the ocular tumour then every six months for at least ten years. Such screening would involve some form of liver imaging and biochemical liver function tests. Most patients undergoing such screening will probably never develop metastatic disease. In such cases, screening would incur unnecessary expenses both to the patients and to the National Health Service (NHS).

There have been significant discussions regarding the role of routine surveillance for metastatic disease after the definitive treatment of UM, which may be a reflection of different patient populations and different practice patterns between ophthalmologists and oncologists. Risks of excessive diagnosis and false-positive or false-negative results, as well as a very low cost-benefit ratio, should be weighed against the potential benefit that early diagnosis of the recurrent disease could prevent premature death.

As previously described, early detection of asymptomatic metastases may increase the ability to identify the disease since certain potentially curative treatments for liver metastases could be attempted, reducing the risk of developing significant tumour-related morbidity and identifying patients who may be eligible for participation in clinical trials accessing new agents for the treatment of UM metastases. It should be noted that recent advances in understanding the underlying biology of UM and the development of new-targeted agents now offer new optimism in what was once a bleak landscape. And ultimately, even if the effect of surveillance on survival is minimal, it can provide to the patient and family another valuable advantage, including better emotional well-being and the chance of making plans for the future.

Although prospective, randomized, and routine surveillance studies of UM have not been reported, they were conducted in patients with resected colorectal cancer who did not demonstrate a survival benefit of surveillance in these patients [231]. In contrast, there are only a few sporadic reports of surveillance in patients with UM, some of them suggesting a survival benefit due to the identification of patients eligible for resection or other loco-regional treatment techniques for metastatic liver disease. However, the effects of waiting time bias in these reports are not clear, and no studies have been reported demonstrating convincing evidence of a survival advantage with routine surveillance practice. These data cast doubt on the utility of surveillance for metastatic UM. Although several proposals have been suggested, there is currently no universally accepted screening approach. Remaining pertinent questions such as: whether routine surveillance should be conducted; who should be monitored for surveillance; how often tests should be done; duration of follow-up; and what are the optimal surveillance methodologies. Because there is a lack of consensus regarding routine surveillance not only in UM but in many types of cancer, it is important that patients have clear instructions about the 'pros and cons' of surveillance as well as the existing surveillance options.

1.7.7 Elaboration of a clinical risk-assessment tool

Survival analysis is an important part of medical research as it allows clinicians to review their practice and plan treatment effectively. It is also of equal importance to patients as it gives them the opportunity to make choices and plan care for their dependents. Survival curves can be generated for various subgroups to investigate the importance of individual variables in predicting outcome. However, in several different variables outcome, the number of subgroups with distinct combinations of variables increases rapidly, and the number of cases in the reference set that match exactly the risk profile in any test case will generally be too small for meaningful prediction. Clinicians routinely make diagnostic and therapeutic decisions based on the patient's prognosis. In addition, prognostic information is also important in counselling patients and family members in this critical scenario. However, clinicians generally believe that their predictions may be inaccurate. In recent years, specific diagnostic processes, and health technology assessment (HTA) tests have been developed in response to the increased pressure from the health systems to decide not only which tests to perform but also the best way from the information provided.

Therefore, it was necessary to develop prognostic models that allow the identification of influential variables in the prediction of patient outcomes and the use of these multiple risk factors in a systematic and reproducible way to the evidence-based methods. The reliability of the models depends on the informed use of statistical methods, in combination with prior knowledge of the disease. Prognostic models are statistical models that combine two or more items of patient data to predict clinical outcome. Multiple prognostic models for UM have been accumulated for decades, but none of them is widely used in clinical practice.

The prognostic models that have been used for the prognosis of UM take into account the several strongest prognostic parameters in UM which have been incorporated into statistical systems created, using test and validation sets for prognostic prediction. These models have been shown to increase prognostic accuracy, in some centres. Prognostic models have been

widely used for patient counselling and to determine the frequency and model of screening to be applied into certain health systems [169]. A series of combined prognostic models has been designed and validated by some centres of ocular oncology worldwide [219,220,232-236].

1.8 The Liverpool Uveal Melanoma Prognosticator Online (LUMPO)

A prognostic tool for predicting probability of survival of patients treated with UM has been developed by the team in Liverpool over a number of years [219,220,233,237]. The Liverpool Ocular Oncology Clinic (LOOC) was the first specialist centre to present personalised curves for UM patients generated from a combination of clinical, histopathological and genetic factors. These have been incorporated into a prognostic tool called the Liverpool Uveal Melanoma Prognostication Online (LUMPO); (www.lumpo.net), [236] to establish the prognosis for UM patients according to the initial tumour characteristics and cytogenetic data. It includes anatomical predictors, such as the largest basal diameter of the tumour, tumour thickness, ciliary body involvement and extra-ocular dissemination; histological predictors, including epithelioid cell type, presence of closed loops and tumour mitotic count; and genetic predictors, which include loss of one copy of chromosome 3 [238].

LUMPO was trained using existing data sets from patients treated with UM, with an average follow-up ranging to more than 20 years (1984-2009) [236]. LUMPO produces estimates relevant for each individual patient. This is because the multivariate analysis includes not only clinical features but also the histological grade of malignancy and tumour genetics. The output generates a survival curve for the patient as compared with an age and gender-matched healthy individual. A pictogram was also designed to facilitate communication with patients.

The first version of LUMPO was validated externally for the first time in 2015, in the Department of Ophthalmology, at the University of Medical Sciences in Poznan, Poland [239]. This study aimed to test the prognosticator in a homogeneous group of patients treated with

ruthenium brachytherapy, in which the genetic analysis was not performed. More recently, it was validated in the USA in 2016, in a cohort of patients treated at the University of California, San Francisco (UCSF) [240]. A retrospective study review was performed on 390 patients treated between 2002 and 2007 for UM at UCSF, and 1175 patients with similar characteristics treated at the LOOC. The results of the study revealed that there were differences between the two patient cohorts, especially regarding the clinical and anatomical characteristics, the type of treatment and the genetic data.

Since the first version of LUMPO was created in 2011, the scientists who developed the tool have continued to improve the program. A transitional version (LUMPO2) was then created, but it was never utilised in the clinic, as the revised third version LUMPO3, quickly overtook it [241]. This new tool incorporates information from chromosome 8q and calculates survival using competing risk methods (**Figure 1.17**). The updated LUMPO3 tool also includes a function that calculates the screening interval based on the 'number needed to scan' (NNS) metric (**Figures 1.18 and 1.19**). To use this function, the user is prompted to enter the time when the initial scan was performed, the desired NNS and an estimate of time from onset of metastases to death. LUMPO3 uses this information to calculate the time point of the subsequent scan. This functionality has not been validated as a surveillance tool yet.

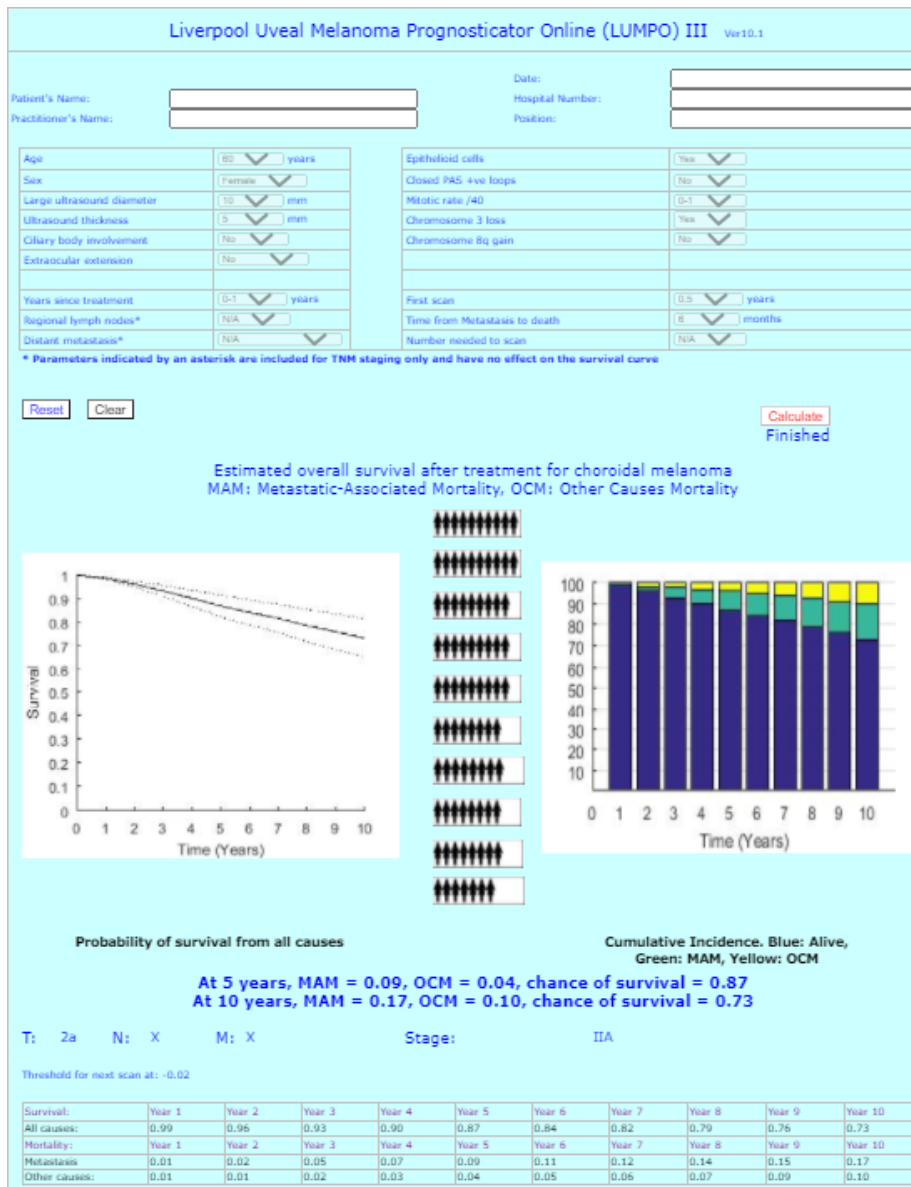


Figure 1.17 Example of a personalized survival curve representing a hypothetical 60-year-old female patient with a UM 10mm in diameter and 5mm thick. The tumour contains epithelioid cells with chromosome3 loss but no other histologic / cytogenetic risk factors. The model shows that at 5 years after treatment the patient has a 9% probability of dying from metastases, 4% probability of dying from an unrelated cause, therefore 87% probability of surviving 5 years or more. (Accessed from lumpo.net 24 August 2020).

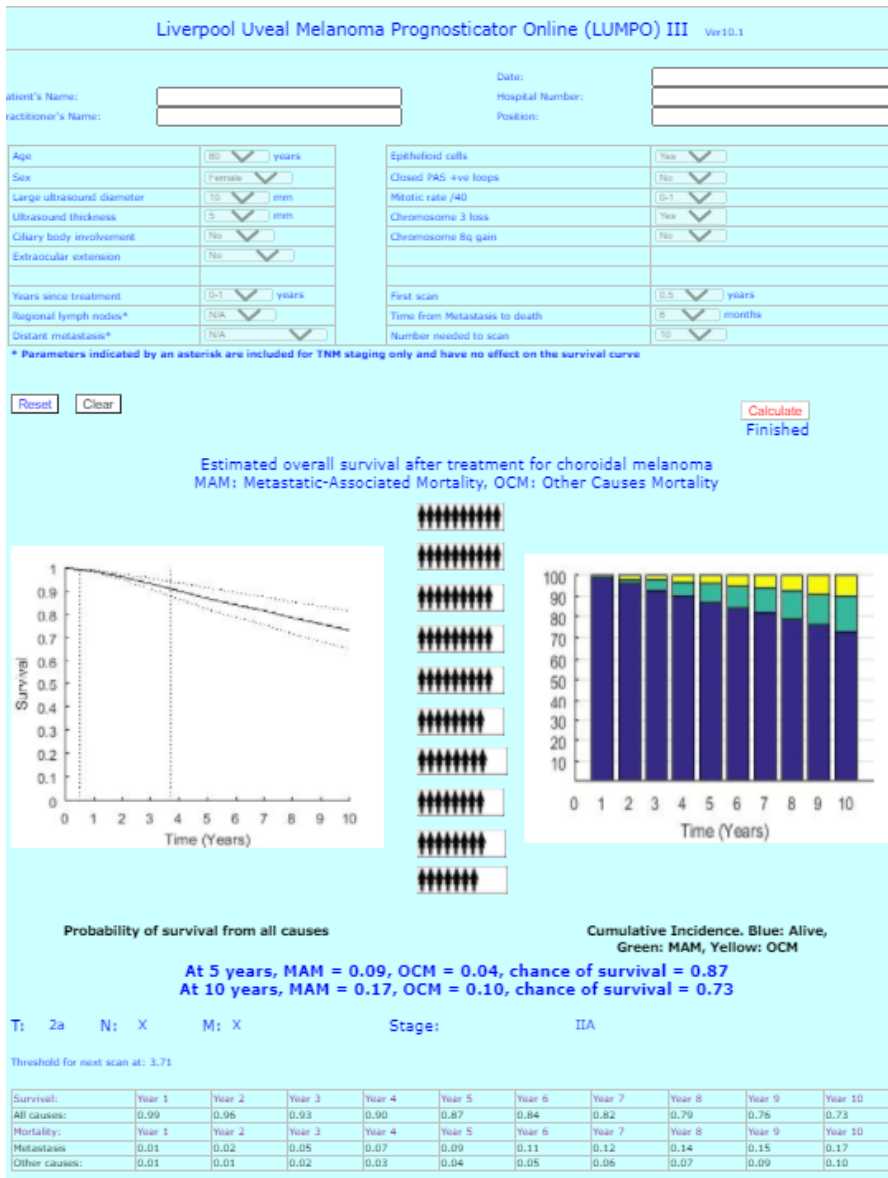


Figure 1.18 The same hypothetical patient above with an initial liver scan performed 6 months after treatment as per usual practice. The estimated time from the onset of metastases to death was 6 months and the NNS was 10. The model uses this information to calculate the time of the next scan which is 3.71 years. (Accessed from lumpro.net 24 August 2020).

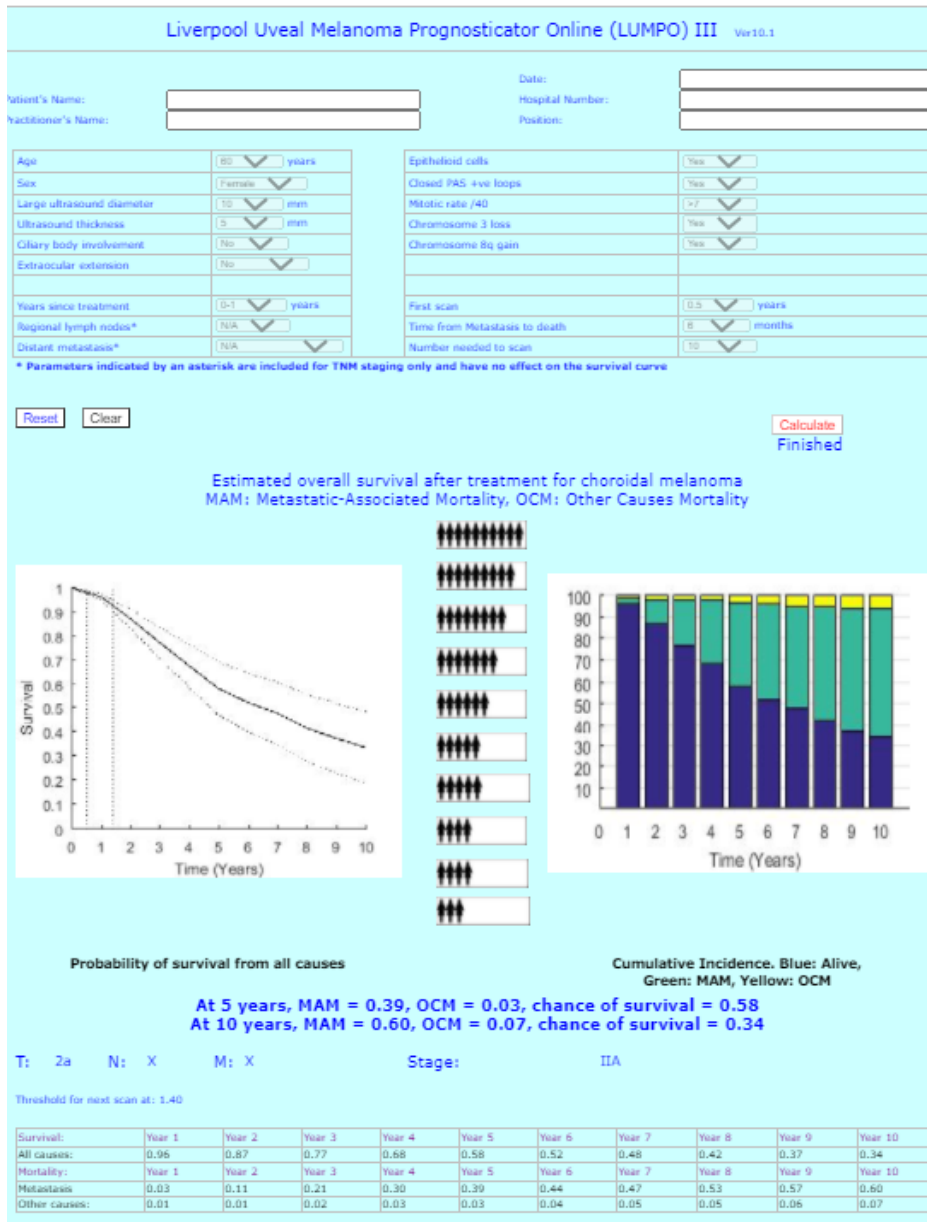


Figure 1.19 The same hypothetical patient above but with more risk factors including the presence of closed loops, higher mitotic rate and chromosome 8q gain. The time of the second scan is now 1.4 years associated with a higher probability of developing metastases at 39%. (Accessed from *lumponet* 24 August 2020).

In the past, several models were developed using neural networks in which pathological, clinical and genetic data were integrated to increase the prognostic accuracy so that the probability of survival for individual patients was relevant [122,124,125]. Validation studies showed that when clinical and laboratory data sets were available, these models functioned adequately in patients treated for local resection or enucleation [216]. However, the prediction was not reliable when only biopsy samples were analysed, such as in patients treated with radiotherapy or phototherapy. This is because biopsies prevented mitotic counts and assessment of extravascular artery patterns and because neural networks failed to adequately compensate for missing data. Such lack of information has become more common in recent years, since prognostic biopsies for irradiated melanomas have become routine.

Prognostic models have been widely used for patient counselling and to determine the frequency and model of screening to be applied to specific health systems [242]. A series of combined prognostic models have been designed and validated by some centres of ocular oncology worldwide, some in Liverpool [219,220,232,233], and others at other institutions overseas [234,235] (**Table 1.4**) but none of them are as widely used in clinical practice as LUMPO and LUMPO3.

Table 1.4: Summary of alternative prognostic models in UM

Authors	Name of the model	Strengths and weaknesses
<p>Kaiserman, Rosner et al. (2005)</p>	<p>ANN</p>	<p>Strengths: ANN could help predict the prognosis of an individual case of UM based on information available to the clinician at the time of brachytherapy and during follow-up.</p> <p>Weaknesses: Some risk factors did not reached statistical significance, possibly attributed to the small sample size used, compared to the large number of predictive factors included in the analysis.</p>
<p>Vaquero-Garcia et al., (2017)</p>	<p>PRiMeUM</p>	<p>Strengths: Provides prognostic information for personalised risk of metastases in UM using clinical and chromosomal information.</p> <p>Weaknesses: Not all risk factors included. Not possible to collect information related to cytology because of small cells collected during FNAB procedure.</p>

1.9 Outline of the thesis

The main aim of this thesis was to test the robustness of LUMPO, and in particular its latest version, i.e. LUMPO3.

The aims and objectives of this thesis are described in greater detail below, as well as with a brief explanation of the content of each chapter.

In **Chapter 2**, the characteristics of the liver scan reports of patients diagnosed with UM were analysed. The data from these cases corresponded to a period of eleven years were collected and included specific data such as: the median time from the treatment of the primary tumour to the detection of metastases, and the time from the detection of metastases to death, when metastases occurred, and its characteristics (for example, number, size, and location). Results of this study were published in *Computers and Biology Medicine*. 2021 Mar; 130:104221. doi: 10.1016/j.compbimed.2021.104221. Epub.

Subsequently, the hypothetical costs of liver surveillance were examined demonstrating the cost-benefit analysis of LUMPO3, this time using a new model that was an output of LUMPO3. The costs of all scans performed, and the number of missed metastases were analysed. In addition, estimated costs savings were calculated which would be obtained by using LUMPO3-advised liver surveillance strategies, as discussed in **Chapter 3**. Results of this study were also published in *Computers and Biology Medicine*. 2021 Mar; 130:104221. doi: 10.1016/j.compbimed.2021.104221. Epub.

To demonstrate that LUMPO3 has a good ability to discriminate between UM patients who died and those who survived, in independent data sets, LUMPO3 was subjected to a multicentric validation test, and the results showed that it is a reasonably accurate tool and valuable for predicting all-cause mortality in UM patients, despite clinical, histopathological and genetic differences between the various cohorts studied. Kaplan-Meier curves for all causes of mortality were presented. The calibration graphs showing the expected probabilities of actuarial survival showed a good agreement between the observed and predicted

probabilities, as detailed in **Chapter 4**. The results were published in *Cancers (Basel)*. February 18, 2020; 12 (2): 477. doi: 10.3390 / cancers12020477.

Finally, in **Chapter 5**, the results of each chapter were discussed and summarized in one conclusion. Recommendations for future research were made considering the implications of the findings made, highlighting how the contributions during this research were contributing to knowledge in the field of ocular oncology.

Chapter 2

Liver-screening analysis to identify uveal melanoma metastases in patients treated at the Liverpool Ocular Oncology Centre between the years 2008-2018

2.1 Introduction

Hepatic metastases are the leading cause of death in patients with UM [132]. In contrast to most cancers, <1% of UM patients have metastatic disease at the time of the initial diagnosis [143]. Although time to metastases varies - and can even be up to 42 years after the diagnosis of UM - [243], it is usually identified about 3 years after the diagnosis of the primary tumour [169]. The median survival time after the diagnosis of metastases is 13 months [244]. It has been reported that some patients in whom the liver metastases are resected may survive longer, although resection requires timely detection of metastases [244,245].

Taking into consideration the long time period during which metastases can occur, it is essential to create a rational surveillance program. Aspects related to the different types of investigations used in screening protocols for metastatic disease in UM was mentioned in the Introduction in **Chapter 1**. However, there are other important factors in the management of liver surveillance that are crucial for the early and pre-symptomatic identification of metastases, such as the patients' compliance to the surveillance examinations. Some studies on metastatic surveillance of patients with a variety of malignancies, such as breast-, colon and prostate cancer, have indicated that patient's socioeconomic, demographic, and psychological factors all play a key role in patients' ability to follow the recommendations of the surveillance programs [246,247]. Other aspects that may interfere with compliance to surveillance protocols are the patient's age, comorbidities, and degree of understanding of their illness as well as anxiety regarding the disease process [246,247]. All these elements are taken into account when designing liver surveillance programs.

Considering the high rates of metastases in UM patients, there is a significant interest in the development of improved methods for liver surveillance for metastases detection [248]. Currently, each institution has its modality and image frequency for the screening of UM metastases, and there is no consensus protocol. The frequency varies depending on the participation in ongoing clinical trials and the spread risk of the tumour as indicated by its stage

at diagnosis, its histological features, and its genetic profile.

2.1.1 Risk stratification

As mentioned in **Chapter 1**, the risk of metastases in UM depends on several factors, including clinical and pathological characteristics of the tumour – i.e., its size and location, and molecular genetic abnormalities, such as one copy of chromosome 3 (monosomy 3) and gain of copies of the long arm of chromosome 8 (polysomy 8q). These factors are associated with higher metastatic risk than others. Generally, oncologists recommend more intensive surveillance for patients with 'high-risk' UM [249]. The definition of UM patients at high risk of metastases (and associated death) varies but can be determined using the AJCC/TNM staging (8th edition) [250], the Cancer Genome Atlas (TCGA) classification [251], from prognostic biopsies where cytogenetic tests are performed [72], or using prognostic models that incorporate various prognostic factors [235,241]. The UM guideline development group (GDG) [252] suggested that several factors are included in UM patients at high-risk, such as the large size of the tumour, ciliary body involvement, and the AJCC staging with a prognosis of >30% probability of death in 5 years.

2.1.2 Surveillance protocols

In Europe, the usual surveillance practice is: liver US performed every 6 months for 10 years, and in the case of a suspected localized lesion, CT or MRI is performed [253]. In the UK, the GDG [252] uses a systematic evidence-based approach to make recommendations in critical areas of UM management. Regarding the surveillance of patients followed after the primary treatment of UM, it was outlined that it should be conducted by a multidisciplinary group of specialists that includes ophthalmologists, oncologists, radiologists and oncology nursing and hepatic services. They also recommend that, regardless of the degree of risk of developing metastases, all patients should undergo a holistic evaluation, which consists of an assessment where the risks, benefits and consequences of entering a surveillance program are discussed. Thus, it was defined that high-risk UM patients should have a semi-annual lifelong surveillance, which includes specialized nursing support, clinical reviews and specific liver

imaging exams by non-ionizing modality, such as MRI and US. Due to the high doses of radiation, ionization modalities such as PET and CT are not considered recommended for UM surveillance [252].

The Scottish Consensus Statement Group (SCSG) [254] suggested that the surveillance protocol should be individualized for each patient and discussed at the time of diagnosis, to be reviewed periodically if necessary. They recommended for high-risk UM patients, MRI with and without contrast at time of the diagnosis, and then semi-annual MRI without contrast according to the protocol. For low-risk patients, they recommend liver US at time of the diagnosis, half-yearly liver US, and should there be limited visualization or any suspicious findings, they indicate MRI with contrast, and the additional surveillance modality to be done later [254].

As mentioned in the **Chapter 1**, the COMS [143] conducted in the USA also described screening procedures reporting the predictive value of liver function tests (LFTs), chest X-rays (CXR) and liver imaging for the detection of melanoma metastases as a routine follow-up after treatment for UM, and concluded that periodic screening for UM metastases is essentially beneficial when patients are eligible to be candidates for clinical trials for optimistic treatments, or when effective treatments are available. Similar to these guidelines, there are others at the national level [158,255-257]; however, so far, no international consensus measures have been outlined. It should also be mentioned that in some countries, due to the limited impact of liver screening on survival in UM, it is believed to have no benefit and not undertaken [147,258-260].

2.1.3 Surveillance modality

There is a significant variation in the modalities of obtaining images of the liver for surveillance of UM patients. In the UK, in some centres, MRI with or without contrast is used in high-risk UM patients, while in other centres, a liver evaluation is performed initially where only US is used. Only when abnormalities are detected, surveillance continues with other modalities [252]. Balasubramanya et al. reported that CT is the most performed imaging modality for assessing melanoma metastases in their melanoma clinic, like others in the USA. They suggest that it has considerable advantages, both for the imaging quality and for being well tolerated and widely available. Its disadvantages include it being relatively insensitive to small liver lesions, specifically those smaller <1 cm; in these cases, MRI is undertaken [170]. Choudhary et al. analysed the utility of liver US in patients undergoing liver surveillance after primary treatment for UM to detect asymptomatic liver metastases: they selected hepatic US instead of CT or MRI referring to factors, such as not using contrast material, easiness of administration, and prevention of radiation [261].

In summary, liver US it is a non-invasive imaging modality, it has no side effects, is inexpensive and widely available; however, it is operator dependent, and it may not be possible to scan the entire liver due to some patients' larger body mass index. In comparison, MRI with contrast is considered a more specific modality for detecting small liver metastases and is thought to be more sensitive than CT [170,262,263]. However, it is expensive and may not be suitable for all patients, such as patients with metallic implants or who suffer from claustrophobia [264]. Some studies have reported that with repeated MRI with contrast, there may be an accumulation of contrast medium in the brain [265].

To conclude, in addition to the significant variability in the type and frequency of surveillance implemented for metastatic disease in UM, there is no convincing evidence that UM screening prolongs life, and there is no consensus regarding liver surveillance in UM patients, with respect to the modality used and the frequency of screening. These factors led us to investigate and correlate in detail the characteristics of UM patients included in liver screening

programs, from the time of diagnosis of their primary UM to the time of detection of metastases and their subsequent follow-up.

The objectives of **Chapter 2** were to: (1) calculate the number of scans and screening modality in patients undergoing liver screening in Liverpool; (2) determine factors, such as time from the primary treatment of UM to the detection of metastases and time from the detection of metastases to death; and to (3) describe characteristics of the detected metastases such as; number, its size and location.

2.2 Patients and Methods

2.2.1 Study design

Patients diagnosed with UM and who had a primary treatment between 1988 and 2018 at the LOOC were identified by the OOB (**Figure 2.1**). The identified patients seen at LOOC between 2008 and 2018 had given their consent to review of their health-related records for research purposes. The NHS/Hospital numbers for the identified patients were passed to me in an encrypted/ password-protected spread sheet for review of their liver scan reports whose examinations were performed in the following Trusts; the Liverpool University Hospitals NHS Foundation Trust (LUHFT), the Clatterbridge Cancer Centre (CCC) and the Aintree University Hospital NHS Trust (AUHT) following both Health Research Authority (HRA) (NRES REC REF: 18/NW/0748), and Confidentiality Advisory Group (18/CAG/0181) approval. An account was created at the LUHFT, which provided me with access to review of patients corresponding data from the 3 above-mentioned hospitals. When available, liver scan data were reviewed and relevant information was collected through the hospital software called CRIS (Clinical Record Interactive System).

The liver scan reports found through CRIS provided the information previously detailed in an available proforma (**Appendix 1**), in which the variables were coded, in order to facilitate the collection and analysis of data (**Appendix 2**). These variables were detailed as follows: patient's demographic (age and sex); anatomical data - such as tumour largest basal diameter (LBD), ultrasound height (UH), ciliary body involvement (CBI), extraocular extension (EOE)-; histological data including presence or absence of epithelioid cells (Epi), presence or absence of extravascular closed connective tissue loops (loops), and mitotic count per 40 high powered fields (Mitoc); as well as tumour cell genetic data, including information on status of chromosomes 1p, 3, 6p, 6q, 8p and 8q.

In order to account for the unreported values in the categories Epi, Loops, Mitoc, status of chromosomes 1p, 3, 6p, 6q, 8p and 8q, the category not available (N/A) was included when it

was not possible to access the result of the corresponding tests due to factors such as: failure to perform or report a biopsy; when the information to all chromosomes was not available; and when a genetic test was not taken. The category 'others' was also included, for describing a mix of alterations in the status of the genetic factors, as follows: 1) gain and unclassified - for chromosome 1p; 2) partial loss, unclassified and allelic imbalance - for chromosome 3; 3) loss, unclassified - for chromosome 6p, 8p and 8q, and 4) unclassified - for chromosome 6q.

The variable 'Mitoc' was categorized according to the number of mitoses per 40 high powered fields, divided into 4 groups as follows: group 1 (0-1 mitoses), group 2 (2-3 mitoses), group 3 (4-7 mitoses) and group 4 (>7 mitoses).

The modality of imaging used and referred to in the reports of the hospitals accessed were MRI, US and CT. Data from these liver scan reports included:

- 1) When the first liver scan occurred;
- 2) The number of liver scans performed;
- 3) The number, size and location of metastases detected;
- 4) Time from primary treatment to the detection of the first metastases; and
- 5) Time from the detection of metastases to death.

The description of how metastases were diagnosed was presented as follows: 1) diagnosis by clinical imaging - when metastases were detected through the liver screening; and 2) diagnosis at autopsy - when metastases were detected by histopathological examination post-mortem, for these cases, it was assumed that the date of the diagnosis of the metastases was the date of death.

Depending on the diagnosis from the pathology report post-mortem, the cause of death was specified whether due to metastatic disease, another disease or another unspecified cause.

The follow-up time for this study was defined as the time interval between the date of primary treatment and the date of the last follow-up at the time of study closure – i.e., 15th of May of 2020.

After collecting these data from the liver scan reports, the dataset was then returned to the OOB custodian, Dr Helen Kalirai, BSc. PhD. Postdoctoral Research Fellow at UoL, who replaced patient identifiers with a unique OOB identifier (ID) and added the patient's clinical, histological, genetic, follow-up and outcome data for completion of patient's data before creating a research database for this study (**Figure 2.1**). The Cancer Registry of the National Health Service (NHS) automatically provided the certified cause of death, with patients being flagged at the time of diagnosis.

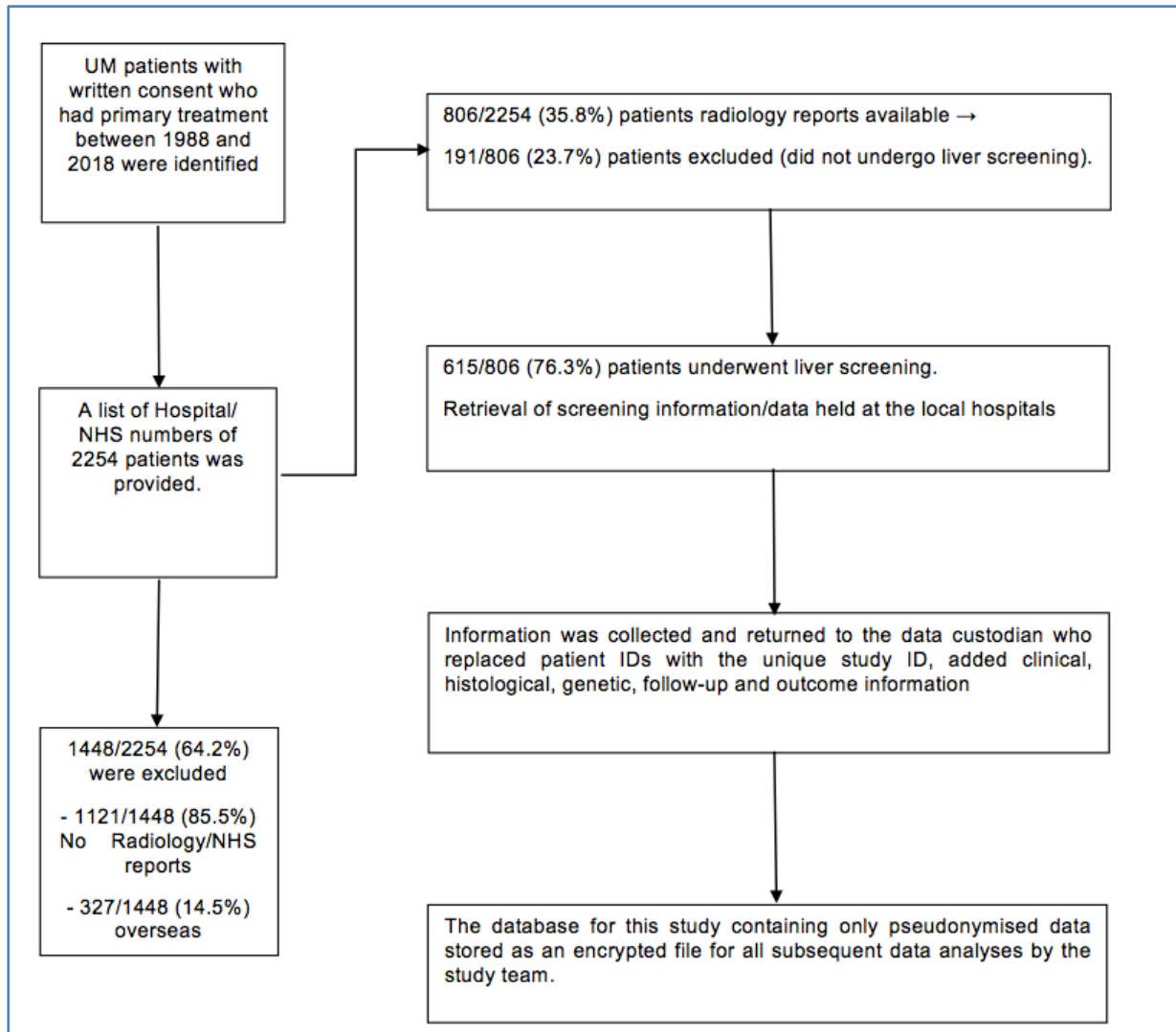


Figure 2.1 Flow diagram for data collection for Liver-screening analysis to identify uveal melanoma metastases in patients treated at the LOOC (image published in *Comput. Biol. Med.* 2021 Mar; 130:104221. doi: 10.1016/j.combiomed.2021.104221. Epub. 2021 Jan 20).

2.2.2 Data Collection

A retrospective review was performed of data from the UM patients identified by the OOB with the diagnosis of UM who had primary treatment between 1988 and 2018. 2254 patients seen at LOOC over the mentioned period were approved by the OOB (**Figure 2.1**). Of these, 1448/2254 (64.2%%) patients were excluded as no radiological reports were found in the LUHFT, presumably because most of these patients had their examinations in other hospitals, or had not undergone any radiological examination. So, 806/2254 (35.2%%) had radiological reports in LUHFT; however, of the 806 UM patients, 191 (23.7%%) patients did not appear to have any liver surveillance, instead they had other radiological examinations e.g. CXR, X-ray of the extremities, abdominal US for the diagnosis of concurrent abdominal diseases not related to liver metastases, etc.

In total, 615 radiological liver screening reports of UM patients were found for our analysis. Patients were categorized into year groups, according to the year they had commenced their treatment at the LOOC. In total, there were 11 year groups. There were also 11 patients included in the group of 2008, whose primary treatment was performed prior to the period established for this study, but who had second or more treatments during the defined study period. These included: 1 UM case from 1988; 1 from 1996; 1 from 1997; 1 from 2001; 1 from 2004; 1 from 2005; and 5 UM cases from 2007.

Data were collected, filed, and processed in Excel format (Microsoft, Inc., UoL, UK) and SPSS Statistics V27. After transferring the data to Dr Helen Kalirai for compilation, the dataset was returned to me, to Professor Azzam Taktak, Consultant Clinical Scientist at the LUHFT, and to Dr Antonio Eleuteri, Mathematician at the Department of Clinical Engineering at the LUHFT, for statistical analysis and model construction (**Figure 2.1**). The description of the new model designed to predict the onset of metastases, which is an output of LUMPO, will be discussed in **Chapter 3**.

2.2.3 Data for analyses

As above, patients were categorized into eleven 1-year groups (2008-2018). Categorical variables of sex, CBI, EOE, Epi, Loops, Mitoc, chromosome 1p, 3, 6p, 6q, 8p and 8q status, type of primary treatment, and outcome were summarized with counts. The variables – i.e., age, LDB, UH, follow-up, type of liver scan, largest diameter of the largest metastases (LDLM), time to detected metastases, and time from the onset of metastases until death - were summarized as median with range and categorized according to the group in which the patients were included.

A distribution was used to group primary UM into categories based on the AJCC tumour nodal metastases (TNM) staging (8th edition), which comprises the UM thickness (height), the largest basal diameter of the tumour, involvement of the ciliary body, and any extraocular extension of the tumour. In this study, the UM were subdivided into the T1, T2, T3 and T4 categories, with their respective subcategories a, b, c, and d, please refer to **Table 1.1** in **Chapter 1**.

The number of scans per patient was divided into groups with time intervals of 5 years each (1-5, 6-10, 11-15, 16-20 and >20), reporting the number of scans undertaken in each patient per year.

To distribute patients according to the regularity of liver screening, patients were categorized into 2 groups: “regular” liver surveillance - when the frequency of surveillance included more than 1 scan, and “irregular” liver surveillance - when for various possible reasons patients underwent only 1 scan. These reasons varied considerably between patients, such as the presence of comorbidities, distance to hospitals, anxiety associated with surveillance, motivation and compliance, amongst other factors.

The number of metastases detected was subdivided in 3 groups (0, 0-1 and >1), according to the size description in the scan reports. This distribution was created in this way because not all scan reports quantified metastases, i.e., in a considerable number of cases, the term

"multiple" or "various" metastases was used when more than 1 was diagnosed.

A distribution that allowed the appropriate number of patients with metastases according to the diameter of the largest liver metastases detected, was used including them in groups of 30 mm size (< 30mm, 31-80mm and >80mm), in concordance with the AJCC /TNM in cancer substaging of metastatic UM [266]. Here, "M" describes systemic metastases, where: M0 – No distant metastases present, M1 - Distant metastases present, with subcategories a, b, c, and Mx - unknown. Please refer to **Table 1.2** in **Chapter 1**.

In order to include all patients according to the time when metastases occurred and to the patients' characteristic, 3 groups of patients were defined:

Group 1 - *Characteristics of 108/615 (17.5%) UM patients who developed metastases within 2 years of diagnosis of the primary UM.*

Group 2 - *Characteristics of 121/615 (20%) UM patients who developed metastases after 2 years of diagnosis of the primary UM.*

Group 3 - *Characteristics of 386/615 (62.76%) UM patients in whom metastases were not demonstrated in Liverpool throughout the liver screening study period.*

2.2.3.1 Statistical analysis

Survival analysis of all prognostic factors, including gender, tumour size, epithelioid cells, closed loops, high mitotic count, ciliary body involvement, extraocular melanoma, and copy number of chromosomes status associated with development of metastatic UM, was undertaken using Kaplan-Meier survival curves and tables for all UM. Survival time was calculated from the date of the treatment of the primary UM until death, or the end of this study, on the 15th of May 2020. All analyses were performed using SPSS Statistics V27 (IBM).

2.3 Results

2.3.1 Baseline characteristics of the patients

The cohort used for this study comprised 615 cases with data reviewed and collected from liver scans of patients diagnosed and treated for UM at the LOOC. Of these, 45 UM cases were in 2008; 47 in 2009; 52 in 2010; 80 in 2011; 54 in 2012; 57 in 2013; 66 in 2014; 57 in 2015; 51 in 2016; 50 in 2017; and 56 in 2018 (**Table 2.1**).

2.3.1.2 Demographic and clinical analysis

Table 2.1 summarises the general characteristics of these 615 UM patients. As can be seen in this table, the study of 615 enrolled patients consisted of 278/615 (45.2%) females and 337/615 (54.8%) males. The median age at primary treatment was 61 years (range 22-94 years). The tumours had a median LBD of 14.6 mm (range 2.4 – 26 mm) and a median UH of 6.3 mm (range 0.7 – 20.2 mm). 183/615 (29.8%) UM involved the ciliary body, and 57/615 (9.3%) UM had EOE. It was not possible to obtain information on the measurements of the primary UM of two patients as this information was not included in the database.

2.3.1.3 Histological analysis

As mentioned in Material and Methods, the histological information regarding the morphology of the UM cells was not available for all subjects. This was due to the range of tumour material sent in for histological examination – i.e. intraocular biopsies would be worked up for cytology, whilst any tumour excisions or enucleations would be paraffin embedded and analysed using histological sections. Therefore, the information gained varied according to tissue processing. Where the information was available, 334/578 (57.8%) UM contained epithelioid cells, 238/363 (65.6%) had PAS+ 'loops', and 369/369 (100%) mitotic counts per 40 high-powered fields had between 1 to more than 7, with the following subsets; 1 – 31/369 (8.4%); 2 – 121/369 (32.7%); 3 – 141/369 (38.2%); and 4 – 76/369 (20.6%) (**Table 2.1**). The analysis for epithelioid cells was missing in 37/615 (6.1%) UM; PAS+ loops was missing in 252/615 (41%) UM; and Mitoc was missing in 246/615 (40%) UM.

2.3.1.4 Genetic analysis

Genetic information was also not available for all UM: this was due to varying reasons – e.g. the patient had not consented to tumour genetic testing; there was insufficient material for testing (e.g. tiny intraocular UM biopsies), and/or the extracted tumour DNA was of poor quality due to fixation reasons. Further, chromosome copy number variation is assessed in two differing ways at the LOOC – using MSA and MLPA [267]. In MSA, only chromosome 3 status is evaluated; using MLPA, chromosomes 1, 3, 6 and 8 are assessed.

Therefore, information to alterations in the subsets of chromosomes were available as follows: chromosome 3 for 392/615 (63.7%) tumours (monosomy, partial loss, unclassifiable). The copy number status of chromosomes 1p, 6p, 6q, 8p and 8q (gain, loss, or unclassifiable) was available for subsets with the following values; Chromosome 1p 175/615 (28.4%), chromosome 6p 216/615 (31.1%), chromosome 6q 139/615 (22.6%), chromosome 8p 161/615 (26.2%) and chromosome 8q 294/615 (47.8 %). Information regarding changes in chromosomes 1p, 6p, 6q, 8p and 8q was missing in 183/615 (30%) UM; chromosome 3 in 65/615 (10.6%); and chromosome 8q was missing in 182/615 (29.6%) UM.

2.3.1.5 Follow-up and outcome analysis

The 615 UM patients had a median follow-up time of 5.1 years (range 0.2 – 32 years) (**Table 2.1**). Additionally, in this table it can be seen that of the total patients studied, 375/615 (61%) were alive at the study closure, i.e., 15th of May of 2020. Unfortunately, 240/615 (39%) patients had died whose causes of death were: metastatic UM in 187/240 (77.9%); in 24/240 (10%), their death was attributed to other causes; and in 29/240 (12.1%) UM patients, the cause of death was unknown (**Figure 2.2**).

Overview of patients included in the study

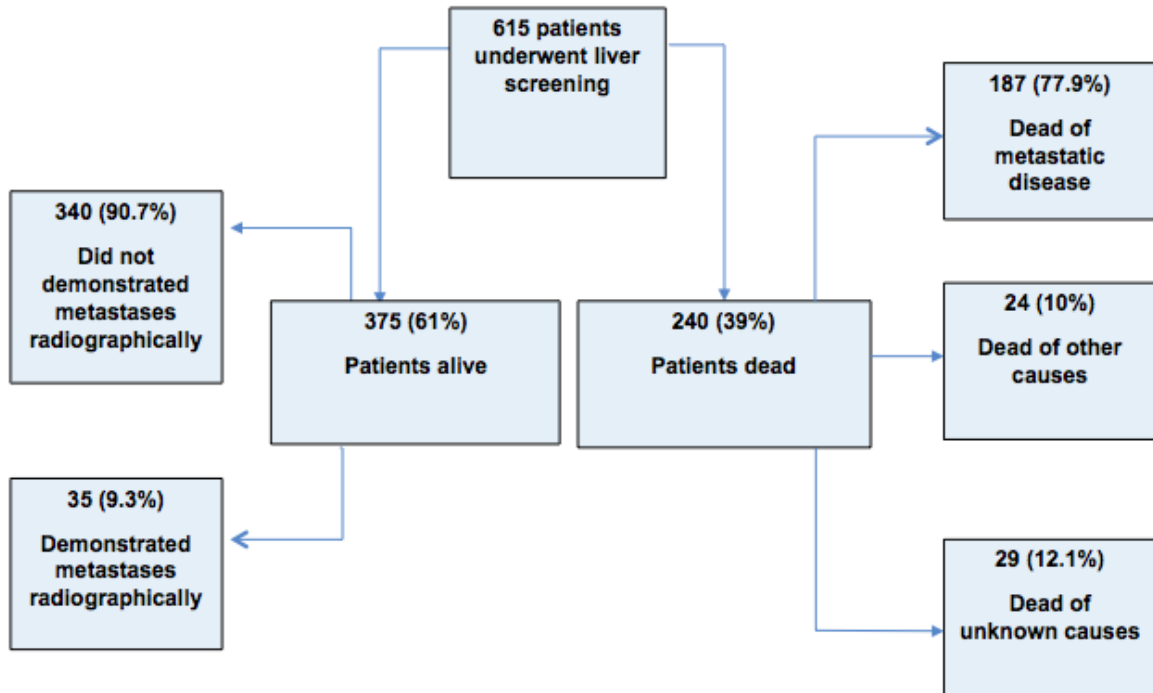


Figure 2.2 Overview of patients included in the Liver-screening analysis to identify uveal melanoma metastases in patients treated at the LOOC between the years 2008-2018.

Table 2.1: Patient Characteristics, overall data (2008-2018)

Patients features	Years											Total
	2008	2009	2010	2011	2012	2013	2014	2015	2016	2017	2018	
	Number of patients											
	45	47	52	80	54	57	66	57	51	50	56	615
Age at primary treatment (years)												
Median	56	59	61	60	62	60	62	64	63	57	63	61
(Range)	(25-74)	(24-82)	(29-90)	(22-94)	(28-88)	(28-87)	(27-81)	(32-88)	(23-82)	(32-86)	(35-89)	(22 – 94)
Sex												
Female												
Male	18	24	27	38	19	23	30	33	22	16	28	278
	27	23	25	42	35	30	36	24	29	34	28	337
LBD (mm)												
Median	15.6	15.1	15.1	14.4	15.2	14.3	13.6	14.2	13.5	13.3	13.4	14.6
(Range)	(9.8-20.9)	(5.8-23.6)	(4.5-26)	(3.6-22.2)	(6.3-22.6)	(2.4-21.2)	(5.1-23.6)	(4.3-22.5)	(5.4-21.8)	(7.7-21.7)	(2.9-22.6)	(2.4–26)
UH (mm)												
Median	7.1	6.2	7.1	6.7	7.9	7.7	6.8	6.4	7.0	6.1	6.0	6.3
(Range)	(1.5-14.8)	(0.9-14.5)	(0.7-14.9)	(0.9-15.4)	(1.5-18.3)	(1.4-14.6)	(0.9-16.7)	(1-18.5)	(1.3-16)	(1.1-20.2)	(1.1-13.6)	(0.7–20.2)
CBI												
No												
Yes	31	33	35	62	36	39	49	34	31	40	42	432
	14	14	17	18	18	18	17	23	20	10	14	183
Extraocular Melanoma												
No	40	47	46	77	46	53	55	53	44	46	51	558
Yes	5	0	6	3	8	4	11	4	7	4	5	57
Epithelioid cells present												
No	19	17	17	30	19	21	27	25	20	20	29	244
Yes	24	26	32	48	33	33	34	28	24	26	26	334
N/A ¹	2	4	3	2	2	3	5	4	7	4	1	37
Closed PAS+ Loops												
No	18	7	15	30	11	13	20	4	1	5	1	125
Yes	13	14	23	24	25	24	21	28	25	17	24	238
N/A ²	14	26	14	26	18	20	25	25	25	28	31	252
MITOC												
0-1	5	2	3	3	3	7	5	0	2	1	0	31
2-3	14	3	10	13	6	13	12	14	18	5	13	121
4-7	8	11	11	15	20	16	16	17	5	12	10	141
> 7	3	8	14	24	7	1	8	4	1	4	2	76
N/A ²	15	23	14	25	18	20	25	22	25	28	31	246
Chr1p												
Normal	31	25	28	29	15	22	26	28	16	21	16	257
Loss	8	13	7	22	15	14	16	11	11	8	10	135
Other ¹	0	0	4	12	11	6	3	0	3	0	1	40
N/A ²	6	9	13	17	13	15	21	18	21	21	29	183
Chr3												
Normal	17	8	12	19	7	21	12	17	8	18	19	158
Monosomy	0	30	25	51	35	23	34	30	29	21	27	330
Other ²	3	0	5	5	7	6	16	6	8	6	3	62
N/A ⁴		9	10	5	5	7	4	4	6	5	7	65
Ch6p												
Normal	23	24	25	9	16	14	22	26	22	17	18	216
Gain	14	9	12	19	7	16	20	13	7	12	8	137
Other ³	2	5	2	35	18	12	3	0	1	0	1	79
N/A ³	6	9	13	17	13	15	21	18	21	21	29	183

Table 2.1: (Continued) Patient Characteristics, overall data (2008-2018)

Patients features	Years											Total
	2008	2009	2010	2011	2012	2013	2014	2015	2016	2017	2018	
	Number of patients											
	45	47	52	80	54	57	66	57	51	50	56	615
Ch6q												
Normal	28	28	24	34	24	21	35	30	23	23	23	293
Loss/Gain	9	8	8	18	8	16	6	8	7	6	4	98
Other ¹	2	2	7	11	9	5	4	1	0	0	0	41
N/A ²	6	9	13	17	13	15	21	18	21	21	29	183
Chr8p												
Normal	24	21	23	34	16	19	39	28	20	26	21	271
Loss/Gain	13	14	13	24	18	11	6	11	10	3	6	129
Other ¹	2	3	3	5	7	12	0	0	0	0	0	32
N/A ²	6	9	13	17	13	15	21	18	21	21	29	183
Chr8q												
Normal	12	14	17	18	10	13	15	15	8	11	6	139
Gain	24	20	23	29	27	22	30	24	20	18	20	257
Other ³	3	4	0	16	4	7	0	0	2	0	1	37
N/A ²	6	9	12	17	13	15	21	18	21	21	29	182
Follow-up time (years)												
Median	9.5	6.7	6.7	6	5	5.5	4.8	4.2	3.2	2.7	1.8	5.1
(Range)	(1.5-32)	(0.4-11.2)	(0.8-10.2)	0.2-9.3)	(0.4-8.3)	(0.9-7.3)	(0.6-6.3)	(0.7-5.3)	(0.2-4.3)	(0.7-3.3)	(0.8-2.3)	(0.2-32)
Outcome												
Alive												
Dead	22	19	21	39	23	38	38	39	36	47	53	375
	23	28	31	41	31	19	28	18	15	3	3	240
Cause of death												
Metastatic	21	24	20	33	29	15	20	10	12	1	2	187
Other	2	4	4	8	1	3	1	0	1	0	0	24
Unknown	0	0	7	0	1	1	7	8	12	2	1	29
<p><i>N/A1 = no biopsy taken</i> <i>N/A2 = no biopsy taken or not reported</i> <i>N/A3 = no genetic testing undertaken or only MSA analysis of Chr3 performed</i> <i>N/A4 = no genetic testing undertaken</i> <i>Other1 = Gain, unclassified</i> <i>Other2 = Partial loss, unclassified, allelic imbalance.</i> <i>Other3 = Loss, unclassified.</i> <i>Other4 = Unclassified.</i></p>												

2.3.2 Type of primary treatment performed

The 615 patients seen at the LOOC underwent different types of surgical and non-surgical treatments, as can be seen in **Table 2.2**. It can be observed that enucleation was most often performed in 314/615 (51.1%), followed by plaque brachytherapy in 131/615 (21.3%), and proton beam irradiation in 118/615 (19.2%).

Table 2.2: Type of primary treatment

Type of primary treatment	Years											Total
	2008	2009	2010	2011	2012	2013	2014	2015	2016	2017	2018	
	Number of patients											
	45	47	52	80	54	57	66	57	51	50	56	615
Enucleation	20	20	28	44	32	33	37	31	26	20	23	314
PRXT	9	15	13	16	10	8	14	11	8	8	19	131
PBR	9	8	3	12	9	10	11	12	15	18	11	118
Local Resection	7	3	6	7	3	2	3	1	1	1	1	35
Endoresection	0	1	2	1	0	4	1	2	1	2	1	15
Endoresection + PRXT	0	0	0	0	0	0	0	0	0	1	1	2

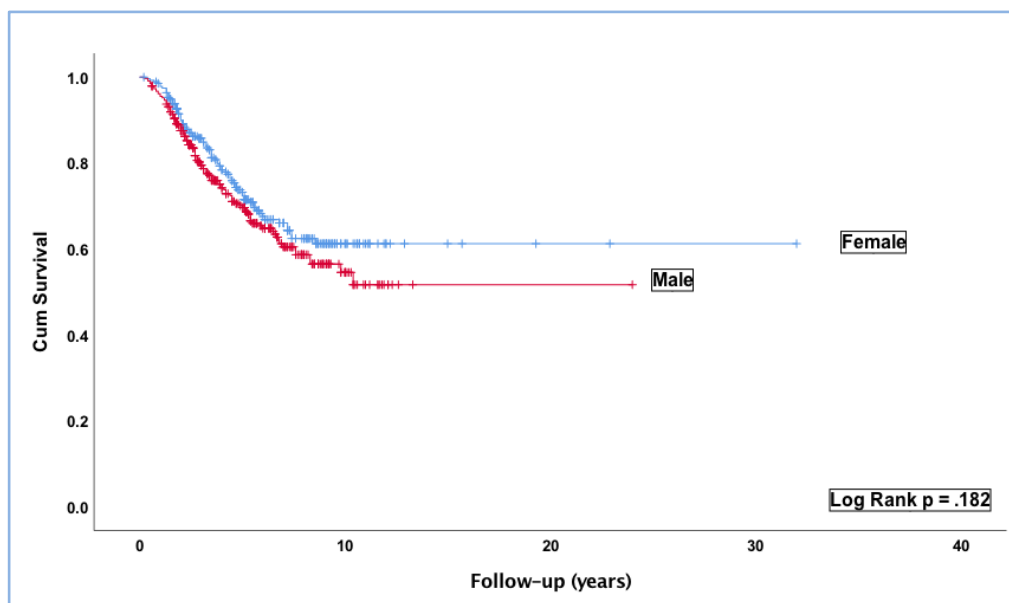
PBR – Proton beam irradiation; PRXT – Plaque Brachytherapy

2.3.3 Survival

All prognostic factors related to LUMPO3 were analysed for this study. Kaplan-Meier survival curves were analysed specifically for each predictor factor.

2.3.3.1 Gender

Kaplan-Meier survival curves and tables were examined for all patients stratified according to gender. Log-rank tests were utilised to compare survival across gender ($p= 0.182$). As mentioned above, the majority of patients in this study were males [337/615 (54.8%)]. These patients also had a higher number of detected metastases 136/337 (40.4%) compared to females 93/278 (33.5%), as well as higher metastatic mortality 108/337 (32.1%) versus 79 (28.4%) in females (**Figure 2.3**). The survival was also compared and was improved for females.

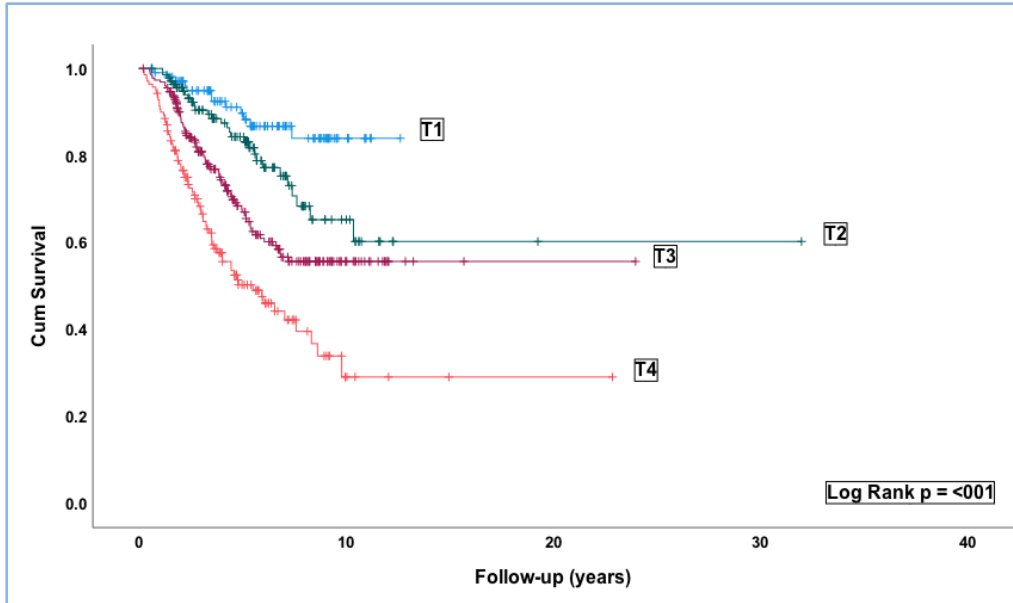


Gender	Number of patients (%)	Number of metastases (%)		Number of Events %		Censored %		Mean survival (years)	95% confidence interval		
									Lower	Upper	
Female	278/615	45.2%	93	33.5%	79	28.4%	199	71.6%	21.116	19.104	23.128
Male	337/615	54.8%	136	40.4%	108	32.1%	229	68.0%	14.526	12.952	16.101
Overall	615	100%	229	37.4%	187	30.5%	426	69.6%	19.828	18.292	21.364

Figure 2.3: Kaplan-Meier survival curve and table for all primary UM stratified according to gender. All patients were classified as: female ($p = .182$) 278 patients and male ($p= .182$) 337 patients. The number of metastases detected in each group of patients was calculated, and the number of events indicates the number of patients who died of liver metastases.

2.3.3.2 Primary tumour size

Kaplan-Meier survival curves and tables were examined for all primary UM stratified according to the classification of the 8th edition of AJCC staging for UM, whose categories are listed in **Table 1.1 (Chapter 1)**. Log-rank tests were utilised to compare survival across the 4 groups ($p = <0.001$). Of the 615 primary UM, the majority of UM [226/615 (36.9%)] were classified as T3. Patients with larger tumours (T4) were those with the highest number of detected metastases, [82/140 (58.6%) patients]. The number of metastases detected, and metastatic mortality was significantly associated with the increase in the size of the primary UM (**Figure 2.4**). Survival was compared for all categories. In this study, it was found that increasing in tumours category was significantly associated with reduced survival (**Figure 2.4**).

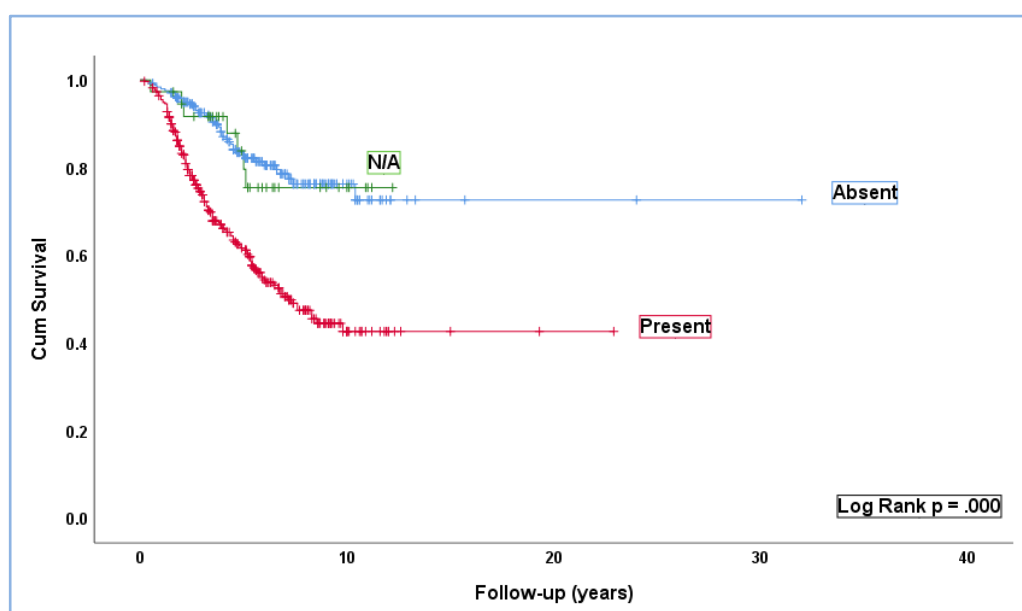


Primary tumour TNM stage	Number of patients (%)	Number of metastases (%)		Number of events %		Censored %		Mean survival (years)	95% confidence interval	
		Number	%	Number	%	Number	%		Lower	Upper
T1	107/613	16	15%	12	11.2%	95	88.8%	11.263	10.542	11.983
T2	140/613	37	26.5%	29	20.7%	111	79.3%	21.526	17.916	25.135
T3	226/613	94	41.6%	76	33.6%	150	66.4%	14.936	13.349	16.523
T4	140/613	82	58.6%	70	50%	70	50.0%	9.490	7.304	11.676
Overall	613	229	37.4%	187	30.5%	426	69.5%	19.691	18.139	21.243

Figure 2.4: Kaplan-Meier survival curve and table for all primary UM stratified according to TNM staging based on the AJCC (8th Edition) classification. Based on tumour categories, all UM were classified as follows: T1 ($p = <0.001$) in 107 patients T2 ($p = <0.001$) in 140 patients, T3 ($p = <0.001$) in 226 patients, and T4 ($p = <0.001$) in 140 patients. The number of metastases detected in each category of tumours was calculated, and the number of events indicates the number of patients who died of liver metastases.

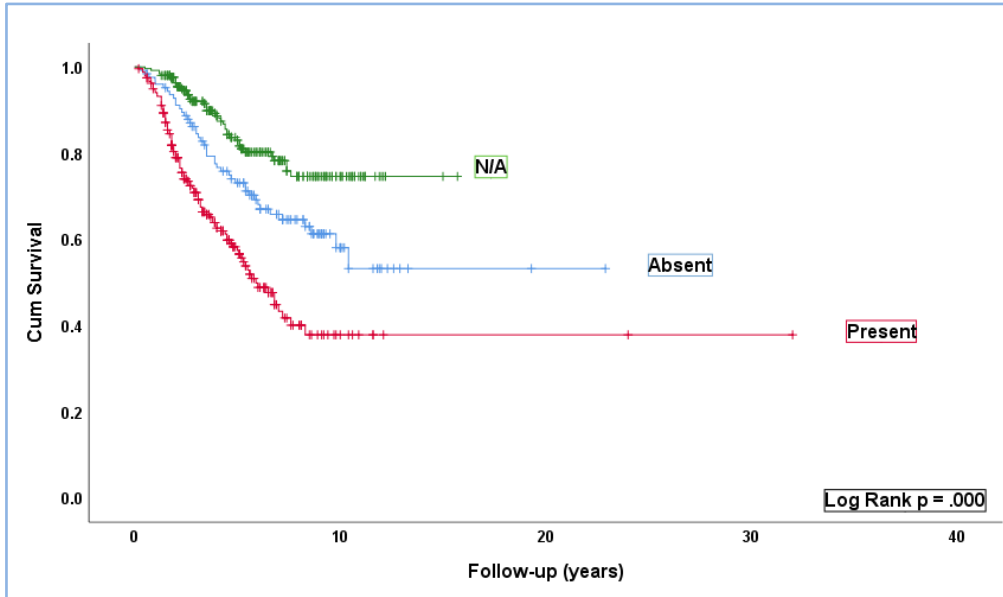
2.3.3.3 Primary tumour histopathological features

Kaplan-Meier survival curves and tables were examined for all UM stratified according to primary tumour histopathological features (epithelioid cells, closed vascular loops, and mitotic count per 40 high-powered fields). Presence of epithelioid cells was associated with worse outcome (Log Rank, $p= 0.000$) (**Figure 2.5**). Presence of closed vascular loops was significantly associated with metastatic disease and metastatic death (Log Rank, $p= 0.000$) (**Figure 2.6**). Mitotic count showing more than 7 per 40 high-powered fields was associated with poor outcome (Log Rank, $p= 0.000$) (**Figure 2.7**).



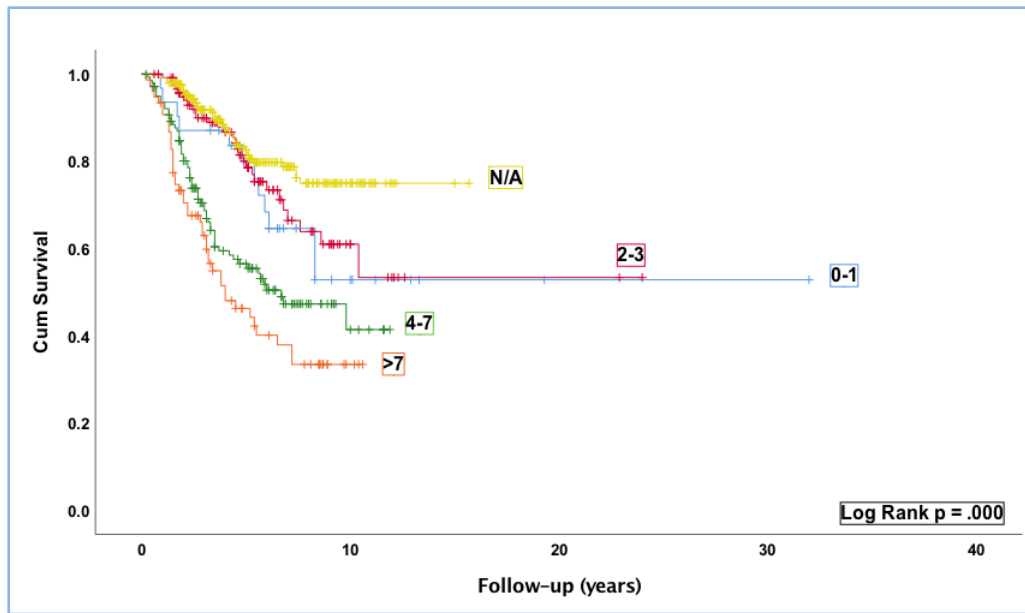
Epithelioid cells	Number of patients (%)		Number of metastases (%)		Number of events %		Censored %		Mean survival (years)	95% confidence interval	
										Lower	Upper
Absent	244/615	39.7%	55/244	22.5%	42	17.2%	202	82.8%	24.570	22.224	26.915
Present	334/615	55.9%	167/334	50%	138	41.3%	196	58.7%	12.016	10.668	13.364
N/A	37/615	6%	7/37	19%	7	18.9%	30	81.1%	10.107	8.774	11.473
Overall	615	100%	229	37.4%	187	30.4%	428	69.6%	19.828	18.292	21.364

Figure 2.5: Kaplan-Meier survival curve and table where patient survival was stratified according to epithelioid cells status: Absence of epithelioid cells ($n=244/615$), presence of epithelioid cells ($n=334/615$), and N/A (not available) ($37/615$). The number of metastases detected in each category was calculated, and the number of events indicates the number of patients who died of liver metastases.



Closed Loops	Number of patients (%)		Number of metastases (%)		Number of events %		Censored %		Mean survival (years)	95% confidence interval	
										Lower	Upper
Absent	125/615	20.3%	54/125	43.2%	44/125	35.2%	81	64.8%	14.537	12.419	16.656
Present	238/615	38.7%	119/238	50%	101/238	42.4%	137	57.6%	14.401	11.811	16.991
N/A	252/615	41%	56/252	22.2%	42/252	16.7%	210	83.3%	12.798	12.011	13.385
Overall	615	100%	229	37.4%	187	30.4%	428	69.6%	19.828	18.292	21.364

Figure 2.6: Kaplan-Meier survival curve and table where patient survival was stratified according to closed loops status: PAS+ loops absent (n=125/615), presence of PAS+ loops (n=238/615), and N/A (252/615). The number of metastases detected in each category was calculated, and the number of events indicates the number of patients who died of liver metastases.

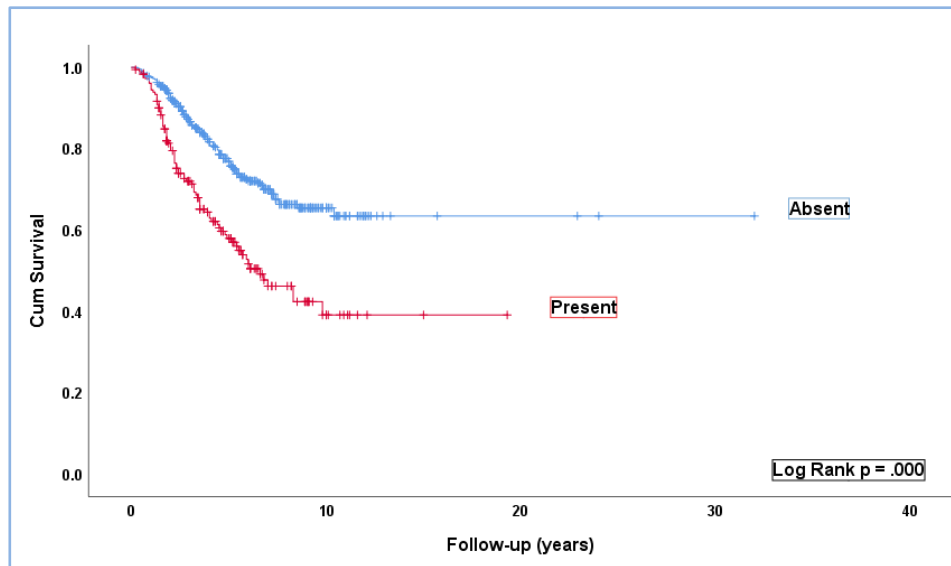


Mitotic count	Number of patients (%)		Number of metastases (%)		Number of events %		Censored %		Mean survival (years)	95% confidence interval	
										Lower	Upper
0-1	31/615	5.1%	14/31	45.2%	12/31	38.7%	19	61.3%	19.268	13.781	24.755
2-3	121/615	19.7%	39/121	32.2%	29/121	24%	92	76.0%	15.511	12.646	18.337
4-7	141/615	22.9%	74/141	52.5%	62/141	44%	79	76.0%	7.057	6.197	7.917
>7	76/615	12.4%	47/76	61.8%	43/76	56.6%	33	43.4%	5.516	4.558	6.474
N/A	246/615	40%	55/246	22.4%	41/246	16.7%	205	83.3%	12.814	12.020	13.607
Overall	615	100%	229	37.4%	187	30.4%	428	69.6%	18.828	18.292	21.364

Figure 2.7: Kaplan-Meier survival curve and table where patient survival was stratified according to mitotic counts per 40 high-powered fields. Based on the subsets analysed, the results were as following: between 0-1 (n= 31/615), 2-3 (n= 121/615); 4-7 (n= 141/615); >7 (n= 76/615), and N/A (n= 246/615). The number of metastases detected in each category was calculated, and the number of events indicates the number of patients who died of liver metastases.

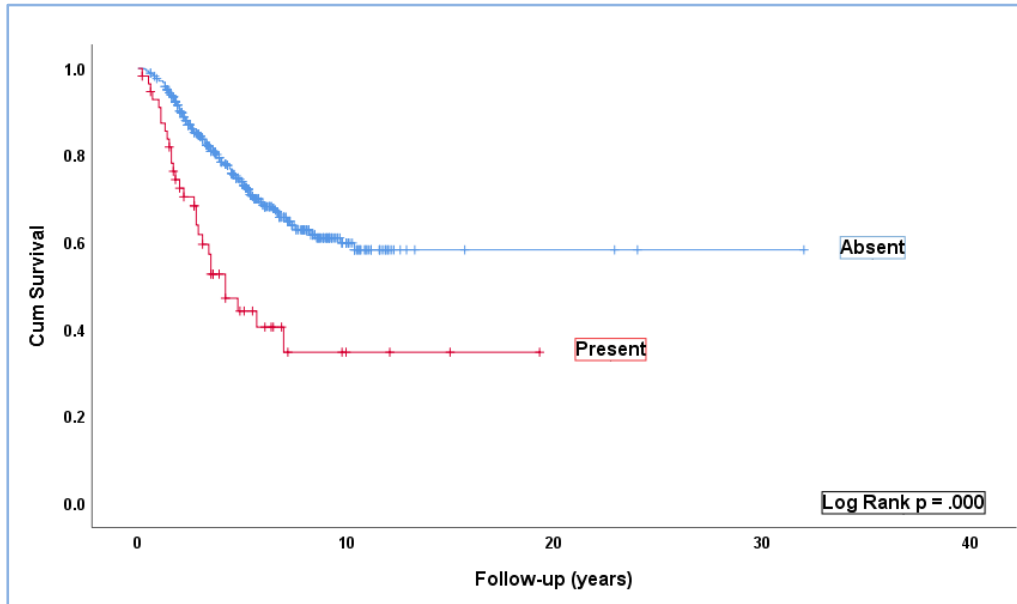
2.3.3.4 Primary tumour clinical features

Kaplan-Meier survival curves and tables were examined for all UM stratified according to primary tumour ciliary body involvement and extraocular extension. Ciliary body involvement was associated with poor outcome (Log Rank, $p= 0.000$) (**Figure 2.8**). Extraocular extension was associated with reduced survival (Log Rank, $p= 0.000$) (**Figure 2.9**).



Ciliary body involvement	Number of patients (%)	Number of metastases (%)		Number of events %		Censored %		Mean survival (years)	95% confidence interval		
									Lower	Upper	
Absent	432/615	70.2%	136/432	31.5%	107/432	24.8%	325	75.2%	21.903	20.139	23.666
Present	183/615	29.8%	93/183	50.8%	80/183	43.7%	103	56.3%	9.905	8.411	11.398
Overall	615	100%	229	37.4%	187	30.4%	428	69.6%	19.828	18.292	21.364

Figure 2.8: Kaplan-Meier survival curve and table where patient survival was stratified according to ciliary body involvement. Absence of ciliary body involvement ($n=432/615$), presence of ciliary body involvement ($n=183/615$). The number of metastases detected in each category was calculated, and the number of events indicates the number of patients who died of liver metastases.

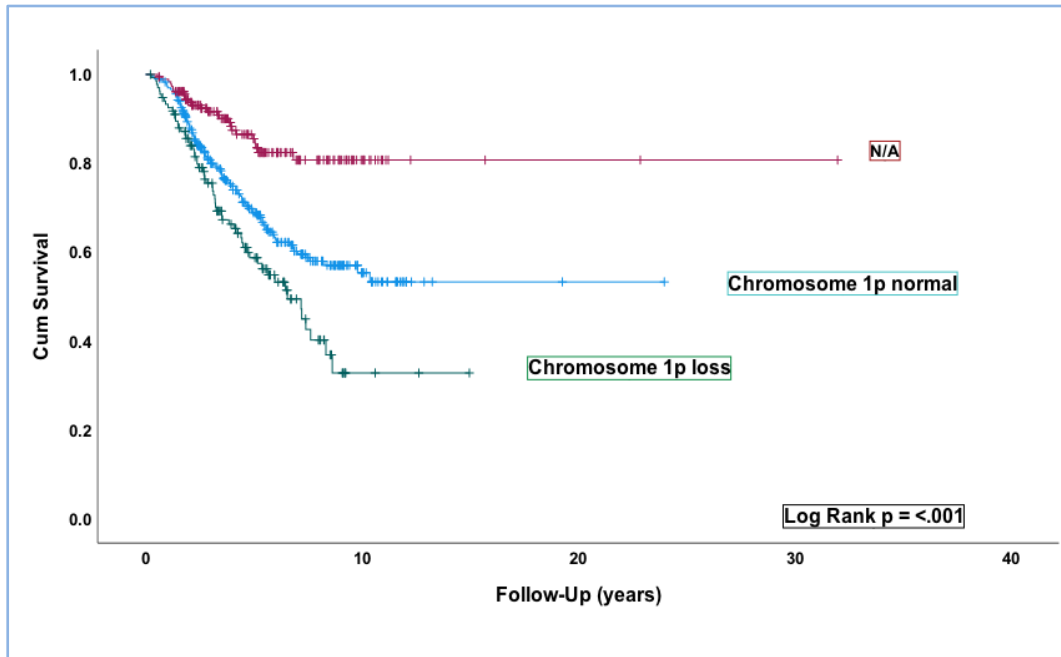


Extraocular extension	Number of patients (%)		Number of metastases (%)		Number of events %		Censored %		Mean survival (years)	95% confidence interval	
										Lower	Upper
Absent	558/615	90.7%	195/558	34.9%	158/558	28.3%	400	71.7%	20.474	18.851	22.098
Present	57/615	9.3%	34/57	59.6%	29/57	50.9%	28	49.1%	8.622	6.052	11.192
Overall	615	100%	229	37.4%	187	30.4%	428	69.6%	19.828	18.292	21.364

Figure 2.9: Kaplan-Meier survival curve and table where patient survival was stratified according to extraocular extension. Absence of extraocular extension ($n=558/615$), presence of extraocular extension ($n=57/615$). The number of metastases detected in each category was calculated, and the number of events indicates the number of patients who died of liver metastases.

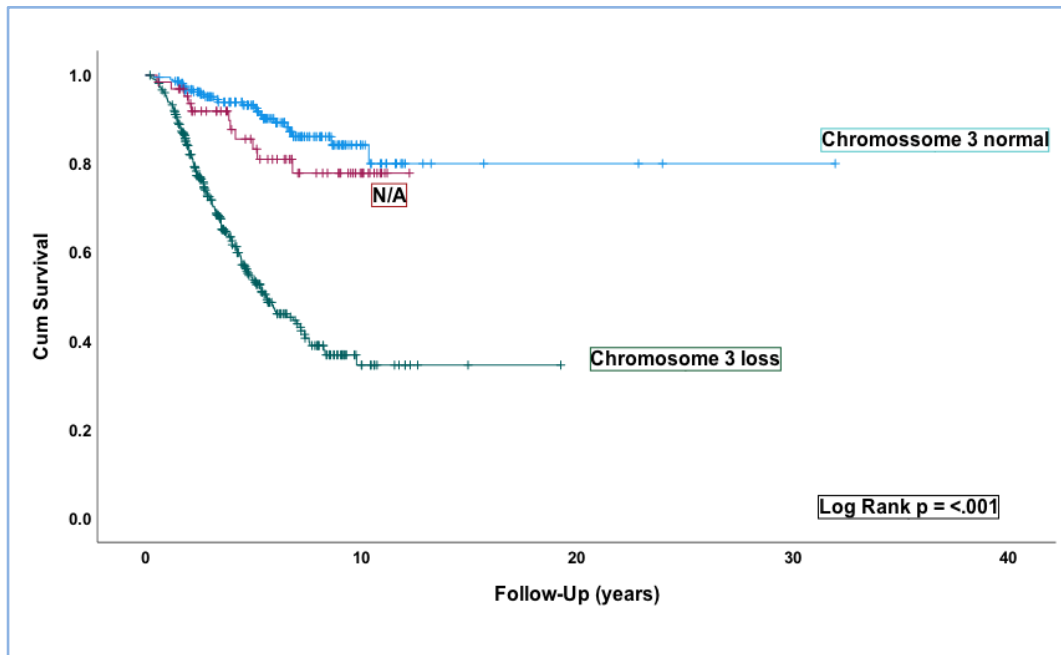
2.3.3.5 Primary tumour chromosomal status

Kaplan-Meier survival curves and tables were examined for all UM according to chromosome status. Log-rank tests were used to compare survival across the 6 groups. Loss of chromosome 1p was associated to poor survival (Log rank, $p = <0.001$) (**Figure 2.10**). Monosomy 3 was significantly associated with metastatic disease and poor survival (Log rank $p = <0.001$) (**Figure 2.11**). With regard to chromosome 3, it was also found that 65/615 (10.6%) patients in whom it was not possible to obtain genetic tests (N/A) had a lower survival than patients with normal status. When data was analysed in detail, and correlated the sizes of the tumours with chromosomes status, it was found that of all chromosome 3 not available (N/A) UM, 28/64 (35.9%) were categorized as T3 and T4, which may explain the low survival in this group of patients (**Appendix 3**). Gain in chromosome 6p was associated with improved survival (Log rank $p = <0.001$); conversely, chromosome 6p normal status was associated with a reduced survival (**Figure 2.12**). In a deeper analysis, it was found that 231/295 (78.4%) of UM with normal Chromosome 6p status coincided with monosomy 3 (**Appendix 4**). Alterations in chromosome 6q were associated with reduced outcome (Log rank $p = .002$); similarly, chromosome 6q normal status was also associated with decreased survival time (Log rank, $p = <0.001$) (**Figure 2.13**). Chromosome 6q normal was associated with 231/335 (69%) of monosomy 3 and with 198/335 (59%) of gains of chromosome 8q (**Appendix 4**). Alterations in chromosome 8p were associated with reduced survival time (Log rank, $p = <0.001$) (**Figure 2.14**), whereas gain of chromosome 8q was significantly associated with metastatic disease, and poor survival (Log rank, $p = <0.001$) (**Figure 2.15**).



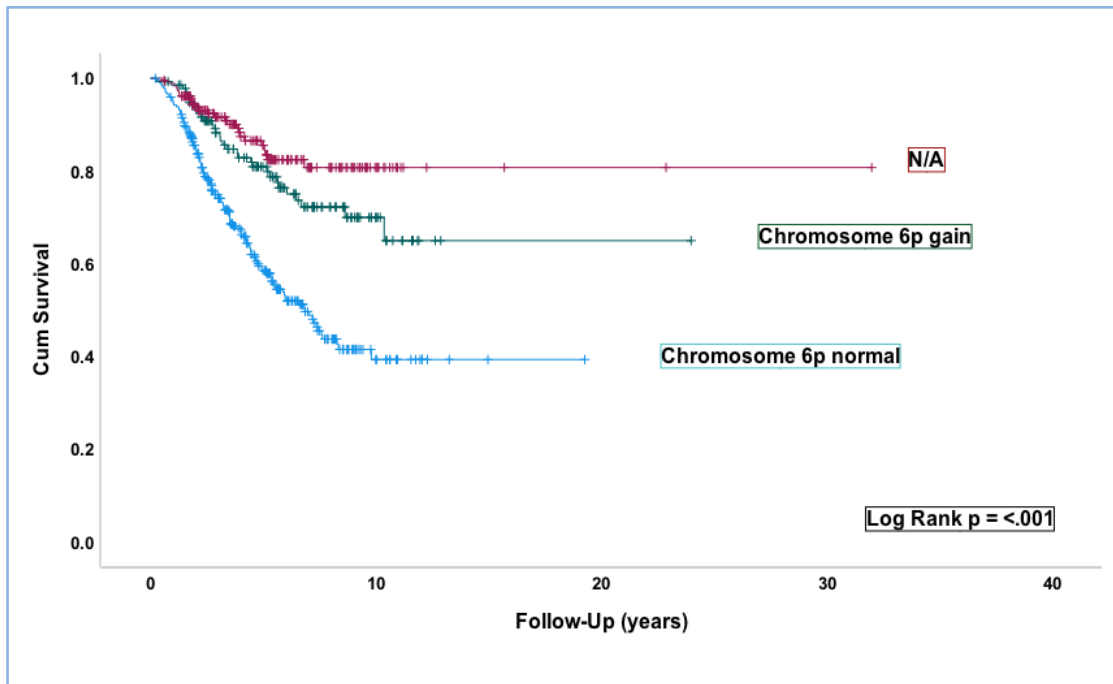
Chr1p	Number of patients (%)		Number of metastases (%)		Number of events %		Censored %		Mean survival (years)	95% confidence interval	
										Lower	Upper
Normal	297	48.3%	124	41.8%	102	34.3%	195	65.7%	14.726	13.256	16.197
Loss	135	29.7%	71	34.8%	60	44.4%	75	55.6%	7.808	6.572	9.045
N/A	183	29.8%	34	18.6%	25	13.7%	158	86.3%	26.481	24.439	28.523
Overall	615	100%	229	37.4%	187	30.4%	428	69.6%	19.742	18.193	21.290

Figure 2.10: Kaplan-Meier survival curve and table where number of metastases, metastatic mortality and patient survival were stratified according to copy number of chromosome 1p normal ($n=297$), loss ($n=135$) and N/A ($n=183$) ($p= < .001$). The number of events indicates the number of patients who died of liver metastases.



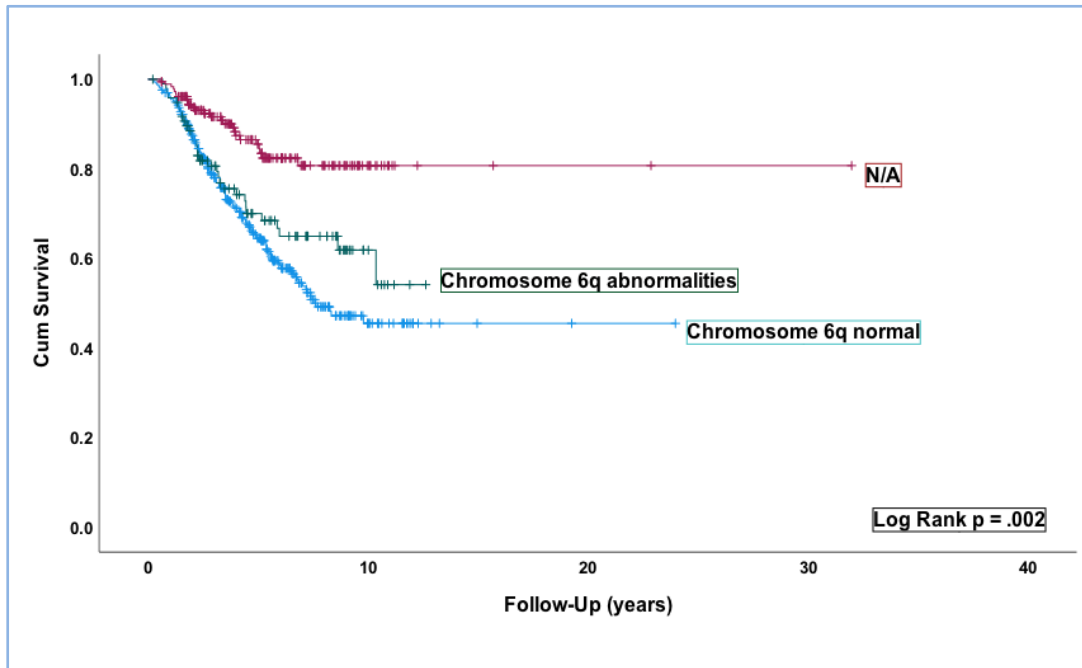
Chr3	Number of patients (%)		Number of metastases (%)		Number of events %		Censored %		Mean survival (years)	95% confidence interval	
										Lower	Upper
Normal	220	35.8%	39	17.7%	23	10.5%	197	89.5%	27.785	24.347	29.223
Loss	330	53.7%	179	54.2%	153	46.4%	177	53.6%	9.211	8.115	10.307
N/A	65	10.6%	11	16.9%	11	16.9%	54	83.1%	10.362	9.364	11.361
Overall	615	100%	229	37.4%	187	30.4%	428	69.6%	19.742	18.193	21.290

Figure 2.11: Kaplan-Meier survival curve and table where number of metastases, metastatic mortality and patient survival were stratified according to copy number of chromosome 3 normal ($n=220$), monosomy ($n=330$) and N/A ($n=65$) ($p= <0.001$). The number of events indicates the number of patients who died of liver metastases.



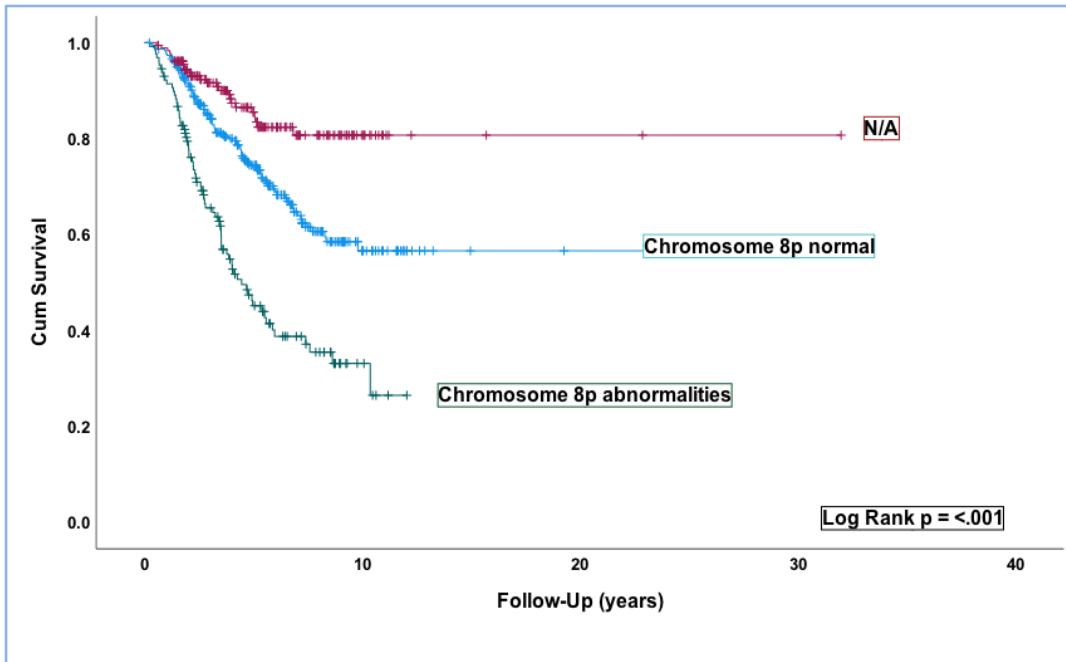
Chr6p	Number of patients (%)		Number of metastases (%)		Number of events %		Censored %		Mean survival (years)	95% confidence interval	
										Lower	Upper
Normal	295	48%	151	51.2%	130	44.1%	165	55.9%	10.005	8.868	11.141
Gain	137	22.3%	44	24.8%	32	23.4%	105	76.6%	17.299	15.124	19.473
N/A	183	22.8%	34	26.5%	25	13.7%	158	86.3%	26.481	24.439	28.523
Overall	615	100%	229	37.4%	187	30.4%	428	69.6%	19.742	18.193	21.290

Figure 2.12: Kaplan-Meier survival curve and table where number of metastases, metastatic mortality and patient survival were stratified according to copy number of chromosome 6p normal ($n=295$), gain ($n=137$) and N/A ($n=183$) ($p= <0.001$). The number of events indicates the number of patients who died of liver metastases.



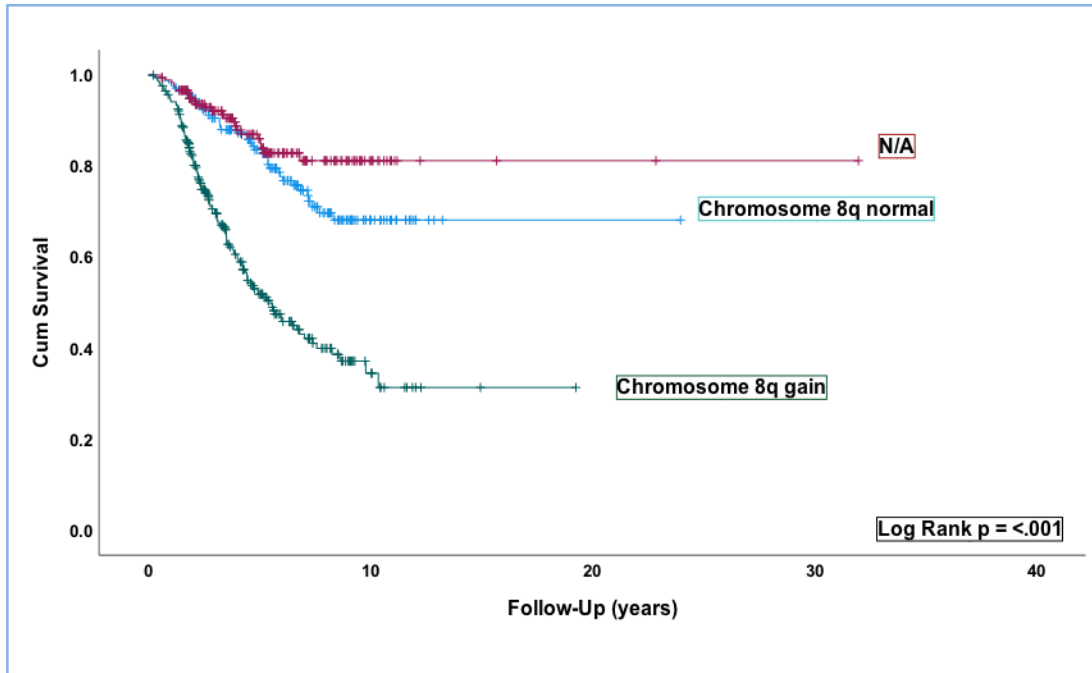
Chr6q	Number of patients (%)		Number of metastases (%)		Number of events %		Censored %		Mean survival (years)	95% confidence interval	
										Lower	Upper
Normal	334	54.3%	160	47.9%	131	39.2%	203	60.8%	13.163	11.753	14.573
Loss/Gain	98	15.9%	35	35.7%	31	31.6%	67	68.4%	8.922	7.874	9.969
N/A	183	36.9%	34	18.6%	25	13.7%	158	86.3%	26.481	24.439	28.523
Overall	615	100%	229	37.4%	187	30.4%	428	69.6%	19.742	18.193	21.290

Figure 2.13: Kaplan-Meier survival curve and table where number of metastases, metastatic mortality and patient survival were stratified according to copy number of chromosome 6q normal ($n=334$), loss/gain ($n=98$) and N/A ($n=183$) ($p= .002$). The number of events indicates the number of patients who died of liver metastases.



Chr8p	Number of patients (%)		Number of metastases (%)		Number of events %		Censored %		Mean survival (years)	95% confidence interval	
										Lower	Upper
Normal	303	49.3%	114	37.6%	91	30.1%	212	70.0%	15.496	14.039	16.953
Loss/Gain	129	21%	81	36.4%	71	55%	58	45.0%	6.078	5.225	6.930
N/A	183	36.9%	34	18.6%	25	13.7%	158	86.3%	26.481	24.439	28.523
Overall	615	100%	229	37.4%	187	30.4%	428	69.6%	19.742	18.193	21.290

Figure 2.14: Kaplan-Meier survival curve and table where number of metastases, metastatic mortality and patient survival were stratified according to copy number of chromosome 8p normal (n=303), loss/gain (n=129) and N/A (n=183) (p= <0.001). The number of events indicates the number of patients who died of liver metastases.



Chr8q	Number of patients (%)		Number of metastases (%)		Number of events %		Censored %		Mean survival (years)	95% confidence interval	
										Lower	Upper
Normal	176	29.6%	50	28.5%	41	23.3%	135	76.7%	17.807	16.170	19.443
Gain	257	41.8%	146	56.8%	122	47.5%	135	52.5%	8.847	7.568	10.127
N/A	182	29.6%	33	18.1%	24	13.2%	158	86.8%	26.621	24.587	28.656
Overall	615	100%	229	37.4%	187	30.4%	428	69.6%	19.742	18.193	21.290

Figure 2.15: Kaplan-Meier survival curve and table where number of metastases, metastatic mortality and patient survival were stratified according to copy number of chromosome 8q normal (n=176), gain (n=257) and N/A (n=182) (p= <0.001). The number of events indicates the number of patients who died of liver metastases.

2.3.4 Liver screening analysis

2.3.4.1 Frequency and modality of the scans

During the screening period, the enrolled patients underwent in total 3854 scans, of which 2419 were MRI; 945 US; and 490 CT (**Table 2.3**). The median number of scans per patient was 6.2 (range 1-40). These data will be analysed in more detail, with respect to the Health Economic Costs, in **chapter 3**.

Table 2.3: Patients grouped according to the modality and the frequency of scans performed

Modality of scan	Years											Total
	2008	2009	2010	2011	2012	2013	2014	2015	2016	2017	2018	
MRI	221	240	152	418	185	165	429	235	182	119	73	2419
Median	6.8	8.3	5.6	7.9	6.2	7.9	8.9	7.1	5.9	4.9	2.9	6.8
Range	(1-22)	(1-21)	(1-16)	(1-21)	(1-19)	(1-17)	(1-21)	(1-12)	(1-14)	(1-12)	(1-9)	(1-22)
US	51	44	79	176	69	73	104	114	59	86	90	945
Median	2.2	1.5	2.3	3.1	1.8	1.6	2.5	2.4	1.6	2.3	1.8	2.1
Range	(1-12)	(1-5)	(1-17)	(1-17)	(1-15)	(1-11)	(1-11)	(1-11)	(1-7)	(1-6)	(1-5)	(1-17)
CT	34	62	36	101	46	23	79	39	30	18	22	490
Median	2.3	3.9	3	3.6	3.8	3.8	3.6	3	2.1	2.3	3.7	3.2
Range	(1-5)	(1-11)	(1-14)	(1-13)	(1-20)	(1-8)	(1-10)	(1-8)	(1-4)	(1-6)	(2-7)	(1-20)
Total	306	346	267	695	300	261	612	388	271	223	185	3854
Median	6.8	7.4	5.1	8.7	5.6	4.6	9.3	6.8	5.3	4.5	3.3	6.2
Range	(1-22)	(1-22)	(1-25)	(1-34)	(1-40)	(1-27)	(1-30)	0	(1-18)	(1-20)	(1-16)	(1-40)

MRI = Magnetic Resonance Imaging
CT = Computed tomography
US = Ultrasound

As described above in the Material and Methods, the number of scans per patient was accessed in 5-year groups. Of the 615 patients, 353 (57.3%) were categorized to group 1-5, 119/615 (19.4%) to group 6-10, 90/615 (14.6%) to group 11-15, 34/615 (5.7%) to group 16-20, and 19/615 (2.9%) to group >20 (Table 2.4).

Table 2.4: Patients grouped according to the number of scans per patient

Liver Scans	Years											Total
	2008	2009	2010	2011	2012	2013	2014	2015	2016	2017	2018	
	Number of patients											
	45	47	52	80	54	57	66	57	51	50	56	615
Number scans												
1-5	22	24	34	36	38	42	17	28	25	37	50	353
6-10	10	10	9	12	5	6	18	13	21	11	4	119
11-15	8	6	5	19	5	6	24	11	4	1	1	90
16-20	4	5	3	9	2	0	4	4	1	1	1	34
>20	1	2	1	4	4	3	3	1	0	0	0	19

2.3.4.2 Regularity of liver surveillance

Each UM patient enrolled in the study underwent a number of scans, as indicated. From our retrospective analysis, it was observed that some patients ceased their screening program for varying reasons, i.e., presumably, patients underwent the rest of the follow-up in local hospitals at their request, or the program screening has ended. As mentioned in the Material and Methods, liver screening in this study was considered to be “regular” (*when more than one scan was performed*) or “irregular” (*when for different possible reasons only one scan was performed*). Therefore, it was found that; 407/615 (66.2%) patients had regular scanning in Liverpool, while in 208/615 (33.8%) patients, scanning was ‘irregular’. Kaplan-Meier survival curves and tables were examined for all patients according to the regularity of the liver screening (Log rank test, $p = 0.043$). An improvement in survival was observed in patients who had “regular” scanning (Figure 2.15).

Of the patients who had regular scanning, 246/407 (60.4%) never demonstrated metastases, while 161/407 (39.6%) patients were diagnosed of hepatic metastases, 142/161 (88.2%) of

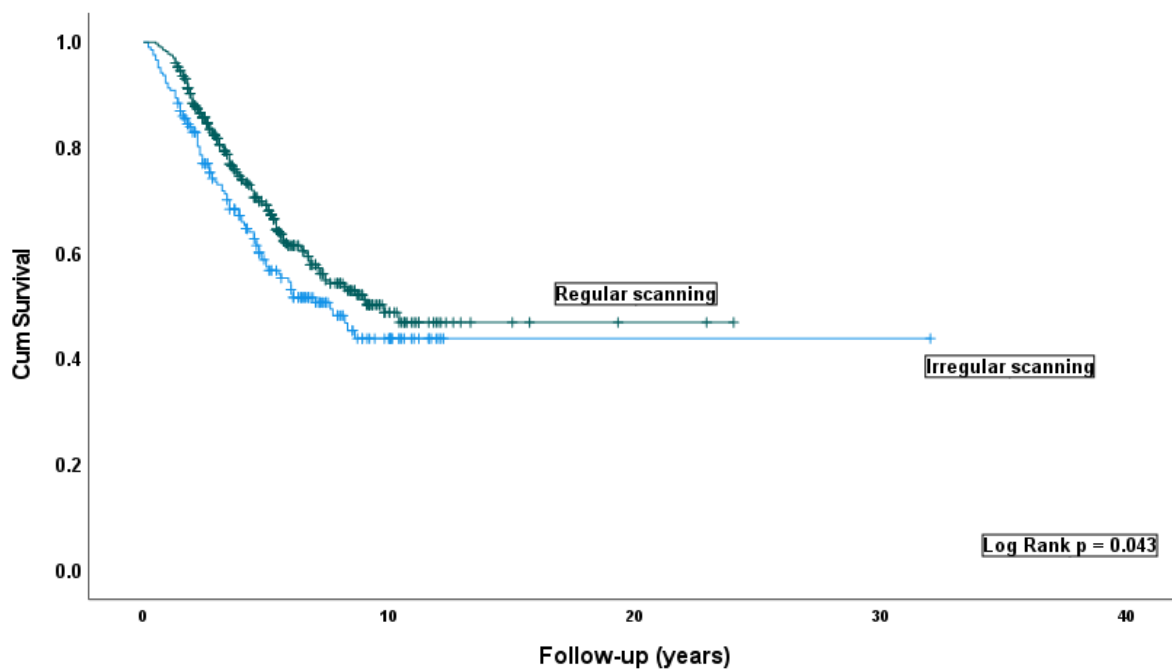
whom through the liver screening, and in 19/161 (11.8%) patients, metastases were only detected post-mortem.

With regard to UM patients in the “irregular” scanning cohort, in 68/208 (32.7%) of the patients, metastases were detected with no metastases being observed in 140/208 (67.3%) patients. Most of these metastases were detected post-mortem 60/68 (88.2%). Unfortunately, all of these patients died, 67/68 (98.5%) of liver metastases, and 1/68 (1.5%) patient of unknown causes (**Figure 2.16**). Due to the fact that a considerable number of patients had irregular surveillance, the general characteristics of patients with irregular surveillance were analysed in detail as shown in **Table 2.5**.

This group of patients with the ‘irregular’ surveillance comprised 119/208 (57.2%) males and 89/208 (42.8%) females with a median age of 62 years at primary management (range, 23-87 years). The median LBD and UH of the primary UM had a median of 15.3 mm and 7.8 mm, respectively. 76/208 (36.5%) involved the ciliary body and 24/208 (11.5%) had EOE. 106/208 (51%) UM contained epithelioid cells and 92/208 (44.2%) contained PAS+ loops. Mitotic count was assessed in 148/208 (71.2%) tumours; most between 4-7 mitotic figures in 40 high-powered fields 58/148 (39.2%). The majority of the cases were monosomy 3 - 98/208 (47.1%), and showed chromosome 8q gains in 91/208 (43.8%).

Patients had a median time from primary treatment to the first and only scan of 0.4 years (4 months) (range, 0.1-26.1 years). The most frequent modality of scan was US - 179/208 (86.1%), with 6/179 (3.4%) in patients who developed metastases and 173/179 (96.6%) in patients who did not demonstrated metastases by clinical imaging. In 8/208 (4%) patients, metastases were detected in the only scan performed.

The median follow-up time was 4.9 years (range, 0.2-32 years). At the end of this study 116/208 (55.8%) patients of this group were still alive, and 92/208 (44.2%) died whose causes were: melanoma metastases in 67/92 (72.8%), other causes in 9/92 (9.8%), and unknown causes in 16/92 (17.4%) patients (**Table 2.5**).



Regularity Of scanning	Total Number (%)	Absence of Metastases (%)	Number of metastases detected		Number of events (%)	Censored		Sig.	Mean survival (years)	95% confidence interval	
			Ante-mortem (%)	Post-mortem (%)		Number	Percent			Lower	Upper
Regular	407 (66.2%)	246 (60.4%)	142 (34.9%)	19 (4.7%)	120 (29.5%)	259	63.6%	P= .043	16.033	13.656	18.411
Irregular	208 (33.8%)	140 (67.3%)	8 (3.8%)	60 (28.8%)	67 (32.2%)	116	55.8%	P= .043	13.617	12.272	14.962
Overall	615	386 (62.8%)	150 (24.4%)	79 (12.8%)	187 (30.4%)	375	61.0%		16.971	15.470	18.471

Figure 2.16 Kaplan-Meier survival curve and table for patients stratified according to regularity of the liver screening. Based on regularity of the scanning, all Patients were classified as: Regular ($p = .043$) in 407 patients, and Irregular ($p = .043$) in 208 patients. Patients were also stratified according to the development of metastases. It was calculated the number of patients who did not developed metastases, and patients who developed metastases. Metastases were stratified according to the method metastases were detected (ante-mortem, and post-mortem). The number of events indicates the number of patients who died of liver metastases.

Table 2.5: Characteristics of 208 patients who had only one scan during the liver screening study

Features of the patients	Years											Total
	2008	2009	2010	2011	2012	2013	2014	2015	2016	2017	2018	
	Number of patients											
	13	12	24	22	28	32	14	17	16	11	19	208
Age at Primary treatment (Years)												
Median (Range)	52 (34-69)	59 (28-82)	63 (31-90)	65 (33-93)	64 (34-86)	62 (28-87)	63 (43-81)	68 (34-88)	63 (23-82)	54 (32-55)	63 (65-87)	62 (23-87)
Sex												
Female	6	5	10	11	10	12	6	7	9	3	10	89
Male	7	7	14	11	18	20	8	10	7	8	9	119
LBD (mm)												
Median (Range)	14.5 (10-19.4)	16.2 (5.8-23.6)	17.1 (7.8-23.8)	16.4 (5.8-22.2)	16.1 (7.1-20.4)	15.4 (6.3-21.2)	14.9 (5.9-21.7)	15.5 (5.6-22.3)	13.6 (6.8-20.0)	12.4 (8.8-16.3)	14.0 (5.5-20)	15.3 (5.5-23.8)
UH (mm)												
Median (Range)	6.5 (1.5-12.5)	6.1 (1.4-12.3)	7.7 (1.4-14.9)	8.2 (1.3-13)	8.4 (2.3-18.3)	8.3 (1.7-14.5)	8.3 (1.6-16.6)	10.2 (1.2-18.5)	6.9 (1.8-14.0)	5.7 (3.0-9.8)	6.9 (2.5-13.6)	7.8 (1.2-18.5)
CBI												
No	12	7	14	14	17	20	8	8	8	10	14	132
Yes	1	5	10	8	11	12	6	9	8	1	5	76
Extraocular Melanoma												
No	12	12	21	21	23	28	10	15	15	10	17	184
Yes	1	0	3	1	5	4	4	2	1	1	2	24
Epithelioid cells present												
No	6	4	8	10	11	14	6	9	7	7	9	91
Yes	5	7	14	12	15	17	7	8	7	4	10	106
N/A ¹	2	1	2	0	2	1	1	0	2	0	0	11
Closed PAS+ Loops												
No	3	3	7	12	5	9	5	12	0	2	0	58
Yes	3	5	10	7	15	18	6	5	9	2	12	92
N/A ²	7	4	7	3	8	5	3	0	7	7	7	58
MITOC												
0-1	1	1	3	0	2	7	3	0	0	0	0	17
2-3	2	4	1	6	2	7	2	7	7	1	6	45
4-7	2	0	7	5	11	12	5	7	2	3	4	58
>7	1	3	6	8	5	1	1	1	0	0	2	26
N/A ²	7	4	7	3	8	5	3	2	7	7	7	60
Chr1p												
Normal	7	8	13	9	8	14	8	12	3	4	6	92
Loss	3	1	3	5	8	11	2	3	5	2	5	48
Other ¹												
N/A ³	3	3	8	8	12	7	4	2	8	5	8	68
Chr3												
Normal	9	5	6	3	3	12	5	7	5	5	11	71
Monosomy	2	4	12	9	20	15	7	8	6	4	7	94
Other ²												
N/A ⁴	2	3	6	10	5	5	2	2	5	2	1	43
Chr6p												
Normal	3	5	11	9	10	9	6	9	7	1	9	79
Gain	6	2	5	7	2	10	4	6	1	5	2	50
Other ³												
N/A ³	4	5	8	6	16	13	4	2	8	5	8	79

Table 2.5: (continued)

Features of the patients	Years											Total
	2008	2009	2010	2011	2012	2013	2014	2015	2016	2017	2018	
	Number of patients											
	13	12	24	22	28	32	14	17	16	11	19	208
Chr6q												
Normal	6	6	7	11	13	15	8	12	6	4	11	99
Loss/Gain	3	2	4	7	4	11	1	3	2	2	1	40
Other ^d												
N/A ^e	4	4	13	4	11	6	5	2	8	5	7	69
Chr8p												
Normal	7	6	8	5	8	12	9	10	5	6	10	86
Loss/Gain	2	3	6	10	10	7	2	5	3	0	2	50
Other ^d												
N/A ^e	4	3	10	7	10	13	3	2	8	5	7	72
Chr8q												
Normal	3	2	7	5	5	9	2	8	2	3	3	49
Gain	5	5	11	10	14	14	9	7	5	3	8	91
Other ^d												
N/A ^e	5	5	6	7	9	9	3	2	9	5	8	68
Time to the only scan (years)												
Median	3.1	0.4	0.8	0.3	0.2	0.2	0.2	0.1	0	0.2	0.1	0.4
(Range)	(0-26)	(0-4.6)	(0-9.4)	(0-2.3)	(0-4.4)	(0-3.2)	(0-2.1)	(0-2.1)	(0-0.1)	(0-1)	(0-0.6)	(0.1-25.1)
Liver screening in patients in whom metastases were not detected antemortem, but were found post-mortem												
HMDA	4	4	8	9	17	9	4	2	3	0	0	60
Modality of the scans												
MRI	3	0	1	3	3	0	0	0	0	0	0	11
US	1	4	6	6	14	9	4	2	3	0	0	48
CT	0	0	1	0	0	0	0	0	0	0	0	1
Liver screening undertaken in patients in whom metastases were found antemortem												
HMDCI	0	1	2	2	1	0	0	2	0	0	0	8
Modality of the scans												
MRI	0	0	0	0	1	0	0	1	0	0	0	2
US	0	1	2	2	0	0	0	1	0	0	0	6
CT	0	0	0	0	0	0	0	0	0	0	0	0
Liver screening in patients not demonstrating metastases												
Modality of the scans												
MRI	5	0	4	4	7	2	1	1	0	0	1	25
US	8	10	17	16	20	30	13	14	16	11	18	173
CT	0	1	1	0	0	0	0	0	0	0	0	2
Outcome												
Follow-up Time (Years)												
Median	11	7.4	6.2	4.7	4.4	5.4	4.3	3.7	3.0	2.4	1.8	4.9
(Range)	(2.3-32)	(0.4-11.2)	(0.8-10.1)	(0.2-9.2)	(0.4-8.1)	(0.9-7.3)	(0.6-6.3)	(0.7-5.2)	(0.2-4.2)	(0.6-2.8)	(1.4-2.1)	(0.2-32)
Status												
Alive	8	7	9	7	9	21	6	9	11	10	19	116
Dead	5	5	15	15	19	11	8	8	5	1	0	92
Cause of death												
Metastatic	4	5	10	11	18	9	4	3	3	0	0	67
Other	1	0	1	4	1	1	0	0	1	0	0	9
Unknown	0	0	4	0	0	1	4	5	1	1	0	16

HMDA: Hepatic metastases diagnosed by autopsy

HMDCI: Hepatic metastases diagnosed by clinical imaging

2.3.4.3 Detection of metastases at time of the primary treatment

In many centres, liver imaging tests are performed at the time of diagnosis or only when treatment of the primary UM is planned. In the present study, 286/615 (46.5%) had their first scan at the time of the first treatment. Of these, in 7/286 (2.4%) patients, metastases were detected in the liver scan. 6/286 (2.1%) patients had liver lesions suspicious of metastases, which were confirmed in subsequent examinations between 0 and 6 years later (**Figure 2.17**).

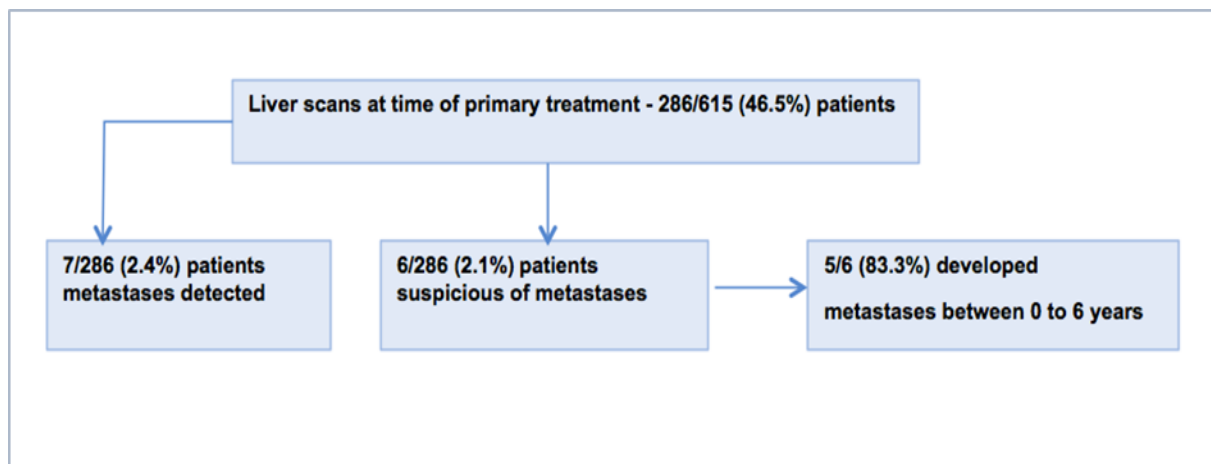


Figure 2.17 Patients who had a first liver scan at time of the primary treatment.

2.3.5 Management of metastatic disease

Screening detected metastases in 150/615 (24.4%) patients (**Figure 2.18**). However, after the provision of information from the pathology reports into the study, it was found that a total of 187/615 (30.4%) patients were diagnosed of metastatic disease post-mortem. It would appear that in 79/187 (42.3%) of these patients, metastases were never detected during the liver screening period. There was no access to information on the detection of these metastases ante-mortem, because the patients underwent liver surveillance examinations in other hospitals and metastases were detected in those hospitals, or the surveillance program for certain patients has been interrupted; and/or patients abandoned the surveillance program.

Thus, a total of 229/615 (37.3%) patients were diagnosed of liver metastases during this study. It can also be shown in **Figure 2.18** that a total of 108/150 (93.9%) patients in which melanoma

metastases were detected by clinical imaging, died. 4/150 (3.5%) patients died of other causes unrelated to UM metastases, and 3/150 (3.5%) died of unknown causes. 35/150 (23.3%) patients developed UM metastases at some point during the course of their illness and were still alive at the end of this study.

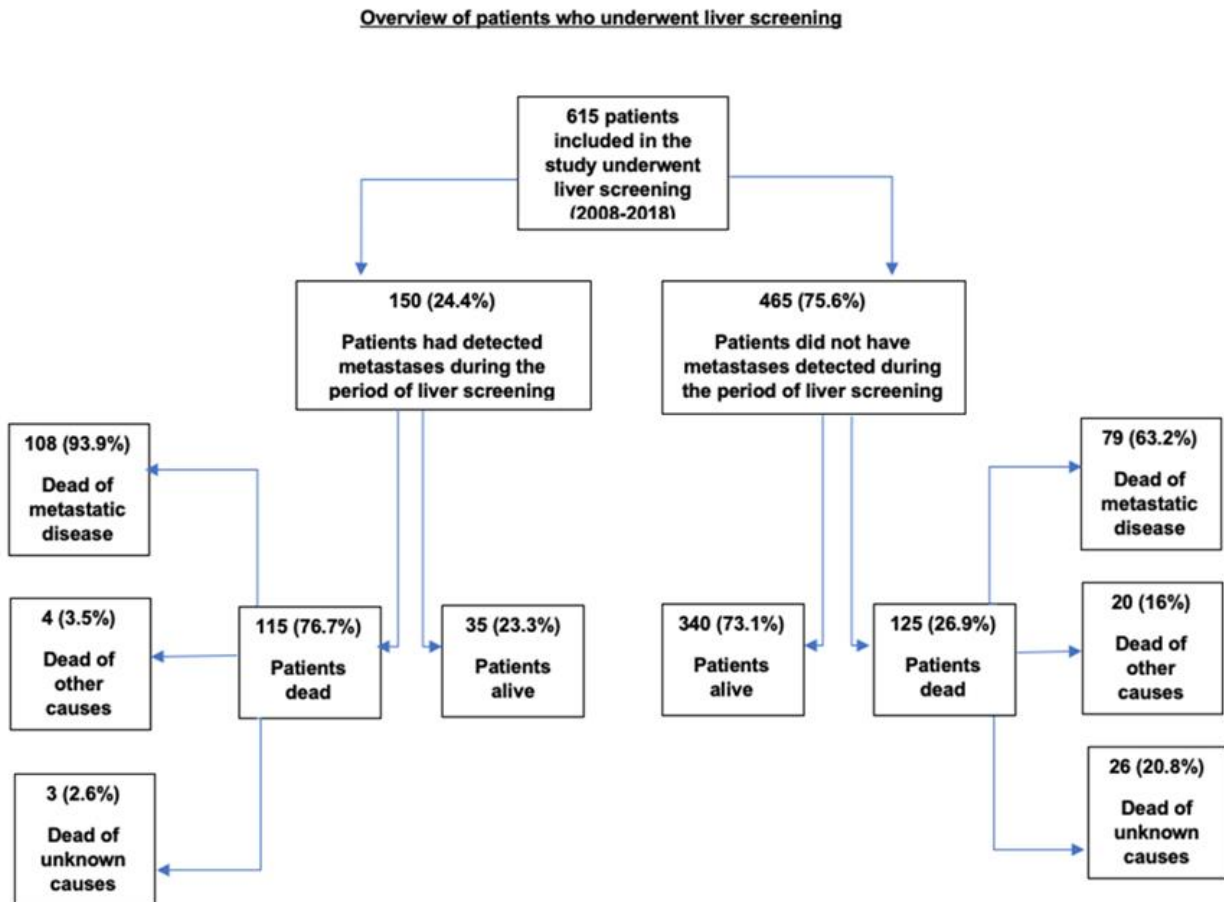


Figure 2.18 Patients distribution scheme. This scheme represents the assessment of the 615 patients initially evaluated regarding their outcome considering the detection of metastases and cause of death.

2.3.5.1 Characteristic of detected hepatic metastases through liver surveillance

With respect the number of metastases detected through the clinical imaging, 17/150 (11.3%) patients had between 0-1 metastases, and 133/150 (86.7%) had more than 1 metastases (Table 2.6).

Table 2.6: Number of liver metastases detected through liver surveillance in the 615 UM patients

Number of Metastases per patient	Years											Total
	2008	2009	2010	2011	2012	2013	2014	2015	2016	2017	2018	
0	25	30	38	54	42	52	46	42	40	46	50	465
0 - 1	4	1	2	4	0	1	0	2	1	2	0	17
> 1	16	16	12	22	12	4	20	13	10	2	6	133
Total	45	47	52	80	54	57	66	57	51	50	56	615

The metastases detected were categorized according to their size, location and AJCC TNM staging. The median LDLM was 35.98 mm (range 4-196 mm). Most of the metastases were located in both hepatic lobes 70/150 (46.7%). With regard to the size of metastases, most measured less than 30 mm [87/150 (58%)] and hence categorized as M1a; 50/150 (33.3%) measured between 31 and 80 mm (M1b); and 13/150 (8.7) % measured more than 80 mm (M1c) (Table 2.7). Of these 150 patients, 18 (12%) were found to have extrahepatic metastases, located in the lung, skin, bone, peritoneum, and para-aortic lymph nodes (Table 2.8).

Table 2.7: Size, location and TNM staging of the detected metastases (n=150 patients)

Characteristic of the metastases	Years											Total
	2008	2009	2010	2011	2012	2013	2014	2015	2016	2017	2018	
	Number of patients											
	20	17	14	26	12	5	20	15	11	4	6	150
LDLM (mm)												
Median	38.3	48.7	18.9	26.7	21.8	29.9	65.8	27.6	33.4	33.95	33.2	35.98
Range	(4-167)	(8-127)	(6-42)	(10-63)	(5-84)	(9-76.7)	(10-196)	(4-68)	(5-77)	(16-82)	(10-104)	(4-196)
Location of metastases												
Right Lobe	10	13	6	6	3	1	7	2	3	1	2	54
Left Lobe	3	1	0	8	0	2	3	4	2	3	0	26
Bilobar	7	3	8	12	9	2	10	9	6	0	4	70
AJCC TNM category,												
<30 mm (M1a)	13	7	12	15	9	4	4	10	6	3	4	87
31-80mm (M1b)	4	9	2	11	2	1	10	5	5	0	1	50
>80mm (M1c)	3	1	0	0	1	0	6	0	0	1	1	13

*LDLM - Largest diameter of the largest metastases.
AJCC TNM - American Joint Committee on Cancer - Tumour, Node, Metastases System.*

Table 2.8: Extra hepatic metastases in the 150 patients in whom metastases were detected during the liver screening study

Extra hepatic metastases (M1)	2008	2009	2010	2011	2012	2013	2014	2015	2016	2017	2018	Total
Lung	0	0	1	2	0	0	1	0	0	0	1	5
Systemic carcinomatosis	1	0	1	1	0	0	0	0	0	0	0	3
Lung + subcutaneous + bone	0	1	0	0	0	0	1	0	0	0	0	2
Bone + para-aortic lymph nodes	1	0	0	0	0	0	0	0	0	0	0	1
Lung + peritoneum + bone	0	0	0	0	0	0	0	0	0	0	1	1
Lung + subcutaneous	0	0	0	1	0	0	0	0	0	0	0	1
Peritoneum	1	0	0	1	0	1	0	0	0	0	0	3
Bone	0	0	0	1	0	0	0	0	0	0	0	1
Lung + peritoneum + subcutaneous	0	1	0	0	0	0	0	0	0	0	0	1
Total	3	2	2	6	0	1	2	0	0	0	2	18

M1: TNM staging - There is metastases to other parts of the body.

2.3.5.2 Metastases-related mortality

Of the 150 patients whose metastases were demonstrated by clinical imaging, 81 (54.7%) developed metastases within 2 years after the primary treatment of the tumour; 27/150 (18%) developed metastases between 2-3 years; and in 42/150 (28%) patients' metastases developed after 3 years of the primary treatment (**Table 2.9**). The median time observed between the primary treatment and the detection of the first metastases was 2.6 years (range 0 to 17.8 years). The median time between the detection of the first metastases to death was 1 year (range 0.1-4.3 years). Of the 115 patients who died, 98 (85.2%) died within 2 years after the development of metastatic disease; 11/115 (9.6%) died 2-3 years later, and 6/115 (5.2%) patients died after 3 years of the first detected metastases. 35/150 (23.3%) patients were still alive at the close of this study. This group of 35 patients had a median follow-up time of 7 years (range, 1.6-19.3). The median time from the primary treatment to the first metastases was 4.6 years (range, 0.2-17.8). Of these, 5/35 (14.3%) patients developed metastases within 1 year, 3/35 (8.6%) between 1-2 years, 8/35 (22.9%) between 2-3 years, and 19/35 (54.3%) after 3 years.

Table 2.9: 150 UM Patients grouped according to time to first metastases detection to death

Time (years)	Years											Total
	2008	2009	2010	2011	2012	2013	2014	2015	2016	2017	2018	
	Number of patients with detected metastases											
	20	17	14	26	12	5	20	15	11	4	6	150
Primary treatment to 1st metastases												
< 2	8	11	9	14	6	1	7	7	9	3	6	81
2-3	3	2	1	4	1	2	7	4	2	1	0	27
> 3	9	4	4	8	5	2	6	4	0	0	0	42
First metastases to death												
< 2	10	14	10	18	9	2	15	9	9	0	2	98
2-3	4	1	1	2	0	1	2	0	0	0	0	11
> 3	0	2	2	2	0	0	0	0	0	0	0	6
Time from primary treatment to first metastases												
Median	5.2	2.2	1.9	2.4	2.8	3.2	2.6	2.1	1.3	1.3	0.7	2.6
(Range)	(0.4-17.8)	(0.1-6.9)	(0.1-4.7)	(0.1-8.4)	(0.1-6.5)	(1.2-6.3)	(0.7-4.6)	(0.1-4.3)	(0.4-2.7)	(0.2-2.7)	(0.1-1.2)	(0.1-17.8)
Time from onset metastases to death												
Median	1.0	1.5	1.5	1.0	0.5	0.8	1.1	0.6	0.6	0	0.4	1.0
(Range)	(0.1-3.0)	(0.4-4.1)	(0.1-4.3)	(0.1-3.9)	(0.1-2.0)	(0.1-2.8)	(0.1-2.2)	(0.1-2.0)	(0.3-1.3)	0	(0.1-1.4)	(0.1-4.3)
Outcome												
Alive	6	0	1	4	3	2	3	6	2	4	4	35
Death	14	17	13	22	9	3	17	9	9	0	2	115

2.3.6 Categorizing 615 patients into 3 groups according to when and whether patients had metastases

As mentioned in Material and Methods, the 615 patients were categorized into three distinct groups. Clinical, histological, and genetic characteristics, and also the findings on liver screening, and outcome of the patients, are listed in tables 2.10, 2.11 and 2.12. Overall, it was found an improvement in survival from Group 1, Group 2 to Group 3 (log rank, $p = <0.001$) (Figure 2.19).

Table 2.10 shows the 108 UM patients (Group 1) who developed metastases *within 2 years after the diagnosis of the primary tumour*. This group of patients consisted of 59/108 (54.6%)

males and 49/108 (45.4%) females with a median age of 66 years at primary management (range, 38-93 years). In 81/108 (75%) patients, the diagnosis of metastases was demonstrated by clinical imaging, and in 27/108 (25%) patients, the metastases were established at autopsy.

The primary UM of this Group had a median LBD of 17 mm (range, 7-26 mm), and a median UH of 9 mm (range, 1.5-20 mm). 51/108 (47.2%) involved the ciliary body and 20/108 (18.5%) had extraocular extension. 82/108 (75.9%) tumour samples contained epithelioid cells and 70/108 (64.8%) contained PAS+ loops. Mitotic count could be assessed in 87/108 (80.5%) tumours, with most showing between 4-7 mitotic figures in 40 high-powered fields 40/87 (45.9%). The majority of the cases were monosomy 3 - 91/108 (84.3%).

With respect to liver screening findings, in patients in whom metastases were found ante-mortem, a total of 588 scans were performed 190 times in 81 patients, with a median of 7.3 scans per patient (range, 1-25). 324/588 (55.1%) of these scans were MRI, 161/588 (27.4%) were CT and 103/588 (17.6%) were US.

In the 27 UM patients in whom the metastases were detected at post-mortem only (within 2 years of diagnosis of the primary UM), a total of 36 scans has been performed, with a median of 1.1 (range, 1-4). 10/36 (27.8%) of these scans were MRI, 3/36 (8.3%) were CT and 23/36 (63.9%) were US. Overall, the 108 patients in this group averaged 5.7 scans per patient (range, 1-40). The median follow-up was 1.9 years (range, 0.2-5.6 years).

At the time of study closure, on 15/05/2020, only 8/108 (7.4%) Group 1 patients were alive, 100/108 (92.6%) had died; 96/100 (96%) from metastatic disease, 3/100 (3%) patients died from other causes, and 1/100 (1%) patient died from unknown causes.

Table 2.10: Characteristics of 108 uveal melanoma patients who developed metastases within 2 years of diagnosis of the ocular tumour

Features of the patients	Years											Total
	2008	2009	2010	2011	2012	2013	2014	2015	2016	2017	2018	
	Number of patients											
	8	13	12	15	14	5	11	9	11	4	6	108
Age at Primary treatment (Years)												
Median	62	64	67	61	72	70	67	63	70	73	61	66
(Range)	(41-69)	(44-82)	(53-80)	(38-93)	(57-88)	(56-81)	(39-88)	(34-88)	(45-80)	(68-80)	(42-65)	(38-93)
Sex												
Female	2	7	5	7	7	0	6	8	5	2	0	49
Male	6	6	7	8	7	5	5	1	6	2	6	59
LBD (mm)												
Median	17.7	16	17.6	17.2	16.4	16.6	17.5	18.5	15.4	17.5	18.3	17
(Range)	(9.8-21)	(10-20.3)	(9.7-26)	(15-21)	(7-22.6)	(14-18.2)	(13.9-21)	(14-22.5)	(9.4-22)	(14.5-22)	(13.3-23)	(7-26)
UH (mm)												
Median	6.8	6.5	10.6	10.3	8.8	12.1	9.2	9.2	8.6	10.6	8.2	9
(Range)	(2.2-12)	(1.6-12.3)	(2.8-15)	(1.8-15.4)	(1.5-17.4)	(10-14.6)	(4.5-16.6)	(3.9-15)	(2.9-16)	(4.7-20)	(4.1-13)	(1.5-20)
CBI												
No	4	8	7	10	9	3	5	3	5	1	2	57
Yes	4	5	5	5	5	2	6	6	6	3	4	51
Extra ocular Melanoma												
No	7	13	10	13	9	5	6	8	10	3	4	88
Yes	1	0	2	2	5	0	5	1	1	1	2	20
Epithelioid cells present												
No	3	3	2	3	2	1	1	3	2	1	2	23
Yes	5	10	10	12	11	4	10	6	7	3	4	82
N/A ¹	0	0	0	0	1	0	0	0	2	0	0	3
Closed PAS+ Loops												
No	2	1	2	5	2	1	2	1	0	0	1	17
Yes	3	8	10	8	10	4	8	6	6	3	4	70
N/A ¹	3	4	0	2	2	0	1	2	5	1	1	21
MITOC												
0-1	0	0	0	0	0	3	1	0	0	0	0	14
2-3	2	0	1	1	1	1	2	0	2	0	2	12
4-7	2	3	4	4	9	1	3	6	3	2	3	40
>7	1	6	7	8	2	0	4	1	1	1	0	31
N/A ²	3	4	0	2	2	0	1	2	5	1	1	21
Chr1p												
Normal	1	5	7	5	4	1	5	5	4	2	3	48
Loss	7	7	2	7	4	3	5	1	2	1	2	35
Other ¹	0	0	2	2	3	0	0	0	4	0	0	0
N/A ²	0	1	1	1	3	1	1	3	1	1	1	25
Chr3												
Normal	1	1	1	0	1	1	0	1	0	0	1	7
Monoosomy	7	11	9	15	12	4	10	7	8	3	5	91
Other ¹	0	0	2	0	0	0	1	0	1	1	0	5
N/A ²	0	1	0	0	1	0	0	1	2	0	0	5
Chr6p												
Normal	5	8	9	2	3	2	4	5	5	1	2	46
Gain	3	1	1	3	1	0	5	1	2	2	3	22
Other ¹	0	2	1	9	7	2	1	0	0	0	0	22
N/A ²	0	2	1	1	3	1	1	3	4	1	1	18

Table 2.10: (continued)

Features of the patients	Years											
	2012	2012	2012	2012	2012	2012	2012	2012	2012	2012	2012	2012
	Number of patients											
	8	13	12	15	14	5	11	9	11	4	6	108
Chr8q												
Normal	4	11	9	2	5	1	8	4	5	1	5	55
Loss/Gain	4	0	1	3	3	2	1	1	2	2	0	19
Other ^a	0	1	1	9	3	1	1	1	0	0	0	17
N/A ^b	0	1	1	1	3	1	1	3	4	1	1	17
Chr8p												
Normal	2	4	8	8	4	1	6	1	4	3	4	45
Loss/Gain	6	6	2	5	6	1	4	5	3	0	1	39
Other ^a	0	2	1	1	1	2	0	0	0	0	0	7
N/A ^b	0	1	1	1	3	1	1	3	4	1	1	17
Chr8q												
Normal	0	3	1	5	0	1	1	0	0	0	1	12
Gain	8	8	11	8	11	2	9	7	7	3	4	77
Other ^a	0	1	0	1	0	1	0	0	0	0	0	3
N/A ^b	0	1	0	1	3	1	1	2	4	1	1	16
Time to the first scan (years)												
Median	0.3	0.2	0.2	0.1	0.1	0	0.1	0	0.5	0.2	0.3	0.2
(Range)	0-0.6)	(0-0.8)	(0-0.4)	(0-0.4)	(0-0.4)	(0-0.01)	(0-0.4)	(0-0.1)	(0-1.7)	(0-0.4)	(0-1.2)	(0-1.7)
Liver screening in patients in whom metastases were not detected antemortem, but were found post-mortem												
HMDA	0	2	3	1	8	4	4	2	2	1	0	27
Scans per patient												
Median	0	1	1	1	1.2	1.7	2	1	1	2	0	1.3
(Range)	-	-	-	-	(1-2)	(1-4)	(1-4)	-	-	-	-	(1-4)
Modality of the scans												
MRI	0	0	1	0	2	2	3	0	0	2	0	10
US	0	2	1	1	7	4	4	2	2	0	0	23
CT	0	0	1	0	0	1	1	0	0	0	0	3
Liver screening undertaken in patients in whom metastases were found antemortem												
HMDCI	8	11	9	14	6	1	7	7	9	3	6	81
Scans per patient												
Median	6.7	8	6.6	5.5	4.7	9	8.6	8.4	6.4	13	9.6	7.3
(Range)	(3-12)	(1-17)	(1-25)	(1-12)	(2-7)	9	(6-12)	(1-23)	(2-12)	(8-20)	(3-16)	(1-25)
Modality of the scans												
MRI	36	44	33	41	13	5	38	32	33	21	28	324
US	9	9	8	16	9	1	11	12	9	9	10	103
CT	9	34	19	19	6	3	11	15	16	9	20	161
Outcome												
Follow-up Time (Years)												
Median	2.1	2.5	2.2	1.6	1.2	1.4	2.3	2.2	1.8	2.6	1.8	1.9
(Range)	(1.5-3.5)	(0.4-5.1)	(0.8-5.6)	(0.2-4.0)	(0.4-2.7)	(0.9-1.8)	(1-3.5)	(0.7-4.7)	(1.4-3.6)	(0.6-2.8)	(1.1-2.3)	(0.2-5.6)
Status												
Alive	0	0	0	0	0	0	0	1	0	3	4	8
Dead	8	13	12	15	14	5	11	8	11	1	2	100
Cause of death												
Metastatic	7	13	11	15	14	5	9	8	11	1	2	96
Other	1	0	1	0	0	0	1	0	0	0	0	3
Unknown	0	0	0	0	0	0	1	0	0	0	0	1
<i>HMDA: Hepatic metastases diagnosed by autopsy</i> <i>HMDCI: Hepatic metastases diagnosed by clinical imaging</i>												

Table 2.11 shows 121 UM patients (Group 2) *who developed metastases after 2 years of diagnosis of the primary tumour*. This group comprised 77/121 (63.6%) males and 44/121 (36.4%) females, with a median age of 60 years at primary treatment (range, 27-87 years). In 69/121 (57%) patients, the diagnosis of metastases was demonstrated by clinical imaging, and in 52/121 (43%) patients, the metastases were established at autopsy.

The primary tumours had a median LBD of 15.3 mm (range, 4.3-22 mm), and a median UH of 7.4 mm (range, 1-18.3 mm). 42/121 (47.2%) UM involved the ciliary body and 14/121 (18.5%) had EOE. Epithelioid cells were observed in 85/121 (70.2%) tumours and PAS+ loops in 49/121 (40.5%) tumours. Mitotic count was assessed in 87/121 (71.9%) tumours, the majority 34/87 (39.1%) showing between 4-7 mitotic figures in 40 high-powered fields. Most of the cases presented chromosome 3 loss, 88/121 (72.7%).

Liver screening in those patients in whom metastases were shown ante-mortem totalled 1012 scans, undertaken 169 times in 69 patients, median 14.6 (1-40). Of these scans, 637/1012 (62.9%) were MRI, 262/1012 (25.9%) was CT and 113/1012 (11.2%) was US. In those UM patients in whom the metastases were found post-mortem, a total of 104 scans were undertaken, 62 times in 52 patients, with a median of 2 scans per patient (range, 1-4). Of these scans, 60/104 (57.7%) were MRI, 3/104 (2.9%) was CT and 41/104 (39.4%) was US. Overall in this group, patients had an average of 9.3 scans per patient (range, 1-40).

The median follow-up was 5.5 years (range, 2.2-19.3 years). At the end of the study, 27/121 (22.3%) patients in this group 2 were alive, 94/121 (77.7%), patients had died; 91/94 (96.8%) from metastatic disease, 1/94 (1.1%) patient died from other causes, and 2/94 (2.1%) patients died from unknown causes.

Table 2.11: Characteristics of 121 patients who developed metastases after 2 years of diagnosis of the ocular tumour

Features of the patients	Years											
	2008	2009	2010	2011	2012	2013	2014	2015	2016	2017	2018	Total
	Number of patients											
	20	11	10	23	18	12	15	8	3	1	0	121
Age at Primary treatment (Years)												
Median	57	59	63	58	61	62	61	64	62	66	0	60
(Range)	(25-74)	(30-81)	(41-84)	(22-81)	(28-85)	(32-87)	(33-75)	(53-77)	(51-75)	(66)	0	(22-87)
Sex												
Female	7	4	5	13	3	5	4	3	0	0	0	44
Male	13	7	5	10	15	7	11	5	3	1	0	77
LBD (mm)												
Median	15.1	16.7	16.5	14.4	15.7	16.2	15.3	13.7	12.5	16.6	0	15.3
(Range)	(10-20.6)	(9.7-22)	(11-21.4)	(4.4-19.5)	(6.3-19.9)	(10-19.5)	(9.2-19.6)	(4.3-20.4)	(9.6-16.8)	-	0	(4.3-22)
UH (mm)												
Median	7.8	8.3	7.94	6.1	7.7	8.5	8.7	4.6	4.5	10.4	0	7.4
(Range)	(2.3-14.8)	(3.2-13.9)	(3.7-12.9)	(1.2-12.7)	(2.3-18.3)	(4.5-12.7)	(3.8-14.7)	(1-10.7)	(2.5-6.6)	-	0	(1-18.3)
CBI												
No	12	6	6	19	7	7	13	7	1	1	0	79
Yes	8	5	4	4	11	5	2	1	2	0	0	42
Extra ocular Melanoma												
No	17	11	8	22	15	12	10	8	3	1	0	107
Yes	3	0	2	1	3	0	5	0	0	0	0	14
Epitheloid cells present												
No	7	2	2	4	6	3	4	3	1	0	0	32
Yes	13	8	8	19	11	9	10	4	2	1	0	85
N/A ¹	0	1	0	0	1	0	1	1	0	0	0	4
Closed PAS+ Loops												
No	10	4	2	8	3	4	5	1	0	0	0	37
Yes	5	1	6	11	9	5	7	3	1	1	0	49
N/A ²	5	6	2	4	6	3	3	4	2	0	0	35
MITOC												
0-1	3	1	1	2	1	1	1	0	0	0	0	10
2-3	6	0	0	7	3	5	4	2	0	0	0	27
4-7	3	6	3	3	6	3	6	2	1	1	0	34
>7	2	0	4	7	2	0	1	0	0	0	0	16
N/A ²	6	4	2	4	6	3	3	4	2	0	0	34
Chr1p												
Normal	12	7	6	7	5	5	9	3	1	1	0	56
Loss	6	4	2	10	6	2	3	2	1	0	0	20
Other ¹	0	0	1	3	3	3	2	0	0	0	0	12
N/A ²	2	0	1	3	4	2	1	3	1	0	0	17
Chr3												
Normal	6	1	1	6	0	2	2	1	1	0	0	20
Monosomy	13	10	8	16	14	9	11	5	2	0	0	88
Other ²	0	0	0	1	2	0	2	1	0	1	0	7
N/A ¹	1	0	1	0	2	1	0	1	0	0	0	6
Chr6p												
Normal	13	8	7	6	8	1	9	4	2	1	0	59
Gain	4	2	1	4	1	4	4	1	0	0	0	21
Other ²	1	1	1	10	5	5	1	0	0	0	0	24
N/A ²	2	0	1	3	4	2	1	3	1	0	0	17

Table 2.11: (continued)

Features of the patients	Years											Total
	2008	2009	2010	2011	2012	2013	2014	2015	2016	2017	2018	
	Number of patients											
	20	11	10	23	18	12	15	8	3	1	0	121
Chr8q												
Normal	15	8	6	11	9	3	11	5	2	1	0	71
Loss/Gain	3	3	0	4	2	4	1	0	0	0	0	17
Other ^a	0	0	3	5	3	3	1	0	0	0	0	16
N/A	2	0	1	3	4	2	2	3	1	0	0	17
Chr8p												
Normal	11	7	3	10	2	3	13	4	1	1	0	55
Loss/Gain	6	4	4	7	8	5	1	1	1	0	0	37
Other ^a	1	0	2	3	4	2	0	0	0	0	0	12
N/A	2	0	1	3	4	2	1	3	1	0	0	17
Chr8q												
Normal	5	4	2	5	0	2	2	1	1	0	0	22
Gain	12	6	7	9	10	7	12	4	1	1	0	69
Other ^a	1	1	0	6	4	1	0	0	0	0	0	13
N/A	2	0	1	3	4	2	1	3	1	0	0	17
Time to the first scan (years)												
Median	3.7	0.16	1	0.7	0.38	0.09	0.35	0.42	0.72	0.14	0	0.99
(Range)	(0-13.9)	(0-0.45)	(0-4.4)	(0-6.7)	(0-4.7)	(0-0.45)	(0-4.16)	(0-2.1)	(0-1.84)	-	-	(0-13.95)
Liver screening in patients in whom metastases were not detected antemortem, but were found post-mortem												
HMDA	8	5	5	11	12	8	2	0	1	0	0	52
Scans per patient												
Median	2.4	4	1	3	1.2	1.2	1	0	1	0	0	2
(Range)	(1-7)	(1-6)	1	(1-11)	(1-2)	(1-2)	1	-	-	-	-	(1-11)
Modality of the scans												
MRI	14	17	0	24	3	2	0	0	0	0	0	60
US	3	3	5	8	11	8	2	0	1	0	0	41
CT	2	0	0	1	0	0	0	0	0	0	0	3
Liver screening undertaken in patients in whom metastases were found antemortem												
HMDCI	12	6	5	12	6	4	13	8	2	1	0	69
Scans per patient												
Median	10	16	7.4	18.1	19.5	20	16.3	12.2	13.5	9	0	14.6
(Range)	(2-20)	(9-22)	(1-11)	(7-34)	(1-40)	(8-27)	(4-30)	(1-20)	(9-18)	9	0	(1-40)
Modality of the scans												
MRI	90	73	16	136	74	58	115	49	20	6	0	637
US	7	5	11	11	9	4	35	28	1	2	0	113
CT	23	18	10	70	34	18	62	20	6	1	0	262
Outcome												
Follow-up Time (Years)												
Median	8.5	5.2	6	5.4	4.9	4.4	4.6	4.4	3.2	3.1	0	5.5
(Range)	(2.2-19.3)	(2.7-5.6)	(2.9-9.8)	(2.2-9.3)	(2.7-8)	(2.29-7.2)	(2.8-6.1)	(2.3-5.3)	(1.2-4.0)	-	-	(2.2-19.3)
Status												
Alive	6	0	1	4	3	2	3	5	2	1	0	27
Dead	14	11	9	19	15	10	12	3	1	0	0	94
Cause of death												
Metastatic	14	11	9	18	15	10	11	2	1	0	0	91
Other	0	0	0	1	0	0	0	0	0	0	0	1
Unknown	0	0	0	0	0	0	1	1	0	0	0	2
<i>HMDA: Hepatic metastases diagnosed by autopsy</i> <i>HMDCI: Hepatic metastases diagnosed by clinical imaging</i>												

Table 2.12 shows 386 UM patients (Group 3) *in whom metastases were not demonstrated in LUHFT throughout the liver screening study period*. This group included 201/386 (53.1%) males and 185/386 (46.9%) females. The median age was 59 years at primary treatment range (range, 23-94 years).

The primary tumours had a median LBD of 13.2 mm (range, 2.4-23.6 mm), and a median UH of 6 mm (range, 0.7-18.5 mm). Of these 90/386 (23.3%) UM involved the ciliary body and 23/386 (5.9%) had EOE. Epithelioid cells were observed in 167/386 (43.3%) tumours and PAS+ loops in 119/386 (30.9%) tumours. Mitotic count was assessed in 195/386 (50.5%) UM, with 82/195 (42.1%) between 2-3 mitotic figures in 40 high-powered fields. The majority of the UM patients had tumours with chromosome 3 loss, 151/386 (39.1%).

A total of 2114 scans were undertaken 491 times in this Group of 386 patients, median 5.5 per patient (range, 1-22), of which MRI 1388/2114 (65.7%), CT 61/2114 (2.9%), and US 665/2114 (31.5%). The median follow-up was 5.8 years (range, 0.2-32 years). At the end of the study, 340/386 (88.1%) patients in this group were alive. Unfortunately, 46/386 (11.9%) patients had died; all of them from causes unrelated to UM. Twelve of these 46 patients (26.1%) died within 2 years after the primary treatment, and 34/46 (73.9%) patients died after 2 years of the primary treatment.

Table 2.12: Characteristics of 386 UM patients in whom metastases were not demonstrated in Liverpool throughout the liver screening study period

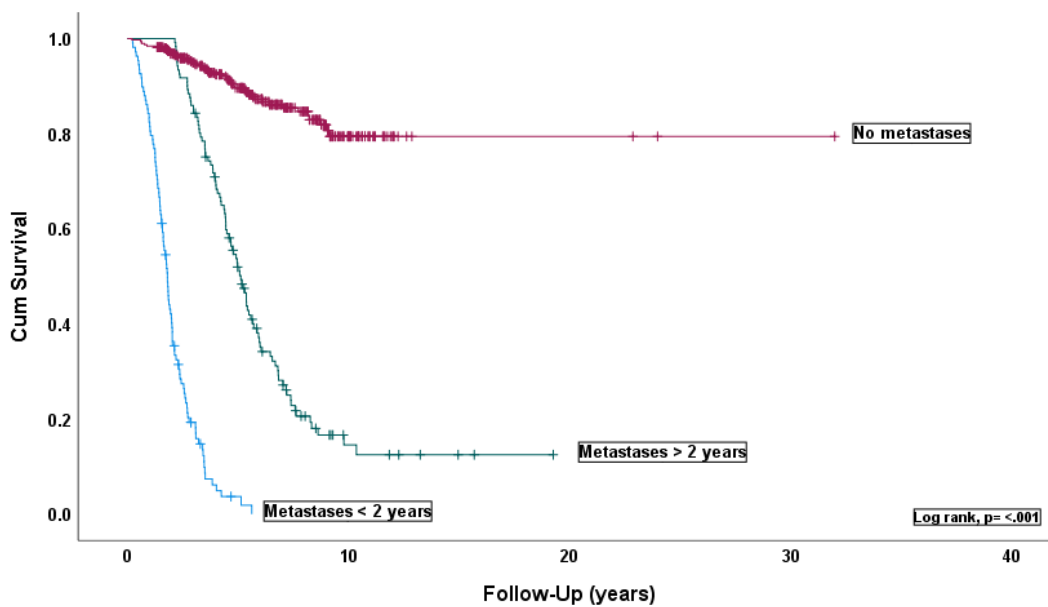
Features of the patients	Years											Total
	2008	2009	2010	2011	2012	2013	2014	2015	2016	2017	2018	
	Number of patients											
	17	23	30	42	22	40	40	40	37	45	50	386
Age at Primary treatment (Years)	52	57	58	61	58	59	61	63	61	56	63	59
Median (Range)	(29-67)	(24-81)	(29-80)	(32-94)	(41-75)	(28-86)	(27-81)	(32-83)	(23-82)	(32-86)	(35-89)	(23-94)
Sex												
Female	9	13	17	18	9	18	20	22	17	14	28	185
Male	8	10	13	24	13	22	20	18	20	31	22	201
LBD (mm)												
Median (Range)	15.2 (10-19.4)	13.8 (6-23.6)	13.6 (4.5-2.4)	13.4 (3.6-22.2)	14.1 (7.5-20.4)	13.5 (2.4-21.2)	11.9 (5.1-23.6)	13.2 (5.6-22.3)	13 (5.4-20)	12.9 (7.7-19.5)	12.8 (2.9-20.5)	13.2 (2.4-23.6)
UH (mm)												
Median (Range)	6.4 (1.5-10.3)	5.1 (0.9-14.5)	5.4 (0.7-11.7)	5.7 (0.9-12.9)	7.4 (1.7-16.8)	6.9 (1.4-14.5)	5.4 (0.9-16.7)	7.3 (1.2-18.5)	6.7 (1.3-13.3)	5.6 (1.1-13.4)	5.7 (1.1-13.6)	6 (0.7-18.5)
CBI												
No	15	19	22	33	20	29	31	24	25	38	40	296
Yes	2	4	8	9	2	11	9	16	12	7	10	90
Extra ocular Melanoma												
No	16	23	28	42	22	36	39	37	31	42	47	363
Yes	1	0	2	0	0	4	1	3	6	3	3	23
Epithelioid cells present												
No	9	12	13	23	11	17	22	19	17	19	27	189
Yes	6	8	14	17	11	20	14	18	15	22	22	167
N/A ¹	2	3	3	2	0	3	4	3	5	4	1	30
Closed PAS+ Loops												
No	6	2	11	17	6	8	13	2	1	5	0	71
Yes	5	5	7	5	6	15	6	19	18	13	20	119
N/A ²	6	16	12	20	10	17	21	19	18	27	30	196
MITOC												
0-1	2	1	2	1	2	3	3	0	2	1	0	10
2-3	6	3	9	5	2	7	6	12	16	5	11	27
4-7	3	2	4	8	5	12	7	9	1	9	7	34
>7	0	2	3	9	3	1	3	3	0	3	2	16
N/A ³	6	15	12	19	10	17	21	16	18	27	30	34
Chr1p												
Normal	12	13	15	17	6	16	12	20	11	18	13	153
Loss	1	2	3	5	5	9	8	8	8	7	8	64
Other ⁴	0	0	1	7	5	3	1	0	2	0	1	20
N/A ⁵	4	8	11	13	6	12	19	12	16	20	28	149
Chr3												
Normal	10	6	10	13	6	18	10	15	7	18	18	131
Monosomy	5	9	8	20	9	10	13	18	19	18	22	151
Other ⁶	0	0	3	4	5	6	13	5	7	4	3	50
N/A ⁷	2	8	9	5	2	6	4	2	4	5	7	54
Chr6p												
Normal	5	8	9	1	5	11	9	17	15	15	16	111
Gain	7	5	10	12	5	12	11	11	5	10	5	93
Other ⁸	1	2	0	16	6	5	1	0	1	0	1	33
N/A ⁹	4	8	11	13	6	12	19	12	16	20	28	149

Table 2.12: (continued)

Features of the patients	Years											Total
	2008	2009	2010	2011	2012	2013	2014	2015	2016	2017	2018	
	Number of patients											
	17	23	30	42	22	40	40	40	37	45	50	386
Chr8q												
Normal	9	9	10	12	10	17	16	21	16	21	18	159
Loss/Gain	2	5	6	13	3	10	4	7	5	4	4	63
Other ^a	2	1	3	4	3	1	1	0	0	0	0	15
N/A ^b	4	8	11	13	6	12	19	12	16	20	28	149
Chr8p												
Normal	11	10	16	16	10	15	20	23	15	22	17	175
Loss/Gain	1	4	2	12	4	5	1	5	6	3	5	48
Other ^a	1	1	1	1	2	8	0	0	0	0	0	14
N/A ^b	4	8	11	13	6	12	19	12	16	20	28	149
Chr8q												
Normal	7	7	14	8	10	10	12	14	7	11	5	105
Gain	4	6	5	12	6	13	9	14	12	14	16	111
Other ^a	2	2	0	9	0	5	0	0	2	0	1	21
N/A ^b	4	8	11	13	6	12	19	12	16	20	28	149
Time to the first scan (years)												
Median	3.8	1.54	1.2	0.35	0.2	0.38	0.30	0.20	0.10	0.24	0.2	0.55
(Range)	(0-26)	(0-9)	(0-9.4)	(0-2.4)	(0-0.6)	(0-3.2)	(0-2.6)	(0-2.8)	(0-0.79)	(0-1.25)	(0-0.56)	(0-26)
Liver screening findings												
Scans per patient												
Median	6.7	6.1	5.4	8.8	6	3.9	8.3	5.8	4.9	3.8	2.5	5.5
(Range)	(1-22)	(1-20)	(1-18)	(1-18)	(1-22)	(1.14)	(1-17)	(1-17)	(1-13)	(1-8)	(1-6)	(1-22)
Modality of the scans												
MRI	81	106	102	217	93	98	273	144	129	90	45	1388
US	32	25	54	140	33	56	72	72	46	75	80	665
CT	0	10	6	11	6	1	5	4	8	8	2	61
Outcome												
Follow-up Time (Years)												
Median	14.2	9.7	8.7	8.0	7.5	6.4	5.6	4.7	3.6	2.7	1.8	5.8
(Range)	(6.1-32)	(3.6-11.2)	(1.6-10.2)	(1.3-9.3)	(0.9-8.3)	(2.6-7.3)	(0.6-6.3)	(1.8-5.3)	(0.2-4.3)	(0.6-3.3)	(0.8-2.3)	(0.2-32)
Status												
Alive	16	19	20	35	20	36	35	33	34	43	49	340
Dead	1	4	10	7	2	4	5	7	3	2	1	46
Cause of death < 2 years before primary treatment												
Other	0	0	1	3	1	0	0	0	1	0	0	6
Unknown	0	0	0	0	0	0	1	1	1	2	1	6
Cause of death > 2 years before primary treatment												
Other	1	4	2	4	0	3	0	0	0	0	0	14
Unknown	0	0	7	0	1	1	4	6	1	0	0	20
HMDA: Hepatic metastases diagnosed by autopsy												
HMDCI: Hepatic metastases diagnosed by clinical imaging												

2.3.7 Survival for the 3 categorized groups of patients: 1) developed metastases within 2 years 2) after 2 years 3) never demonstrated metastases

Kaplan-Meier survival curve and table were examined for all patients according to the 3 groups categorized on when and whether they developed metastases. Log-rank tests were used to compare survival across the 3 groups ($p = <.001$). Patients from Group 1 were associated to the poorest outcome. Group 2 was significantly associated with metastatic disease and poor survival. Group 3, was associated with improved outcome (**Figure 2.19**).



Groups	Total Number of patients (%)		Number of events %		Censored %		Sig.	Mean survival (years)	95% confidence interval	
									Lower	Upper
1	108	17.6%	100	92.6%	8	7.4%	P= <.001	2.011	1.791	2.232
2	121	19.6%	94	77.7%	27	22.3%	P= <.001	6.810	5.778	7.841
3	386	62.8%	46	11.9%	340	88.1%	P= <.001	26.484	24.847	28.071
Overall	615	100%	240	30.3%	375	61.1%		5.065	15.440	18.471

Figure 2.19: Kaplan-Meier survival curve and table where all the patients were stratified according to when and whether developed metastases; Group1 - patients diagnosed of metastases within 2 years ($n=108$), Group 2 - patients diagnosed of metastases after 2 years ($n=121$), and Group 3 - patients who have never been diagnosed of metastases ($n=386$), ($p = <0.001$). The number of events indicates the total number of patients who died.

2.4 Discussion

In this study, I undertook an extensive retrospective analysis of liver surveillance scans in 615 UM patients diagnosed at the LOOC between 2008-2018. Although several studies have investigated the impact of surveillance in UM patients, the current study is important because I used a 'real world' dataset – with its associated strengths and weaknesses - that correlated the characteristics of UM patients included in liver screening programs with the features of the primary tumours, examining particularly the onset of the metastases and the scanning characteristics of the metastases.

The main 'top level' findings of my analyses are summarised under the following subheadings, and will be discussed in more detail below:

A – Frequency of UM metastases: Of all 615 UM patients reviewed over an 11-year period, 386/615 (62.8%) patients did not demonstrate metastases in scans available at LUHFT, 229/615 (37.3%) developed metastases, and 18/229 (7.9%) patients had extrahepatic metastases.

B – Primary UM size and risk of metastases: This analysis demonstrated that 107/613 (17.4%) primary UM were categorised as T1; 140/613 (22.8%) as T2; 226/613 (36.8%) as T3; and 140/613 (22.8%) as T4. Increasing size of the primary UM and increasing tumour TNM category were associated with increasing number of metastases (T4 - 58.6%), melanoma specific mortality (T4 - 50%), and reduced survival (T4 – 9.4 years). Of the 140 T4-primary UM, 5 (3.6%) patients had synchronous with M1c metastases.

C – Primary UM genetics and risk of metastases: Patients who developed metastases had large primary UM, the majority of which demonstrated monosomy 3 (54.2%) and chromosome 8q gain (56.8%). Liver surveillance was undertaken more frequently in these high-risk UM patients, and the survival mean time was 9.2 and 8.8 years, respectively, (range, 8.1-10.3, and 7.5-10.1 years, correspondingly).

D – Liverpool liver surveillance – detected metastases, number, and type of scans:

Within the liver surveillance programme performed in Liverpool, metastases were detected in 150 (24.4%) patients, and in 465 (75.6%) patients, metastases were not detected by clinical imaging during the study period. In the 150 patients, metastases were diagnosed mostly by MRI – in total 961 scans were performed over 11 years in these patients, with an average of 7 scans per patient; followed by CT – 423 scans, with a median of 3.8 scans per patient, and US - 216 scans, with 2 scans per patient. Liver surveillance showed that the most frequent modality was MRI for all patients, with a total of 2419/3854 (62.8%) examinations and an average of 6.8 scans per patient.

E. UM metastases characteristics in the Liverpool liver surveillance programme:

Most patients in whom metastases were detected by imaging had multiple metastases 133/150 (88.7%). The majority of metastases were categorized as M1a - measuring less than 30 mm 87/150 (58%). From the metastases categorized as M1a, 24/87 (27.6%) had primary tumours with T4 stage, whereas M1b metastases had 16/50 (32%) primary UM T4, and M1c metastases had 5/13 (38.5%) primary tumours T4.

F. Outcome of patients with UM metastases in the Liverpool liver surveillance programme:

81/150 (54%) of the patients in whom clinical imaging metastases were detected, developed the metastases within 2 years after the primary treatment of the tumour. The median time to metastases was 2.6 years, and the median time to death after the detection of metastatic disease was 1 year (range 0.1-4.3 years). However, there were still 27/229 (11.8%) patients who developed metastases in two years, but these were detected only at post-mortem, in which it was not possible to obtain information such as: 1) when these metastases were diagnosed, 2) if metastases were detected during the period of liver surveillance in other hospitals, or 3) if metastases were ever detected ante-mortem.

G. Three groups of patients stratified according to when and whether patients had metastases: This analysis showed that it was possible to stratify the 615 patients into three distinct groups according to when and whether metastases occurred. In **Group 1**, patients developed metastases within two years of the treatment of the primary tumours and were associated with a worse outcome: [100/108 (92.6%)] died, [96/100 (96%)] of which from melanoma metastases. **Group 2**, patients developed metastases 2 years after the treatment of primary tumours. These patients had improved outcome than Group 1. [94/121 (77.7%)] of the patients died, [91/94 (96.8%)] of liver metastases. Patients from **Group 3** never demonstrated metastases and were associated with an improved outcome. At the end of the study, 46/386 (11.9%) patients had died, none of them due to liver metastases.

H - Regularity of liver surveillance: This analysis demonstrated that not all UM patients had a regular scanning interval. In most patients [407/615 (66.2%)], the results of scanning were considered regular (more than 1 scan); however, the remaining patients [208/615 (33.3%)], liver screening was considered irregular (only 1 scan performed). Factors associated with patients' follow-up were some of the limitations of this study, which may have influenced the absence of a number of surveillance imaging.

2.4.1 Frequency of UM metastases

The incidence of UM metastases varies between studies in the literature. Our results (37.3%) are similar to those of Diener-West et al. [143] who analysed 2,320 cases of UM, in which metastases were detected in 32% using LFTs, CXR and diagnostic imaging to detect UM metastases. Rantala et al. (2021) [268] also described 32% of metastases in their study to assess patients with liver metastases managed with the best supportive care.

In contrast, Eskelin et al. [158] in a study of 390 UM patients over an 11-year period, reported 62/390 (15.9%) of UM metastases, but only 37 (59.8%) patients had hepatic metastases only, the remaining 25 (40.3%) patients having extrahepatic metastases, either both liver and other sites, or other sites only. Although this figure differs to our analysis (37.3%), in the same study 26.1% of UM patients were diagnosed on the basis of symptoms, since the study criteria included not only liver imaging, but also LFT values. Other studies also showed variability in the percentage of detected metastases: Frenkel et al. (13%) [204], Gomez et al. (71.1%) [245], and Rantala et al. reported that 72% of the patients developed only hepatic metastases [269]. Such variability can be explained by the type of studies undertaken, and the detection methods of UM metastases in the liver.

2.4.2 Primary UM size and risk of metastases

There are numerous studies that investigate the prediction and risk of mortality from UM [235,244,270,271] and liver surveillance to detect liver metastases [143,158,169,170,252,253,269,272-274]; however, none have undertaken such a wide analysis as that conducted here, combining clinical, histomorphological and genetic data. The risk of developing metastases in UM is determined by several factors, which include clinical and pathological characteristics, such as the size and location of the tumour [275] as well as molecular genetic abnormalities, mainly the loss of chromosome 3 [219].

In the current study, in the 613/615 (99.7%) patients in whom the tumour measurements were obtained, the median tumour diameter and thickness was 14.6 mm (range, 2.4-26mm), and

6.3 mm (range, 0.7-20.2 mm), respectively. Similar data were found in a study by Damato et al. [72] in Liverpool, where the tumours had a mean LBD of 15.4 mm, and a mean thickness of 8.1 mm. A greater percentage of metastases was detected in UM with LBD of >18 mm (72.7%) and UH (12.1-15.0 mm) (73.5%), respectively. Other studies [276-279] also reported tumour size, as strongly associated with metastatic risk. Shields et al. [274] conducted a study in which they evaluated patients for the onset of UM metastases, using US measurements of the primary UM, particularly in cases where genetic tests or histopathological evaluation could not be obtained. In their analysis, Shields et al. analysed the risk of metastases based on a single millimetre increment in tumour thickness. They reported that tumour size significantly determined metastases risk with metastatic UM being observed in all 12% patients over a 38 years' time period: 5% incidence in patients with small UM (0-3.0 mm); 12.8% in patients with medium-sized melanomas (3.1-8.0 mm); and 21.8% for large melanomas (>8 mm).

As mentioned above, the frequency of metastases found was higher at 229/615 (37.3%), however our results were in agreement in that an increasing size of UM was significantly associated with detection of metastases (T4 – 58.6%, $p = <.001$), and poor survival (T4 – 9.4 years, $p = <.001$). This study is in agreement that the size of the tumour, is in fact a risk factor for poor outcome as previously described [102,280].

In this analysis, the focus was a comprehensive review of the features of liver imaging performed after the treatment of the primary UM; however, in a detailed analysis of the primary tumours, a strong correlation was also observed between the increase in tumour size and chromosomal abnormalities. For example, the metastatic risk seen in T1 (17.5%), T2 (22.8%), tumours versus T3 (36.9%) and T4 (22.8%) tumours for genetic alterations, suggested that medium and large UM carry a substantially higher risk of changes compared to small UM, suggesting that an early intervention could prevent the accumulation of such genetic changes.

Rantala et al. [269] evaluated the sensitivity of US as a screening modality in the detection of metastases in primary UM patients when associated with LFTs and confirmatory MRI in case

of detection of a suspected lesion. They categorized the sizes of primary tumours according to AJCC-TMN in; T1 (10%), T2 (39%), T3 (41%), T4 (10%), and 41% involved the ciliary body or the sclera [269]. Kujala et al. [278] classified UM as T1 (24%), T2 (33%), T3 (31%), and T4 (12%). Comparatively, in the present study a higher percentage for T4 tumours was found (22.8%, $p = <.001$). A gradual increasing risk for metastases was noticed with the increasing category of the tumours (T1 – 15%, T2 – 26.5%, T3 – 41.6%, and T4 – 58.6%), and other studies have shown the same [132,143,281]. Survival analysis confirmed tumour size to be a risk factor for metastases and mortality (Log rank, $p = <.001$). The risk of synchronous metastases has been reported in the literature [269,282]. Garg et al. [283] analysed ocular and systemic findings in patients with metastatic disease. They reported that 1.9% of UM patients had clinical metastases (stage IV), having reported that patients with synchronic metastases had larger UM, as well as more frequent involvement of the ciliary body and extra-scleral extension, concluding that although the tumours with higher stage have been associated with the risk of metastases at diagnosis, some small T1 tumours were classified as stage IV at initial presentation. In the present study, 5/140 (3.6%) of the primary tumours categorized as T4 had synchronic metastases M1c; 1/5 (20%) patient had involvement of the ciliary body and 2/5 (40%) had extra-scleral extension. This is in agreement with the study by Garg et al. who also reported that stage IV patients were more likely to develop multi-organ diseases, supporting a whole-body initial staging of all UM patients [283].

2.4.3 Primary UM genetics and risk of metastases

Although tumour size remains one of the most important clinical predictive factors, it is not the only parameter-influencing prognosis [274]. Several factors must be considered [284]. Damato et al. [72] in their analysis of prognostic factors predicting metastatic death, included genetic analysis and reported that the most important independent predictors were the basal diameter of the tumour, histopathology of epithelioid cells and the loss of chromosome 3. The study also confirmed that monosomy 3 is associated with a high rate of metastatic death in the first 5 years after treatment for UM. Their results showed monosomy 3 (47.2%), and chromosome 8 gain (37.1%).

In our current study, cytogenetic data were comparatively similar to the study of Damato et al., monosomy 3 (53.7%), and chromosome 8q gain (41.8%). These figures had a greater correlation with liver metastases and metastatic death.

As described in previous studies, monosomy 3 and gains in chromosome 8q are associated with a poor prognosis for survival [72,98,105,121,285], and this study confirms this. In the current analysis, I was able to demonstrate a significant association between chromosome 3 and 8 abnormalities with poor survival. Chromosome 3 loss (46.4% - 9.2 years, $p = <.001$); gains or loss in chromosome 8p (55% - 6 years, $p = <.001$) and gains in chromosome 8q (47.5% - 8.8 years $p = <.001$).

In 2020, Damato et al. [271] also described poor outcome associated with monosomy 3. They reported a parsimonious model developed to estimate mortality from melanoma metastases in patients with choroidal melanoma when it was not possible to apply either the LUMPO algorithm, or the TNM staging system. In a cohort of 8,348 patients with choroidal melanoma, Damato et al. found 4,174 (50%) who had chromosome 3 status. 1,553 (18.6%) of the patients died, where 956 (61.5%) deaths were attributed to UM metastases. The most informative predictors of metastatic death were LBD and chromosome 3 status. In our analysis, corresponding numbers were found – that is, of the 330 (53.7%) patients who had monosomy

3 UM, 179/330 (54.2%) had metastases, and 153/330 (46.4%) died of melanoma metastases. However, with regard to the overall mortality of the 615 patients studied here compared to their figures, higher percentages were found: the number of patients who died was 240/615 (39%), of which 187/240 (77, 9%), due to liver metastases.

In the current analysis, I demonstrated a significant correlation between loss of chromosome 1p and metastatic death, and a decrease in overall survival (44.4% - 7.8 years, $p = <0.001$). Consistent with these findings, in a study analysing the genotypic profile of 452 choroidal melanomas with MLPA, Damato et al. [99] also reported that the increase in mortality is correlated with loss of 1p, as well as loss of chromosome 3 and gain of chromosome 8q. Another study showing consistency with our findings was the analysis of Kilic et al. [286]. Conversely, abnormalities of chromosome 6p are described as almost mutually exclusive to monosomy 3 and are therefore associated with a good prognosis [102,286]. This analysis also showed gains in chromosome 6p associated with a decreased metastatic death and improved survival: (23.4% - 17.3 years, $p = <.001$).

2.4.4 Liverpool liver surveillance – detected metastases, number and type of scans

As previously shown, surveillance allows early detection of metastases before symptoms develop, even though the debate on which tests will be most effective and the most beneficial cost-benefit ratio continues. Although a survival benefit for surveillance has not yet been proven, most centres perform periodic screening of all patients with high-risk UM, and surveillance is now considered good clinical practice [254].

In 2004, Diener-West et al. [143] in a study by the COMS Group, reported that in a cohort of 2320 patients, 714 (32%) patients developed metastases and 679 (95.1%) died, 675 (99.4%) with confirmed metastases and 4 (0.6%) had clinical suspicion and histopathological confirmation of melanoma metastases. They considered that the use of LFTs associated with diagnostic imaging has a high specificity and predictive value, but a low sensitivity, and that better tests would be needed to identify melanoma metastases earlier. In the present study,

we did not include the analysis of LFTs or other tests used for metastatic screening. Comparatively, it was found 37.3% of metastases, 24.4% diagnosed clinically, and 12.8% by pathologic confirmation; in these patients, metastases have not been demonstrated ante-mortem but may eventually be developed at different stages of the disease. For various reasons already mentioned previously, many patients did not continue their surveillance programs, and it was not possible to obtain this information.

Marshall et al. [169] conducted a prospective study to evaluate the detection of asymptomatic UM liver metastases by MRI. 188 patients were included in which the 5-year mortality prediction exceeded 50%. The median follow-up time was 28.8 months (range, 1-118 months). The screening was continued for a minimum period of 5 years, until the detection of metastases. Six months of MRI screening detected metastases in 83 (92%) of the 90 patients who developed systemic disease. They concluded that performing MRI for a period of 6 months in patients at high risk of developing metastases before the onset of symptoms increases the possibilities for early treatment of metastases and participation in clinical trials. Conversely, in our study, the liver screening period was defined to 11 years, with an additional follow-up period of 15 months (until 30th of March 2020) and a surveillance modality constituted of MRI, US, and CT. The median follow-up time was 5.1 years (range 0.2-32 years). A relatively lower number of metastases 229 (37.4%) were detected. The retrospective modality of this study did not enable the attainment of information on follow-up for a certain number of patients in whom there was no continuity of the surveillance, and consequently, an amount of metastases were not identified.

On average, metastatic disease is detected about 3 years after the diagnosis of the primary tumour [169]. At the time of the primary diagnosis, less than 4% of UM patients have occult liver metastases [259]. Once diagnosed, metastases are predictive of poor survival [287]. In the recent study published by Rantala et al. [269], they analysed the US's inconsistency with CT or MRI and compared CT and MRI. They reported that of the 215 selected patients; metastases were detected in 10 (4.7%) patients before the tumour's primary treatment. A total

of 155 (72%) liver metastases were detected, with 215 (47.7%) US, 167 (37.1%) CT and 69 (15.3%) MRI. They opted for the US as their first imaging modality, except for CT in 18 patients (8%) and MRI in 2 (0.9%) patients. The median interval was 17 days (range, 0-56 days) from the first to the second imaging modality, US, CT, and MRI.

In our analyses, there were only a few similarities, since our study period was longer, and we did not analyse the specificity of the examinations, but their frequency and the characteristics of the liver metastases. In the 150 patients in whom metastases were demonstrated by imaging, 1600 scans were performed, of which 961/1600 (60.1%) was MRI, 423/1600 (26.4%) was CT and 216/1600 (13.5%) was US. The MRI was the most used, because it is considered to be the study choice for evaluating metastases in high-risk patients or when abnormalities are detected in some centres in the UK [252], particularly in Liverpool [169]. Due to the characteristics of melanoma metastases, in which even very small melanotic deposits can be seen as bright foci, MRI is considered to be more specific and at least more sensitive than CT to detect metastases, and US is even less specific, and additionally it is highly operator-dependent, time-consuming and technically challenging [170]. In this study, it was demonstrated that in 286/615 (46.5%) patients the first scan was performed on the eve of the primary treatment of the tumour, and in 7/286 (2.4%) patients it were detected metastases at time of primary treatment, as also referred in other studies [288]. Albert et al. reported that, while patients are being examined for preoperative metastases, an increasing number of patients with metastatic UM are being identified before primary treatment [289].

2.4.5 UM metastases characteristics in the Liverpool liver surveillance programme

In this study, during the liver screening analysis it was found that of most patients presented multiple metastases 133/150 (88.7%). Conversely, Rivoire et al. [183] described a total of 602 patients treated for UM who had an abdominal US scan every 6 months over a period of 14 years. 10.5% of the patients developed liver metastases as the first extraocular metastatic site. When possible, liver surgery was performed. Most of the patients 39.3% had < 4 liver metastases, 34% had between 5 and 8 liver metastases, and 27% of the patients had <10 metastases.

The median LDLM of the metastases identified in this study was 35.98 mm (range, 41-196 mm). 87/150 (58%) patients had metastases with less than 30 mm (M1a), 50/150 (33%) had between 30 and 80 mm (M1b), and 13/150 (9%) patients had metastases with more than 81 mm (M1c).

Comparatively, other studies reported metastases with smaller sizes. Rantala et al. [269] reported 380 patients undergoing liver surveillance. They found a median LDLM of 26 mm (range, 6-130). Other study describing the characteristics of liver surveillance was from Marshall et al. [169], in which they described 90 patients who developed metastases. Here again describing smaller metastases, 66% of patients had metastases with less than 20 mm, 21% between 25 and 50mm, 8% 50-100 mm and 6% > 100 mm. Servois et al. [253] reported a study of preoperative staging of hepatic metastases from UM, also describing metastases with smaller size. Of the 28 lesions resected, in 27 metastases confirmed surgically and histologically, 32.3% were smaller than 5 mm, 25.9% measured between 5 and 10 mm, and 40.7% measured more than 10 mm. Smaller metastases were also found in the study by Rivoire et al. [183] describing treatment procedures for hepatic metastases in UM and reported that the diameter of the largest metastases was < 30 mm (median, 12 mm; range, 5-75 mm). However, a study from Eskelin et al. [158] describing screening for melanoma metastases reported larger metastases than those found in our study, the median LDLM was 48 mm (range 10-300 mm).

2.4.6 Outcome of patients with UM metastases in the Liverpool liver surveillance programme

As previously mentioned, in this study were detected metastases in 229 patients; however, in patients in whom metastases were detected at autopsy, it was not possible to obtain the time in which metastases occurred after primary treatment. Thus, the following results are related to metastases detected by clinical imaging. 81/150 (54%) patients developed metastases within 2 years after primary treatment. Overall, 115/150 (76.7%) patients died 1 year after the detection of the first metastases (range, 0.1-4.3 years).

Rietschel et al. [163] evaluated survival parameters in metastatic UM. They found 119 patients with metastases over a 10-year period. The estimated median overall survival was 12.5 months. The median time to the detection of metastases was 4.4 years (range, 0.2-9.9 years), and the median follow-up of the survivors was 17 months. 22% patients were alive at 4 years. Comparing to our analysis, we found an estimated median overall survival of 3.5 years. The median time to metastases was shorter - 2.6 years (range, 0.1-17.8 years). 35/150 (23.3%) patients diagnosed of metastases ante-mortem were alive at the close of this study, for a follow-up time - 2.5 years (range, 0.4-7.7 years) after the detection of the metastases.

Other previous studies have reported survival data for metastatic UM. Rivoire et al. [183] reported similarities: time to metastases of 29 months and, 87% patients died within 2 years after the diagnosis of metastases compared with 85.5% in our analysis. In contrast, they reported an improved median follow-up time of survivors of 29 months. Lane et al. [217] described a poor median survival time after the diagnosis of metastases of 3.9 months. Unlike our study, the median time from the initial treatment of the tumour to metastases was 3.45 years, and the overall survival rate was 13% in 1 year. In total, only 11.7% of patients survived for more than 1 year.

Lorigan et al. [150] in a study on the prevalence and location of UM metastases reported 92% of detected metastases. In 61% patients, metastases were detected 4.3 years after the

treatment of the primary tumour. A poorer survival after metastases was observed, 95.5% of patients died 10 months after the diagnosis of metastases, compared with 85.5% who died within two years of diagnosis in our study. Only 2.7% of patients were alive after metastases, with progressive disease, compared to 23.3% who survived up to 2.5 years after the detection of metastases in this analysis.

2.4.7 Three groups of patients stratified according to when and whether developed metastases

For the identification of patients at high risk of developing metastatic disease, many anatomical, histological and, more recently, genomic prognostic characteristics have been used [122,290-292]. Mazloumi et al. [291] investigated the accuracy of the TCGA classification by comparing it with the AJCC classification system. Based on the tumour largest basal diameter, thickness, location, and EOE, tumours were classified according to the AJCC into 4 tumour categories, 17 subcategories, and 4 stages. TCGA classification was based on genetic results into 4 classes: A, B, C, and D. Patients classified according to the AJCC, the main differences were: the category of more advanced tumours had a shorter follow-up time, a greater number of metastases and poor outcome, and the median time to metastases was shorter. Comparisons of the AJCC tumour categories and stages with TCGA classification showed that more advanced TCGA classes were associated with more advanced AJCC categories. The results suggested that the TCGA classification provides greater precision than AJCC categories for predicting UM metastases.

In contrast in this study, 3 groups of patients (Groups 1, 2, 3) were stratified according to the time of the development of the metastases, integrating clinical and cytogenetic characteristics of the patients, as well as the characteristics of the liver screening and outcome. The results showed that the distinct characteristics in each group, differentiated patients as having: better, intermediate and worse outcome ($p = <.001$).

The comparison showed that in Group 1 (*patients who developed metastases within two years*) the tumours were larger, (LDB median 17 mm and UH median 9 mm), and had a higher incidence of monosomy 3 [91/108 (84.3%)] and gains of chromosome 8q [77/108 (71.3%)]. The median frequency of scans was 5.7 examinations per patient. The comparison between groups in this study, also demonstrated that patients from Group 1 had worse outcome. A shorter follow-up time (1.9 years), a higher mortality rate 100/108 (92.6%), in which metastatic death was 96%, and a survival rate of 8/108 (7.4%) at 1.9 years of follow-up was shown.

Although with some similar characteristics, in Group 2 (*patients who developed metastases after 2 years of primary treatment*) It was verified smaller tumours than Group 1 (LDB median 15.3 mm and UH median 7.4 mm), the incidence of monosomy 3 was lower [88/121 (72.7%)] and also gains of chromosome 8q [69/121 (57.1%)]. They had higher median frequency of scanning - 9.2 scans per patient, compared to 5.7 examinations per patient in Group 1. In a retrospective study conducted by Davanzo et al. [292] patients were categorized as low-, unknown- and high risk. The group of patients at low risk and unknown risk was recommended a less frequent standard surveillance protocol, while for patients identified as high risk of metastases, was recommended referral to an oncologist and an intensive protocol was advised. In our analysis, regardless of the highest frequency of examinations found in Group 2, when analysing Groups 1 and 2 together, which were the total of patients who developed metastases, we found a higher average of scans per patient compared to Group 3. Regarding the outcome, in Group 2 was improved: mortality rate - 94/121 (77.7%) and survival - 27/121 (22.3%) at the 5.5 years of follow-up; however, metastatic death (96.8%) was similar to Group 1.

The group of *patients in which metastases have never been demonstrated* (Group 3), tumours had smaller size, (LDB median 13.2 mm and UH median 6 mm) and most of the genetic factors presented mainly normal status, except for chromosome 3, which presented 151/386 (39.1%) of monosomy 3, compared to 131/386 (33.9%) of normal status, and chromosome 8q gain with 11/386 (28.8%) compared to 105/386 (27.2%) of normal status. The frequency of imaging

was lower (5.5 scans per patient). Also in Group 3, patients had better outcome than Groups 1 and 2. The mortality rate was 46/386 (11.9%) and the survival rate was 340/386 (88.1%) at 5.8 years of follow up. The mortality rate in Group 3 was considerably lower in relation to Groups 1 and 2; but nevertheless it was found that there was a percentage of patients - 12/46 (26.1%), who died within two years after the primary treatment and although they died due to causes unrelated to UM and no metastases were detected, it cannot be exclude the fact that there could have been unidentified micro metastases, which could develop later [145]. The risk of metastatic disease, although lower in this group of patients, is not completely absent and, some studies [293-296] indicate that the surveillance program should continue, as well as patients should be encouraged to adhere to the recommended surveillance. Other studies [261,292] also indicate that only when suspicious lesions are found, patients should have more frequent routine confirmatory examinations.

An analysis performed by Singh et al. [297] published results in which patients were grouped according to the molecular prognosis. Those with tumours with disomy of chromosome 3, class 1 GEP and absence of mutation in the *BAP1* or *SF3B1* gene, were considered patients with good prognosis, and those who had monosomy 3, class 2 GEP, or presence of *BAP1* or *SF3B1* gene mutation, were considered patients with poor prognosis. No difference was demonstrated between small tumours with poor prognosis and large tumours with good prognosis, and no patient with small tumours with a good prognosis died of metastatic disease. Their analysis also reported that the broad classification of distributing patients into groups with good or bad prognosis used in current practice, does not depend only on the test used, and it is considered insufficient because within the group with worse prognosis the pattern of mortality may be initial or late and seems to be determined by the genetic profile. They established that the preferred method for the prognosis could be the mutational subtyping of UM.

Conversely, in our analysis due to variations in the intensity and frequency of the scanning, we wanted to know if there were any factors related to the patient, or primary tumour that were

associated with specific surveillance characteristics, which helped to stratify patients into 3 groups and verify that the patients at higher risk: developed metastases and the surveillance was more frequent. In the above-mentioned study from Davanzo et al. [292] on risk-stratified systemic surveillance in UM, a statistically significant difference in the risk of metastases was reported between the low-risk group and the unknown-risk group compared to the high-risk group ($p < 0.001$). All detectable metastases developed in the high-risk group. High-risk patients had more scans performed and were also more likely to perform any scan and have more intensive surveillance.

2.4.8 Regularity of liver surveillance in the real world

Regular surveillance can result in early detection of metastases in resectable stages. Oncologists generally recommend more frequent and/or more intensive surveillance for patients with metastatic high-risk [292]. Due to the lack of solid evidence on liver surveillance for the detection of melanoma metastases, more studies should be conducted to assess the efficacy of surveillance in reducing mortality. Studies on surveillance performed for other cancers, such as primary liver cancers and colorectal cancers [231,298,299], showed a survival benefit for surveillance receivers.

In this study, we investigated the outcome of patients with UM who received the surveillance program, and when analysing patients according to the regularity of liver surveillance, it was found that; scanning was regular in 407/615 (66.2%), and irregular in 208/615 (33.8%) patients. A considerably greater number of metastases were detected through the regular screening programme 161/407 (39.6%), compared with the irregular screening 8/208 (3.8%); although in this latter group, 60/208 (28.8%) patients had their metastases recorded at autopsy. There is a possibility that these patients have continued their surveillance program in other hospitals, and the surveillance was not analysed in this study. Overall mortality increased in the irregular group 92/208 (44.2%) than in the regular surveillance group 148/407 (36.4%). Metastatic mortality for the irregular group was statistically higher 67/208 (32.2%) compared to the regular group 120/407 (29.5%), ($p = 0.043$).

Our results showed some consistency with a study conducted by Khalili et al. [298] reporting the effectiveness of US surveillance for hepatocellular carcinoma. They also reported a better outcome for regular versus irregular liver surveillance. Patients were categorized into 3 groups: regular surveillance, irregular surveillance, or first surveillance (tumour detected in the first scan). The results of surveillance showed that when they used the Milan criteria for transplantation as outcome, (77%), (61%), and (74%) patients performing regular, irregular, and first surveillance, respectively, had tumours that met the transplant criteria. The difference between regular and irregular surveillance was statistically significant ($p = 0.03$). When they used the Barcelona Clinic Liver Cancer (BCLC) staging system, (80%), (68%), and (76%) patients who had regular, irregular and first surveillance had their tumours detected in BCLC curative stages. They concluded that a high success rate in surveillance of hepatocellular carcinoma was achieved by regularly using US.

In another study described by Kwon et al. [299] in which they analysed the impact of national surveillance for liver cancer, they grouped patients into surveillance and non-surveillance. The mortality rate of patients who participated in liver surveillance was 22% lower than that of those who did not participate. The survival probability of the surveillance group was statistically higher over the entire follow-up period ($p < 0.0001$) compared to the group who did not participate. The study highlighted the survival benefit in patients who participated in the liver surveillance program.

In summary, I have undertaken a detailed analysis of liver scans in 615 UM patients diagnosed at the LOOC and found that the onset of metastases is related to the size and genetic profiles of the primary UM. Liver surveillance did enable detection of the metastases earlier, and in some cases enabled prolonged survival via metastasectomy. These data are of value in considering the costs of surveillance programmes (as to be discussed in **Chapter 3**) as well as of potential modifications and revisions of prognostic algorithms for UM (see **Chapter 4**).

Chapter 3

Analysis of costs of liver screening for metastases in patients treated at the Liverpool Ocular Oncology Centre between the years 2008 and 2018 using the LUMPO3

3.1 Introduction

3.1.1 Factors associated with follow-up liver screening

Given the relatively high incidence of metastatic disease involving the hepatic parenchyma, liver surveillance is a widespread practice in cancer management. As already mentioned in **Chapter 1**, various diagnostic tests have now been indicated for the detection of metastases [160,165,167,169,173].

Literature on metastatic surveillance on patients with a variety of cancers - such as uveal and skin melanoma, hepatocellular carcinoma, colorectal, and pancreas [231,292,300-302] - suggests that there are advantages of liver surveillance, such as early detection of metastases and reassurance of the patient. Detecting metastases in a timely fashion may lead to changes in the management, such as local liver treatment with ablation or resection, targeted or traditional systemic chemotherapy, or enrolment in clinical trials of new treatments, leading to better survival results [293,294]. Mitchell et al. in a study on the experience of uveal melanoma follow-up care, reported that several patients indicated a preference for more liver scans during follow-up, which made them feel reassured [300]. However, some studies reported that some disadvantages could include: exposure to radiation, which may lead to an increased risk of cancer in the future [248,303]; incidental findings during examinations, such as suspicious or benign lesions that are later considered harmless but that cause unnecessary investigations and anxiety to patients [304], imaging-guided biopsies as a result of suspicious findings, to prove or exclude melanoma metastases [305] and possible concomitant complications of these tests, such as biopsy bleeding.

3.1.2 Cost-effectiveness of liver surveillance

Several studies have evaluated the sensitivity and cost-effectiveness of liver surveillance in patients with various malignancies [301,306,307]. Although previous studies have shown that overall survival does not improve with early detection of metastases, more recent studies have suggested that survival is better in patients with smaller metastases and asymptomatic

patients. However, intensive imaging follow-up programs tend to increase costs either for healthcare systems or patients and can constitute a risk for patients. Currently, assessing the utility of liver routine screening remains controversial. To date, limited data suggest that liver surveillance is cost-effective or has a significant impact on UM patients concerning life expectancy. There are not many studies that investigate the cost-effectiveness of liver surveillance in patients with UM, studies of other cancers have reported costs, [306,307]. However, in UM, some of the published studies reported costs and benefits of single images [269,308] before surgical resection of metastases or follow-up imaging to assess response to treatment.

Frequent liver surveillance can constitute either a financial, time, and psychological burden for patients and the results obtained in the "real world" may be very different from what would be expected by oncology researchers [309]. Evaluating the functionality of liver surveillance is not simple. Eskelin et al. [158] suggested that the combination of LFTs and half-yearly US can detect up to 98% of metastases, but the authors recognized that the costs of these programs are not guaranteed until more effective systemic therapies are available. It is important to note that screening programs, when implemented early, will lead to the improvement of screening protocols. Gombos et al. [161] reported that not all patients indicated, as being at high risk would be good candidates for therapy, in which case they will not be indicated for early detection of metastases. Therefore, guidelines for screening asymptomatic patients with UM should be based on scientific data that indicate routine observations because early detection and intervention significantly alter patient's morbidity and mortality.

3.1.3 Clinical prediction models

Prognostic tools used to estimate the risk of metastatic death and also to predict the time when this may occur are considered of great value to patients [235,241]. Considering that the spread of the tumour is rarely detectable at the time of primary ocular treatment, and assuming these tools are sufficiently reliable, they would allow personalized medical care to allow patients at low risk of metastases to be reassured and, in contrast, patients with the likelihood of developing the disease could be included in special programs, such as personalized counselling and systemic surveillance. Prognostic models designed to predict survival or risk of metastases after the treatment for UM based on clinical, tumour characteristics and cytogenetic risk factors, or even on the gene expression profile have been reported [124,219,235,236,240,241,310]. Prognostic models are abundant in the medical literature [311,312], but few of the models are implemented or used in clinical practice [312]. Worse still, few models are evaluated for their impact on health outcomes. Prognostic models are a formal combination of several predictors from which the risks for a specific end point can be calculated for each patient.

A newly-developed prognostic model needs to be validated with patient data not used in the development process and, preferably, selected from different configurations [313]. Validation studies provide estimates of the ability of a model to discriminate between patients with different risk groups and of the agreement between predicted and observed risks [314].

As referred in **Chapter 1**, the Liverpool Uveal Melanoma Prognosticator Online (LUMPO) model was developed, which estimates life expectancy using risk factors and mathematical models based on machine learning algorithms (7 -9). When LUMPO3 was improved and validated in Liverpool [241], it was considered a reliable and personalized prognosticator of metastatic death and capable of being used as a decisive support tool for the individual management of patients in a clinical context. Since routine liver screening for UM metastases is time-consuming and expensive for patients and healthcare services, this has encouraged us to use the LUMPO3 prognostic tool, to potentially increase the cost-effectiveness of

providing services, reducing the number of screening examinations. This time, a new prediction model was designed, which is an output of LUMPO3, that demonstrated that it is possible to reliably predict the time of the onset of metastases, and also to implement different screening strategies in patients with UM. Results of this study were recently published [315].

The objective of **Chapter 3** was to: (1) validate LUMPO3 in Liverpool, essentially to examine LUMPO3's ability to predict the appearance of liver metastases in patients treated at the LOOC; and (2) to determine the costs of liver screening in patients with UM.

3.2 Material and Methods

There were 615 eligible patients for our retrospective observational cohort study who were previously treated for primary UM at the LOOC, between 1988 and 2018, and who underwent liver surveillance between 2008-2018. Clinical data on this cohort study have been published previously [315]. Data from these patients were analysed concerning the identification and characterization of hepatic metastases through liver screening and later correlated with demographic, primary tumours, follow-up, and outcome data, as already outlined in **Chapter 2**.

3.2.1 Data Collection

A detailed retrospective review of data from UM patients identified by OOB with the diagnosis of UM who underwent liver screening between 2008-2018 was performed. A total of 615 radiological reports of liver screening from UM patients were found. The relevant clinical data of the enrolled patients related to imaging studies, such as demographic information (gender, age), features of the liver imaging, follow-up and outcome were retrieved from the electronic medical records at the LUHFT. These information collected through a hospital software called CRIS, provided data whose details are available in a existing proforma (**Appendix 6**).

All patients were categorized into the 11-year period according to the year they performed the primary treatment or, in some cases secondary treatment, at the LOOC. The following variables were analysed according to the information found in the patients' scan reports:

3.2.1.1 Data from scan reports

- 1) Scan reports for all patients:
 - a. When the first liver scan occurred;
 - b. The total number of liver scans performed;
 - c. The number of scans per year;
 - d. The performed scanning modality (MRI, CT, or US)

- 2) Patients in whom metastases were detected:
 - a. Metastases diagnosed by clinical imaging - metastases were detected through liver screening;
 - b. Metastases diagnosed by autopsy - metastases were detected post-mortem through histopathological examination;
 - c. The number of scans from the primary treatment to the detection of the first metastases;
- 3) Patients who never developed metastases:
 - a. The median time from the treatment of the primary tumour to the last scan performed;
 - b. The total numbers of scans until the last scan.

3.2.1.2 Occurrence of metastases

The time of occurrence of metastases was calculated for all patients who demonstrated metastases during the liver screening program. The time to detection of metastases was calculated from the date of treatment of the primary UM until the date of detection of the first metastases. The percentages of metastases detected at different times were also calculated. All analyses were performed using SPSS Statistics V27 (IBM).

3.2.1.3 Cost analysis of imaging

For this study, the unit costs of the scans were specifically calculated, without considering other associated costs such as material and equipment used during the procedures, or human resources involved. The costs of scans performed were obtained based on the direct costs of each of the studies performed (MRI, CT, and US), from the price list cited in the National Institute of Health and Care Excellence (NICE) liver cancers guideline, the price year adopted was 2021 [316] (**Table 3.1**). In this guideline, the costs related to MRI it varies from £138 to £250 per examination, the costs of CT from £83 to £172 per study, and the costs of the US ranged from £52 to £161. Maximum and minimum prices were obtained, as listed in the NICE guidance.

The total costs were calculated as the costs of each scan and presented as follows:

- 1) The costs of all scans performed until the detection of metastases;
- 2) The costs of all scans until the last scan performed in patients who did not develop metastases;

Data were collected, filed, and processed in Excel format (Microsoft, Inc., UoL, UK) and SPSS Statistics V27. As described in **Chapter 2**, after transferring the data to Dr Helen Kalirai for compilation, the dataset was returned to me, to Professor Azzam Taktak, and to Dr Antonio Eleuteri, for statistical analysis and model construction.

Table 3.1: Costs of MRI, CT, and US according to NICE guidelines

Currency	Currency Description	Unit Cost
RD01A	Magnetic Resonance Imaging Scan of One Area, without Contrast, 19 years and over	£138
RD01B	Magnetic Resonance Imaging Scan of One Area, without Contrast, between 6 and 18 years	£142
RD01C	Magnetic Resonance Imaging Scan of One Area, without Contrast, 5 years and under	£144
RD02A	Magnetic Resonance Imaging Scan of One Area, with Post-Contrast Only, 19 years and over	£164
RD02B	Magnetic Resonance Imaging Scan of One Area, with Post-Contrast Only, between 6 and 18	£207
RD02C	Magnetic Resonance Imaging Scan of One Area, with Post-Contrast Only, 5 years and under	£229
RD03Z	Magnetic Resonance Imaging Scan of One Area, with Pre- and Post-Contrast	£199
RD04Z	Magnetic Resonance Imaging Scan of Two or Three Areas, without Contrast	£152
RD05Z	Magnetic Resonance Imaging Scan of Two or Three Areas, with Contrast	£202
RD06Z	Magnetic Resonance Imaging Scan of more than Three Areas	£202
RD07Z	Magnetic Resonance Imaging Scan Requiring Extensive Patient Repositioning	£250
RD40Z	Ultrasound Scan with duration of less than 20 minutes, without Contrast	£52
RD41Z	Ultrasound Scan with duration of less than 20 minutes, with Contrast	£65
RD42Z	Ultrasound Scan with duration of 20 minutes and over, without Contrast	£63
RD43Z	Ultrasound Scan with duration of 20 minutes and over, with Contrast	£41
RD44Z	Ultrasound Scan, Mobile or Intraoperative Procedures, with duration of less than 20 minutes	£70
RD45Z	Ultrasound Scan, Mobile or Intraoperative Procedures, with duration of 20 to 40 minutes	£118
RD46Z	Ultrasound Scan, Mobile or Intraoperative Procedures, with duration of more than 40 minutes	£161
RD20A	Computerised Tomography Scan of One Area, without Contrast, 19 years and over	£83
RD20B	Computerised Tomography Scan of One Area, without Contrast, between 6 and 18 years	£97
RD20C	Computerised Tomography Scan of One Area, without Contrast, 5 years and under	£66
RD21A	Computerised Tomography Scan of One Area, with Post-Contrast Only, 19 years and over	£107
RD21B	Computerised Tomography Scan of One Area, with Post-Contrast Only, between 6 and 18 years	£133
RD21C	Computerised Tomography Scan of One Area, with Post-Contrast Only, 5 years and under	£172
RD22Z	Computerised Tomography Scan of One Area, with Pre- and Post-Contrast	£105
RD23Z	Computerised Tomography Scan of Two Areas, without Contrast	£93
RD24Z	Computerised Tomography Scan of Two Areas, with Contrast	£104
RD25Z	Computerised Tomography Scan of Three Areas, without Contrast	£103
RD26Z	Computerised Tomography Scan of Three Areas, with Contrast	£115
RD27Z	Computerised Tomography Scan of more than Three Areas	£111

3.2.2 LUMPO3 model Validation

Statistical analyses were performed using semiparametric competing risks model of metastases onset, integrated in the class of semiparametric transformation models. To perform the internal validation of LUMPO3, the model developed by Antonio Eleuteri et al. [241] was used to predict the appearance of liver metastases in patients diagnosed with UM, and also calculate liver screen intervals. There were two predictors considered, both resulting from the LUMPO3 model: the first being a linear combination of age and sex (linear predictor of death due to causes other than metastases *lpod*) and the second is a linear combination of age, sex, LBD, EOE, UH, Epi, Loops, Mitoc, chromosome 3 loss, chromosome 8 gain (linear predictor of death due to metastases, *lpmd*). For this validation, whose objective was to verify the ability of LUMPO3 to predict the onset of metastases and also calculate the number of scans that could be avoided; only the *lpmd* was used, due to its specificity in relation to death caused by metastases.

The model was validated for discrimination and calibration, which are two measures to characterize the performance of a mathematical model [317]. Discrimination is described as quantifying the model's ability to correctly classify subjects into appropriate risk categories, such as low, medium, high, etc. Perfect discrimination would be observed if a model placed each individual in the class to which he or she really belongs. Calibration is described as verifying to what extent the predicted probabilities numerically agree with the actual results. Good model discrimination does not always indicate good calibration and vice versa. Harrell [317] suggests that good discrimination is always preferable whenever one has to choose which method should receive the main focus, and this is possible because it will always be conceivable to recalibrate since for true discrimination this is not possible [317].

One measure of discrimination used was the area under the receiving operating characteristic (ROC) curve (AUC), which is a graph showing the performance of a classification model at all classification thresholds [318]. This curve plots two parameters: true positive rate and false positive rate. It is a graphical representation of the relationship between sensitivity and

specificity and helps to decide the ideal model, determining the best limit for the diagnostic test. Sensitivity, specificity and precision are statistics widely used to describe a diagnostic test. In particular, they are used to quantify how good and reliable a test is [242]. Sensitivity measures the effectiveness of the test in detecting a positive disease, while specificity estimates the probability that patients without disease can be correctly excluded.

It was also of interest to assess whether there is a difference in the cumulative incidences of onset of metastases. In most clinical studies, estimating the cumulative incidence function (or the probability of experiencing an event at a given time) is of primary interest. The cumulative incidence of mortality up to a given time is the likelihood that an individual will die at that time. It is the sum of the incidences of mortality that occurred until that moment.

In order to predict the cost of scans performed, the *lpmd* feature of LUMPO3 was specifically chosen for this study, due to its specificity of predict death due of metastases. The *lpmd* feature has a numerical constitution ranging from - infinity to + infinity. To obtain a variety of predictions, 3 decision thresholds ("-1", "0" and "+1") were chosen. The predictions of *lpmd* were categorized as "recommended" and "not recommended". Based whether the *lpmd* score was above or below the threshold respectively.

The number of scans that would be hypothetically not performed according to the *lpmd* score was calculated as well as the number of metastases that would have been missed. The calculations for the number of unnecessary scans were based on the assumption that all patients considered to be at low risk would perform a surveillance program defined for up to 5 years after the initial diagnosis, similar to what is described in some surveillance programs for UM [169,319] and for other types of cancers [320-325].

3.3 Results

3.3.1 Overall imaging utilization

Among the 615 UM patients who underwent liver surveillance, a total of 3854 imaging procedures were performed between 2008-2018. The general utilisation of abdominal surveillance images after the treatment of the primary tumour was highest in the years 2011 and 2014, which were the years when there was a greater number of patients, which may be due to administrative reasons. Between 2017 and 2018 there was a decrease in the utilisation of scanning imaging probably because it was the last years of the study and if patients were diagnosed in those years, they would be starting their liver surveillance program, which is likely to increase in subsequent years (**Figure 3.1**).

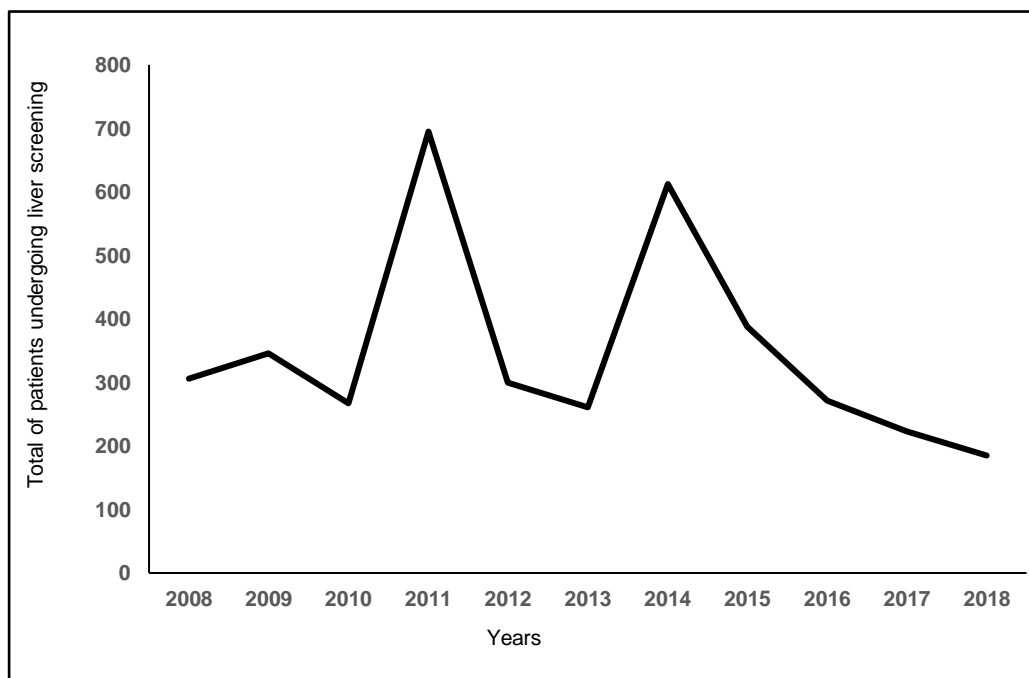


Figure 3.1 Annual rate of imaging utilization per patient. Frequency of imaging scans per patient within 11 years of liver surveillance for uveal melanoma patients.

3.3.2 Imaging modality

Among the 615 patients undergoing liver screening, the majority of UM patients underwent MRI (n = 2419 [62.8%]); followed by patients who underwent US (n = 945 [24.5%]), and CT (n = 490 [12.7%]) (**Table 3.2**). The general annual use of MRI, US, and CT was also higher in the years 2011 and 2014. However, in 2018 there was a great decrease in MRI examinations and in contrast more US were performed, probably because these patients were starting the surveillance program and at this stage more US are usually performed and the MRI is only used when suspected lesions appear (**Figure 3.2**).

Table 3.2: Modality and frequency of scans performed

Frequency of scans	Scans modality						Total all scans
	MRI		US		CT		
	Nº patients	Total MRI	Nº patients	Total US	Nº patients	Total CT	
1	67	67	298	298	58	58	423
2	34	68	46	92	29	58	218
3	13	39	24	72	17	51	162
4	26	104	21	84	11	44	232
5	25	125	18	90	12	60	275
6	26	156	7	42	4	24	222
7	20	140	4	28	9	63	231
8	19	152	4	32	3	24	208
9	14	126	4	36	1	9	171
10	20	200	5	55	3	30	285
11	22	242	1	12	2	22	276
12	17	204	3	39	1	13	256
13	9	117	1	15	1	14	146
14	10	140	1	16	-	-	156
15	10	150	2	34	-	-	184
16	8	128	-	-	-	-	128
17	7	119	-	-	-	-	119
18	1	18	-	-	-	-	18
19	1	19	-	-	-	-	19
20	1	20	-	-	1	20	40
21	3	63	-	-	-	-	63
22	1	22	-	-	-	-	22
Total	615	2419	615	945	615	490	3854

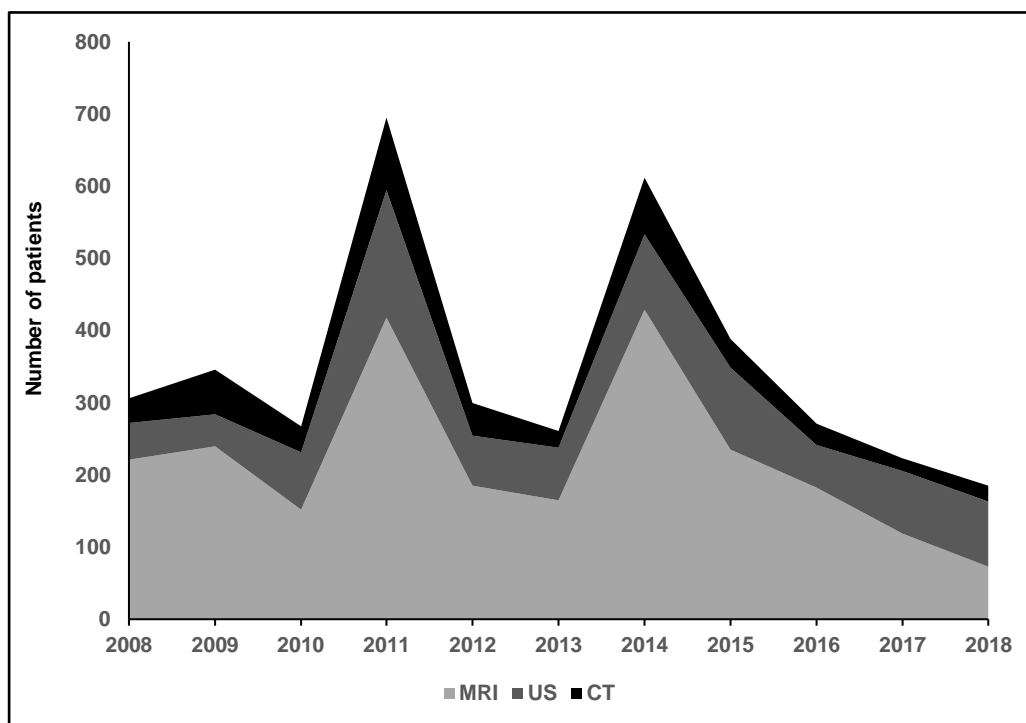


Figure 3.2 Frequency of imaging modality per patient within 11 years of liver surveillance for UM patients. The overall yearly utilization of MRI, CT and US scanning varied over time, but the greatest increase in imaging was largely in 2011 and 2014. In addition, these patients were twice as likely to have a high frequency of imaging compared with the rest of patients.

3.3.3 Factors associated with follow-up imaging

3.3.3.1 Time and number of scans until the detection of metastases in 150 patients whose metastases were detected through liver surveillance

During this study, it was possible to verify how many scans patients were submitted to before the metastases were detected and the median time from the diagnosis to the detection of metastases. As mentioned in **Chapter 2**, patients who developed metastases were divided into two groups: patients in whom metastases were detected by clinical imaging (n = 150), and patients in whom metastases were detected by autopsy (n=79). In the 150 patients, the median time from the diagnosis to the detection of the first metastases was 2.6 years (range,

0-17.8) (**Figure 3.3**). A total of 793 scans were performed during these period before the detection of metastases (**Figure 3.4**).

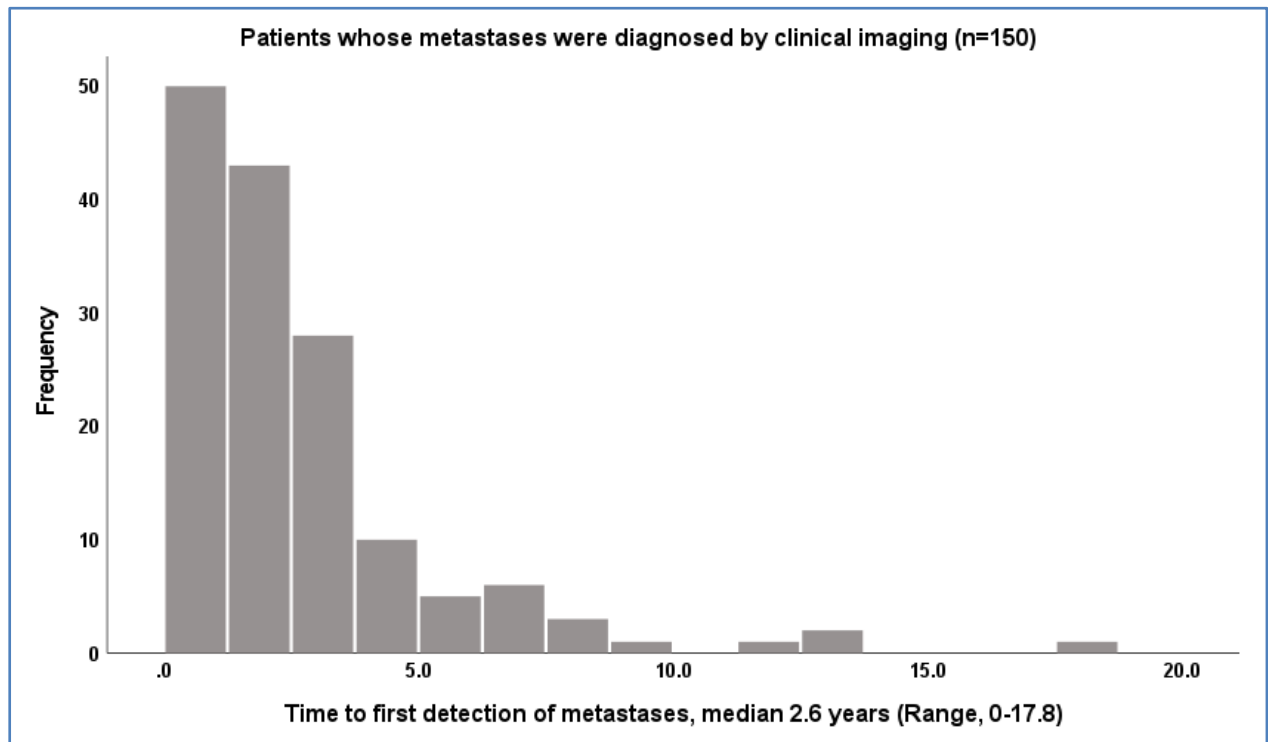


Figure 3.3 Patients whose metastases were diagnosed by clinical imaging – time to the first detection of metastases.

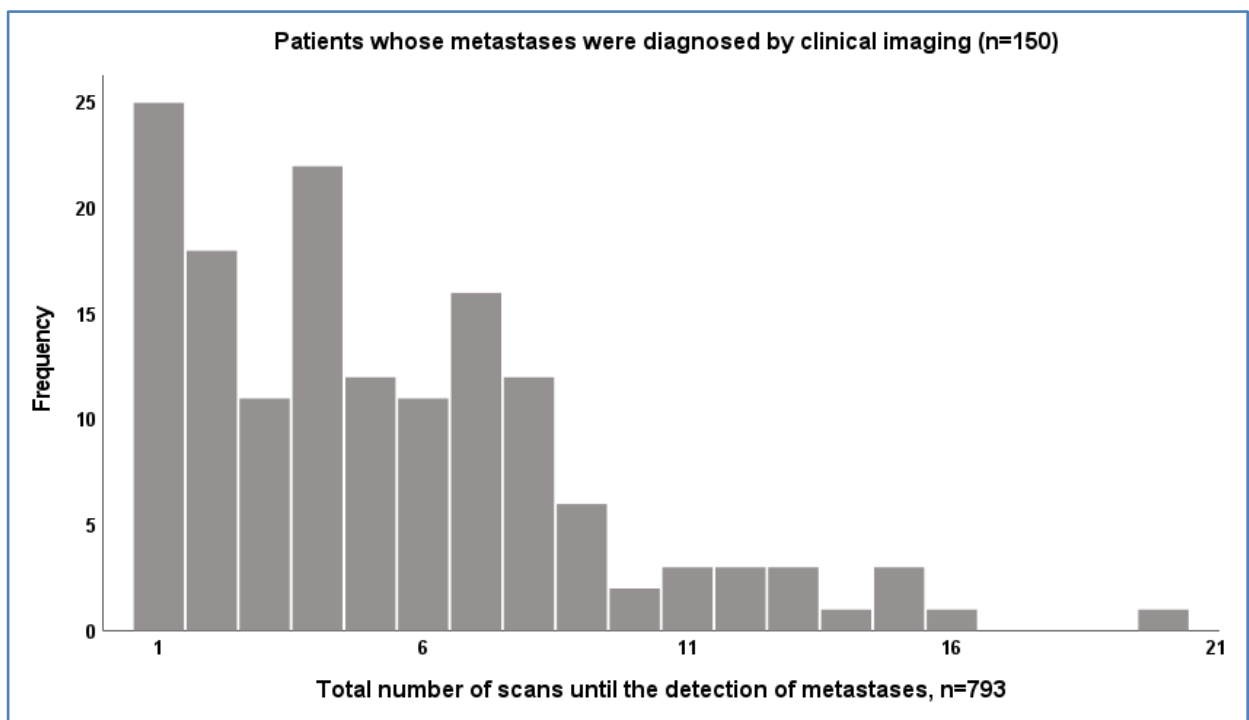


Figure 3.4 Patients whose metastases were diagnosed by clinical imaging – total number of scans until the detection of metastases.

The interpretation of the frequency of scans in 150 patients revealed the following trend: In 25/150 (16.7%) patients, metastases were diagnosed in the first scan performed. Most patients 74/150 (49.3%) in whom metastases were detected during the liver screening study performed between 2-6 scans, that is, in total 283/793 (30.7%) examinations were performed in these 74 patients up to the detection of metastases. This group of 74 patients also had the highest number of events at the end of the study 60/150 (52.2%). On the other hand, 39/150 (26%) patients who underwent between 7-11 examinations had a higher frequency of examinations than the previous group, totalling 315/793 (39.7%) scans. This could be because suspicious lesions may have been found and, consequently, the intensity of the scanning increased. Finally, a group of 12/150 (8%) patients underwent between 12-20 examinations each, making a total of 170/793 (21.4%) scans (**Table 3.3**).

Table 3.3: Number of scans until the detection of metastases and number of events

Frequency of scans until detection of metastases	Total of patients	Total of scans	Number of events	Censored	
				Number	Percent
1	25	25	22	3	12%
2	18	36	14	4	22.2%
3	11	33	10	1	9.1%
4	22	88	17	5	22.7%
5	12	60	10	2	16.7%
6	11	66	9	2	18.2%
7	16	112	10	6	37.5%
8	12	96	10	2	16.7%
9	6	54	2	4	66.7%
10	2	20	1	1	50.0%
11	3	33	3	0	0.0%
12	3	36	1	2	66.7%
13	3	39	2	1	33.3%
14	1	14	0	1	100.0%
15	3	45	3	0	0.0%
16	1	16	1	0	0.0%
20	1	20	0	1	100.0%
Overall	150	793	115	35	23.3%

3.3.3.2 Time and number of scans until the detection of metastases in 79 patients whose metastases were detected by autopsy

Interpretation of liver surveillance data from 79 patients whose metastases were detected by autopsy revealed a median time of 3.3 years (Range, 0.4-8.6 years) until the detection of metastases (autopsy) (**Figure 3.5**). In total, 140 scans were performed until metastases were detected (**Figure 3.6**). Interestingly, 60/79 (75.9%) patients in this group only performed 1 scan over the liver surveillance program.

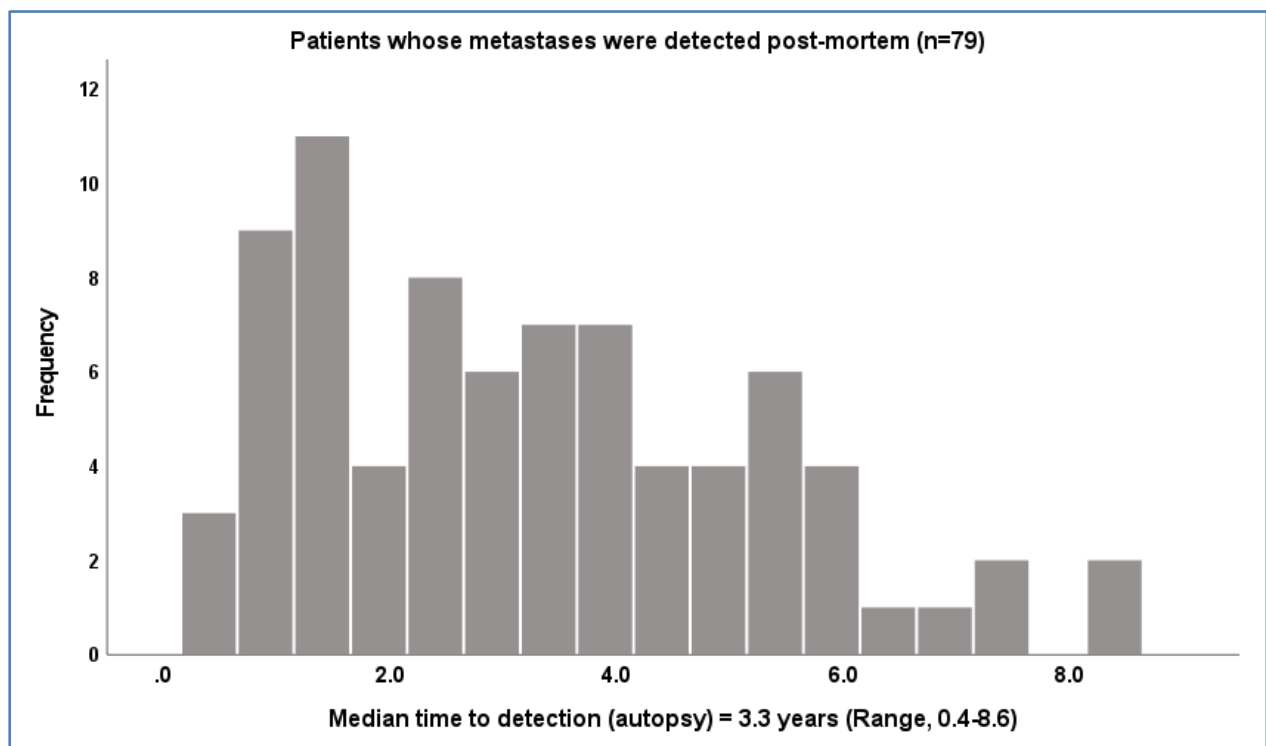


Figure 3.5 Patients whose metastases were detected by autopsy – median time until the detection of metastases

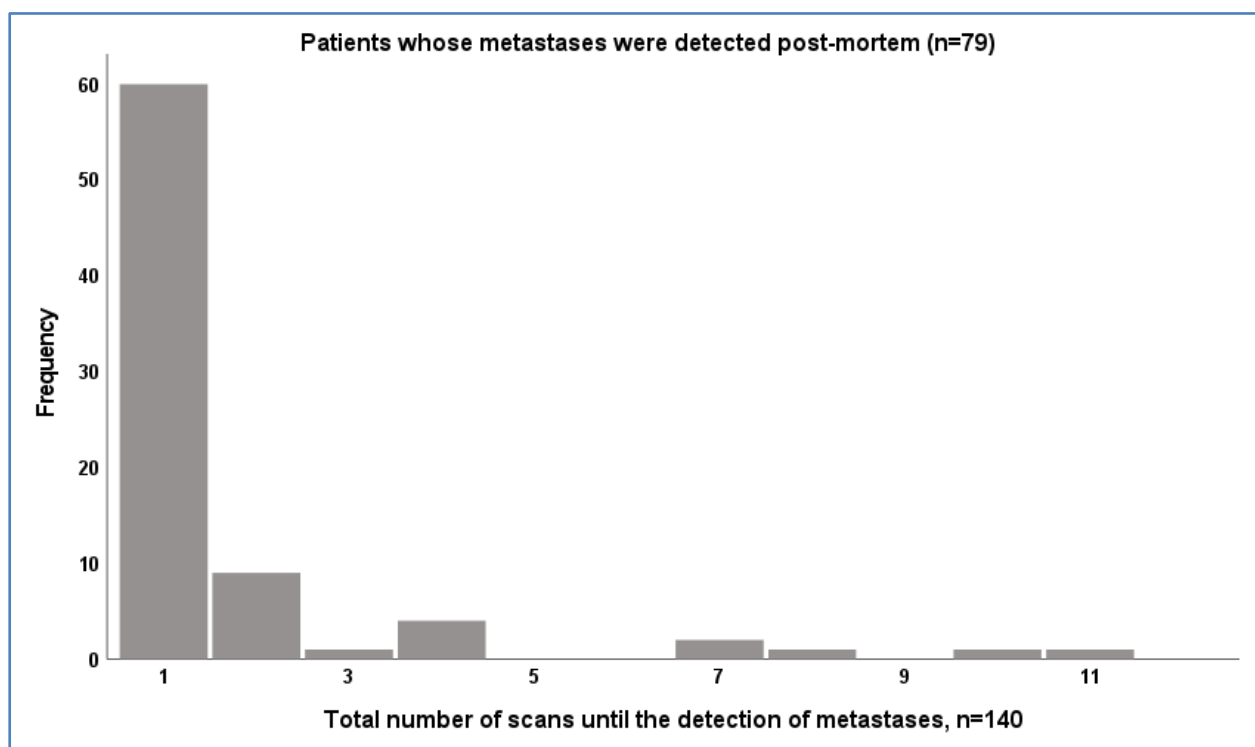


Figure 3.6 Patients whose metastases were detected by autopsy – total number of scans until the detection of metastases.

Although this group of patients performed a reduced number of scans during the study, metastases were detected post-mortem, it was unclear whether these patients had no indication to continue the screening program, or if the program continued in other institutions.

Table 3.4 shows that these patients had an irregular liver surveillance, the majority of patients 60/79 (75.9%) performed only 1 scan over the study period. A more detailed analysis showed that these 60 patients had a median follow-up time of 3 years (range, 0.2-8.6), and the median time from the primary treatment to the first and only scan was 0.2 years (range, 0.0-2.3 years), which indicates that these patients missed 2.8 months of liver surveillance in the hospitals where we performed this analysis, having them however all died of liver metastases.

Table 3.4: Frequency of scans in 79 patients whose metastases were detected at autopsy

Frequency of scans until detection of metastases	Total of patients	Total of scans	Valid percent
1	60	60	75.9
2	9	18	11.4
3	1	3	1.3
4	4	16	5.1
7	2	14	2.5
8	1	8	1.3
10	1	10	1.3
11	1	11	1.3
Overall	79	140	100.0

3.3.3.3 Time and number of scans in 386 patients who never demonstrated metastases during the liver screening study

In this analysis, we found that the trend among all groups of patients was that a large percentage of patients underwent only one examination. In this group of 386 patients, the following was observed: the median time from primary treatment to the last scan was 3 years (range, 0.0-26.1 years) (**Figure 3.7**). In total, 2114 examinations were performed on 386 patients during the study period, with no metastases detected (**Figure 3.8**). 140/386 (36.3%) of these patients underwent only 1 scan, which was 6.6% (140/2114) of the total of scans in this group. **Table 3.5** shows that of the 140 patients who underwent only 1 scan; the number of patients who died was 24/140 (17.2%). Overall, in this group of 386 patients, 46/386 (11.9%) individuals died, 24/46 (52.2%) of them performed only 1 scan. This may indicate that these patients could have other chronic diseases and could not continue the liver surveillance program, as they would be being treated primarily for these diseases.

Regarding the frequency of scans, in this study it was shown that, in this group, some patients performed an excessive number of scans, and it will be seen later in this chapter that many of these scans would be unnecessary. The observed trend was that a greater number of examinations were performed in a reduced number of patients.

The following predisposition was verified: 114/386 (29.5%) patients performed between 2-6 scans, which totalled 437/2114 (20.8%) scans, 4 scans per patient. 75/386 (19.4%) patients performed between 7-11 scans, comprising 692/2114 (32.7%) scans, 9 scans per patient. 42/386 (10.9%) patients performed between 12-16 scans, consisting of 575/2114 (27.2%) scans, 14 scans per patient, and finally, 15/386 (3.9%) patients performed 17-22 scans, totalling 214/2114 (10.2%) scans, 18 scans per patient (**Table 3.5**).

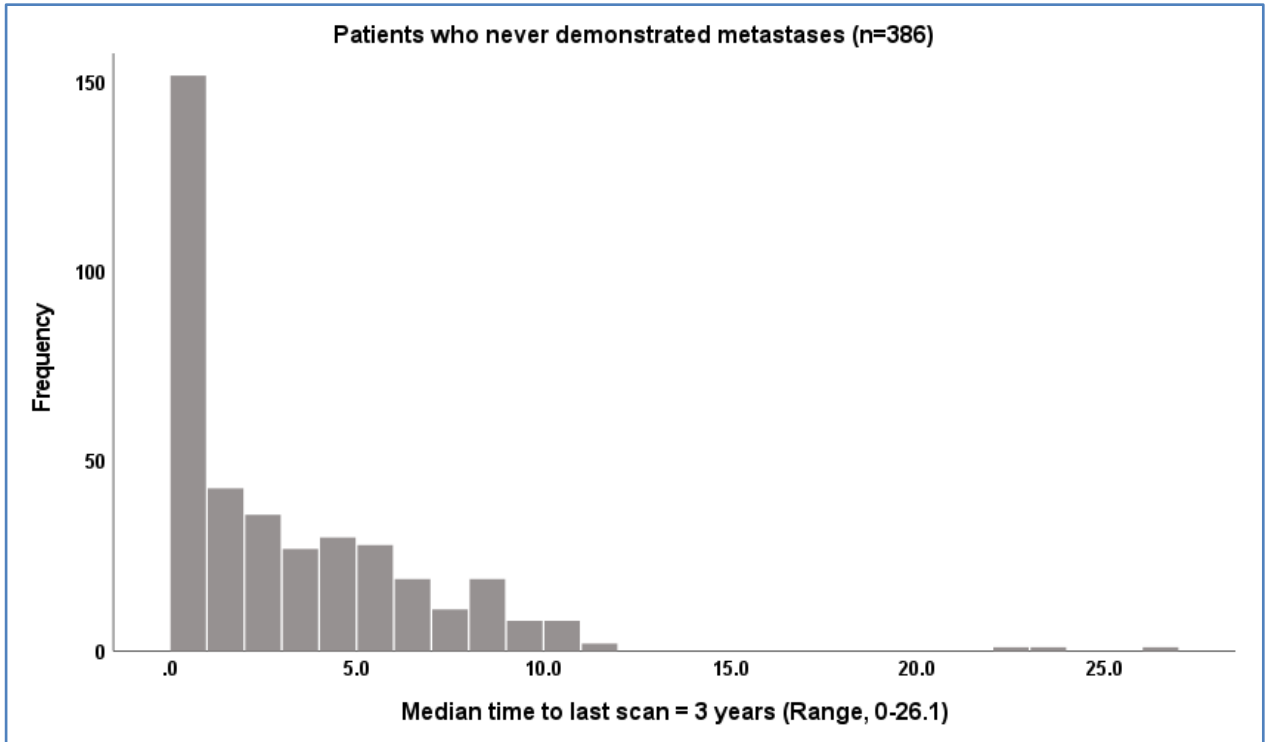


Figure 3.7: 386 patients who did not demonstrated metastases grouped according to the total number of scans and time to the last scan.

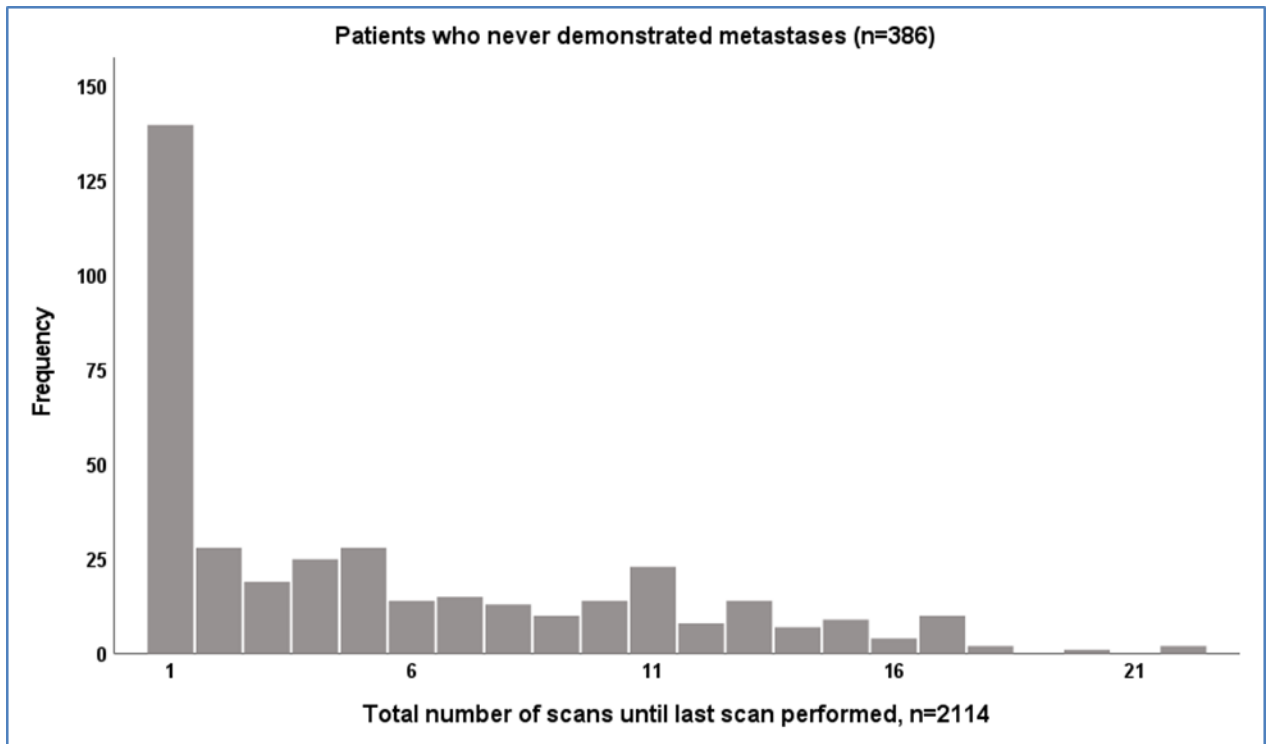


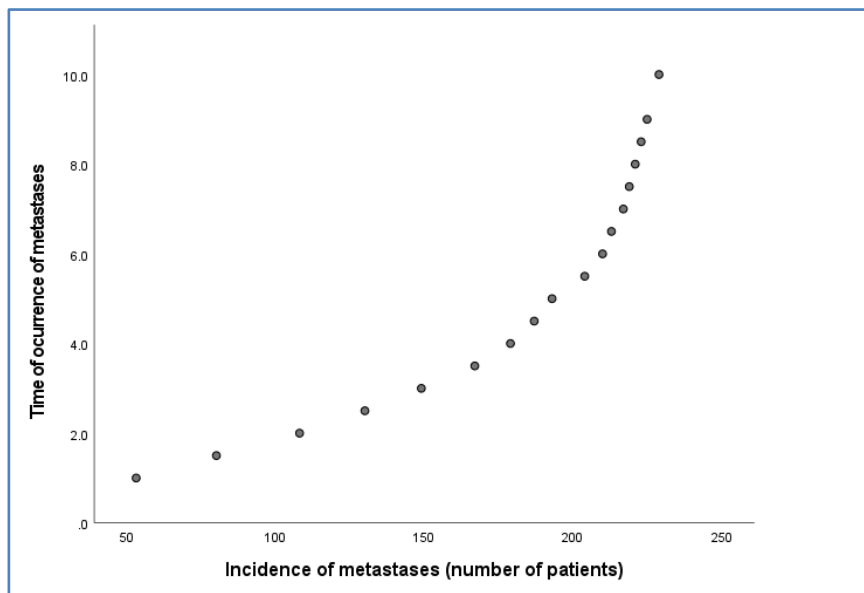
Figure 3.8: 386 patients who did not demonstrated metastases grouped according to the total number of scans and time to the last scan.

Table 3.5: Frequency of scans in 386 patients who never developed metastases

Frequency of scans until the last scan performed	Total of patients	Total of scans	Number of events	Censored	
				Number	Percent
1	140	140	24	116	82.9%
2	28	56	8	20	94.7%
3	19	57	1	18	91.1%
4	25	100	2	23	92.0%
5	28	140	4	24	85.7%
6	14	84	2	12	85.7%
7	15	105	1	14	93.3%
8	13	104	2	11	16.7%
9	10	90	0	10	100.0%
10	14	140	0	14	100.0%
11	23	253	0	23	100.0%
12	8	96	0	8	100.0%
13	14	182	2	12	85.7%
14	7	98	0	7	100.0%
15	9	135	0	9	100.0%
16	4	64	0	4	100.0%
17	10	170	0	10	100.0%
18	2	36	0	2	100.0%
20	1	20	0	1	100.0%
22	2	44	0	2	100.0%
Overall	386	2114	46	340	88.1%

3.3.4 Incidence of metastases

The time of occurrence of metastases were examined for all UM patients during the liver surveillance program. **Figure 3.9** shows the frequency of metastases detected for all patients in this study at different time points. In 53/229 (23.2%) patients, metastases were detected one year after the treatment of the primary tumour, in 193/229 (84.3%) 5 years later, and in 226/229 (98.6%) after 10 years.



Metastases	
Incidence	Time of occurrence (years)
53/229 (23.2%)	1
108/229 (34.9%)	2
149/229 (65.1%)	3
179/229 (72.9%)	4
193/229 (84.3%)	5
208/229 (90.8%)	6
217/229 (94.6%)	7
220/229 (96.1%)	8
225/229 (98.3%)	9
226/229 (98.6%)	10

Figure 3.9: Cumulative Incidence of metastases at different time points of the development of the disease for all 229 patients diagnosed of metastases.

3.3.5 Costs analysis of imaging

3.3.5.1 Costs of imaging for patients who developed metastases

The estimated costs for the different modalities of scanning used in the liver surveillance program in this study were calculated. As described in Material and Methods, scan costs were calculated based on the minimum and maximum costs available at the NICE guidelines. For patients who developed metastases, 1740 scans were performed whose costs were estimated between £191,147 and £367,931 (**Table 3.6**).

3.3.5.2 Costs of imaging for patients who did not develop metastases

For patients who did not develop metastases, 2114 scans were performed, whose total costs were estimated between £225,983 and £443,942 (**Table 3.7**).

Table 3.6: Estimated costs of liver imaging for patients who developed metastases, based on the NICE guidelines

Type scan	Number of scans	NICE minimum cost/scan	NICE maximum cost/scan	Minimum total cost	Maximum total cost
MRI	1031	£140	£250	£144,340	£257,750
CT	429	£83	£172	£35,607	£73,788
US	280	£40	£130	£11,200	£36,400
Total	1740			£191,147	£367,938

Table 3.7: Estimated costs of liver imaging for patients who did not develop metastases, based on the NICE guidelines

Type scan	Number of scans	NICE minimum cost/scan	NICE maximum cost/scan	Minimum total cost	Maximum total cost
MRI	1388	£140	£250	£194,320	£347,000
CT	61	£83	£172	£5,063	£10,492
US	665	£40	£130	£26,600	£86,450
Total	2114			£225,983	£443,942

3.3.6 Statistical analysis results

3.3.6.1 Model validation

3.3.6.2 Discrimination and calibration

As mentioned in Material and Methods, for this new feature resulting from the LUMPO3 model, the predictor considered for this study was *the lpmd* representing a *linear predictor of death due to metastases*. This model was previously validated via bootstrap resampling in terms of discrimination and calibration. By using the new feature, it was verified that the performance of discrimination was consistent over time. **Table 3.8** demonstrates the Area under the ROC within 0.5 to 10 years (2000 samples, 95% confidence interval). **Figure 3.10** shows a ROC graph demonstrating the consistent performance of discrimination over 5 years. **Table 3.9** shows 9 different scenarios represented according to the cumulative incidence of the initial development of metastases and the linear predictor of metastatic death, in terms of decision thresholds. In this case, sensitivity, specificity, and negative and positive predictive values within 5 years were calculated for each decision thresholds. Model calibration was carried out by comparing the number of events observed with the expected onset of metastases. These estimates are shown in **Figure 3.11**, in which it can be seen a good agreement between the observed and predicted events.

Table 3.8 Area under the ROC

Time (years)	AUC (95% CI)
0.5	0.85 [0.76, 0.92]
1	0.86 [0.80, 0.90]
2	0.87 [0.83, 0.91]
3	0.86 [0.82, 0.89]
4	0.85 [0.81, 0.88]
5	0.85 [0.81, 0.88]
6	0.85 [0.81, 0.89]
7	0.84 [0.80, 0.88]
8	0.84 [0.80, 0.88]
9	0.84 [0.78, 0.88]
10	0.84 [0.77, 0.89]

(Table published in *Comput. Biol. Med.* 2021 Mar; 130:104221. doi: 10.1016/j.combiomed.2021.104221. Epub. 2021 Jan 20).

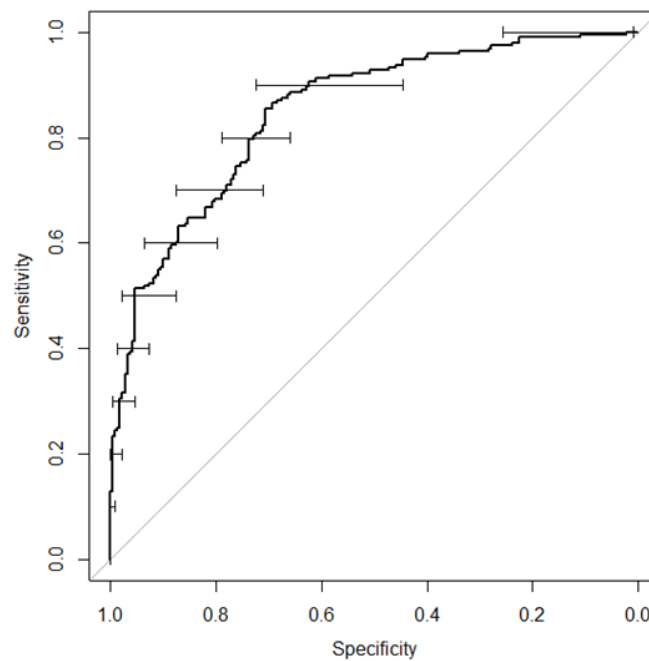


Figure 3.10: ROC graph at 5 years with a bootstrapped 95% confidence interval on specificity (image published in *Comput. Biol. Med.* 2021 Mar; 130:104221. doi: 10.1016/j.combiomed.2021.104221. Epub. 2021 Jan 20).

Table 3.9: Sensitivity, specificity, positive and negative predictive values within 5 years, for different decision thresholds

Cumulative incidence of metastases onset decision threshold	Linear predictor of metastatic mortality decision threshold	Sensitivity	Specificity	Positive Predictive Value	Negative Predictive Value
0.10	- 1.00	0.99 [0.97, 1.00]	0.18 [0.13, 0.23]	0.52 [0.50, 0.53]	0.95 [0.88, 1.00]
0.15	- 0.29	0.96 [0.93, 0.98]	0.36 [0.30, 0.42]	0.57 [0.55, 0.60]	0.91 [0.85, 0.96]
0.20	0.25	0.92 [0.88, 0.96]	0.51 [0.44, 0.58]	0.62 [0.59, 0.66]	0.88 [0.83, 0.93]
0.25	0.69	0.89 [0.84, 0.93]	0.65 [0.59, 0.72]	0.69 [0.65, 0.73]	0.87 [0.82, 0.91]
0.30	1.08	0.81 [0.75, 0.87]	0.72 [0.66, 0.77]	0.72 [0.67, 0.76]	0.81 [0.76, 0.86]
0.35	1.43	0.70 [0.64, 0.77]	0.78 [0.72, 0.83]	0.74 [0.69, 0.79]	0.75 [0.70, 0.79]
0.40	1.76	0.64 [0.58, 0.71]	0.85 [0.81, 0.90]	0.79 [0.74, 0.85]	0.73 [0.69, 0.77]
0.45	2.07	0.55 [0.48, 0.62]	0.90 [0.86, 0.94]	0.83 [0.78, 0.89]	0.69 [0.66, 0.73]
0.50	2.38	0.44 [0.37, 0.51]	0.95 [0.92, 0.98]	0.89 [0.83, 0.95]	0.66 [0.63, 0.69]

(Table published in *Comput. Biol. Med.* 2021 Mar; 130:104221.doi:10.1016/j.combiomed.2021.104221. Epub. 2021 Jan 20).

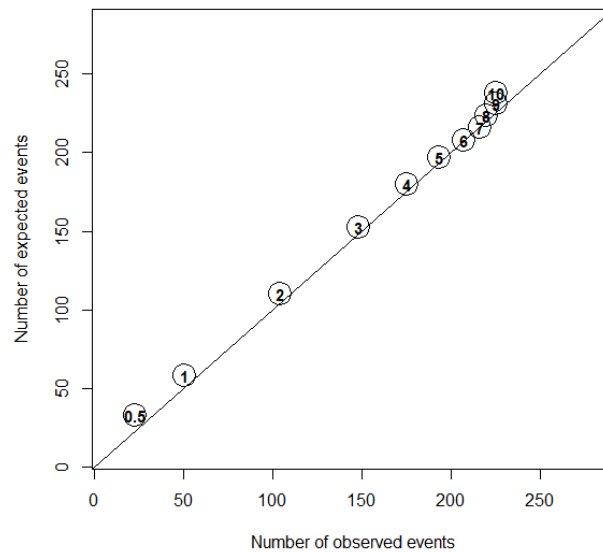


Figure 3.11: Comparison of observed and expected number of metastases onset events within 0.5 to 10 years since management (Image published in *Comput. Biol. Med.* 2021 Mar; 130:104221.doi:10.1016/j.combiomed.2021.104221. Epub. 2021 Jan 20).

3.3.6.3 Cost analysis of liver scanning

The total costs of the provision of health services could potentially be decreased with the application of LUMPO3 by reducing the number of screening examinations. The percentage of patients who had cost savings at different decision threshold points based on the analysis of the *lpmd* is summarized below.

As mentioned in Materials and Methods, using the *lpmd* feature, predictions were made in whose patients, scans were recommended and those who were not recommended, using three different thresholds. As shown in **Table 3.10**, more patients are recommended to have scans using a lower threshold (-1), and fewer metastases would be missed. However, as the threshold value increased, fewer patients were recommended scans, but contrary, more metastases would be missed during the screening study, and a higher significant number of scans would be hypothetically not performed in patients whose scans were not recommended.

The cost savings of scans that would not hypothetically be performed were calculated, both for patients whose predictions of *lpmd* scans were recommended and for patients whose examinations were not recommended. For example, as shown in **Table 3.11**, using a threshold of -1, a series of scans performed could be avoided. In that case, a total of 185 recommended scans would not be performed. This corresponds to a potential saving of costs of between £23,758 and £42,422; approximately half of the total costs of scans actually performed during the study for this selected group of patients. Differently, still for a threshold of -1, when the predictions calculated for patients in which scans would not be recommended, it was found that as this group of patients was of low risk, all examinations that were actually performed would not be recommended (341 examinations), and a saving of between £32,584 and £66,986 hypothetically would be obtained (**Table 3.12**).

Table 3.10: Cost analysis using the *lpmd* for different decision threshold points regarding the number of metastases missed and avoided scans.

Linear predictor of death due to metastases (<i>lpmd</i>)						
Decision thresholds	Number of patients whose scans were recommended	Number of metastases missed	Number of scans that hypothetically would not be performed (n=patients) (m=median scans/patient)	Number of patients whose scans were not recommended	Number metastases missed	Number of patients/scans that hypothetically would not be performed (m=median/patient)
- 1	546	0	185 (n=29, m=6.4)	69	2/69 (3%)	46/341 (m=7.4)
0	431	0	143 (n=22, m=6.5)	184	12/184 (6.5%)	111/860 (m=7.7)
+ 1	309	0	36 (n=5, m=5.0)	306	35/306 (11.4%)	139/1170 (m=8.4)

Table 3.11: Cost analysis using the *lpmd* for different thresholds regarding cost savings for recommended scans.

<i>lpmd</i>	Scans recommended Vs scans performed/hypothetically not performed												
	Number of scans actually performed	Modality of scans			Estimated costs		Number of patients that would not perform scans	Number of scans that hypothetically would not be performed (m=median scans/patient)	Modality of scans			Estimated savings	
		MRI	CT	US	Minimum cost	Maximum cost			MRI	CT	US	Minimum cost	Maximum cost
- 1	475	383	16	76	£58,260	£108,030	29	185 (m=6.4)	151	6	28	£22,758	£42,422
0	362	317	11	34	£46,840	£85,320	22	143 (m=6.5)	123	6	14	£18,278	£33,702
+ 1	86	62	2	17	£9,560	£18,010	5	36 (m=5.0)	27	2	7	£4,226	£8,004

Table 3.12: Cost analysis using *lpmd* for different thresholds regarding cost savings for scans not recommended.

Number of scans not recommended in patients with low risk of metastases according to <i>lpmd</i>							
<i>lpmd</i>	Number of patients that would not perform scans	Number of scans that hypothetically would not be performed	Modality of scans			Estimated savings	
			MRI	CT	US	Minimum cost	Maximum cost
- 1	46	341	186	8	147	£32,584	£66,986
0	111	860	495	22	343	£84,846	£172,124
+ 1	139	1170	742	34	394	£122,462	£242,562

3.4 Discussion

This study showed a comprehensive retrospective analysis of liver screening characteristics of 615 UM patients diagnosed at the LOOC between 2008-2018. In my detailed examination, the intensity and frequency of the liver scans were evaluated, as well as the number of examinations performed in which no metastatic lesions were detected, which allowed the calculation of the number of scans that could be avoided during the liver surveillance program. For this study, a new feature of the prediction model was designed which demonstrated that it is possible to safely predict the time for the onset of metastases in UM patients, and is also possible to use the model to assess the number of scans that could be avoided using specificity as a guideline. The results of this study showed the following findings:

A) Overall imaging utilization and imaging modality: A total of 3854 imaging procedures were performed between 2008-2018 among the 615 UM patients who underwent liver surveillance during that period. Most of these patients underwent MRI (n = 2419 [62.8%]); followed by US (n = 945 [24.5%]) and CT (n = 490 [12.7%]).

B) Time and number of scans until the detection of metastases: It was demonstrated that in the 150 patients diagnosed by imaging, a total of 793 liver scans were performed until the detection of metastases, within a median time of 2.6 years (range, 0-17, 8 years) from the diagnosis to the detection of the first metastases. In contrast, in the 79 patients whose metastases were detected at autopsy, 140 examinations were performed until the detection of metastases. The average time from the treatment of primary tumours to the detection of metastases was 3.3 years (range: 0.4-8.6 years). Interestingly, 60/79 (75.9%) patients in this group underwent only 1 scan during the liver surveillance program. This group of patients performed a reduced number of scans during the study; however, metastases were detected post-mortem.

C) Time and number of scans in 386 patients who never demonstrated metastases during the liver screening study: In total, 2114 examinations were performed on these 386 patients during the study period, with no metastases detected. 140/386 (36.3%) of these patients underwent only 1 scan. The median time observed from primary treatment to the last scan was 3 years (Range, 0.0-26.1).

D) Cost analysis of imaging: Scanning costs were calculated based on the minimum and maximum costs available in the NICE guidelines. For patients who developed metastases, 1740 scans were performed, whose costs were estimated between £191,000 and £368,000. For patients who did not develop metastases, 2114 examinations were performed, whose total costs were estimated between £226,000 and £444,000. Overall, £417,000 minimum, and £812,000 maximum costs were valued for the 3854 scans performed in 615 patients enrolled in the screening program.

E) Discrimination and calibration, cumulative incidences of onset of metastases, and cost analysis of liver scanning for LUMPO3 validation using *lpmd*: Calibration measures were used to compare the number of events observed versus the expected onset of metastases. It was demonstrated a good agreement between the observed and the predicted. With the application of LUMPO3, it was demonstrated that reducing the number of screening examinations could potentially decrease the costs of providing health services.

3.4.1 Overall imaging utilization and imaging modality

The current study found a total of 3854 imaging procedures that were performed between 2008-2018 amongst the 615 UM patients who underwent liver surveillance during that period. Most of these patients underwent MRI (n = 2419 [62.8%]).

The results of other studies on liver surveillance in the literature were relatively consistent with the present analysis. Hyder et al. [321] evaluated post-treatment surveillance of patients with colorectal cancer and liver metastases (CRLM) treated surgically. They reported that of the 1739 patients with CRLM who underwent metastasectomy, about 5707 examinations were performed from the surgical treatment until five years after surgery or death. This corresponded to about 3.2 scans per patient in that period, compared with the present study, in which there were about 6.3 scans per patient during the 11-year study period. The authors demonstrated a significant increase in the use of surveillance imaging overtime after surgery for CRLM, which they suggested was due to factors associated with the characteristics of the patient or the geographical location of the hospital. With respect to the scanning modality, when comparing the Hyder study with ours, CT (97%) was more used frequently than MRI (7%) and PET (18%), contrasting to our study where the MRI was more frequent (62.8%). The study of Rantala et al. also published results different from ours: the majority of scans performed were US 215/451 (47.7%), in 215 patients diagnosed with liver UM metastases who underwent a total of 451 examinations [269]. These differences may have numerous reasons, including the cancer type and the availability of technologies (and their preference of usage) in the healthcare systems.

3.4.2 Time and number of scans until the detection of metastases

In the present study, it was demonstrated that in the 150 UM patients whose metastases were diagnosed by imaging, a total of 793 liver examinations were performed until the detection of metastases. Conversely, the 79 patients whose metastases were detected at autopsy underwent a much smaller number of scans until metastases were diagnosed (n=140 scans). The median time from diagnosis to detection of the first metastases was 2.6 years (range, 0-

17, 8 years). Similar findings have been reported in a survival study in patients with pre-symptomatic diagnosis of metastatic UM conducted by Kim et al. [326]. They described that the average time from the diagnosis of the primary tumour to the diagnosis of metastases was 31.4 months (2.6 years) in the asymptomatic group compared to 40.3 months (3.4 years) in the symptomatic group; however, they mentioned that this difference was not statistically significant ($P = 0.14$), and that this median time of interval occurred without metastases for the asymptomatic group (31.4 months) was comparable to that of asymptomatic patients in other studies [163,327], that included images as part of the liver surveillance program, such as in the present study, but they did not study the characteristics of the scanning performed during liver screening.

Intensive surveillance after diagnosis of UM in high-risk patients has been reported in the literature [143,245,254,261,269,292,328]. The impact of follow-up based on CT to detect recurrence of resectable disease after surgery for CRLM was evaluated in a study by Gomez et al. [329]. They reported that all patients who had CRLM resection and survived the perioperative phase underwent a surveillance program with a frequency of 3 months during the first 2 years. Their analysis reported an average number of 6.2 scans performed in the first 2 years. In the 444 patients who developed recurrence, it was detected during the 2 years after the initial liver resection in 402 patients. The average number of scans performed for recurrence was 10.9. Comparing the imaging surveillance program of the present study, it should be noted that all patients who developed metastases underwent a median of 7.6 scans per patient during the 11 years period of the study, and during the period until the detection of metastases (2.6 years) a median of 4 scans per patient were performed.

3.4.3 Time and number of scans in 386 patients who never demonstrated metastases during the liver screening study

386/615 (62.8%) patients who never developed metastases during the study underwent 2114 examinations. This number of scans could be considered excessive for this group of patients. Considering that they represented a group with a low risk profile for developing metastases, as mentioned in **Chapter 2**. As will be seen below, the cost analysis of liver scanning is described. When using the predictions of the new feature of LUMPO (*lpmd*) for these 386 patients, using the decision threshold point of -1, which demonstrated the best-expected results. It was found that from the group of 546 patients whose examinations were considered recommended, 319/546 (58.4%) patients were part of this group of 386 patients who never developed metastases during the study. Thus, according to the *lpmd* feature, for 319 patients in whom scans were recommended, about 185 scans would be avoided. In addition, it was also found that 119/319 (37.3%) of these patients only performed 1 scan during the study, and unfortunately, we did not know if they would have continued the program and performed more scans.

67 of the 69 (97.1%) patients considered not recommended by using the best decision threshold point in this study, were part of this group of 386 patients. 21/67 (30.4%) of them also performed only 1 scan. According to the *lpmd* feature, for those patients whose examinations were not recommended, around 341 scans would be avoided. In total, in this group, about 526/2114 (24.9%) examinations would be avoided.

In this analysis, it was found that 140/386 (36.3%) patients underwent only 1 scan during the period of study. Maeda et al. [330] described an MRI screening trial for liver metastases in 159 patients with locally controlled choroidal melanoma. They reported an MRI follow-up interval of approximately 5.7 years (range, 1.2–6.6) since diagnosis. Consistently, in our study, the median follow-up time for all 615 patients was 5.1 years (range 0.2-32), but precisely the average time from the primary treatment to the last scan was 3 years (range, 0-26.1 years).

They reported the number of scans per patient, and 38% of patients performed only 1 scan. Similarly, in the present study, 33.8% (208/615) of the total number of patients underwent only one scan, and in this specific group of patients 36.3% (140/386) also underwent only 1 scan.

3.4.4 Cost analysis of imaging

Scanning costs were calculated based on the minimum and maximum costs available in the NICE guidelines. For UM patients who developed metastases, 1740 scans were performed, whose costs were estimated between £191K and £368K. For UM patients who did not develop metastases, 2114 examinations were performed, whose total costs were estimated between £226K and £444K.

The surveillance imaging involves considerable financial costs. Previous studies have referred to the costs of imaging tests used in surveillance for different cancers [244,301,306,307,331,332]. For instance, at the University of Nebraska Medical Centre [333], total costs ranging from \$34,655 to \$72,710 were reported for patients who received between 5 and 10 screening images of abdominal, pelvis or chest CT or PET/CT. The cost per CT is \$6,931, and CT/PET is \$7,271. They considered it a significant impact to health services, mainly due to the lack of proof of benefit. Their report described questions about the frequency of imaging in patients with lymphoma in the US. The required recommended routine did not provide evidence that the imaging would improve overall survival or provide other benefits. They referred to Voss et al. [334] suggesting that the scanning could improve survival in children with high-risk Hodgkin's lymphoma, for whom highly curative saliva therapy is available. In other words, the greater possibility of recurrence would increase the positive predictive value of an image with abnormal findings.

Merrill et al. [331] analysed the utility and costs of routine staging examinations in early-stage breast cancer, and reported that the total cost of non-indicated staging scans was \$308,932.98 during the period of study, with an amount of \$5,720.98 per patient. They concluded that using the recommended staging criteria suggested by The American Society of Clinical Oncology

(ASCO) [335] contributed to reducing the total number of scans, false-positive examinations and costs of imaging. However, there were no changes in the detection of asymptomatic metastases.

Podlipnik et al. [332] evaluated the cost-effectiveness analysis of the imaging strategy for intensive monitoring of patients with malignant melanoma with a high risk of recurrence. A cost analysis was performed for each follow-up of 1805 abdomen, chest and pelvis CT scans, and 1683 MRI scans of the brain. The 290 patients with AJCC stage IIB, IIC and IIID melanoma were scanned every 6 months and were removed from the study after completing a 5-year follow-up or when metastases were detected. They reported the costs for each study performed, in which CT cost €184 per study and brain MRI with contrast of €177 per study. A decision tree model was created for each of the screening strategies involving image studies and a cost-effectiveness analysis was performed. 44.5% of patients developed metastases detected by various methods, of which 58.9% were detected by imaging. The total cost of the follow-up study was €630,011, with a cost of €2172 per patient. The cost per patients with metastases diagnosed by CT came to €115,526.70 at year 5. They concluded that CT scan was a cost-effective strategy from the first to fourth year of follow-up, whereas brain MRI was cost-effective only during the first year after melanoma treatment. The present study did not involve the creation of a decision tree model as a screening strategy, but it was calculated the total costs of scanning for the liver screening program, which was irregular for a substantial number of patients. The minimum and maximum costs of scans per patient were calculated; whose values were between £678 and £1320 per patient, respectively. The 615 patients enrolled in the screening program for 11 years performed in total 3854 scans, whose minimum and maximum costs were £417K and £812K, correspondingly. It should be noted that different programs for screening for metastases have been mentioned so far and each with its own characteristics. It should be highlighted that the costs of these programs differ from one another depending on the duration of the program, the modality of scanning used, the prices

utilized by each society, how patients are selected for inclusion in the protocols, and the benefits acquired for patients and health systems.

3.4.5 Discrimination and calibration, cumulative incidences of onset of metastases, and cost analysis of liver scanning for LUMPO3 validation using *Ipmd*

3.4.5.1 LUMPO3 model performance

This study demonstrated that the discrimination performances of the new feature of LUMPO3 were consistent over time. Calibration performance demonstrated a good agreement between the observed and the predicted, when comparing the number of metastases observed versus expected metastases.

Prognostic factors in patients with UM hepatic metastases have been evaluated in diverse retrospective studies [148,259,327,336]. Other studies described more recently, also refer to the use of imaging to assess liver invasion as determining factors for survival in addition to prognostic factors [279,337,338]. A nomogram to assist in decision-making regarding the choice of treatment for patients with UM liver metastases, selected by liver MRI, was developed by Mariani et al. [339]. For the construction of the prognostic nomogram for overall survival, four predictor factors were used, including disease-free interval between UM and UM liver metastases, LDH value, and number and size of UM liver metastases on MRI. The performance of the model was assessed in terms of discrimination, in which the model predicted well the survival after metastases of patients in 71% of cases. In terms of calibration, the model's calibration curves were evaluated the three times used in the nomogram: 6-, 12- and 24 months. They reported that the calibration of the nomogram was better at 24 months than at 12 and 6 months because, at 6 months, the model tended to overestimate the patient's survival. The study showed good calibration performance, the survival predicted by the model was very close to the observed survival. The result of multivariate analysis also confirmed almost exclusive liver involvement when patients developed metastases in 90% of cases.

Comparatively, the present model was designed to including prognostic factors of the patient and the primary tumour, different from the Mariani nomogram, which included characteristics of the hepatic metastases among other prognostic factors. When comparing Mariani's analysis to the current model, the former demonstrated good discrimination for a 24-month period, while the *Ipmd* discrimination performances were consistent over 5 years of the study. Another study, in which a nomogram was also developed that incorporated prognostic factors, including the percentage of liver involvement, LDH levels, World health Organization (WHO) performance status [340], and disease-free interval, is the study by Valpione et al. [337]. The model accurately predicts the prognosis of UM Metastases and can be helpful in decision-making and risk stratification for clinical trials. The nomogram, by reliably stratifying the prognosis for patients with UM metastases, can be of great assistance to oncologists who treat patients with UM metastases in order to adjust the different forms of treatment, and thus enabling to a better administration of resources.

Online prognostic models for other cancers have also been described in the literature, such as the study by Gray et al. [320] that validated PREDICT, an online tool for prognostic benefit and treatment for patients with early breast cancer. The tool's purpose is to assist the Doctor in making decisions about adjuvant therapy after breast cancer surgery. This algorithm has been updated since the first publication in 2010 [324,341,342], the most recent version including prognostic factors such as age at diagnosis, tumour size, lymph node status, histological characteristics of the tumour, in addition to the prognostic factors incorporated in the previous model, the prognostic markers *HER2* status and *Ki-67*.

When comparing the present model with Gray's model, the same as in our study, the calibration assessment was obtained by comparing the predicted results with the results observed in the validation data. In the validation of the PREDICT prognostic tool, a good performance was demonstrated concerning discrimination and calibration. Similar to the previous LUMPO3 model, in the PREDICT model, the discrimination of the PREDICT score as a prognostic index was assessed by calculating the ROC AUC for 5 and 10-year mortality,

both for breast cancer and all-cause mortality. It is worth highlighting that the novel prognostic feature, the *lpmd*, demonstrated that the time of onset of metastases in UM patients could be reliably predicted. Furthermore, through a good choice of a decision threshold, each of these thresholds, which have different properties that include sensitivity, specificity, and positive and negative predictive values, can allow different screening strategies to be adopted in UM patients.

3.4.5.2 Cost analysis of liver scanning using the *lpmd*

To the best of our knowledge, the current study represents the most recent cohort of patients assessed for cost analysis of liver screening using LUMPO3 and demonstrates that routine liver screening for UM metastases is time-consuming and expensive for patients and healthcare professionals.

Frequent screening examinations represent both time and financial burden on individuals, in addition to the adverse or harmful psychological effects of unnecessary scans. The literature on surveillance of UM patients suggests that the psychological variable plays an essential role in the patient's desire and ability to adhere to surveillance programs [343,344]. The anxiety experienced while waiting for the results or associated with any false-positive results can lead to stages of depression, as documented in the study by Hope-Stone et al. [345]. Patients felt that the prognostic information did not alleviate the uncertainty regarding their prognosis and that this uncertainty still obscured their lives. The different prognoses received generated different experiences of uncertainty. Another study on the patient's experience with ocular melanoma is the study by Afshar et al. [309] describing that many patients were dissatisfied with low financial and psychological counselling. Emotions can also lead to low adherence to surveillance programs. In fact, what is observed in the "real world" during surveillance programs may differ from what would be recommended by oncologists.

With the application of LUMPO3, it has been shown that reducing the number of screening examinations could represent a potential cost saving for health services. This study

demonstrated that it would be possible to save costs of unnecessary scans performed, both in patients whose LUMPO3 predictions recommended scans and in those where they were not recommended. These estimates were calculated using different decision threshold points.

In the scans recommended by the *lpmd*, it was found that metastases would not be missed at all thresholds evaluated, but some of the recommended scans were found to be excessive; therefore, several scans estimated would hypothetically not be performed, that is, in some patients, these scans were performed over a long period, which was unnecessary as most of them had a low risk of developing metastases. Scans not recommended were associated with a more significant number of scans that would be avoided, but also a considerable number of metastases would be missed. The tendency was that the higher the threshold value, the greater the number of metastases missed and also the number of scans performed that would be avoided. Thus, the lowest decision threshold was considered the best predictor. For example, using a threshold of -1, a total number of 185 scans recommended by the *lpmd* corresponding to costs between £23K and £42K would be avoided. Furthermore, at this threshold, all scans not recommended, hypothetically would not be performed, minimum costs of £33K and maximum costs of £67K would be avoided.

The impact of adopting the imaging recommendations of the ASCO, which recommends avoiding routine staging in newly diagnosed patients with early-stage breast cancer, was examined by the study by Merrill et al. [331]. The staging scans were considered "indicated" and "non-indicated" by adopting the ASCO recommendations. The results showed that the examinations indicated had a significantly greater detection of metastatic disease and changes in the patient's treatment. 43.2% (41/95) of the scans were considered indicated and 56.8% (54/95) non-indicated. Indicated scans statistically detected a more significant number of metastases (22%) than the non-indicated scans. The scans indicated were also statistically more probable than the scans not indicated to result in changes in the clinical management of patients. They concluded that non-indicated staging scans cost at least \$5,700 per patient and are associated with an even higher false-positive rate (37%). Adopting ASCO's

recommendations for staging imaging early-stage breast cancer could have prevented 54 examinations, improved patient care, and led to cost savings. This study, unlike our study, by not using a prognostic method for the scanning recommendations, did not report whether metastases would have been missed. But they reported that there was a percentage of patients with false-positive results who were submitted to additional evaluations, leading to an increase in costs.

Comparatively, in the present study, although the scan recommendation methods are different, the results have some consistencies. Using the preferable predictor as example (-1), the number of recommended patients was 546/615 (88.8%) who underwent 3470/3854 (90%) scans, and as mentioned above, 185/3470 (5.3%) excessive scans were performed on 29 patients. Recommended scans detected almost all metastases diagnosed through scanning 148/150 (98.7%). 69/615 (11.2%) patients were not recommended to perform scans, but actually, 384/3854 (10%) scans were performed in these patients. In this group of patients, metastases were missed in 2/150 (1.3%) patients, and 46 patients performed 341/384 (88.8%) unnecessary scans. Recommended but avoidable scans (185 scans for 29 patients) cost a minimum of £785 and a maximum of £1463 per patient, while non-recommended scans (341 scans for 46 patients) cost a minimum £708 and a maximum of £1456 per patient.

Several limitations of these analyses should be considered. Examinations relating to metastatic UM may have been undertaken elsewhere and thus would not be recorded in this study for the costs to be calculated. In addition, a potential range of other health care resources that may be affected were not evaluated, such as costs associated with medical staff, patient management, or costs related to innovative treatments during clinical trials.

These risks are predicted due to errors in all prognostic tests and algorithms, which are not 100% accurate as observed in surveillance programs for other cancers, which do not follow a defined time pattern and can often be truncated in about 5 years after the initial diagnosis [320-325]. The LUMPO3 algorithm has improved with the data collected at LOOC and

elsewhere, especially with significant molecular testing improvements over the past decade. However, LUMPO3 can be further refined by incorporating information about the status of genetic mutations in UM such as *BAP1*, *SF3B1* and *EIFAX1*, using bespoke NGS panels [121], or substitute immunohistochemical markers [117,118].

In summary, in this chapter, I performed a retrospective analysis of the “real world” of liver scans in 615 UM patients diagnosed at the LOOC. Their data were used to construct a predictive model of metastases (*lpmd*), an output of LUMPO3. This model was designed to predict the time of onset of metastases in UM patients in a reliable way. The model provided decision thresholds, which allowed predicting different scenarios for recommending screening strategies in UM patients. A cost analysis on all scans that hypothetical would not be performed decreased the frequency of regular screening for UM patients, depending on the risk of developing metastases. However, these calculations must be balanced, taking into account the risk of under-diagnosing some metastases.

Chapter 4

External Validation of LUMPO3

4.1 Introduction

In medicine, the development of prognostication models allows for the identification of variables that influence the prediction of the patient's outcome and also the use of these various risk factors that should be used in a systematic and reproducible manner in accordance with methods based on evidence [242]. As mentioned in **Chapter 3**, the use of suitable methods both for the development of the model and for the development of prognostic indexes and risk groups based on the models are a requirement for the appropriate selection and the use of prognostication models in clinical practice. Models need to be validated, and model performance measures reported in order to assess reliance and generalizability for use. In order to be able to understand whether a given prognosis model or prognosis index provides us with a useful tool helping to inform the patient's treatment, it is necessary to report the accuracy of the model's predictions, either in terms of demonstrating how the model separates the individuals who develop the results of those who do not, and also the comparison that demonstrates the proximity of the expected risks to the actually observed risks. Presently, several model performance proceedings are been used; however, due to the range of different clinical decisions directed from prognostic models, there is no consensus on which are the most clinically worthwhile [318].

In UM, only a limited number of studies (reviewed in **Chapter 1**) have been published to date validating prognostic models, and the majority of them have been validated internally [219,221,232-235]. To externally validate the performance of a prediction model across multiple populations and to evaluate different implementation strategies, multivariate meta-analysis can be used [346,347]. External validation means evaluating the performance of a model already developed when adapted to an independent data set, that is, data collected as part of a distinct exercise from the development of the original model.

Before their implementation, predicting risk models need to be validated against external data and compared with those used for the development of the model. This is best achieved using data from individual participants in various studies so that the performance of the model can

be examined and quantified in various populations of interest. A good prediction model will perform satisfactorily on average across all external validation data sets and crucially little or no performance heterogeneity across studies.

As in **Chapter 1**, the first version of LUMPO was for the first time externally validated in 2015, using data from the Department of Ophthalmology, University of Medical Sciences in Poznan Poland [239]. The likelihood of metastases-free survival at three years, five and ten years were obtained for each patient using LUMPO accessed online and then compared to the existing follow-up data. This validation study concluded that LUMPO is a useful tool for calculating survival probabilities in an individual patient with UM. However, the authors highlighted that the accuracy of the prognosis would potentially be improved with the use of cytogenetic data, which was lacking in their analyses [239]. In 2016, LUMPO was newly validated externally with data from the USA [240], this validation was performed using a cohort of UM patients treated at the University of California, San Francisco (UCSF) [240]. When evaluating these data, it was found that the two patient cohorts showed differences in relation to clinical and anatomical characteristics, probably because they were not defined and measured in a standardized manner. There were also differences in the type of treatment provided to UM patients in the two centres, and, furthermore, genetic data were unavailable within the UCSF dataset at that time [240]. Despite these differences, the external validation showed that LUMPO accurately estimated all-cause mortality for UM patients treated at UCSF.

As mentioned in **Chapter 1**, the revised version of LUMPO (called LUMPO3) incorporated additional information on chromosome 8q and also calculating survival using competing risk methodology [241]. In that study, estimates of crude cumulative incidence from the raw data showed that metastatic death has a different pattern from death due to other causes, thereby necessitating the need for a competing risks model. Such a model facilitates prediction of metastatic death as a distinctive event from other causes of death. LUMPO3 was internally validated using bootstrap resampling [241].

These encouraging results served as the basis for this study, to proceed with the improvement of the tool and the creation of the new improved version, based on the new information previously described. Survival calculations are known to greatly improve with the incorporating of genetic information. As mentioned above, in this new version, competing risk methods as well as UM parameters have also been incorporated to stratify patients into groups of low risk, low intermediate risk, high intermediate risk and high risk for the development of metastases and, thus, assist surveillance strategies. This division into four groups was decided after reviewing data from studies from Paris [290], Liverpool [348] and TCGA [122], where there appear to be four prognostic groups, according to the results of the DNA and RNA analysis.

Based on the fact that this new version of LUMPO has not been externally validated, and that a large cohort of UM data coming from several ocular oncology centres from countries in Europe and the USA could be collated, we undertook the external validation of the UM prognostic model, LUMPO3.

The objective of **Chapter 4** was to perform an external validation of an updated prognostic tool, LUMPO3. This was achieved by: 1) the collection of relevant independent data from members of the European Group of Ophthalmic Oncology (OOG; www.oogeu.com) and eye oncology centres located in the USA facilitated by the LOORG. 2) performing the external validation of LUMPO3 as a tool to estimate all-cause mortality, in which mortality from all causes was estimated from LUMPO3 adding the probability of metastatic death and death from other causes.

4.2 Methods

4.2.1 Study design

Our study was proposed as a multicentre project that allowed the recruitment of a sufficient number of patients using the existing clinical network within the OOG and the USA. An invitation for participation in this external validation of LUMPO3 was made in November 2017 to fourteen centres involved in the OOG and collaborative studies (**Figure 4.1**). After sharing the study proposal with the collaborating centres, initially, twenty centres expressed interest in participating, of which seven centres collaborated in the study: Leiden University Medical Centre (LUMC), Leiden and Erasmus Medical Centre Hospital (EMCH), Rotterdam in the Netherlands, University of California San Francisco (UCSF), U.S.A., University Hospital Schleswig-Holstein (UHS) in Rostock, Germany, the Helmholtz Institute of Eye Diseases (HIED) in Moscow, Russia, S.C. Oculistica Oncologica (SCOO) in Genoa, Italy, and University Hospital of Essen (UHE) Germany). Ethical approval was obtained from the local research ethics committee; the Health Research Authority (NRES REC ref 18/NW/0748). The study followed the tenets of the Declaration of Helsinki. Anonymised data were transferred from external centres according to local approvals.

Standard clinical, histopathological, and cytogenetic proforma were shared to collect information uniformly by the participating centres. **Appendix 7** shows proforma for data collection at the initial presentation. The clinical proforma was based on the data collection form used for the internal validation of LUMPO for patients seen at LOOC [219,236]. All variables included in the proforma have been coded so that there was a clear and transparent report for the model, so it could be used in a uniform way. **Appendix 8** shows table with inserted variables for the model, including its description and coding scheme.

The following desirable data were requested for the study: demographic data - sex and age; anatomical data that included tumour thickness, ultrasound or histopathological measurements of largest basal tumour diameter, presence or absence of ciliary body

involvement and presence or absence of EOE; histological data including presence or absence of extravascular matrix loops, presence or absence of epithelioid cells, and mitotic cell count per 40 high power fields; and genetic data that include the status of chromosomes 3 and 8q. Complete descriptions of how genetic data were obtained and classified were also requested, such as FISH methods, MLPA [123] or other methods.

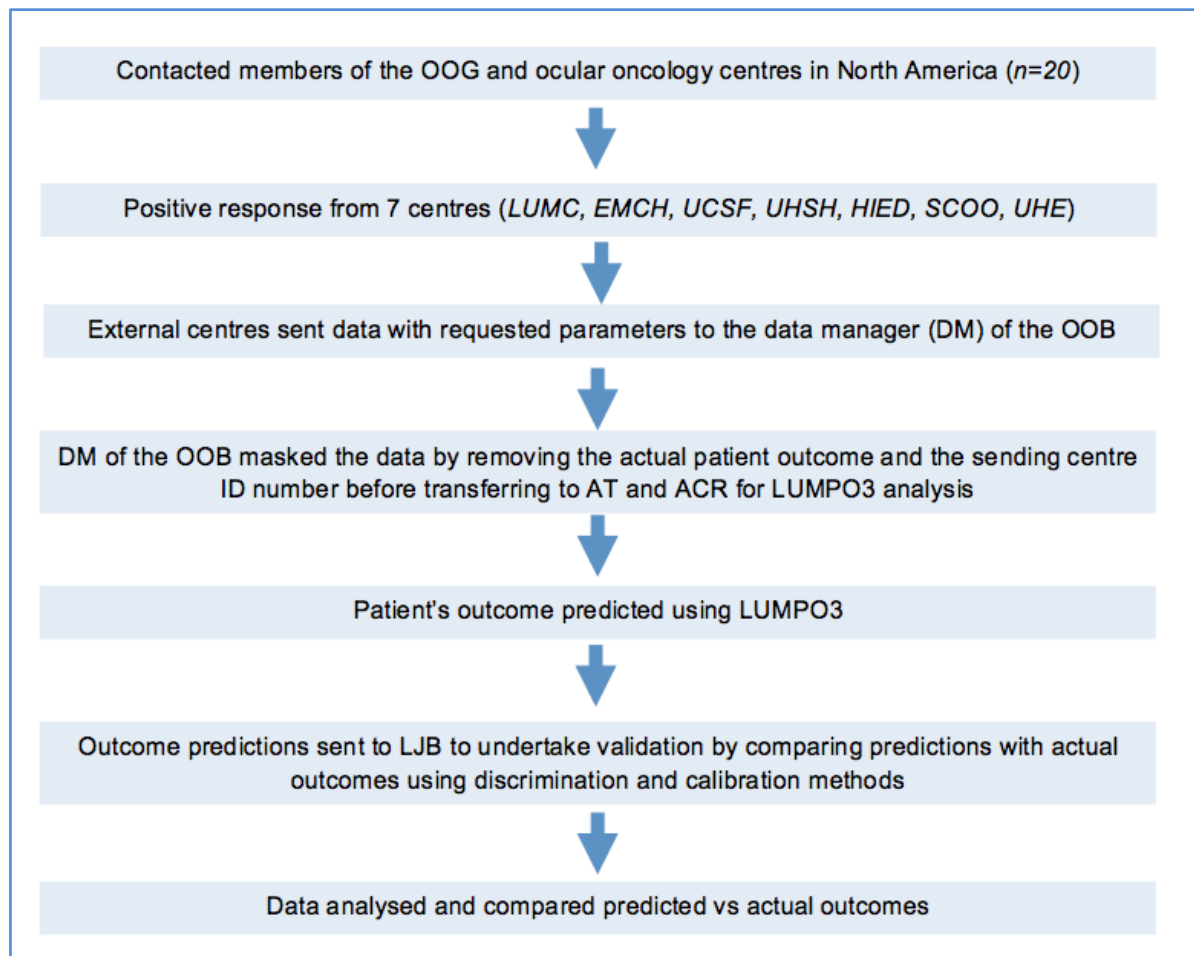


Figure 4.1. Flow Diagram External Validation LUMPO3 (image published in *Cancers - Basel*. February 18, 2020; 12 (2): 477. doi: 10.3390 / cancers12020477.)

4.2.2 Patient recruitment and sample collection

Data were collected from all patients diagnosed and / or treated for UM at collaborating centres. These data were acquired retrospectively from the years 2006 to 2016, allowing adequate time to obtain sufficient survival information.

Each of the external centres provided anonymised data. All patients received a unique study identification number (UIN) and the data were pseudo-anonymised before being entered into the study database, in accordance with their local institutional policies and guidelines to export patient data.

Cases in which the missing data included age or sex were excluded, as it was established that these variables are essential as predictors of results [238]. The data were transferred to the data manager (DM) at the LBIH at the University of Liverpool (UoL), who subsequently masked centre identification and the patient outcomes before passing the data sets for LUMPO3 analysis. Using LUMPO3, outcomes were predicted by Professor Azzam Taktak (AT), Consultant Clinical Scientist and Honorary Professor, Department of Clinical Physics and Engineering, UoL, and myself. The data were then compared with the actual outcomes by a neutral mediator and Post-doctoral Fellow in Biostatistics at the UoL, Dr Laura J. Bonnet (LJB), to determine the performance of the LUMPO3 tool. The comparative results were analysed as below using statistical methods (**Figure 4.1**).

4.2.3 Demographics of patients whose tumours were treated

Demographics and tumour data from all patients treated at the above-mentioned external centres were analysed and compared. Survival data were compared using the Kaplan-Meier analysis, the performance of the model being assessed by the calibration method Harrell C-Index [237,349], which is frequently used to assess the performance of the predictions in survival analyses.

4.2.4 Statistical analyses

Using the LUMPO3 model designed by Dr Antonio Eleuteri et al. [241] to predict the probability of survival at annual intervals for each UM patient [241] to perform external validation, survival predictions were sent to an independent statistician, who used methods of discrimination and calibration [350] for the analyses. As described in **Chapter 3**, discrimination can be defined as the ability of the prognostic model to differentiate between those who experienced the event during the study and those who did not, and calibration indicates the model's ability to demonstrate how close the probability of the event predicted by the model corresponds with the observed probability [350] (please refer to **Chapter 3** for further details).

Harrell's C statistic was used to measure the model's discriminative ability. For measurement, a scale ranging from 0.5 (representing no better than chance) to 1 (representing a perfect discrimination) was used. A pooled estimate of discrimination was also used, in which a meta-analysis of random effects was used to calculate it. This estimate was then responsible for the correlation between the studies [349]. Calibration was evaluated graphically [350]; when the predicted and observed probabilities correspond across the range of probabilities, the graphs show a 45° line. In this study, statistical analyses were performed with the R statistical software version 3.5.0.

4.3 Results

4.3.1 Characteristics of the patients

A total of 1836 data from patients diagnosed with UM (ciliary body and choroidal) were recruited from seven collaborating Ocular Oncology Centres: These included 1086 patients from Leiden (LUMC), 218 from Rotterdam (EMCH), 138 from San Francisco (UCSF), 138 from Rostock (UHSH), 134 from Moscow (HIED), 739 from Genoa (SCOO), and 49 from Essen (UHE). These data can be seen in **Table 4.1**. In this table, we can also verify original data from the Liverpool dataset that was used for the development of the model for comparison purposes.

4.3.2 Demographic and clinical analysis

As can be seen in **Table 4.1**, comparing all data sets, cases treated in Moscow tended to be female 84/134 (63%) compared to male 50/134 (37%) ($p = 0.001$). The other centres that also had highest percentage of female were Rostock 80/138 (58%) and Essen 27/49 (55%).

Patients from Moscow were relatively younger, median age 53 years (range, 22-84) compared to all the other centres ($p < 0.001$), and tumours were larger: median LDB of 15.4 mm (range 7-22 mm), and median UH of 9.1 mm (range, 1-17 mm) ($p < 0.001$). Similarly, tumours from Genoa were large, with a median LDB of 15.5 mm (range, 9-23 mm) and median UH of 10.8 mm (range, 3-22 mm) ($p < 0.001$). It was also found that patients from Moscow and Essen had the highest percentage of ciliary body involvement, 41/134 (31%) and 15/49 (31%), respectively. From the comparisons, it was also verified that the Leiden dataset, had a higher percentage of patients with extraocular melanoma 228/1086 (21%) compared to patients treated at the other centres ($p < 0.001$).

4.3.3 Histological analysis

It was also verified a difference between the prevalence of tumours containing epithelioid cells among the eight groups, in which this variable was reported: these results were considerably lower in tumours in San Francisco than in in the other centres 31/138 (45%) ($p = 0.032$), and much less frequent in Rostock 1/138 (3%) ($p < 0.001$). In contrast, patients from Genoa had the highest percentage; all the 56 patients analysed presented epithelioid cells ($p < 0.001$). These results were followed by the dataset of Leiden 720 (67%) and Rotterdam 144 (66%) ($p < 0.001$). The presence of closed PAS + loops was analysed only by the centres of Liverpool, Leiden, and Rotterdam, whose results were 597 (50%), 346 (60%), and 88 (42%) respectively. Furthermore, of the 5 centres which analysed the mitotic count, a variety results were found. In the centres with higher percentages, the following was found; whereas Liverpool UM showed more 0-2 (414) 23% mitoses per 40 high powered fields, tumours from Leiden showed more between 3-4 (291) 29%, and tumours from Rotterdam showed principally >7 (81) 49%.

4.3.4 Genetic analysis

All participating centres presented results of genetic data for the status of chromosome 3, but these results were not verified in the Rostock dataset (**Table 4.1**). **Table 4.1** also shows that most centres also provided information about the status of chromosome 8q, contrary to Rostock and Essen who did not present this data. Of all the data cohorts that presented genetic data, the patients from Genoa had the highest percentage of alterations in both chromosome 3 and chromosome 8q comparing to Liverpool cases ($p < 0.001$) and ($p = 0.001$), respectively. It was also found that there was a moderate difference between the Liverpool and Rotterdam data sets regarding the percentage of alterations in chromosome 3 ($p = 0.02$) and a considerable difference for chromosome 8q ($p < 0.001$).

4.3.5 Follow-up and outcome analysis

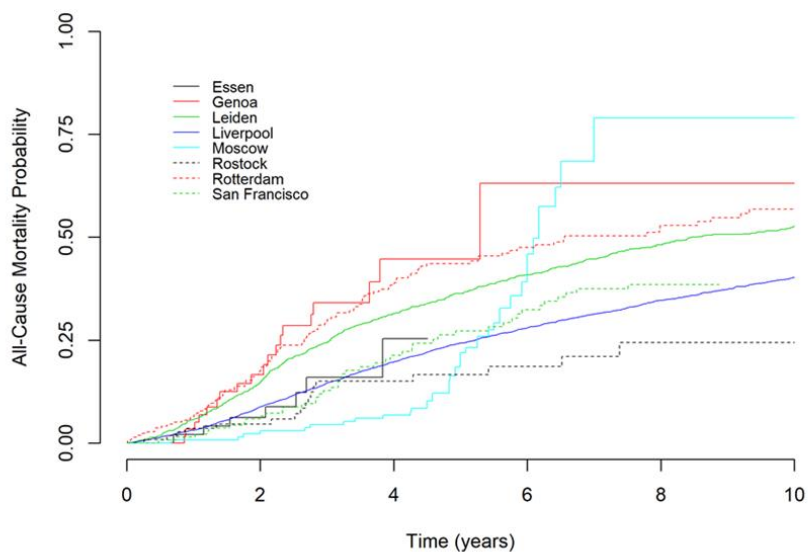
We found that there was diversity regarding the average follow-up time among external participants (variation, 0.7 – 6.5 years). The shortest average follow-up time was observed in San Francisco (7 months), and the longest period was observed in Liverpool and Leiden (6.5 and 5.2 years, respectively). To present all-cause mortality based on the Liverpool data set and external data sets, Kaplan-Meier curves were presented, as shown in **Figure 4.2**. It can be seen that Essen and San Francisco data sets were the closest to the Liverpool dataset.

Table 4.1. Patient characteristics. Development data (Liverpool) and external validation data (from seven ocular oncology centres—Leiden, Rotterdam, San Francisco, Rostock, Moscow, Genoa, and Essen)

Characteristics (n, %)	Liverpool	Leiden	Rotterdam	UCSF	Rostock	Moscow	Genoa	Essen	Total
	(n=4145)	(n=1086)	(n=218)	(n=138)	(n=138)	(n=134)	(n=73)	(n=49)	(n=5981)
Mean age at primary treatment (years, range)	61.4 (12-98)	60.7 (6-93)	62 (22-95)	60 (20-89)	64.8 (11-95)	53 (22-84)	62 (28-90)	63.8 (21-91)	61 (6-98)
Sex (%)									
Female	2010 (48)	498 (46)	111 (50.5)	67 (49)	80 (58)	84 (63)	26 (36)	27(55)	2903 (48)
Male	2135 (52)	588 (54)	107 (49.5)	71 (51)	58 (42)	50 (37)	47 (64)	22 (45)	3078 (52)
Missing	0	0	0	0	0	0	0	0	0
LDB (mm) mean	12.4	11.2	12.9	11.	11.3	15.4	15.5	13.8	12.3
Range	(1.2-28)	(0.4-30)	(3-22)	(4.8-20)	(2-22.4)	(7.3-21.9)	(9-23)	(5.5-21.3)	(0-30)
Missing	110	0	4	4	0	0	0	0	118
UH (mm) mean	5.3	5.6	7.4	5.3	5.2	9.1	10.8	8.6	5.6
Range	(0.4-20)	(0.5-17.0)	(1.0-22)	(0.9-14.1)	(0.7-16)	(1.0-17)	(3-22)	(1.3-16.2)	(0.9-22)
Missing	98	1	6	0	0	0	1	0	106
CBI (n, %)									
No	3036 (73)	803 (74)	154 (71)	132 (84)	130 (94)	93 (69)	63 (86)	33 (69)	4354 (74)
Yes	1108 (27)	283 (26)	64 (29)	6 (16)	8 (6)	41 (31)	10 (14)	15 (31)	1525 (26)
Missing	1	0		100	0	0	0	1	102
Extraocular Melanoma (n, %)									
No	3872 (93)	848 (79)	191 (88)	134 (99)	130 (96)	119 (89)	73 (100)	35 (92)	5402 (90)
Yes	273 (7)	228 (21)	27 (12)	1 (1)	5 (4)	15 (11)	0 (0)	3 (8)	552 (10)
Missing	0	10	0	3	3	0	0	11	27
Epithelioid cells present (n, %)									
No	915 (42)	351 (33)	74 (34)	38 (55)	31 (97)	61 (46)	0 (0)	-	1470 (39)
Yes	1268 (58)	720 (67)	144 (66)	31 (45)	1 (3)	71 (53)	56 (100)	-	2291 (61)
Missing	1962	15	0	69	106	2	17	49	2220
Closed PAS + Loops (n, %)									
No	600 (50)	230 (40)	124 (58)	-	-	-	-	-	954 (48)
Yes	597 (50)	346 (60)	88 (42)	-	-	-	-	-	1031 (52)
Missing	2948	510	6	138	138	134	73	49	3996
Mitoc (n, %)									
0	673 (38)	173 (17)	14 (8)	1 (20)	32 (100)	-	-	-	893 (30)
1	414 (23)	282 (28)	27 (16)	0 (0)	0 (0)	-	-	-	723 (24)
2	366 (21)	291 (29)	45 (27)	0(0)	0 (0)	-	-	-	706 (24)
3	307 (17)	264 (26)	81 (49)	4 (80)	0 (0)	-	-	-	652 (22)
Missing	2385	76	51	133	106	134	73	49	3007

Table 4.1: (Continued)

Characteristics (n, %)	Liverpool	Leiden	Rotterdam	UCSF	Rostock	Moscow	Genoa	Essen	Total
	(n=4145)	(n=1086)	(n=218)	(n=138)	(n=138)	(n=134)	(n=73)	(n=49)	(n=5591)
Chr 3 loss (n, %)									
No	333 (55)	201 (50)	100 (46)	22 (58)	-	77 (57)	27 (39)	37 (76)	797 (53)
Yes	269 (45)	202 (50)	117 (54)	16 (42)	-	57 (43)	43 (61)	12 (24)	716 (47)
Missing	3543	683	1	100	138	0	3	0	4468
Chr 8q gain (n, %)									
No	330 (55)	186 (53)	82 (38)	21 (55)	-	97 (72)	23 (34)	-	739 (52)
Yes	272 (45)	162 (47)	136 (62)	17 (45)	-	37 (28)	45 (66)	-	669 (48)
Missing	3543	738		100	138	0	5	49	4573
Follow-up time (years) mean									
(range)	6.5 (0.01-37.5)	5.2 (0-43)	4.0 (0-23)	0.7 (2-8.9)	2.7 (0-16.2)	5.0 (0.7-55)	2.0 (0-11.6)	2.7 (0.7-4.5)	6.5 (0-55)
Missing	28	0	0	0	0	0	0	0	0
Outcome (n, %)									
Alive	2480 (60)	440 (41)	98 (45)	94 (68)	121 (88)	92 (69)	54 (74)	42 (86)	3421 (57)
Death	1665 (40)	646 (59)	120 (55)	44 (32)	17 (12)	42 (31)	19 (26)	7 (14)	2560 (43)
Missing	0	0	0	0	0	0	0	0	0
Cause of Death (n, %)									
Other	773 (46)	291 (45)	36 (30)	-	4 (27)	5 (12)	2 (11)	2 (33)	1110 (43)
Possible UM metastases	0	0	0	-	6 (40)	10 (24)	1 (11)	1 (17)	19 (2)
Definitely UM metastases	893 (54)	355 (55)	78 (70)	-	5 (33)	27 (64)	16 (84)	3 (50)	1377 (55)
Missing	2	0	6	44	2	0	0	1	55



Centre	0	1	2	3	4	5	6	7	8	9	10
Essen	49	48	40	18	8	0	0	0	0	0	0
Genoa	73	57	37	20	8	3	2	1	1	1	1
Leiden	1086	956	824	697	610	545	490	441	398	361	333
Liverpool	4145	3864	3529	3182	2814	2512	2226	1932	1651	1442	1265
Moscow	134	133	131	126	119	71	18	3	1	1	1
Rostock	138	103	82	64	52	47	39	29	17	13	8
Rotterdam	218	204	174	142	111	90	78	62	53	45	38
San Francisco	138	136	130	110	86	72	66	61	41	0	0

Figure 4.2 Kaplan–Meier estimates of all-cause mortality for the centres involved in the study. The Liverpool development dataset is shown in solid blue line for comparison. The figure shows that datasets from Essen and San Francisco had the closest match to the Liverpool dataset. The numbers below the figure are the number of subjects at risk entering the corresponding time point for each dataset (Image published in *Cancers - Basel*. February 18, 2020; 12 (2): 477. doi: 10.3390 / cancers12020477).

4.3.5 Statistical Analyses

4.3.5.1 Discrimination

C statistic can be interpreted as the probability that a given subject in a group of events has a higher predicted probability of having an event, than a subject in the group of non-events [351]. In this study, C statistics were evaluated annually for all participating centres for up to 4 years (**Table 4.2**). Values varied from 0.64 (San Francisco) to 0.85 (Essen) in year 1, up to 0.65 (Moscow) to 0.89 (Essen) in year 4.

The pooled estimates of discrimination were reasonably steady over the years at 0.72 (0.68 to 0.75) in year 1 and 0.73 (0.70, 0.77) in years 2 to 4. This generally indicates a good ability of the model LUMPO3 to discriminate in independent data sets, between all those patients who died and those who survived.

**Table 4.2. LUMPO3 discrimination performance — per year
up to 4 years of follow- up**

Dataset	1 year	2 years	3 years	4 years
Essen	0.85 (0.72, 0.98)	0.87 (0.77, 0.98)	0.89 (0.80, 0.98)	0.89 (0.80, 0.98)
Genoa	0.78 (0.68, 0.88)	0.78 (0.68, 0.88)	0.78 (0.69, 0.88)	0.78 (0.69, 0.88)
Leiden	0.72 (0.70, 0.74)	0.73 (0.71, 0.75)	0.73 (0.71, 0.75)	0.73 (0.71, 0.75)
Moscow	0.65 (0.56, 0.74)	0.64 (0.54, 0.75)	0.65 (0.54, 0.75)	0.65 (0.54, 0.75)
Rostock	0.70 (0.57, 0.84)	0.72 (0.59, 0.84)	0.71 (0.57, 0.84)	0.71 (0.58, 0.84)
Rotterdam	0.73 (0.69, 0.78)	0.74 (0.69, 0.78)	0.74 (0.69, 0.78)	0.74 (0.69, 0.78)
San Francisco	0.64 (0.56, 0.72)	0.66 (0.58, 0.74)	0.66 (0.58, 0.74)	0.66 (0.58, 0.74)
Pooled estimate	0.72 (0.68, 0.75)	0.73 (0.70, 0.77)	0.73 (0.70, 0.77)	0.73 (0.70, 0.77)

(Table published in *Cancers - Basel*. February 18, 2020; 12 (2): 477. doi: 10.3390 / cancers12020477.)

4.3.5.2 Calibration

Figure 4.3 shows the calibration graphs that show the predicted probabilities of the result compared to the actuarial survival estimates. As can be seen, the graphs, in general, showed good agreement between the observed and predicted probabilities. In the Essen and Genoa data sets, the limited event data was responsible for the large confidence ranges. Leiden's data suggested that LUMPO3 overestimated the probability of survival, whereas the data from Moscow suggested that LUMPO3 underestimated mortality, in spite of the fact that the event rate was found to be relatively low in the Moscow data set.

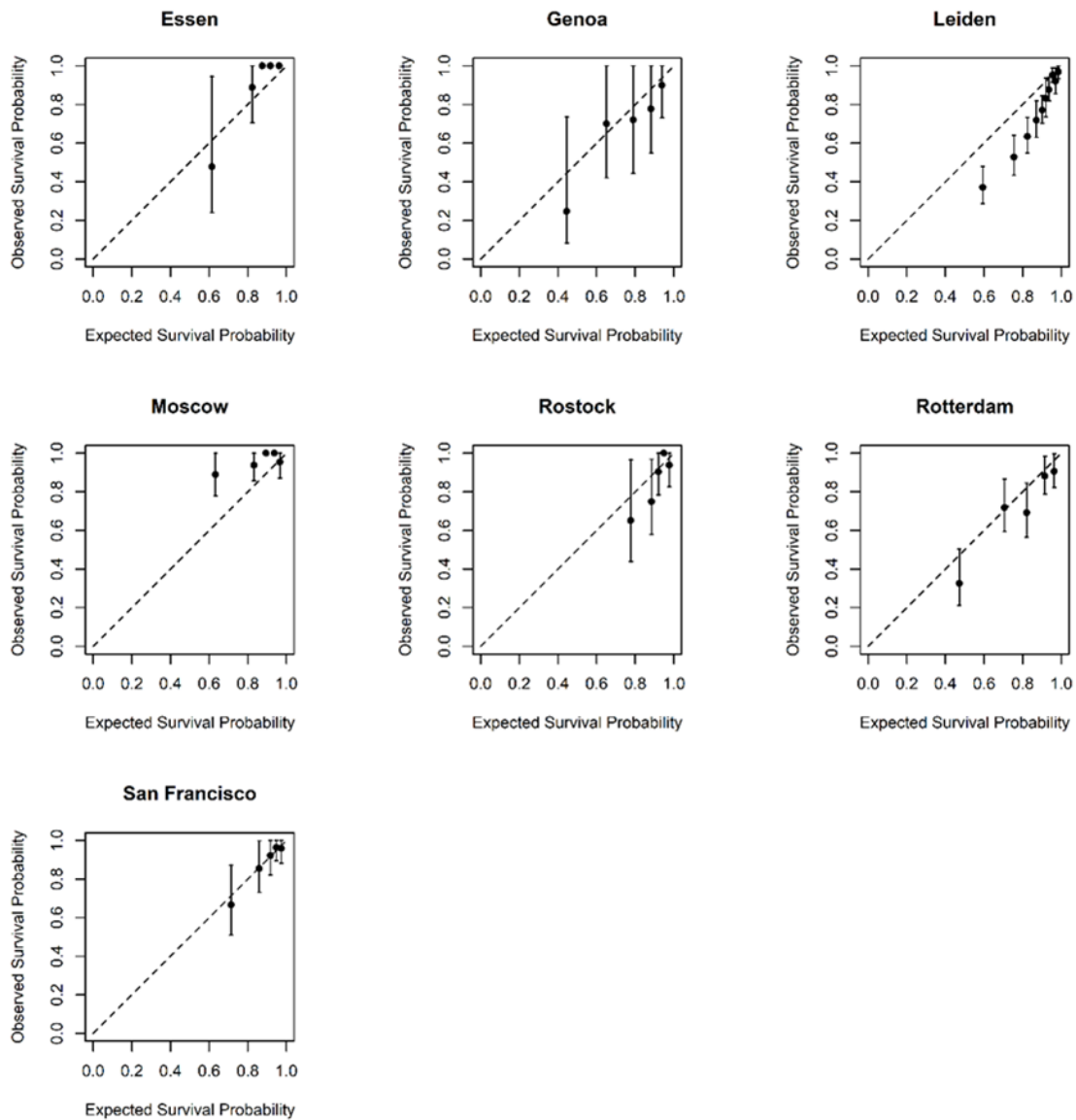


Figure 4.3 Calibration graphs showing the comparison of observed and predicted survival in each of the external data sets for 3 years after treatment. The individuals were divided into five different prognostic groups according to the expected survival and the average expected survival for each group was plotted against the observed survival. The dashed diagonal line is the equality line and, therefore, the markers along this line show a perfect agreement between their predicted and observed survival (Image published in *Cancers - Basel*. February 18, 2020; 12 (2): 477. doi: 10.3390 / cancers12020477).

4.4 Discussion

At the end of this study, in May 2019, this was the first international multi-centre collaborative study to successfully validate and demonstrate the value of a multiparameter prognostic tool in UM, the LUMPO3, which was developed in large, well-defined datasets, and robust statistical modelling used for personalized stratification of patients in relation to metastatic risk and all-cause mortality.

Currently, as far as we know, there are no validated multifaceted tools that take into account clinical, histopathological and genetic tests to predict the patient's prognosis. These tools are crucial to making a reliable decision that helps us to identify patients who may be harmed either physically or psychologically by disease management. Although this is not a major concern in cancers with a relatively good prognosis and several treatment options with proven clinical benefit, it is a crucial determinant of clinical treatment. A reliable prognostic tool would help oncologists to select candidates for invasive or potentially toxic treatments that should be reserved for patients with a longer life expectancy.

In the primary UM, numerous prognostic factors have been identified, these can be used alone and in combination to predict the risk of metastases. These factors can be divided into three main categories: clinical, histological and genetic [102]. The resulting prognostic tools - the prognostic models, have been of great help as they have led to personalized screening regimes [169,218,245] and targeted recruitment for clinical trials for adjuvant therapies. The AJCC TNM staging system for UM is a prognostic tool that combines multiple factors that incorporates the size of the tumour, its location and extraocular dissemination. However, the genetic characteristics of UM are not included [250]. This differed to our present study where sufficient genetic data were available [310], thus enhancing the prognostic accuracy of the model [241]. It is possible to improve the accuracy of the prognostic tools by combining several factors. This is evidenced by the improved prognostic accuracy of the AJCC staging system when the status of chromosomes 3 and 8q are included. In this study by Dogrusoz et al. [352], the AJCC staging system has been validated for use as a prognostic parameter in UM. They

studied whether adding information about the status of chromosome 3 and 8q provided additional information about the prognosis in UM and further improved the prognostic value of this staging system.

A prognostic nomogram has been developed to demonstrate the additive effect of genetic factors and AJCC staging on the prognosis, but it still requires additional validation using a larger study group [353]. In this study, the prognostic effect of genetic evaluation was reinforced by the assessment of AJCC staging in patients with alterations in the number of copies of chromosomes, while Normal genetic status predicted favourable survival, regardless of the AJCC stage. However, in my study, in addition to having used a large cohort of different cases mix, LUMPO3 model was able to accurately predict survival probabilities even in the absence of some prognostic factors.

The prediction tool - Predicting Risk of Metastases in UM (PRiMeUM) utilizes a multivariate method to predict the risk of metastases within 48 months of treatment for the primary tumour. An accuracy of about 85% (derived from the AUROC analysis) was achieved with a logistic regression model using a combination of clinical and genetic factors. However, the PRiMeUM tool has not yet been externally validated [235]. In contrast, in this study, our model not only calculated the risk of metastatic death but also all-cause mortality. Regarding accuracy achieved, it showed a discriminative capacity that varied from 0.72 in year 1 and 0.73 in years 2 and 4, and a discriminative capacity that showed a good agreement between the observed and predicted probabilities.

Kaiserman et al. developed an artificial neural network to predict 5-year survival with brachytherapy. This network incorporates only demographic and clinical data and, again, uses only data collected at a single centre. An accuracy of 84% was achieved (c-index 0.81) when 16 neurons were used in this artificial neural network [234].

In other studies, such as Onken et al. [126], in which the correlation between the number of events and the GEP classification was examined in a short follow-up time (17.4 months) [126],

and in Plasseraud et al., on the other hand, the correlations between pathological characteristics and molecular class in UM were analysed, with an average follow-up of 27.3 months [296]. However, none of the studies analysed the calibration aspect of providing an accurate probability of survival, and both had short follow-up times. But despite these weaknesses, these studies illustrated an initial promise for the role of GEP in decision-making in UM.

In this chapter, I demonstrated that sufficient data were collected to perform a reliable validation of the LUMPO3 model's prognostic accuracy. Despite the differences between the cohorts, the model is capable stratifying the prognosis for patients with UM and appears to be a valuable tool for predicting all-cause mortality in patients with UM. This model may, therefore, inform management choices of physicians when treating UM patients, permitting a better provision of resources with regard to systemic surveillance. Further, the incorporation of key mutations as described in the primary UM may occur in later versions, and also if there were a possibility to recalibrate the model, the predictions would be adapted to external data with distinct baseline risk rates.

Chapter 5

Summary

5.1 Conclusions and Future Directions

The purpose of this thesis was to perform a retrospective study, analysing different aspects of data collected in liver scan reports of patients with UM; and to further use these data to examine whether LUMPO3 was robust and able to predict the onset of metastases in patients in Liverpool, and to determine the cost analysis of liver screening for the detection of metastases in these patients; and lately validate LUMPO3 externally.

In **Chapter 2**, I analysed retrospectively liver surveillance scan reports in detail from 615 UM patients diagnosed at the LOOC between 2008-2018. The importance of this study was primarily because I used a 'real world' dataset demonstrating the associated strong and weak specificities, which correlated the characteristics of UM patients included in UM programs. By performing the review of these radiological reports, and later combining them with clinical, histological, genetic, follow-up and outcome data, I was able to confirm that patients in whom liver metastases were detected had characteristics in their primary tumours, confirming previous studies that suggested that UM with larger size, monosomy 3 and chromosome 8q gain are associated with worse outcome.

The percentage of metastases found was consistent with other studies; however, it was interesting to observe that a substantial percentage of metastases was detected post-mortem, likely due to the irregular liver screening program in some UM patients. Additionally, I showed that in UM patients who underwent regular liver surveillance more metastases were detected. Other studies for UM and other cancers also reported that regular surveillance resulted in detection of metastases at resectable stages. I was able to demonstrate that of the UM patients in whom metastases were detected by clinical imaging, 54% developed metastases within 2 years after the primary treatment of the tumour, and 65% of patients died within two years after detection of metastases.

In this study, I also demonstrated that the cohort of 615 UM patients had distinct characteristics that enabled to categorize them into three different groups according to when and whether they developed metastases, with the poorest outcome being found in the group of patients who developed metastases within two years.

My study had some limitations, factors associated with patients' follow-up may have influenced the absence of a certain number of surveillance imaging, and it was also not possible to investigate this, as the information was not available in the database. Of the 2254 patients diagnosed and treated in the LOOC, approved by the OOB, 1448 (64%) were excluded because they did not have radiological reports in their hospital records. Of these, 14.5% were overseas patients. These patients were seen at the LOOC only for the treatment of their primary UM, and then returned to their countries of origin where they would continue their follow-up. Moreover, in the remaining 85.5% of the patients, no radiological report was found, probably because they had their radiological examinations performed in local hospitals close to their area of residence.

In order to have access to the route of this important number of patients, it would be necessary to retrieve the summary letters through their general practitioners (GPs), who would have the results of their radiological examinations. Although this approach was considered, it was not feasible during the covid pandemic, when GPs were under immense pressure doing virtual consultations, away from their practices.

The absence of certain high-risk patients to a regular surveillance program can also be explained by patient-related factors: e.g., in the case where patients have comorbidities, such as other primary cancers or other chronic diseases, and the primary treatment is directed

towards these illnesses. This may have resulted in the patient leaving the surveillance program due to a second illness in an advanced stage, or even decide to interrupt the program.

More research is needed on liver surveillance programs, as regular screening enabled earlier detection of metastases, allowing a prolonged survival in these cases through metastasectomy.

In this study, I demonstrated that most UM metastases (84%) were detected within 5 years after treatment of the primary tumour, and this can be considered to be an indicator to guide strategies for liver surveillance programs for UM patients. Current recommendations for follow-up surveillance include a combination of factors, ranging from risk stratification to patient factors, e.g., age, patient adherence to liver surveillance programs, or patient comorbidities. In addition, the overall success of surveillance for early detection of curable metastases will depend on the commitment of practitioners and the patients to adhere to the surveillance programs.

Therefore, a personalized follow-up routine can be recommended based on the data presented in this study. If surveillance is selected, the interval can be adapted to the estimated risk of developing metastases, considering more intensive surveillance for patients at higher risk. Taking into account that most low-risk patients in the present analysis did not develop metastases during the study period, liver surveillance would not be recommended for these patients. For high-risk patients, liver surveillance could be limited to 5 to 10 years, as 84% of metastases were detected within 5 years after primary tumour treatment in the present study, and at 10 years of follow-up, 99% of metastases had already been detected.

Another important factor to be considered in liver surveillance programs is the screening limit in elderly patients, especially in patients over 80 years of age. Surveillance recommendations should be tempered, with some factors (e.g., comorbidities and motility issues) should be considered when recommending liver surveillance in elderly patients. The ability and adequacy of surgical resections or chemotherapy in such patients should also be thought about carefully, as many patients may not be able to tolerate surgical or adjuvant therapy and, therefore, should not undergo liver surveillance.

As verified in this study, only 6% of patients were >80 years old and, in 25% of them, metastases were detected by clinical imaging during the study period. The median time until the last scan performed was 1.4 years in this group of patients. Hence, the recommendation for this age group of patients, would be to reduce or not perform liver screening, since the objective of liver surveillance is the detection of curable metastases. Most of these patients underwent palliative treatment, with only 8% undergoing liver resection and who had a very short overall survival.

In **Chapter 3**, I performed a detailed examination of the liver screening reports of 615 patients with UM, in which the modality and frequency of liver scans were assessed, as well as the number of scans performed until the detection of metastases, and all scans performed in patients that never demonstrated metastases. I was able to calculate the costs of all scans performed, both on patients who developed metastases and those who never showed metastases, using the NICE liver cancers guideline as a reference.

For this study, a new feature of LUMPO was designed, the *lpmd*, which demonstrated that it was possible to reliably predict the time of the onset of the metastases in UM patients. To

validate the model, discrimination measures that demonstrated a consistent performance of the model over 5 years were observed. Calibration measures were also used to compare the occurrence of observed metastases with the expected metastases, and the performance of the model demonstrated a good agreement between the observed and the predicted occurrence of metastases.

When I used the *lpmd* score, it was possible to calculate for which patients the scans were recommended, and in those scans could possibly be reduced in number or avoided. This was possible because 3 different decision thresholds were used, defining, within the numerical representation that the model attributed to each patient, which patients would be recommended scans or not. In addition, I was able to demonstrate in how many UM patients hypothetically could have not had the examinations as their risk of metastases was so low, and yet, in how many patients' metastases would have been missed, should they not have undergone the scans.

The decision thresholds used allowed predicting different scenarios to recommend screening strategies in UM patients. In addition, cost saving analysis on all examinations that hypothetical would not be performed suggested a decrease in the frequency of regular scanning for UM patients.

Subsequent work can validate and further improve the accuracy of our prognostic tool. For this, immunohistochemistry or molecular genetic tests could be used, which indicates the presence of somatic mutations in UM cells. Ongoing basic research may allow the development of adjuvant systemic clinical trials and other procedures to be more precisely targeted at high-risk metastatic UM patients. Additionally, future explicit prospective studies

with full cost-benefit analyses may demonstrate considerable cost savings by decreasing the frequency of regular screening for UM patients, determined by their risk. However, these calculations must be balanced, taking into account that there is a risk of missing some metastases in a small number of patients.

Future prospective works can be recommended; for example, when designing these prospective studies, the following aspects can be taken into account: 1) studies on the analysis of the quality of life of patients that may include various aspects, such as the impact of their illness and liver surveillance, anxiety and other emotions felt during screening, as well as waiting for results; 2) the financial costs from the patient's perspective, which include a potential range of aspects such as travel expenses, days off, parking fees, child care, etc., 3) a potential range of other health resources that could be affected, including human resources involved and other hospital costs. Furthermore, the costs of likely innovative treatments included in clinical trials should be considered, and potentially what the health implications are and any potential differences in health outcomes.

In **Chapter 4**, I organised a multicentre study comprising a cohort of 1,836 UM patients from 7 collaborative external centres. This was the only study to date validating a prognostic model for UM, using such a large cohort and with a variety of cases. By performing this multivariate analysis of clinical, histopathological and genetic factors to predict the patient's prognosis, using the LUMPO3 prognostic tool, I was able to demonstrate that the tool is sufficiently robust to make a reliable decision that helps to identify patients who may be physically or psychologically impaired during disease management.

This research highlighted the utility of using enough data that was collected to perform a reliable validation of the predictive accuracy of the LUMPO3 model. As a result of this study, I demonstrated that despite the differences between cohorts, the model is able to stratify prognosis for patients with UM and appears to be a valuable tool for predicting all-cause mortality in patients with UM.

In conclusion, the work of this thesis has provided further insight into UM prognostication. The understanding of a prognostic model for UM patients can help inform the choices of strategies for the follow-up of these patients, allowing better provision of resources with regard to systemic surveillance. I and others demonstrate the need to use prognostic models in UM patients. Prognostication is an important tool, but it is not always used in clinical practice, or it is under-used. Medical decision-making in daily clinical practice can have a greater impact when using prognostic tools as a strategic assistance. Patients with advanced terminal illnesses such as cancer will be able to have personalized prognostic assistance when using prognostication as a support for planning advanced care for their illness. However, the final challenge remains its application in future clinical practice. Looking to the future, collaborative efforts in conjunction with multi-integrated functional studies in larger cohorts of UM patients are essential to improve patient care and outcomes.

Appendices

Appendix 1 – Proposal Sample study 1 (Proforma)

Study Number	Age at Primary treatment	Gender	Date of primary treatment	Type of primary treatment	Epithelioid cells	Loops	Mitotic Count	LBD	UH
1	67	1	15/04/2008	Enucleation	0	1	2	19.3	8.6
5	53	1	18/03/2008	Enucleation	1	1	4	20	8.3

EOE	CBI	Chr1	Chr3	Chr6p	Chr6q	Chr8p	Chr8q	Total number of scans	Number of MRI	Number of CT
0	1	0	1	0	0	0	0	17	17	0
1	0	0	1	0	0	1	1	16	10	5

Number of US	Time from primary treatment to first scan	Date of the first scan	Date of the next scan	Number of Metastases	Location of Metastases	Size of the largest Metastases	Date of the first Metastases
0	0	15/04/2008	22/07/2008	0	0	0	0
1	0	18/03/2008	21/03/2008	Multiple	RL	33mm	06/08/2010

Date from the primary treatment to first metastases	Date from the first Metastases to death	Date of death	Date of the last follow-up	Status	Follow-up time
0	0	Alive	01/05/2020	0	12.9
2.39	0.86	15/06/2011	15/06/2011	1	3.2

	A	B	C	D	E	F	G	H	I	J	K	L	M	N	O	P	Q	R	S	T	U	V	W	X	Y	Z	AA	AB	AC	AD	AE	AF	AG	AH	AI	AJ	AK	AL	AM	AN			
67	66	48	1	18/08/09	Local Resectio	1	1	3	16.8	9.5	'3a'	T3	0	0	0	1	0	0	0	0	20/06/16	20/06/16	1	6.8	22	Mult	1	2	70	M1b	17-Nov-14	53	5.3	1.6	22	21	1	20/06/16	18/08/09				
68	67	44	1	13/01/09	Enucleation	1	1	4	16.1	7.5	'3a'	T3	0	0	1	1	1	0	0	1	13/02/12	13/02/12	1	3.1	17	Mult	1	1	35	M1b	18-Jun-10	45	1.4	1.7	17	6	11	13/02/12	13/01/09				
69	68	76	0	04/08/09	PBR	1	N/A	N/A	15.2	7.1	'3b'	T3	1	0	0	1	1	1	0	0	ALIVE	01/05/20	0	10.7	6	0	0	3								6	6		ALIVE	04/08/09			
70	69	67	1	10/02/09	PRXT	1	N/A	N/A	14.2	4.9	'2a'	T2	0	0	0	1	0	0	1	0	22/10/11	22/10/11	1	2.7	4	3	1	1	30	M1a	21-Jul-10	68	1.4	1.3	4	4		22/10/11	10/02/09				
71	70	42	0	24/11/09	PRXT	0	N/A	N/A	12.2	2.9	'2a'	T2	0	0	0	1	0	0	0	0	ALIVE	01/05/20	0	10.4	17	0	0	3								17	16	1		ALIVE	24/11/09		
72	71	28	0	10/11/09	PBR	0	N/A	N/A	17.1	7.7	'3a'	T3	0	0	0	0	1	Other	0	0	ALIVE	01/05/20	0	10.5	1	0	0	3									1		1	ALIVE	10/11/09		
73	72	24	0	19/05/09	PRXT	N/A	N/A	N/A	8.7	2.3	'1a'	T1	0	0	0	N/A	N/A	N/A	N/A	N/A	ALIVE	01/05/20	0	11.0	5	0	0	3									5	5		ALIVE	19/05/09		
74	73	57	1	24/11/09	Enucleation	0	0	3	23.6	3.4	'4a'	T4	0	0	0	0	1	1	0	1	ALIVE	01/05/20	0	10.4	1	0	0	3										1		1	ALIVE	24/11/09	
75	74	74	1	09/01/09	Enucleation	1	1	4	18.2	12.3	'4b'	T4	1	0	1	1	0	0	1	1	12/07/10	12/07/10	1	1.5	1	0	2	1							1.5	1.5	1	1	1	12/07/10	09/01/09		
76	75	64	0	22/09/09	PBR	0	N/A	N/A	15	2.8	'2a'	T2	0	0	0	N/A	N/A	N/A	N/A	N/A	ALIVE	01/05/20	0	10.6	1	0	0	3										1	1		ALIVE	22/09/09	
77	76	74	1	11/12/07	PBR	0	N/A	N/A	20.6	4.6	'4a'	T4	0	0	0	1	0	0	0	1	24/05/12	24/05/12	1	4.5	4	0	2	2							4.5	4.5	4	4		24/05/12	11/12/07		
78	77	68	0	12/06/09	PRXT	N/A	N/A	N/A	6.9	0.9	'1a'	T1	0	0	0	N/A	N/A	N/A	N/A	N/A	ALIVE	01/05/20	0	10.9	6	0	0	3									6	5	1	ALIVE	12/06/09		
79	78	73	0	04/08/09	PRXT	1	N/A	N/A	11.4	5.5	'2a'	T2	0	0	0	N/A	N/A	N/A	N/A	N/A	ALIVE	01/05/20	0	10.7	3	0	0	3									3	1	2	ALIVE	04/08/09		
80	79	73	0	16/10/09	Enucleation	1	0	3	10.1	1.6	'1a'	T1	0	0	0	1	Other	Other	Other	Other	13/02/12	13/02/12	1	2.3	9	Mult	1	1	60	M1b	23-Jul-11	75	1.8	0.6	9	5	3	1	13/02/12	16/10/09			
81	80	48	1	07/12/09	Enucleation	1	1	4	17.7	7.7	'3a'	T3	0	0	0	N/A	N/A	N/A	N/A	N/A	ALIVE	01/05/20	0	10.4	1	0	0	3										1		1	ALIVE	07/12/09	
82	81	47	0	21/08/09	Enucleation	0	1	4	17.6	9.6	'3a'	T3	0	0	1	1	1	0	Other	1	24/06/13	24/06/13	1	3.8	10	1	1	1	41	M1b	28-Jun-11	49	1.9	2.0	10	8	1	1	24/06/13	21/08/09			
83	82	47	1	22/09/09	Local Resectio	0	1	4	14	7.7	'3a'	T3	0	0	1	1	Other	1	Other	Other	ALIVE	01/05/20	0	10.6	20	0	0	3									20	20		ALIVE	22/09/09		
84	83	59	1	01/04/08	PBR	1	1	3	18.9	7.4	'4b'	T4	1	0	0	1	1	1	0	1	03/12/09	03/12/09	1	1.7	7	Mult	1	1	40	M1b	18-Mar-09	60	1.0	0.7	7	3	2	2	03/12/09	01/04/08			
85	84	63	1	14/04/08	PRXT	0	N/A	N/A	17.7	7.1	'3c'	T3	0	1	0	0	0	0	Other	Other	ALIVE	01/05/20	0	12.1	1	0	0	3										1	1	ALIVE	14/04/08		
86	85	90	1	06/01/10	Enucleation	0	1	3	21.2	8.3	'4b'	T4	1	0	1	1	0	0	0	0	16/12/13	16/12/13	3	3.9	1	0	0	3										1	1	16/12/13	06/01/10		
87	86	72	0	15/01/10	Enucleation	1	1	4	19.3	6.1	'4c'	T4	0	1	0	1	0	1	Other	1	02/10/12	02/10/12	2	2.7	6	2	1	1	16	M1a	08-Dec-11	74	1.9	0.8	6	4	2	2	02/10/12	15/01/10			
88	87	64	1	19/01/10	Enucleation	1	1	4	21.8	12.2	'4b'	T4	1	0	0	1	0	1	0	1	05/08/11	05/08/11	1	1.5	1	0	2	1										1	1		05/08/11	19/01/10	
89	88	78	1	19/01/10	Enucleation	0	0	4	19.5	14.9	'4a'	T4	0	0	1	1	0	0	0	1	06/06/11	06/06/11	1	1.4	1	1	1	1	10	M1a	19-Jan-10	78	0.0	1.4	1				1	06/06/11	19/01/10		
90	89	65	1	05/02/10	Enucleation	1	1	4	18.8	9.6	'4b'	T4	1	0	0	1	0	Other	1	1	06/08/15	06/08/15	1	5.5	1	0	2	2										1	1	06/08/15	05/02/10		
91	90	51	1	23/02/10	Local Resectio	0	0	4	10.4	7.4	'2a'	T2	0	0	0	0	0	0	0	0	ALIVE	01/05/20	0	10.2	11	0	0	3										11	10	1	ALIVE	23/02/10	
92	91	63	0	09/03/10	Enucleation	1	1	3	17	8.4	'3b'	T3	1	0	1	1	0	0	0	1	17/04/19	17/04/19	3	9.1	13	0	0	3										13	12	1		ALIVE	09/03/10
93	92	69	0	26/03/10	PRXT	N/A	N/A	N/A	9	1.9	'1a'	T1	0	0	0	N/A	N/A	N/A	N/A	N/A	ALIVE	01/05/20	0	10.1	1	0	0	3											1	1	ALIVE	26/03/10	
94	93	52	0	30/03/10	PRXT	1	N/A	N/A	11.6	3.7	'2a'	T2	0	0	1	1	0	0	1	1	22/08/17	22/08/17	1	7.4	8	4	1	2	13	M1a	20-May-13	55	3.1	4.3	8	2	6	6	22/08/17	30/03/10			
95	94	35	1	06/04/10	Enucleation	1	0	1	10.2	2	'1b'	T1	1	0	0	0	1	Other	1	1	ALIVE	01/05/20	0	10.1	1	0	0	3											1	1	ALIVE	06/04/10	
96	95	80	1	27/04/10	Enucleation	1	1	3	10.5	2.8	'1d'	T1	1	1	0	Other	0	0	0	1	31/01/12	31/01/12	1	1.8	4	3	1	1	27	M1a	22-May-11	81	1.1	0.7	4	4		31/01/12	27/04/10				
97	96	53	0	27/04/10	Enucleation	1	0	3	9.7	14.8	'3b'	T3	1	0	0	1	0	0	1	1	15/10/13	15/10/13	1	3.5	8	2	1	1	6	M1a	12-Jan-12	55	1.7	1.8	8	8		15/10/13	27/04/10				
98	97	81	0	11/05/10	PRXT	1	N/A	N/A	17.6	5.7	'3b'	T3	1	0	0	0	1	Other	0	0	ALIVE	01/05/20	0	10.0	1	0	0	3										1	1		ALIVE	11/05/10	
99	98	42	1	18/05/10	Local Resectio	0	0	3	22.4	11.7	'4a'	T4	0	0	0	N/A	N/A	N/A	N/A	N/A	ALIVE	01/05/20	0	10.0	1	0	0	3										1	1		ALIVE	18/05/10	
100	99	50	0	27/04/10	PBR	1	0	2	9.5	7.5	'2a'	T2	0	0	0	1	1	1	0	0	ALIVE	01/05/20	0	10.0	15	0	0	3										15	15		ALIVE	27/04/10	
101	100	84	0	22/06/10	Enucleation	1	1	3	19.6	12.9	'4d'	T4	1	1	0	1	0	0	1	1	24/12/13	24/12/13	1	3.5	1	0	2	2											1	1	24/12/13	22/06/10	
102	101	79	0	09/07/10	PRXT	0	N/A	N/A	10.8	3.5	'2a'	T2	0	0	0	N/A	N/A	N/A	N/A	N/A	26/09/18	26/09/18	2	8.2	4	0	0	3										4	2	2	26/09/18	09/07/10	
103	102	29	0	20/07/10	Local Resectio	0	0	2	19.3	10.8	'4d'	T4	1	1	0	0	1	1	0	0	ALIVE	01/05/20	0	9.8	5	0	0	3										5	2	1	2	ALIVE	20/07/10
104	103	54	1	20/07/10	Endoresection	1	N/A	N/A	9.9	6	'2a'	T2	0	0	0	0	1	1	0	0	ALIVE	01/05/20	0	9.8	2	0	0	3										2		2	ALIVE	20/07/10	
105	104	51	1	27/07/10	Local Resectio	1	1	4	17.1	7.4	'3a'	T3	0	0	0	1	0	0	1	1	ALIVE	01/05/20	0	9.8	7	3	1	2	12.5	M1a	15-Aug-12	53	2.1	0.0	7	7		ALIVE	27/07/10				
106	105	66	0	03/08/10	PRXT	0	N/A	N/A	15.8	3.4	'3a'	T3	0	0	0	N/A	N/A	N/A	N/A	N/A	ALIVE	01/05/20	0	9.8	1	0	0	3											1	1	ALIVE	03/08/10	
107	106	45	1	06/08/10	Enucleation	1	1	4	15.1	5.5	'3a'	T3	0	0	0	0	0	0	0	0	10/01/16	10/01/16	1	5.4	11	2	1	2	16	M1a	01-Apr-15	50	4.7	0.8	11	6	1	4	10/01/16	06/08/10			
108	107	63	0	10/08/10	Local Resectio	1	1	2	19.5	9.5	'4a'	T4	0	0	0	Other	Other	0	1	1	07/03/13																						

J	A	B	C	D	E	F	G	H	I	J	K	L	M	N	O	P	Q	R	S	T	U	V	W	X	Y	Z	AA	AB	AC	AD	AE	AF	AG	AH	AI	AJ	AK	AL	AM	AN										
271	270	73	1	28/02/12	Enucleation	1	1	3	18.3	17.4	'4a	T4	0	0	0	1	Other	0	0	1	11/07/12	11/07/12	1	0.4	1	0	2	1					0.4	2.0	1				1	11/07/12	28/02/12									
272	271	81	1	08/01/13	Enucleation	1	1	1	18.2	13.2	'4a	T4	0	0	1	1	Other	1	Other	Other	08/12/13	08/12/13	1	0.9	1	0	2	1					0.9	0.4	1			1	1	08/12/13	08/01/13									
273	272	64	1	18/12/12	PRXT	0	N/A	N/A	7.5	2.6	'1a	T1	0	0	N/A	0	N/A	N/A	N/A	N/A	N/A	ALIVE	01/05/20	0	7.4	1	0	0	3										1	1		1	18/12/12							
274	273	56	1	22/01/13	Enucleation	1	1	1	17.6	10.7	'3a	T3	0	0	1	1	Other	Other	Other	1	26/11/14	26/11/14	1	1.8	1	0	2	1					1.8	0.9	1			1		1	26/11/14	22/01/13								
275	274	75	0	25/01/13	Enucleation	0	1	3	15.6	9.7	'3a	T3	0	0	0	0	1	1	Other	1	ALIVE	01/05/20	0	7.3	13	0	0	3										13	12		1	1	ALIVE	25/01/13						
276	275	33	1	29/01/13	PBR	1	N/A	N/A	13.4	4.1	'2a	T2	0	0	Other	Other	1	1	Other	1	ALIVE	01/05/20	0	7.3	1	0	0	3										1		1	1	ALIVE	29/01/13							
277	276	59	0	22/01/13	Endoresection	1	N/A	N/A	5.6	1.4	'1a	T1	0	0	0	0	0	0	0	0	ALIVE	01/05/20	0	7.3	14	0	0	3										14	13		1	1	ALIVE	22/01/13						
278	277	53	1	08/02/13	PBR	1	N/A	N/A	17	7.8	'3b	T3	1	0	N/A	N/A	N/A	N/A	N/A	N/A	18/04/18	18/04/18	1	5.2	27	Mult	1	2	76.7	M1b	08-Jul-15	55	2.4		2.8	27	17	8	2	18/04/18	08/02/13									
279	278	80	0	08/02/13	Enucleation	1	0	3	20	4.1	'4a	T4	1	1	0	Other	1	0	0	1	ALIVE	01/05/20	0	7.2	1	0	0	3											1		1	1	ALIVE	08/02/13						
280	279	54	1	12/02/13	Enucleation	0	1	3	19.5	10.9	'4a	T4	0	0	Other	1	Other	Other	0	01/07/15	01/07/15	1	2.4	1	0	2	2								2.4	2.4	1			1	1	01/07/15	12/02/13							
281	280	77	0	12/02/13	Enucleation	1	0	2	17.9	8.1	'3a	T3	0	0	Other	1	1	0	1	1	25/12/16	25/12/16	1	3.9	8	Mult	1	2	22	M1a	11-May-16	80	3.2		0.6	8	7	1		1	25/12/16	12/02/13								
282	281	45	0	20/02/13	Local Resectio	1	0	3	15.2	8.9	'3a	T3	0	0	0	1	Other	0	0	0	ALIVE	01/05/20	0	7.2	1	0	0	3												1		1	1	ALIVE	20/02/13					
283	282	54	1	12/02/13	Local Resectio	0	0	3	17	9.8	'3a	T3	0	0	Other	1	1	1	Other	Other	ALIVE	01/05/20	0	7.2	1	0	0	3												1		1	1	ALIVE	12/02/13					
284	283	46	1	22/02/13	PBR	1	N/A	N/A	15.8	7.9	'3a	T3	0	0	0	0	1	1	1	1	ALIVE	01/05/20	0	7.2	24	1	1	2	9	M1a	05-Jun-19	52	6.3		0.0	24	17	7				1		1	ALIVE	22/02/13				
285	284	47	0	28/02/13	Enucleation	0	0	2	19.3	13.3	'4a	T4	1	0	0	Other	1	1	Other	0	ALIVE	01/05/20	0	7.2	1	0	0	3												1	1	1	1	ALIVE	28/02/13					
286	285	87	0	01/03/13	Enucleation	1	1	2	18.3	12.6	'4a	T4	1	0	1	1	Other	1	Other	1	15/05/15	15/05/15	1	2.2	1	0	2	2							2.2	2.2	1			1	1	15/05/15	01/03/13							
287	286	40	1	05/04/13	PBR	1	N/A	N/A	6.3	1.9	'1a	T1	0	0	N/A	0	N/A	N/A	N/A	N/A	ALIVE	01/05/20	0	7.1	1	0	0	3												1	1		1	1	ALIVE	05/04/13				
288	287	70	0	08/03/13	PRXT	1	N/A	N/A	10.1	1.7	'1a	T1	0	0	N/A	N/A	N/A	N/A	N/A	N/A	ALIVE	01/05/20	0	7.2	3	0	0	3											3		3		1	ALIVE	08/03/13					
289	288	72	1	12/03/13	PRXT	1	N/A	N/A	14.9	3.9	'2a	T2	0	0	N/A	0	N/A	N/A	N/A	N/A	13/02/16	13/02/16	2	2.9	2	0	0	3												2	1	1		1	13/02/16	12/03/13				
290	289	63	1	18/03/13	PRXT	1	N/A	N/A	13.9	5.7	'2a	T2	0	0	N/A	Other	N/A	N/A	N/A	N/A	ALIVE	01/05/20	0	7.1	10	0	0	3												10	10			1	1	ALIVE	18/03/13			
291	290	64	1	26/03/13	Enucleation	1	1	3	16.1	14.6	'4a	T4	1	0	1	1	0	1	1	1	31/01/14	31/01/14	1	0.9	4	0	2	1							0.9	0.9	4	2	1	1	1	31/01/14	26/03/13							
292	291	32	0	16/04/13	PRXT	1	N/A	N/A	14.4	4.5	'2a	T2	0	0	N/A	1	N/A	N/A	N/A	N/A	ALIVE	01/05/20	0	7.0	21	Mult	1	2	12	M1a	02-Mar-16	35	2.9		0.0	21	17	3	1	1	ALIVE	16/04/13								
293	292	75	0	08/04/11	PRXT	1	0	2	5.8	4.9	'1a	T1	0	0	0	0	1	1	1	1	03/07/13	03/07/13	1	2.2	1	0	2	2							2.2	2.2	1			1	1	03/07/13	08/04/11							
294	293	51	0	03/05/13	PBR	1	N/A	N/A	8	4.1	'1b	T1	1	0	N/A	Other	N/A	N/A	N/A	N/A	ALIVE	01/05/20	0	7.0	12	0	0	3												12	12			1	1	ALIVE	03/05/13			
295	294	64	1	14/08/13	Enucleation	0	0	3	17.2	7.9	'3a	T3	0	0	0	0	1	0	0	0	ALIVE	01/05/20	0	6.9	2	0	0	3												2		2		1	1	ALIVE	14/08/13			
296	295	33	0	14/05/13	Endoresection	0	N/A	N/A	11.2	8.2	'2a	T2	0	0	1	0	Other	0	1	Other	ALIVE	01/05/20	0	7.0	1	0	0	3													1	1		1	1	ALIVE	14/05/13			
297	296	40	1	14/05/13	Enucleation	0	0	2	13.4	6.4	'3a	T3	0	0	0	0	1	Other	Other	Other	ALIVE	01/05/20	0	7.0	12	0	0	3													12	12			1	1	ALIVE	14/05/13		
298	297	70	1	21/05/13	PRXT	0	N/A	N/A	12	2.7	'1a	T1	0	0	N/A	1	N/A	N/A	N/A	N/A	ALIVE	01/05/20	0	7.0	7	0	0	3														7	7			1	1	ALIVE	21/05/13	
299	298	64	1	28/05/13	Enucleation	1	1	3	18	10.9	'3b	T3	1	0	1	1	Other	1	Other	Other	28/08/15	28/08/15	1	2.3	1	0	2	2							2.3	2.3	1			1	1	28/08/15	28/05/13							
300	299	64	1	24/08/13	Endoresection	1	1	N/A	8.7	7	'2c	T2	0	1	0	0	0	0	0	0	ALIVE	01/05/20	0	6.9	1	0	0	3														1	1	1	1	ALIVE	24/08/13			
301	300	81	0	12/07/13	Enucleation	0	1	1	17.1	5.7	'3b	T3	1	0	0	0	1	1	Other	1	ALIVE	01/05/20	0	6.8	1	0	0	3														1	1	1	1	ALIVE	12/07/13			
302	301	53	1	06/08/13	Endoresection	1	N/A	N/A	11.6	12	'3a	T3	0	0	0	0	0	0	0	0	ALIVE	01/05/20	0	6.7	13	0	0	3													13	13			1	1	ALIVE	06/08/13		
303	302	67	1	16/07/13	Enucleation	1	0	3	17.8	6.5	'3a	T3	0	0	0	1	Other	Other	1	1	21/11/15	21/11/15	1	2.4	1	0	2	2							2.4	2.4	1			1	1	21/11/15	16/07/13							
304	303	41	0	19/07/13	PBR	0	N/A	N/A	2.4	N/A	N/A	N/A	0	0	N/A	N/A	N/A	N/A	N/A	N/A	ALIVE	01/05/20	0	6.8	4	0	0	3														4	4			1	1	ALIVE	19/07/13	
305	304	41	0	23/07/13	PBR	0	N/A	N/A	11.8	2.2	'1a	T1	0	0	N/A	N/A	N/A	N/A	N/A	N/A	ALIVE	01/05/20	0	6.8	11	0	0	3														11	11			1	1	ALIVE	23/07/13	
306	305	57	1	08/08/13	Enucleation	1	1	3	10.2	1.7	'1a	T1	0	0	1	1	Other	1	Other	Other	ALIVE	01/05/20	0	6.7	1	0	0	3																1	1	1	1	ALIVE	08/08/13	
307	306	58	0	28/07/13	Enucleation	1	1	3	15.2	10.6	'3a	T3	0	0	0	0	0	0	1	1	ALIVE	01/05/20	0	6.8	8	0	0	3															8	8			1	1	ALIVE	28/07/13
308	307	76	0	06/08/13	Enucleation	0	1	2	13.8	6.5	'3a	T3	0	0	0	1	0	0	1	1	23/07/18	23/07/18	1	5.0	1	0	2	2								5.0	5.0	1			1	1	23/07/18	06/08/13						
309	308	64	1	13/08/13	Enucleation	1	1	3	13.2	6.5	'3a	T3	0	0	Other	Other	Other	0	0	0	ALIVE	01/05/20	0	6.7	1	0	0	3															1	1	1	1	ALIVE	13/08/13		
310	309	86	1	13/08/13	Enucleation	1	1	4	17.2	14.5	'4a	T4	0	0	0	1	0	1	1	1	23/12/15	23/12/15	2	2.4	1	0	0																							

A	B	C	D	E	F	G	H	I	J	K	L	M	N	O	P	Q	R	S	T	U	V	W	X	Y	Z	AA	AB	AC	AD	AE	AF	AG	AH	AI	AJ	AK	AL	AM	AN					
338	337	50	0	18/03/14	Enucleation	0	0	1	23.6	16.7	'4b'	T4	1	0	1	1	0	0	0	0	ALIVE	01/05/20	0	6.1	10	0	0	3									10	9	1	1	ALIVE	18/03/14		
339	338	50	1	25/03/14	Enucleation	1	1	2	16.6	12.4	'4c'	T4	0	1	0	0	0	0	0	0	ALIVE	01/05/20	0	6.1	30	Mult	1	2	37	M1b	22-Jun-16	52	2.2	0.0	0.0	30	21	7	2	ALIVE	25/03/14			
340	339	68	0	25/03/14	PBR	0	N/A	N/A	6.1	3.1	'1b'	T1	1	0	0	N/A	1	N/A	N/A	N/A	N/A	ALIVE	01/05/20	0	6.1	9	0	0	3								9	9			ALIVE	25/03/14		
341	340	75	0	28/03/14	PRXT	N/A	N/A	N/A	13.9	2.5	'2a'	T2	0	0	0	N/A	N/A	N/A	N/A	N/A	21/07/19	21/07/19	3	5.3	7	0	0	3								7		2	5	21/07/19	28/03/14			
342	341	43	1	01/04/14	Enucleation	0	0	1	11.9	7.5	'2b'	T2	1	0	0	0	0	0	0	0	ALIVE	01/05/20	0	6.1	1	0	0	3									1				1	ALIVE	01/04/14	
343	342	61	0	01/04/14	PBR	0	N/A	N/A	7.7	2.2	'1a'	T1	0	0	N/A	Other	N/A	N/A	N/A	N/A	ALIVE	01/05/20	0	6.1	13	0	0	3									13	13			ALIVE	01/04/14		
344	343	55	0	08/04/14	PRXT	0	N/A	N/A	10.8	1.8	'1a'	T1	0	0	N/A	0	N/A	N/A	N/A	N/A	ALIVE	01/05/20	0	6.1	1	0	0	3									1				ALIVE	08/04/14		
345	344	69	0	08/04/14	PRXT	0	N/A	N/A	8.2	2.4	'1a'	T1	0	0	N/A	Other	N/A	N/A	N/A	N/A	ALIVE	01/05/20	0	6.1	11	0	0	3									11			11	ALIVE	08/04/14		
346	345	64	1	08/04/14	Enucleation	0	0	4	10	4.2	'2a'	T2	0	0	0	Other	0	0	0	0	1	ALIVE	01/05/20	0	6.1	11	0	0	3									11	11			ALIVE	08/04/14	
347	346	59	0	08/04/14	Enucleation	1	1	3	21	14	'4b'	T4	1	0	1	1	0	0	0	0	13/09/16	13/09/16	1	2.4	7	Mult	1	1	14	M1a	25-Feb-15	60	0.9	1.6	7	4	2	1	13/09/16	08/04/14				
348	347	52	1	06/05/14	Enucleation	1	1	4	15.4	12.1	'4a'	T4	0	0	1	1	1	0	0	0	08/06/17	08/06/17	1	3.1	6	Mult	1	1	10	M1a	17-Aug-15	53	1.3	1.8	6	4	2	2	08/06/17	06/05/14				
349	348	43	0	20/05/14	Enucleation	1	1	3	21.7	11.2	'4b'	T4	1	0	1	0	1	0	0	1	ALIVE	01/05/20	0	6.0	1	0	0	3									1			1	ALIVE	20/05/14		
350	349	66	1	24/06/14	PBR	1	N/A	N/A	15.3	5.8	'3a'	T3	0	0	0	1	1	0	0	1	ALIVE	01/05/20	0	5.9	20	Mult	1	2	41	M1b	09-Apr-18	70	3.8	0.0	20	16	4			ALIVE	24/06/14			
351	350	38	0	01/07/14	PRXT	0	N/A	N/A	7.4	1.8	'1a'	T1	0	0	N/A	Other	N/A	N/A	N/A	N/A	ALIVE	01/05/20	0	5.8	13	0	0	3									13	13			ALIVE	01/07/14		
352	351	68	0	01/07/14	PBR	1	1	3	10.4	6.2	'2a'	T2	1	1	Other	1	1	0	0	0	04/03/20	04/03/20	1	5.7	29	Mult	1	2	143	M1c	18-Dec-17	71	3.5	2.2	29	16	10	3	04/03/20	01/07/14				
353	352	75	0	08/07/14	Enucleation	0	0	1	17.9	12.1	'4a'	T4	0	0	0	0	1	1	0	1	29/03/19	29/03/19	3	4.7	1	0	0	3									1			1	29/03/19	08/07/14		
354	353	53	0	22/07/14	Enucleation	0	0	2	22.7	9.9	'4a'	T4	0	0	0	0	1	0	0	0	ALIVE	01/05/20	0	5.8	17	0	0	3									17	15	1	1	ALIVE	22/07/14		
355	354	66	0	29/07/14	Enucleation	1	0	3	12.4	8	'3a'	T3	0	0	0	1	1	0	0	1	ALIVE	01/05/20	0	5.8	11	0	0	3									11	11			ALIVE	29/07/14		
356	355	27	0	29/08/14	PRXT	N/A	N/A	N/A	8.5	3	'1b'	T1	1	0	N/A	N/A	N/A	N/A	N/A	N/A	ALIVE	01/05/20	0	5.7	8	0	0	3									8	8			ALIVE	29/08/14		
357	356	63	1	16/09/14	Enucleation	1	1	4	13.8	6.2	'2a'	T2	0	0	0	1	1	0	0	0	13/03/16	13/03/16	1	1.5	9	2	1	1	47	M1b	20-May-15	64	0.7	0.8	9	8	1			13/03/16	16/09/14			
358	357	49	0	09/09/14	Local resection	0	0	2	16	9.6	'3b'	T3	1	0	0	0	1	0	0	1	ALIVE	01/05/20	0	5.6	1	0	0	3									1			1	ALIVE	09/09/14		
359	358	46	1	09/09/14	Enucleation	1	1	2	19.6	14.7	'4b'	T4	1	0	0	1	0	0	0	1	ALIVE	01/05/20	0	5.6	10	Mult	1	2	47	M1b	30-Apr-19	51	4.6	0.0	10	6	3	1		ALIVE	09/09/14			
360	359	78	0	26/09/14	Enucleation	1	0	4	14.2	8	'3a'	T3	0	0	0	1	1	0	0	1	28/02/18	28/02/18	2	3.4	11	Mult	1	1	32	M1b	08-Sep-16	80	2.0	1.5	11	5	5	1	28/02/18	26/09/14				
361	360	66	1	30/09/14	Enucleation	1	1	2	7.1	2.1	'1a'	T1	0	0	0	Other	0	0	0	0	1	ALIVE	01/05/20	0	5.6	10	0	0	3									10	10			ALIVE	30/09/14	
362	361	70	1	21/10/14	Enucleation	1	1	4	13.7	9.9	'3a'	T3	0	0	0	1	0	0	0	0	12/02/19	12/02/19	3	4.3	1	0	0	3									1			1	12/02/19	21/10/14		
363	362	65	0	21/10/14	PBR	0	N/A	N/A	5.5	3.5	'1b'	T1	1	0	N/A	Other	N/A	N/A	N/A	N/A	ALIVE	01/05/20	0	5.5	12	0	0	3									12	12			ALIVE	21/10/14		
364	363	58	0	11/11/14	Local resection	1	1	3	13.8	6.6	'3b'	T3	1	0	0	1	1	1	1	1	04/05/18	04/05/18	3	3.5	9	3	1	1	45.6	M1b	28-Sep-16	60	1.9	1.6	9	7	2			04/05/18	11/11/14			
365	364	33	0	02/12/14	Endoresection	0	N/A	N/A	9.2	6.6	'2a'	T2	0	0	0	1	0	Other	0	1	09/05/19	09/05/19	1	4.4	19	Mult	1	2	76	M1b	09-Nov-17	36	2.9	1.5	19	12	6	1		09/05/19	02/12/14			
366	365	65	1	28/10/14	PBR	1	N/A	N/A	10.4	3.5	'2a'	T2	0	0	0	1	1	1	0	0	ALIVE	01/05/20	0	5.5	12	0	0	3									12	11			ALIVE	28/10/14		
367	366	67	1	21/01/14	Enucleation	1	1	4	17.7	4.7	'3a'	T3	0	1	0	1	0	0	0	0	11/07/15	11/07/15	1	1.5	2	0	2	1									1.5	1.5	2	1	1	11/07/15	21/01/14	
368	367	60	1	21/01/14	Enucleation	1	1	1	20.6	16.6	'4a'	T4	1	1	0	1	0	0	0	1	15/01/15	15/01/15	1	1.0	1	0	2	1								1.0	1.0	1		1	15/01/15	21/01/14		
369	368	62	1	21/01/14	Enucleation	0	1	2	17.3	9.4	'3b'	T3	1	0	0	1	0	0	0	0	ALIVE	01/05/20	0	6.3	1	0	0	3									1			1	ALIVE	21/01/14		
370	369	75	0	21/01/14	Enucleation	1	0	2	16.5	4.5	'3a'	T3	1	1	0	Other	1	0	1	1	26/08/15	26/08/15	1	1.6	4	0	2	1									1.6	1.6	4	2	1	1	26/08/15	21/01/14
371	370	69	1	25/02/14	Enucleation	1	0	3	12.3	8.2	'3c'	T3	0	1	Other	1	0	Other	1	1	26/11/16	26/11/16	1	2.8	1	0	2	2									2.8	2.8	1		1	26/11/16	25/02/14	
372	371	58	1	25/02/14	Enucleation	0	0	1	13.5	11.7	'3c'	T3	0	1	0	1	0	0	0	1	25/05/18	25/05/18	1	4.2	14	Mult	1	2	196	M1c	07-Mar-18	62	4.0	0.2	14	12	2			25/05/18	25/02/14			
373	372	62	1	18/03/14	Enucleation	1	0	3	9	9	'2a'	T2	0	0	0	Other	Other	0	0	0	ALIVE	01/05/20	0	6.1	14	0	0	3									14	14			ALIVE	18/03/14		
374	373	73	1	21/03/14	Enucleation	1	0	3	19.5	4	'4a'	T4	0	0	0	1	0	0	0	1	18/03/17	18/03/17	1	3.0	11	Mult	1	2	115	M1c	03-Apr-16	75	2.4	0.6	11	2	5	4		18/03/17	21/03/14			
375	374	51	1	15/04/14	PRXT	0	N/A	N/A	14.8	4.9	'2a'	T2	0	0	N/A	N/A	N/A	N/A	N/A	N/A	ALIVE	01/05/20	0	6.0	10	0	0	3									10	10			ALIVE	15/04/14		
376	375	78	1	25/04/14	Enucleation	0	0	3	5.9	1.9	'1a'	T1	0	0	0	Other	1	0	0	1	15/12/14	15/12/14	3	0.6	1	0	0	3									1			1	15/12/14	25/04/14		
377	376	62	0	20/05/14	PRXT	N/A	N/A	N/A	13.3	3.8	'2a'	T2	0	0	N/A	Other	N/A	N/A	N/A	N/A	18/06/19	18/06/19	1	5.1	10	Mult	1	2	92	M1c	18-Jul-18	66	4.2	0.9	10	6	3	1		18/06/19	20/05/14			
378	377	75	1	03/06/14	Enucleation	0	0	2	15.3	9.3	'3a'	T3	0	0	1	1	0	0	0	0	22/07/19	22/07/19	3	5.1	13	Mult	1	2	19	M1a	17-May-17	76	3.0	2.2	13									

Appendix 3 - Inserted variables for the model for study 1, including its description and coding scheme

Variable name	Description
Age	Age at the primary treatment
Sex	0 - Female 1 - Male
LBD (mm)	Largest basal diameter from ultrasound in mm
UH (mm)	Ultrasound tumour height in mm
Ciliary Body Involvement (CBI)	0 - No, 1 - Yes
Extraocular Extension (EOE)	0 - No, 1 - Yes
Epithelioid cells present (Epi)	0 - No, 1 - Yes
Close PAS positive loops	0 - No, 1 - Yes
Mitoc	Mitotic count per 40 high power fields 0: 0-1 1: 2-3 2: 4-7 3: >7
Chromosome 1	1 - Abnormal/Loss 0 - Normal
Chromosome 3	1 - Abnormal/Loss 0 - Normal
Chromosome 6	1 - Abnormal/Loss or Gain 0 - Normal
Chromosome 8	1 - Abnormal/Loss or Gain 0 - Normal
Follow-up time	In Years
Cause of Death	0 - Alive 1 - Definitely UM Metastases 2 - Other causes 3 - Unknown causes
Number of scans performed/screening interval	Varied
Metastases state	1 - Metastases 2 - No Metastases 999 - Suspicious
Time from primary treatment to first metastases	In Years
Time from first metastases to death	In Years

Appendix 4 - Correlations between genetics and primary tumour TNM stage according to AJCC 8th edition (cross tabulations)

Chromosome status	Primary tumour TNM stage								Total	Significance (p value)
	T1 (%)	T2 (%)	T3 (%)	T4 (%)	T1 (%)	T2 (%)	T3 (%)	T4 (%)		
Chr 1										
0	35	11.8%	59	19.9%	125	42.1%	78	26.3%	297	<.001
1	12	9%	26	19.4%	59	44.1%	37	27.6%	134	<.001
2	60	33%	55	30.3%	42	23.1%	25	13.7%	182	<.001
Chr 3										
0	50	22.7%	53	24.1%	84	38.2%	33	15%	220	<.001
1	37	11.3%	66	20.1%	128	39%	98	29.8%	329	<.001
2	20	31.3%	21	32.8%	14	21.9%	9	14.1%	64	=.324
Chr 6p										
0	36	12.2%	57	19.3	113	38.3%	89	30.2%	295	<.001
1	11	8.1%	28	20.6%	71	52.3%	26	19.2%	136	<.001
2	60	33%	55	30.3%	42	23.1%	25	13.7%	182	<.001
Chr 6q										
0	41	12.3%	68	20.4%	135	40.4%	90	26.9%	334	<.001
1	6	6.2%	17	17.5%	49	50.5%	25	25.8%	97	<.001
2	60	33%	55	30.3%	42	23.1%	25	13.7%	182	<.001
Chr 8p										
0	36	11.9%	64	49.6%	129	42.7%	73	24.2%	302	<.001
1	11	8.5%	21	16.3%	55	42.6%	42	32.6%	129	<.001
2	60	33%	55	30.3%	42	23.1%	25	13.7%	182	<.001
Chr 8q										
0	21	12%	36	20.6%	82	46.9%	36	20.6%	175	<.001
1	26	10.1%	49	19.1%	102	39.7%	80	31.2%	257	<.001
2	60	33.2%	55	30.4%	42	23.2%	24	13.3%	181	<.001
Total	107	17.5%	140	22.8%	226	36.9%	140	22.8%	613	

Appendix 5 - Associations between chromosomal copy numbers (cross tabulations)

Chromosome status (cross tabulations)																			
Chr 1p	Chr 1p			Chr3			Chr6p			Chr6q			Chr8p			Chr8q			Total
	0	1	2	0	1	2	0	1	2	0	1	2	0	1	2	0	1	2	
0	297	0	0	125	172	0	200	97	0	234	63	0	208	89	0	123	174	0	297
1	0	135	0	23	112	0	95	40	0	100	35	0	95	40	0	52	83	0	135
2	0	0	183	72	46	65	0	0	183	1	0	182	0	0	183	1	0	182	183
Chr 3																			
0	125	23	72	220	0	0	64	84	72	103	45	72	126	22	72	88	61	71	220
1	172	112	46	0	330	0	231	53	46	231	53	46	177	107	46	88	196	46	330
2	0	0	65	0	0	65	0	0	65	1	0	64	0	0	65	0	0	182	65
Chr 6p																			
0	200	95	0	64	231	0	295	0	0	255	40	0	194	101	0	117	178	0	295
1	97	40	0	84	53	0	0	137	0	79	58	0	109	28	0	58	79	0	137
2	0	0	183	72	46	65	0	0	183	1	0	182	0	0	183	1	0	182	183
Chr 6q																			
0	234	100	1	103	231	1	255	79	1	335	0	0	237	97	1	136	198	1	335
1	63	35	0	45	53	0	40	58	0	0	98	0	66	32	0	39	59	0	98
2	0	0	72	72	46	64	0	0	182	0	0	182	0	0	182	1	0	181	182
Chr 8p																			
0	208	95	0	126	177	0	194	109	0	237	66	0	303	0	0	163	140	0	303
1	89	40	0	22	107	0	101	28	0	97	32	0	0	129	0	12	117	0	129
2	0	0	183	72	46	65	0	0	183	1	0	182	0	0	183	1	0	182	183
Chr 8q																			
0	123	52	1	88	88	0	117	58	1	136	39	1	163	12	1	176	0	0	176
1	174	83	0	61	196	0	178	79	0	198	59	0	140	117	0	0	257	0	257
2	0	0	182	71	46	65	0	0	182	1	0	181	0	0	182	0	0	182	182
Total	297	135	183	220	330	65	295	137	183	335	98	182	303	129	183	176	257	182	615

Appendix 6 - Proposal Sample for study 2 (Proforma)

Study Number	Age at Primary treatment	Gender	Date of primary treatment	Follow-up time	Status	Primary treatment to first scan	Number of scans	Date of first metastases	Time to first detection
5	53	1	18/03/2008	3.2	1	0.0	16	06/08/2010	2.4
6	44	0	10/03/2008	11.9	0	0.0	1	0	0

Number of scans until first detection	Time to last scan	<i>Ipmd</i>	Threshold = -1	Number of metastases missed	Number of scans avoided	Threshold = 0	Number of metastases missed	Number of scans avoided
7	3.2	3.409612495	Recommended	0	0	Recommended	0	0
0	0.0	0.097941474	Recommended	0	0	Recommended	0	0

Threshold = +1	Number of metastases missed	Number of scans avoided						
Recommended	0	0						
Not Recommended	0	0						

B	C	D	E	F	G	H	I	J	K	L	M	N	O	P	Q	R	S	T	U	V	W	X	Y	Z	AA	AB	AC	AD	AE	AF	AG
456	0.246	R	0	0	R	0	0	NR	1	0	23	12	8	3	ALIVE	25/08/15	0.0	*****	5	25-Aug-15	0	136	08-Jan-16	0	180	05-Jul-16	0	209	31-Jan-17		
457	2.529	R	0	0	SA	R	0	SA	R	0	SA	10	10	0	0	ALIVE	25/08/15	0.0	*****	10	26-Aug-15	0	98	02-Dec-15	0	203	22-Jun-16	0	179	18-Dec-16	
458	0.319	R	0	0	SA	R	0	SA	NR	0	SA	9	0	0	9	ALIVE	24/06/97	18.1	*****	9	20-Jul-15	0	500	01-Dec-16	0	168	18-May-17	0	89	15-Aug-17	
459	1.921	R	0	0	R	0	0	R	0	0	12	8	4	0	ALIVE	17/05/05	11.8	12.7	4	20-Feb-17	0	236	13-Oct-17	0	33	15-Nov-17	0	61	15-Jan-18		
460	-0.32	R	0	0	SA	NR	0	SA	NR	0	SA	7	0	0	7	ALIVE	30/08/16	0.0	*****	7	30-Aug-16	0	177	23-Feb-17	0	182	24-Aug-17	0	182	22-Feb-18	
461	2.228	R	0	0	SA	R	0	SA	R	0	SA	8	3	3	2	ALIVE	28/01/16	0.1	*****	8	10-Mar-16	0	165	22-Aug-16	0	185	23-Feb-17	0	126	29-Jun-17	
462	-1.1	NR	0	0	SA	NR	0	SA	NR	0	SA	1	0	0	1	ALIVE	14/06/16	0.0	*****	0.0	1	14-Jun-16	0	0	0	0	0	0	0	0	
463	1.864	R	0	0	SA	R	0	SA	R	0	SA	7	7	0	0	ALIVE	09/02/16	0.8	*****	7	22-Nov-16	0	177	18-May-17	0	181	15-Nov-17	0	182	16-May-18	
464	0.931	R	0	0	SA	R	0	SA	NR	0	SA	1	0	0	1	ALIVE	08/03/16	0.0	*****	0.0	1	10-Mar-16	0	0	0	0	0	0	0	0	
465	-0.84	R	0	0	SA	NR	0	SA	NR	0	SA	10	9	0	1	ALIVE	26/04/16	0.3	*****	10	19-Aug-16	0	8	27-Aug-16	0	90	25-Nov-16	0	172	16-May-17	
466	-0.87	R	0	0	SA	NR	0	SA	NR	0	SA	6	0	0	6	ALIVE	03/05/16	0.1	*****	6	23-Jun-16	0	175	15-Dec-16	0	182	15-Jun-17	0	182	14-Dec-17	
467	3.563	R	0	0	R	0	0	R	0	0	12	6	4	2	28/01/18	12/04/16	0.6	0.6	1	30-Nov-16	1	23	23-Dec-16	1	1	24-Dec-16	1	31	24-Jan-17		
468	0.506	R	0	0	SA	R	0	SA	NR	0	SA	13	10	2	1	ALIVE	19/04/16	0.0	*****	13	20-Apr-16	0	98	27-Jul-16	0	194	06-Feb-17	0	190	15-Aug-17	
469	-1.18	NR	0	0	SA	NR	0	SA	NR	0	SA	1	0	0	1	ALIVE	31/05/16	0.0	*****	0.0	1	31-May-16	0	0	0	0	0	0	0	0	
470	0.142	R	0	0	SA	R	0	SA	NR	0	SA	7	7	0	0	ALIVE	12/07/16	0.0	*****	7	13-Jul-16	0	161	21-Dec-16	0	174	13-Jun-17	0	373	21-Jun-18	
471	2.907	R	0	0	SA	R	0	SA	R	0	SA	1	0	0	1	27/01/17	10/05/16	0.0	*****	0.0	1	10-Jun-16	0	0	0	0	0	0	0	0	
472	1.569	R	0	0	SA	R	0	SA	R	0	SA	2	2	0	0	ALIVE	24/05/16	0.2	*****	0.7	2	01-Aug-16	0	189	06-Feb-17	0	0	0	0	0	0
473	-0.75	R	0	0	NR	1	0	NR	1	0	18	14	4	0	ALIVE	17/05/16	0.3	*****	7	01-Sep-16	0	186	06-Mar-17	0	187	09-Sep-17	0	34	13-Oct-17		
474	1.982	R	0	0	SA	R	0	SA	R	0	SA	9	8	0	1	ALIVE	31/05/16	0.0	*****	9	31-May-16	0	28	28-Jun-16	0	184	29-Dec-16	0	184	01-Jul-17	
475	2.961	R	0	0	R	0	0	R	0	0	4	2	1	1	10/10/17	17/06/16	0.2	0.7	2	27-Aug-16	0	152	07-Mar-17	1	31	07-Apr-17	1	36	13-May-17		
476	2.336	R	2	0	R	2	0	R	2	0	1	0	0	1	21/08/18	14/06/16	0.0	2.2	1	14-Jun-16	0	0	0	0	0	0	0	0	0	0	0
477	1.064	R	0	0	R	0	0	R	0	0	9	6	2	1	ALIVE	14/10/16	1.8	2.7	4	16-Aug-16	0	203	07-Mar-19	0	21	28-Mar-19	0	97	03-Jul-19		
478	3.274	R	0	0	R	0	0	R	0	0	10	6	3	1	16/11/18	27/07/16	0.0	*****	6	27-Jul-16	0	81	16-Oct-16	0	173	07-Apr-17	0	185	09-Oct-17		
479	0.14	R	0	0	SA	R	0	SA	NR	0	SA	1	0	0	1	ALIVE	02/08/16	0.1	*****	0.1	1	25-Aug-16	0	0	0	0	0	0	0	0	0
480	0.227	R	0	0	SA	R	0	SA	NR	0	SA	11	9	1	1	ALIVE	02/08/16	0.1	*****	11	02-Aug-16	0	8	10-Aug-16	0	107	25-Nov-16	0	34	29-Dec-16	
481	2.166	R	0	0	R	0	0	R	0	0	7	3	3	3	04/04/18	19/07/16	0.5	0.9	4	09-Jan-17	0	30	08-Feb-17	0	78	27-Apr-17	0	40	06-Jul-17		
482	0.819	R	0	0	SA	R	0	SA	NR	0	SA	9	8	1	0	ALIVE	23/08/16	0.3	*****	9	05-Dec-16	0	18	23-Dec-16	0	7	30-Dec-16	0	153	01-Jun-17	
483	-1.24	NR	0	0	SA	NR	0	SA	NR	0	SA	1	0	0	1	ALIVE	06/09/16	0.1	*****	0.1	1	29-Sep-16	0	0	0	0	0	0	0	0	0
484	-1.16	NR	0	0	SA	NR	0	SA	NR	0	SA	1	0	0	1	ALIVE	23/08/16	0.0	*****	0.0	1	24-Aug-16	0	0	0	0	0	0	0	0	0
485	3.18	R	2	0	R	2	0	R	2	0	1	0	0	1	24/04/18	06/09/16	0.0	1.6	1	06-Sep-16	0	0	0	0	0	0	0	0	0	0	0
486	-1.13	NR	0	0	SA	NR	0	SA	NR	0	SA	7	7	0	0	ALIVE	06/09/16	0.2	*****	7	08-Nov-16	0	211	07-Jun-17	0	189	13-Dec-17	0	189	20-Jun-18	
487	1.937	R	0	0	SA	R	0	SA	R	0	SA	4	4	0	0	ALIVE	13/09/16	0.2	*****	1.7	4	28-Nov-16	0	193	09-Jun-17	0	175	01-Dec-17	0	187	06-Jun-18
488	2.921	R	0	0	SA	R	0	SA	R	0	SA	8	8	0	0	ALIVE	20/09/16	0.0	*****	8	20-Sep-16	0	59	18-Nov-16	0	182	19-May-17	0	188	23-Nov-17	
489	3.994	R	0	0	SA	R	0	SA	R	0	SA	1	0	0	1	12/01/17	29/10/16	0.0	*****	0.0	1	28-Oct-16	0	0	0	0	0	0	0	0	0
490	0.425	R	0	0	SA	R	0	SA	NR	0	SA	7	7	0	0	ALIVE	27/09/16	0.4	*****	7	14-Feb-17	0	179	12-Aug-17	0	193	21-Feb-18	0	173	13-Aug-18	
491	1.869	R	0	0	R	0	0	R	0	0	7	4	1	2	19/11/18	29/09/16	0.0	0.9	3	29-Sep-16	0	144	20-Feb-17	0	177	16-Aug-17	1	36	21-Sep-17		
492	0.819	R	0	0	R	0	0	R	0	0	3	3	0	0	16/12/18	28/10/16	1.8	1.6	1	15-Jun-18	1	70	24-Aug-18	1	114	16-Dec-18	1	36	21-Sep-17		
493	2.245	R	0	0	R	0	0	R	0	0	11	7	3	1	25/08/18	25/10/16	0.3	*****	5	7	06-Feb-17	0	14	20-Feb-17	0	109	09-Jun-17	0	89	06-Sep-17	
494	-1.33	NR	0	0	SA	NR	0	SA	NR	0	SA	1	0	0	1	ALIVE	01/11/16	0.0	*****	0.0	1	01-Nov-16	0	0	0	0	0	0	0	0	0
495	2.525	R	0	0	SA	R	0	SA	R	0	SA	3	2	0	1	ALIVE	11/11/16	0.0	*****	0.6	3	15-Nov-16	0	44	29-Dec-16	0	184	01-Jul-17	0	0	0
496	0.103	R	0	0	R	0	0	R	0	0	2	1	1	0	12/11/18	15/11/16	1.7	1.7	1	11-Jul-18	1	7	18-Jul-18	1	0	0	0	0	0	0	
497	0.94	R	0	0	SA	R	0	SA	NR	0	SA	1	0	0	1	ALIVE	13/12/16	0.4	*****	0.0	1	13-Dec-16	0	0	0	0	0	0	0	0	0
498	-2.19	NR	0	0	SA	NR	0	SA	NR	0	SA	6	6	0	0	ALIVE	12/12/16	0.0	*****	6	09-May-17	0	178	03-Nov-17	0	195	17-May-18	0	167	31-Oct-18	
499	-0.23	R	0	0	SA	NR	0	SA	NR	0	SA	5	0	0	5	ALIVE	13/12/16	0.0	*****	5	13-Dec-16	0	492	19-Apr-18	0	259	03-Jan-19	0	203	25-Jul-19	
500	1.931	R	2	0	R	2	0	R	2	0	1	0	0	1	26/03/18	20/12/16	0.0	1.3	1	20-Dec-16	0	0	0	0	0	0	0	0	0	0	0
501	2.487	R	0	0	SA	R	0	SA	R	0	SA	9	7	1	1	ALIVE	20/12/16	0.0	*****	9	20-Dec-16	0	62	20-Feb-17	0	178	17-Aug-17	0	118	13-Dec-17	
502	1.467	R	0	0	SA	R	0	SA	R	0	SA	9	9	0	0	ALIVE	26/01/16	0.0	*****	9	26-Jan-16	0	83	18-Apr-16	0	171	06-Oct-16	0	179	03-Apr-17	
503	1.947	R	0	0	SA	R	0	SA	R	0	SA	1	0	0	1	27/09/19	22/01/16	0.0	*****	0.2	2	22-Jan-16	0	0	0	0	0	0	0	0	0
504	0.022	R	0	0	SA	R	0	SA	NR	0	SA	6	0	0	6	ALIVE	01/03/16	0.3	*****	6	09-Jun-16	0	210	05-Jan-17	0	182	06-Jul-17	0	238	01-Mar-18	
505	-0.62	R	0	0	NR	1	0	NR	1	0	2	1	0	1	03/06/17	05/04/16	0.3	0.4	2	03-Aug-16	0	34	06-Sep-16	1	0	0	0	0	0	0	0
506	1.341	R	0	0	SA	R	0	SA	R	0	SA	1	0	0	1	ALIVE	01/03/16	0.0	*****	0.0	1	01-Mar-16	0	0	0	0	0	0	0	0	0
507	-0.43	R	0	0	SA	NR	0	SA	NR	0	SA	8	8	0	0	ALIVE	01/03/16	0.0	*****	8	02-Mar-16	0	146	26-Jul-16	0	162	04-Jan-17	0	196	19-Jul-17	
508	1.534	R	0	0	SA	R	0	SA	R	0	SA	7	7	0	0	ALIVE	11/10/16	0.2	*****	7	29-Dec-16	0	184	01-Jul-17	0	179	27-Dec-17	0	192	07-Jul-18	
509	0.621	R	0	0	SA	R	0	SA	NR	0	SA	1	0	0	1	ALIVE	16/02/16	0.0	*****	0.0	1										

B	C	D	E	F	G	H	I	J	K	L	M	N	O	P	Q	R	S	T	U	V	W	X	Y	Z	AA	AB	AC	AD	AE	AF	AG	AH	
570	0,541	R	0	SA	R	0	SA	NR	0	SA	4	2	0	2	ALIVE	16/01/18	0,4			1,3	4	28-Jun-18	0	28	26-Jul-18	0	246	29-Mar-19	0	55	23-May-19		
571	-0,06	R	0	SA	NR	0	SA	NR	0	SA	4	0	0	4	ALIVE	30/01/18	0,3			1,8	4	24-May-18	0	189	29-Nov-18	0	175	23-May-19	0	189	28-Nov-19		
572	3,421	R	0	0	R	0	0	R	0	0	3	1	0	2	ALIVE	09/01/18	1,2	1,2	1			28-Mar-19	1	53	20-May-19	1	1	21-May-19	1				
573	2,913	R	0	0	R	0	0	R	0	0	16	9	7	0	ALIVE	16/03/18	0,2	#####	6	#####	5	21-May-18	0	0	21-May-18	0	16	06-Jun-18	0	117	01-Oct-18		
574	-0,79	R	0	SA	NR	0	SA	NR	0	SA	5	0	0	5	ALIVE	13/02/18	0,1			#####	4	29-Mar-18	0	134	10-Aug-18	0	181	07-Feb-19	0	196	22-Aug-19		
575	-2,03	NR	0	SA	NR	0	SA	NR	0	SA	4	0	0	4	ALIVE	06/03/18	0,1			1,8	4	27-Apr-18	0	230	13-Dec-18	0	182	13-Jun-19	0	182	12-Dec-19		
576	-0,68	R	0	SA	NR	0	SA	NR	0	SA	1	0	0	1	ALIVE	14/03/18	0,5			0,5	1	13-Sep-18	0										
577	-0,87	R	0	SA	NR	0	SA	NR	0	SA	1	0	0	1	ALIVE	13/03/18	0,3			0,3	1	25-Jun-18	0										
578	-2,89	NR	0	SA	NR	0	SA	NR	0	SA	4	0	0	4	ALIVE	27/03/18	0,4			1,9	4	02-Aug-18	0	189	07-Feb-19	0	182	08-Aug-19	0	189	13-Feb-20		
579	2,502	R	0	SA	R	0	SA	R	0	SA	1	0	0	1	ALIVE	10/04/18	0,0			0,0	1	11-Apr-18	0										
580	-0,63	R	0	SA	NR	0	SA	NR	0	SA	4	4	0	0	ALIVE	10/04/18	0,4			1,9	4	16-Aug-18	0	188	20-Feb-19	0	191	30-Aug-19	0	180	26-Feb-20		
581	-0,16	R	0	SA	NR	0	SA	NR	0	SA	1	0	0	1	ALIVE	20/04/18	0,0			0,0	1	21-Apr-18	0										
582	3,469	R	0	SA	R	0	SA	R	0	SA	6	4	2	0	ALIVE	15/05/18	0,0			#####	6	18-May-18	0	87	13-Aug-18	0	191	20-Feb-19	0	182	21-Aug-19		
583	-1,84	NR	0	SA	NR	0	SA	NR	0	SA	2	1	0	1	ALIVE	12/06/18	0,2			0,3	2	30-Aug-18	0	39	08-Oct-18	0							
584	2,204	R	0	SA	R	0	SA	R	0	SA	2	1	0	1	18/03/19	05/06/18	0,0			0,6	2	05-Jun-18	0	206	28-Dec-18	0							
585	-2,37	NR	0	SA	NR	0	SA	NR	0	SA	5	1	0	4	ALIVE	26/06/18	0,0			#####	5	28-Jun-18	0	40	07-Aug-18	0	156	10-Jan-19	0	217	15-Aug-19		
586	2,863	R	0	SA	R	0	SA	R	0	SA	1	0	0	1	ALIVE	19/06/18	0,0			0,0	1	20-Jun-18	0										
587	0,721	R	0	SA	R	0	SA	R	0	SA	4	4	0	0	ALIVE	19/06/18	0,3			1,5	4	26-Sep-18	0	78	13-Dec-18	0	183	14-Jun-19	0	173	04-Dec-19		
588	2,219	R	0	SA	R	0	SA	R	0	SA	1	0	0	1	ALIVE	26/06/18	0,0			0,0	1	27-Jun-18	0										
589	-0,4	R	0	SA	NR	0	SA	NR	0	SA	1	0	0	1	ALIVE	06/07/18	0,1			0,1	1	09-Aug-18	0										
590	-1,59	NR	0	SA	NR	0	SA	NR	0	SA	1	0	0	1	ALIVE	26/06/18	0,0			0,0	1	30-Jun-18	0										
591	1,112	R	0	SA	R	0	SA	R	0	SA	1	0	0	1	ALIVE	03/07/18	0,0			0,0	1	04-Jul-18	0										
592	2,582	R	0	SA	R	0	SA	R	0	SA	1	0	0	1	ALIVE	03/07/18	0,0			0,0	1	04-Jul-18	0										
593	-1,59	NR	0	SA	NR	0	SA	NR	0	SA	3	0	0	3	ALIVE	10/07/18	0,5			1,5	3	17-Jan-19	0	175	11-Jul-19	0	182	09-Jan-20	0				
594	-2	NR	0	SA	NR	0	SA	NR	0	SA	1	0	0	1	ALIVE	17/07/18	0,1			0,1	1	30-Aug-18	0										
595	2,493	R	0	SA	R	0	SA	R	0	SA	3	0	0	3	ALIVE	17/07/18	0,0			1,2	3	17-Jul-18	0	273	16-Apr-19	0	153	16-Sep-19	0				
596	1,281	R	0	SA	R	0	SA	R	0	SA	3	0	0	3	ALIVE	17/07/18	0,0			1,0	3	19-Jul-18	0	196	31-Jan-19	0	161	11-Jul-19	0				
597	0,891	R	0	SA	R	0	SA	R	0	SA	3	2	0	1	ALIVE	31/07/18	0,0			0,8	3	01-Aug-18	0	115	24-Nov-18	0	179	22-May-19	0	183	21-Nov-19		
598	0,698	R	0	SA	R	0	SA	NR	0	SA	5	4	0	1	ALIVE	14/08/18	0,2			#####	5	18-Oct-18	0	185	21-Apr-19	0	178	16-Oct-19	999	26	11-Nov-19		
599	1,954	R	0	SA	R	0	SA	R	0	SA	1	0	0	1	ALIVE	31/07/18	0,0			0,0	1	31-Jul-18	0										
600	1,612	R	0	SA	R	0	SA	R	0	SA	3	3	0	0	ALIVE	07/08/18	0,5			1,5	3	13-Feb-19	0	176	08-Aug-19	0	181	05-Feb-20	0				
601	2,896	R	0	0	R	0	0	R	0	0	8	2	5	1	14/10/19	21/08/18	0,2	0,1	2			22-Aug-18	0	34	25-Sep-18	1	73	07-Dec-18	1	119	05-Apr-19		
602	1,048	R	0	SA	R	0	SA	R	0	SA	3	1	0	2	ALIVE	28/08/18	0,0			1,2	3	12-Nov-18	0	177	08-May-19	0	189	13-Nov-19	0				
603	0,664	R	0	SA	R	0	SA	NR	0	SA	1	0	0	1	ALIVE	14/08/18	0,3			0,3	1	22-Nov-18	0										
604	-0,78	R	0	SA	NR	0	SA	NR	0	SA	1	0	0	1	ALIVE	21/08/18	0,6			0,6	1	14-Mar-19	0										
605	-1,02	NR	0	SA	NR	0	SA	NR	0	SA	2	0	0	2	ALIVE	18/09/18	0,5			1,3	2	21-Mar-19	0	274	20-Dec-19	0							
606	2,172	R	0	SA	R	0	SA	R	0	SA	1	0	0	1	ALIVE	02/10/18	0,0			0,0	1	02-Oct-18	0										
607	1,419	R	0	0	R	0	0	R	0	0	10	6	3	1	ALIVE	09/10/18	0,4			0,9	2	21-Feb-19	0	190	30-Aug-19	1	18	17-Sep-19	1	7	24-Sep-19		
608	0,854	R	0	SA	R	0	SA	NR	0	SA	1	0	0	1	ALIVE	16/10/18	0,0			0,0	1	16-Oct-18	0										
609	-0,1	R	0	SA	NR	0	SA	NR	0	SA	1	0	0	1	ALIVE	06/11/18	0,5			0,5	1	25-Apr-19	0										
610	-0,5	R	0	SA	NR	0	SA	NR	0	SA	3	2	0	1	ALIVE	13/11/18	0,3			1,3	3	04-Mar-19	0	156	07-Aug-19	0	196	19-Feb-20	0				
611	2,75	R	0	SA	R	0	SA	R	0	SA	2	2	0	0	ALIVE	04/12/18	0,4			0,9	2	12-Apr-19	0	182	11-Oct-19	0							
612	2,865	R	0	SA	R	0	SA	R	0	SA	3	2	0	1	ALIVE	11/12/18	0,0			0,8	3	11-Dec-18	0	113	03-Apr-19	0	193	13-Oct-19	0				
613	3,277	R	0	SA	R	0	SA	R	0	SA	1	0	0	1	ALIVE	18/12/18	0,0			0,0	1	18-Dec-18	0										
614	-0,35	R	0	SA	NR	0	SA	NR	0	SA	2	0	0	2	ALIVE	11/12/18	0,2			0,7	2	01-Mar-19	0	174	22-Aug-19	0							
615	1,526	R	0	SA	R	0	SA	R	0	SA	2	0	0	2	ALIVE	28/12/18	0,0			0,4	2	28-Dec-18	0	153	30-May-19	0							

Appendix 8 - Proposal sample for study 3 (proforma)

Study Number	Date of management	Age	Gender	LUD	UH	CBI	EOE	Epi	Loops	Mitoc	Chr3	Chr8	Follow-up	Outcome	CoD
1001	27 November 2006	59.12	1	14	9	0	0	1	NA	NA	1	0	4.76	0	NA
1002	04 March 2010	66.33	0	15	12	1	0	1	1	5	1	1	1.98	1	1

Appendix 9 – Inserted variables for the model of study 3, including its description and coding scheme

Variable name	Description
Age	Age at the first treatment
Sex	0: Female
	1: Male
Largest tumour diameter from ultrasound in mm (LUD)	Mm
Ultrasound tumour height in mm (UH)	Mm
Ciliary Body Involvement (CBI)	0 – No, 1 – Yes
Extraocular Extension (EOE)	0 – No, 1 – Yes
Epithelioid cells present (Epi)	0 – No, 1 – Yes
Close PAS +ve loops	0 – No, 1 – Yes
Mitotic count	
1	0 to 1
2	2 to 3
3	4 to 7
4	> 7
Chr 3 loss	1 – Yes
	0 – No
Chr 8 gain	1 – Yes
	0 – No
Follow-up time	Years
Outcome	Alive
	Death
Cause of Death	Other
	Possible UM metastases
	Definitely UM metastases

REFERENCES

1. Stricklan, D.; Lee, J.A. Melanomas of eye: Stability of rates. *American journal of epidemiology* **1981**, *113*, 700-702.
2. Eagle, R.C. *Eye pathology: An atlas and text*. Lippincott Williams & Wilkins: 2012.
3. Damato, B.E.; Coupland, S.E. Ocular melanoma. *Saudi Journal of Ophthalmology* **2012**, *26*, 137-144.
4. Chang, A.E.; Karnell, L.H.; Menck, H.R. The national cancer data base report on cutaneous and noncutaneous melanoma: A summary of 84,836 cases from the past decade. *Cancer: Interdisciplinary International Journal of the American Cancer Society* **1998**, *83*, 1664-1678.
5. Bishop, K.D.; Olszewski, A.J. Epidemiology and survival outcomes of ocular and mucosal melanomas: A population-based analysis. *International journal of cancer* **2014**, *134*, 2961-2971.
6. Singh, A.D.; Turell, M.E.; Topham, A.K. Uveal melanoma: Trends in incidence, treatment, and survival. *Ophthalmology* **2011**, *118*, 1881-1885.
7. Aronow, M.E.; Topham, A.K.; Singh, A.D. Uveal melanoma: 5-year update on incidence, treatment, and survival (seer 1973-2013). *Ocul Oncol Pathol* **2018**, *4*, 145-151.
8. Singh, A.D.; Topham, A. Incidence of uveal melanoma in the united states: 1973–1997. *Ophthalmology* **2003**, *110*, 956-961.
9. Singh, N.; Bergman, L.; Seregard, S.; Singh, A.D. Uveal melanoma: Epidemiologic aspects. In *Clinical ophthalmic oncology*, Springer: 2014; pp 75-87.
10. Bergman, L.; Seregard, S.; Nilsson, B.; Ringborg, U.; Lundell, G.; Ragnarsson-Olding, B. Incidence of uveal melanoma in sweden from 1960 to 1998. *Invest Ophthalmol Vis Sci* **2002**, *43*, 2579-2583.
11. Rana'a, T.; Cassoux, N.; Desjardins, L.; Damato, B.; Konstantinidis, L.; Coupland, S.E.; Heimann, H.; Petrovic, A.; Zografos, L.; Schalenbourg, A. The pediatric choroidal and ciliary body melanoma study: A survey by the european ophthalmic oncology group. *Ophthalmology* **2016**, *123*, 898-907.
12. Hu, D.N.; Yu, G.P.; McCormick, S.A.; Schneider, S.; Finger, P.T. Population-based incidence of uveal melanoma in various races and ethnic groups. *Am J Ophthalmol* **2005**, *140*, 612-617.
13. Kaneko, A. Malignant ophthalmic tumors. *Nihon rinsho. Japanese journal of clinical medicine* **1993**, *51*, 1013.
14. Egan, K.M.; Seddon, J.M.; Glynn, R.J.; Gragoudas, E.S.; Albert, D.M. Epidemiologic aspects of uveal melanoma. *Survey of ophthalmology* **1988**, *32*, 239-251.

15. Wakamatsu, K.; Hu, D.N.; McCormick, S.A.; Ito, S. Characterization of melanin in human iridal and choroidal melanocytes from eyes with various colored irides. *Pigment cell & melanoma research* **2008**, *21*, 97-105.
16. Ni-Komatsu, L.; Orlow, S.J. Heterologous expression of tyrosinase recapitulates the misprocessing and mistrafficking in oculocutaneous albinism type 2: Effects of altering intracellular pH and pink-eyed dilution gene expression. *Experimental eye research* **2006**, *82*, 519-528.
17. Naumann, G.; Yanoff, M.; Zimmerman, L.E. Histogenesis of malignant melanomas of the uvea: I. Histopathologic characteristics of nevi of the choroid and ciliary body. *Archives of Ophthalmology* **1966**, *76*, 784-796.
18. Yanoff, M.; Zimmerman, L.E. Histogenesis of malignant melanomas of the uvea: Iii. The relationship of congenital ocular melanocytosis and neurofibromatosis to uveal melanomas. *Archives of Ophthalmology* **1967**, *77*, 331-336.
19. Qiu, M.; Shields, C.L. Choroidal nevus in the united states adult population: Racial disparities and associated factors in the national health and nutrition examination survey. *Ophthalmology* **2015**, *122*, 2071-2083.
20. Singh, A.D.; Kalyani, P.; Topham, A. Estimating the risk of malignant transformation of a choroidal nevus. *Ophthalmology* **2005**, *112*, 1784-1789.
21. Sahel, J.A.; Pesavento, R.; Frederick, A.R.; Albert, D.M. Melanoma arising de novo over a 16-month period. *Archives of ophthalmology* **1988**, *106*, 381-385.
22. Shields, C.L.; Qureshi, A.; Mashayekhi, A.; Park, C.; Sinha, N.; Zolotarev, F.; Shields, J.A. Sector (partial) oculo (dermal) melanocytosis in 89 eyes. *Ophthalmology* **2011**, *118*, 2474-2479.
23. Shields, J.A.; Shields, C.L. *Intraocular tumors: An atlas and textbook*. Lippincott Williams & Wilkins: 2015.
24. Shields, C.L.; Kaliki, S.; Livesey, M.; Walker, B.; Garoon, R.; Bucci, M.; Feinstein, E.; Pesch, A.; Gonzalez, C.; Lally, S.E. Association of ocular and oculodermal melanocytosis with the rate of uveal melanoma metastasis: Analysis of 7872 consecutive eyes. *Jama Ophthalmology* **2013**, *131*, 993-1003.
25. Singh, A.D.; De Potter, P.; Fijal, B.A.; Shields, C.L.; Shields, J.A.; Elston, R.C. Lifetime prevalence of uveal melanoma in white patients with oculo (dermal) melanocytosis. *Ophthalmology* **1998**, *105*, 195-198.
26. Gonder, J.R.; Shields, J.A.; Albert, D.M.; Augsburger, J.J.; Lavin, P.T. Uveal malignant melanoma associated with ocular and oculodermal melanocytosis. *Ophthalmology* **1982**, *89*, 953-960.
27. Frangieh, G.T.; El Baba, F.; Traboulsi, E.I.; Green, W.R. Melanocytoma of the ciliary body: Presentation of four cases and review of nineteen reports. *Survey of ophthalmology* **1985**, *29*, 328-334.
28. Smith, J.H.; Padnick-Silver, L.; Newlin, A.; Rhodes, K.; Rubinstein, W.S. Genetic study of familial uveal melanoma: Association of uveal and cutaneous melanoma with cutaneous and ocular nevi. *Ophthalmology* **2007**, *114*, 774-779.

29. Singh, A.D.; Donoso, L.A.; Jackson, L.; Shields, C.L.; De Potter, P.; Shields, J.A. Familial uveal melanoma: Absence of constitutional cytogenetic abnormalities in 14 cases. *Archives of ophthalmology* **1996**, *114*, 502-503.
30. Smith, L.T.; Irvine, A.R. Diagnostic significance of orange pigment accumulation over choroidal tumors. *Am J Ophthalmol* **1973**, *76*, 212-216.
31. Singh, A.D.; Shields, C.L.; Shields, J.A.; De Potter, P. Bilateral primary uveal melanoma: Bad luck or bad genes? *Ophthalmology* **1996**, *103*, 256-262.
32. Pomeranz, G.A.; Bunt, A.H.; Kalina, R.E. Multifocal choroidal melanoma in ocular melanocytosis. *Archives of Ophthalmology* **1981**, *99*, 857-863.
33. Van Raamsdonk, C.D.; Bezrookove, V.; Green, G.; Bauer, J.; Gaugler, L.; O'Brien, J.M.; Simpson, E.M.; Barsh, G.S.; Bastian, B.C. Frequent somatic mutations of gnaq in uveal melanoma and blue naevi. *Nature* **2009**, *457*, 599-602.
34. Gerami, P.; Pouryazdanparast, P.; Vemula, S.; Bastian, B.C. Molecular analysis of a case of nevus of ota showing progressive evolution to melanoma with intermediate stages resembling cellular blue nevus. *The American journal of dermatopathology* **2010**, *32*, 301-305.
35. Shields, C.L.; Manalac, J.; Das, C.; Ferguson, K.; Shields, J.A. Choroidal melanoma: Clinical features, classification, and top 10 pseudomelanomas. *Current opinion in ophthalmology* **2014**, *25*, 177-185.
36. Abdel-Rahman, M.H.; Pilarski, R.; Cebulla, C.M.; Massengill, J.B.; Christopher, B.N.; Boru, G.; Hovland, P.; Davidorf, F.H. Germline *bap1* mutation predisposes to uveal melanoma, lung adenocarcinoma, meningioma, and other cancers. *Journal of medical genetics* **2011**, *48*, 856-859.
37. Abdel-Rahman, M.H.; Sample, K.M.; Pilarski, R.; Walsh, T.; Grosel, T.; Kinnamon, D.; Boru, G.; Massengill, J.B.; Schoenfield, L.; Kelly, B. Whole exome sequencing identifies candidate genes associated with hereditary predisposition to uveal melanoma. *Ophthalmology* **2020**, *127*, 668-678.
38. Njauw, C.-N.J.; Kim, I.; Piris, A.; Gabree, M.; Taylor, M.; Lane, A.M.; DeAngelis, M.M.; Gragoudas, E.; Duncan, L.M.; Tsao, H. Germline *bap1* inactivation is preferentially associated with metastatic ocular melanoma and cutaneous-ocular melanoma families. *PloS one* **2012**, *7*, e35295.
39. Wiesner, T.; Obenaus, A.C.; Murali, R.; Fried, I.; Griewank, K.G.; Ulz, P.; Windpassinger, C.; Wackernagel, W.; Loy, S.; Wolf, I. Germline mutations in *bap1* predispose to melanocytic tumors. *Nature genetics* **2011**, *43*, 1018-1021.
40. Abdel-Rahman, M.H.; Cebulla, C.M.; Verma, V.; Christopher, B.N.; Carson III, W.E.; Olencki, T.; Davidorf, F.H. Monosomy 3 status of uveal melanoma metastases is associated with rapidly progressive tumors and short survival. *Experimental eye research* **2012**, *100*, 26-31.
41. Buecher, B.; Gauthier-Villars, M.; Desjardins, L.; Lumbroso-Le Rouic, L.; Levy, C.; De Pauw, A.; Bombled, J.; Tirapo, C.; Houdayer, C.; Bressac-de Paillerets, B. Contribution of *cdkn2a/p16 ink4a*, *p14 arf*, *cdk4* and *brca1/2* germline mutations in individuals with suspected genetic predisposition to uveal melanoma. *Familial cancer* **2010**, *9*, 663-667.

42. Easton, D.; Steele, L.; Fields, P.; Ormiston, W.; Averill, D.; Daly, P.; McManus, R.; Neuhausen, S.; Ford, D.; Wooster, R. Cancer risks in two large breast cancer families linked to brca2 on chromosome 13q12-13. *American journal of human genetics* **1997**, *61*, 120.
43. Sinilnikova, O.M.; Egan, K.M.; Quinn, J.L.; Boutrand, L.; Lenoir, G.M.; Stoppa-Lyonnet, D.; Desjardins, L.; Levy, C.; Goldgar, D.; Gragoudas, E.S. Germline brca2 sequence variants in patients with ocular melanoma. *International journal of cancer* **1999**, *82*, 325-328.
44. Cruz, C.; Teule, A.; Caminal, J.M.; Blanco, I.; Piulats, J.M. Uveal melanoma and brca1/brca2 genes: A relationship that needs further investigation. *J Clin Oncol* **2011**, *29*, e827-829.
45. Wooster, R.; Neuhausen, S.L.; Mangion, J.; Quirk, Y.; Ford, D.; Collins, N.; Nguyen, K.; Seal, S.; Tran, T.; Averill, D., *et al.* Localization of a breast cancer susceptibility gene, brca2, to chromosome 13q12-13. *Science* **1994**, *265*, 2088-2090.
46. Li, W.; Judge, H.; Gragoudas, E.S.; Seddon, J.M.; Egan, K.M. Patterns of tumor initiation in choroidal melanoma. *Cancer Research* **2000**, *60*, 3757-3760.
47. Singh, A.D.; Rennie, I.G.; Seregard, S.; Giblin, M.; McKenzie, J. Sunlight exposure and pathogenesis of uveal melanoma. *Surv Ophthalmol* **2004**, *49*, 419-428.
48. Vajdic, C.M.; Kricke, A.; Giblin, M.; McKenzie, J.; Aitken, J.; Giles, G.G.; Armstrong, B.K. Sun exposure predicts risk of ocular melanoma in australia. *Int J Cancer* **2002**, *101*, 175-182.
49. Seddon, J.M.; Gragoudas, E.S.; Glynn, R.J.; Egan, K.M.; Albert, D.M.; Blitzer, P.H. Host factors, uv radiation, and risk of uveal melanoma: A case-control study. *Archives of ophthalmology* **1990**, *108*, 1274-1280.
50. Holly, E.A.; Aston, D.A.; Ahn, D.K.; Smith, A.H. Intraocular melanoma linked to occupations and chemical exposures. *Epidemiology* **1996**, 55-61.
51. Ikehata, H.; Ono, T. The mechanisms of uv mutagenesis. *Journal of radiation research* **2011**, *52*, 115-125.
52. Rivolta, C.; Royer-Bertrand, B.; Rimoldi, D.; Schalenbourg, A.; Zografos, L.; Leyvraz, S.; Moulin, A. Uv light signature in conjunctival melanoma; not only skin should be protected from solar radiation. *Journal of human genetics* **2016**, *61*, 361-362.
53. Royer-Bertrand, B.; Torsello, M.; Rimoldi, D.; El Zaoui, I.; Cisarova, K.; Pescini-Gobert, R.; Raynaud, F.; Zografos, L.; Schalenbourg, A.; Speiser, D. Comprehensive genetic landscape of uveal melanoma by whole-genome sequencing. *The American Journal of Human Genetics* **2016**, *99*, 1190-1198.
54. Van Poppelen, N.M.; Vaarwater, J.; Mudhar, H.S.; Sisley, K.; Rennie, I.G.; Rundle, P.; Brands, T.; Van Den Bosch, Q.C.; Mensink, H.W.; de Klein, A. Genetic background of iris melanomas and iris melanocytic tumors of uncertain malignant potential. *Ophthalmology* **2018**, *125*, 904-912.

55. Wilkerson, C.L.; Syed, N.A.; Fisher, M.R.; Robinson, N.L.; Albert, D.M. Melanocytes and iris color: Light microscopic findings. *Archives of ophthalmology* **1996**, *114*, 437-442.
56. Imesch, P.D.; Wallow, I.H.; Albert, D.M. The color of the human eye: A review of morphologic correlates and of some conditions that affect iridial pigmentation. *Survey of ophthalmology* **1997**, *41*, S117-S123.
57. Imesch, P.D.; Bindley, C.D.; Khademian, Z.; Ladd, B.; Gangnon, R.; Albert, D.M.; Wallow, I.H. Melanocytes and iris color: Electron microscopic findings. *Archives of Ophthalmology* **1996**, *114*, 443-447.
58. Menon, I.A.; Wakeham, D.C.; Persad, S.D.; Avaria, M.; Trope, G.E.; Basu, P.K. Quantitative determination of the melanin contents in ocular tissues from human blue and brown eyes. *Journal of Ocular Pharmacology and Therapeutics* **1992**, *8*, 35-42.
59. Tucker, M.A.; Shields, J.A.; Hartge, P.; Augsburger, J.; Hoover, R.N.; Fraumeni, J.F., Jr. Sunlight exposure as risk factor for intraocular malignant melanoma. *N Engl J Med* **1985**, *313*, 789-792.
60. Damato, B.; Singh, A.D. *Clinical ophthalmic oncology: Uveal tumors*. Springer: 2014.
61. Nickla, D.L.; Wallman, J. The multifunctional choroid. *Progress in retinal and eye research* **2010**, *29*, 144-168.
62. McMenemy, P.G.; Saban, D.R.; Dando, S.J. Immune cells in the retina and choroid: Two different tissue environments that require different defenses and surveillance. *Progress in Retinal and Eye Research* **2019**, *70*, 85-98.
63. Freddo, T.F. A contemporary concept of the blood–aqueous barrier. *Progress in retinal and eye research* **2013**, *32*, 181-195.
64. Damato, E.M.; Damato, B.E. Detection and time to treatment of uveal melanoma in the united kingdom: An evaluation of 2,384 patients. *Ophthalmology* **2012**, *119*, 1582-1589.
65. Arentsen, J.J.; Green, W.R. Melanoma of the iris: Report of 72 cases treated surgically. *Ophthalmic Surg* **1975**, *6*, 23-37.
66. Khan, S.; Finger, P.T.; Yu, G.P.; Razzaq, L.; Jager, M.J.; de Keizer, R.J.; Sandkull, P.; Seregard, S.; Gologorsky, D.; Scheffler, A.C., *et al.* Clinical and pathologic characteristics of biopsy-proven iris melanoma: A multicenter international study. *Arch Ophthalmol* **2012**, *130*, 57-64.
67. Qian, Y.; Zakov, Z.N.; Schoenfield, L.; Singh, A.D. Iris melanoma arising in iris nevus in oculo(dermal) melanocytosis. *Surv Ophthalmol* **2008**, *53*, 411-415.
68. Shields, C.L.; Kaliki, S.; Hutchinson, A.; Nickerson, S.; Patel, J.; Kancherla, S.; Peshtani, A.; Nakhoda, S.; Kocher, K.; Kolbus, E., *et al.* Iris nevus growth into melanoma: Analysis of 1611 consecutive eyes: The abcdef guide. *Ophthalmology* **2013**, *120*, 766-772.
69. McLean, I.W.; Foster, W.D.; Zimmerman, L.E.; Gamel, J.W. Modifications of callender's classification of uveal melanoma at the armed forces institute of pathology. *Am J Ophthalmol* **1983**, *96*, 502-509.

70. McLean, I.W.; Saraiva, V.S.; Burnier Jr, M.N. Pathological and prognostic features of uveal melanomas. *Canadian Journal of Ophthalmology/Journal Canadien d'Ophthalmologie* **2004**, *39*, 343-350.
71. Bastian, B.C. The molecular pathology of melanoma: An integrated taxonomy of melanocytic neoplasia. *Annu Rev Pathol* **2014**, *9*, 239-271.
72. Damato, B.; Duke, C.; Coupland, S.E.; Hiscott, P.; Smith, P.A.; Campbell, I.; Douglas, A.; Howard, P. Cytogenetics of uveal melanoma: A 7-year clinical experience. *Ophthalmology* **2007**, *114*, 1925-1931. e1921.
73. McLean, M.I.W.; Foster, W.D.; Zimmerman, L.E. Prognostic factors in small malignant melanomas of choroid and ciliary body. *Archives of ophthalmology* **1977**, *95*, 48-58.
74. Angi, M.; Damato, B.; Kalirai, H.; Dodson, A.; Taktak, A.; Coupland, S.E. Immunohistochemical assessment of mitotic count in uveal melanoma. *Acta Ophthalmol* **2011**, *89*, e155-160.
75. Kivela, T.; Makitie, T.; Al-Jamal, R.T.; Toivonen, P. Microvascular loops and networks in uveal melanoma. *Can J Ophthalmol* **2004**, *39*, 409-421.
76. Folberg, R.; Mehaffey, M.; Gardner, L.M.; Meyer, M.; Rummelt, V.; Pe'er, J. The microcirculation of choroidal and ciliary body melanomas. *Eye (Lond)* **1997**, *11* (Pt 2), 227-238.
77. Mehaffey, M.G.; Folberg, R.; Meyer, M.; Bentler, S.E.; Hwang, T.; Woolson, R.; Moore, K.C. Relative importance of quantifying area and vascular patterns in uveal melanomas. *Am J Ophthalmol* **1997**, *123*, 798-809.
78. Mehaffey, M.G.; Gardner, L.M.; Folberg, R. Distribution of prognostically important vascular patterns across multiple levels in ciliary body and choroidal melanomas. *Am J Ophthalmol* **1998**, *126*, 373-378.
79. Hendrix, M.J.; Seftor, E.A.; Seftor, R.E.; Gardner, L.M.; Boldt, H.C.; Meyer, M.; Pe'er, J.; Folberg, R. Biologic determinants of uveal melanoma metastatic phenotype: Role of intermediate filaments as predictive markers. *Lab Invest* **1998**, *78*, 153-163.
80. Foss, A.J.; Alexander, R.A.; Jefferies, L.W.; Hungerford, J.L.; Harris, A.L.; Lightman, S. Microvessel count predicts survival in uveal melanoma. *Cancer Res* **1996**, *56*, 2900-2903.
81. Folberg, R.; Bernardino, V.B., Jr.; Aguilar, G.L.; Shannon, G.M. Amputation neuroma mistaken for recurrent melanoma in the orbit. *Ophthalmic Surg* **1981**, *12*, 275-278.
82. Daniels, K.J.; Boldt, H.C.; Martin, J.A.; Gardner, L.M.; Meyer, M.; Folberg, R. Expression of type vi collagen in uveal melanoma: Its role in pattern formation and tumor progression. *Lab Invest* **1996**, *75*, 55-66.
83. Weidner, N.; Semple, J.P.; Welch, W.R.; Folkman, J. Tumor angiogenesis and metastasis--correlation in invasive breast carcinoma. *N Engl J Med* **1991**, *324*, 1-8.
84. Weidner, N. Intratumor microvessel density as a prognostic factor in cancer. *Am J Pathol* **1995**, *147*, 9-19.

85. Sakamoto, H. [cancer cells; its characteristics and behavior]. *Nihon Sanka Fujinka Gakkai Zasshi* **1996**, *48*, 683-688.
86. Bronkhorst, I.H.; Ly, L.V.; Jordanova, E.S.; Vrolijk, J.; Versluis, M.; Luyten, G.P.; Jager, M.J. Detection of m2-macrophages in uveal melanoma and relation with survival. *Investigative ophthalmology & visual science* **2011**, *52*, 643-650.
87. Whelchel, J.C.; Farah, S.E.; McLean, I.W.; Burnier, M.N. Immunohistochemistry of infiltrating lymphocytes in uveal malignant melanoma. *Investigative ophthalmology & visual science* **1993**, *34*, 2603-2606.
88. De Cruz Jr, P.O.L.; Specht, C.S.; McLean, I.W. Lymphocytic infiltration in uveal malignant melanoma. *Cancer* **1990**, *65*, 112-115.
89. Streilein, J.W. Ocular immune privilege: Therapeutic opportunities from an experiment of nature. *Nature Reviews Immunology* **2003**, *3*, 879-889.
90. Mantovani, A.; Sozzani, S.; Locati, M.; Allavena, P.; Sica, A. Macrophage polarization: Tumor-associated macrophages as a paradigm for polarized m2 mononuclear phagocytes. *Trends in immunology* **2002**, *23*, 549-555.
91. Krishna, Y.; McCarthy, C.; Kalirai, H.; Coupland, S.E.J.H.p. Inflammatory cell infiltrates in advanced metastatic uveal melanoma. **2017**, *66*, 159-166.
92. Coupland, S.E.; Lake, S.L.; Zeschnigk, M.; Damato, B.E. Molecular pathology of uveal melanoma. *Eye (Lond)* **2013**, *27*, 230-242.
93. Prescher, G.; Bornfeld, N.; Hirche, H.; Horsthemke, B.; Jockel, K.H.; Becher, R. Prognostic implications of monosomy 3 in uveal melanoma. *Lancet* **1996**, *347*, 1222-1225.
94. Tschentscher, F.; Prescher, G.; Horsman, D.E.; White, V.A.; Rieder, H.; Anastassiou, G.; Schilling, H.; Bornfeld, N.; Bartz-Schmidt, K.U.; Horsthemke, B., *et al.* Partial deletions of the long and short arm of chromosome 3 point to two tumor suppressor genes in uveal melanoma. *Cancer Res* **2001**, *61*, 3439-3442.
95. Schoenfield, L.; Pettay, J.; Tubbs, R.R.; Singh, A.D. Variation of monosomy 3 status within uveal melanoma. *Arch Pathol Lab Med* **2009**, *133*, 1219-1222.
96. Scholes, A.G.; Damato, B.E.; Nunn, J.; Hiscott, P.; Grierson, I.; Field, J.K. Monosomy 3 in uveal melanoma: Correlation with clinical and histologic predictors of survival. *Invest Ophthalmol Vis Sci* **2003**, *44*, 1008-1011.
97. Harbour, J.W.; Onken, M.D.; Roberson, E.D.; Duan, S.; Cao, L.; Worley, L.A.; Council, M.L.; Matatall, K.A.; Helms, C.; Bowcock, A.M. Frequent mutation of bap1 in metastasizing uveal melanomas. *Science* **2010**, *330*, 1410-1413.
98. Kilic, E.; van Gils, W.; Lodder, E.; Beverloo, H.B.; van Til, M.E.; Mooy, C.M.; Paridaens, D.; de Klein, A.; Luyten, G.P. Clinical and cytogenetic analyses in uveal melanoma. *Invest Ophthalmol Vis Sci* **2006**, *47*, 3703-3707.
99. Damato, B.; Dopierala, J.A.; Coupland, S.E. Genotypic profiling of 452 choroidal melanomas with multiplex ligation-dependent probe amplification. *Clin Cancer Res* **2010**, *16*, 6083-6092.

100. Onken, M.D.; Worley, L.A.; Harbour, J.W. A metastasis modifier locus on human chromosome 8p in uveal melanoma identified by integrative genomic analysis. *Clin Cancer Res* **2008**, *14*, 3737-3745.
101. Werdich, X.Q.; Jakobiec, F.A.; Singh, A.D.; Kim, I.K. A review of advanced genetic testing for clinical prognostication in uveal melanoma. *Seminars in Ophthalmology* **2013**, *28*, 361-371.
102. Kaliki, S.; Shields, C.L.; Shields, J.A. Uveal melanoma: Estimating prognosis. *Indian journal of ophthalmology* **2015**, *63*, 93.
103. Hausler, T.; Stang, A.; Anastassiou, G.; Jockel, K.H.; Mrzyk, S.; Horsthemke, B.; Lohmann, D.R.; Zeschnigk, M. Loss of heterozygosity of 1p in uveal melanomas with monosomy 3. *Int J Cancer* **2005**, *116*, 909-913.
104. Parrella, P.; Sidransky, D.; Merbs, S.L. Allelotype of posterior uveal melanoma. *Implications for a Bifurcated Tumor Progression Pathway* **1999**, *59*, 3032-3037.
105. Damato, B.; Dopierala, J.; Klaasen, A.; van Dijk, M.; Sibbring, J.; Coupland, S.E. Multiplex ligation-dependent probe amplification of uveal melanoma: Correlation with metastatic death. *Invest Ophthalmol Vis Sci* **2009**, *50*, 3048-3055.
106. Ehlers, J.P.; Worley, L.; Onken, M.D.; Harbour, J.W. Integrative genomic analysis of aneuploidy in uveal melanoma. *Clin Cancer Res* **2008**, *14*, 115-122.
107. Onken, M.D.; Worley, L.A.; Long, M.D.; Duan, S.; Council, M.L.; Bowcock, A.M.; Harbour, J.W. Oncogenic mutations in gnaq occur early in uveal melanoma. *Investigative ophthalmology & visual science* **2008**, *49*, 5230-5234.
108. Van Raamsdonk, C.D.; Griewank, K.G.; Crosby, M.B.; Garrido, M.C.; Vemula, S.; Wiesner, T.; Obenaus, A.C.; Wackernagel, W.; Green, G.; Bouvier, N. Mutations in gna11 in uveal melanoma. *New England Journal of Medicine* **2010**, *363*, 2191-2199.
109. Dono, M.; Angelini, G.; Cecconi, M.; Amaro, A.; Esposito, A.I.; Mirisola, V.; Maric, I.; Lanza, F.; Nasciuti, F.; Viaggi, S., *et al.* Mutation frequencies of gnaq, gna11, bap1, sf3b1, eif1ax and tert in uveal melanoma: Detection of an activating mutation in the tert gene promoter in a single case of uveal melanoma. *Br J Cancer* **2014**, *110*, 1058-1065.
110. Staby, K.M.; Gravdal, K.; Mørk, S.J.; Heegaard, S.; Vintermyr, O.K.; Krohn, J. Prognostic impact of chromosomal aberrations and gnaq, gna 11 and bap 1 mutations in uveal melanoma. *Acta Ophthalmologica* **2018**, *96*, 31-38.
111. Golas, M.M.; Sander, B.; Will, C.L.; Lührmann, R.; Stark, H. Molecular architecture of the multiprotein splicing factor sf3b. *Science* **2003**, *300*, 980-984.
112. Harbour, J.W. Genomic, prognostic, and cell-signaling advances in uveal melanoma. *Am Soc Clin Oncol Educ Book* **2013**, 388-391.
113. Martin, M.; Maßhöfer, L.; Temming, P.; Rahmann, S.; Metz, C.; Bornfeld, N.; van de Nes, J.; Klein-Hitpass, L.; Hinnebusch, A.G.; Horsthemke, B., *et al.* Exome sequencing identifies recurrent somatic mutations in eif1ax and sf3b1 in uveal melanoma with disomy 3. *Nat Genet* **2013**, *45*, 933-936.

114. Ewens, K.G.; Kanetsky, P.A.; Richards-Yutz, J.; Purrazzella, J.; Shields, C.L.; Ganguly, T.; Ganguly, A. Chromosome 3 status combined with *bap1* and *eif1ax* mutation profiles are associated with metastasis in uveal melanoma. *Invest Ophthalmol Vis Sci* **2014**, *55*, 5160-5167.
115. Ventii, K.H.; Devi, N.S.; Friedrich, K.L.; Chernova, T.A.; Tighiouart, M.; Van Meir, E.G.; Wilkinson, K.D. *Brcal*-associated protein-1 is a tumor suppressor that requires deubiquitinating activity and nuclear localization. *Cancer Res* **2008**, *68*, 6953-6962.
116. Koopmans, A.E.; Verdijk, R.M.; Brouwer, R.W.; van den Bosch, T.P.; van den Berg, M.M.; Vaarwater, J.; Kockx, C.E.; Paridaens, D.; Naus, N.C.; Nellist, M., *et al.* Clinical significance of immunohistochemistry for detection of *bap1* mutations in uveal melanoma. *Mod Pathol* **2014**, *27*, 1321-1330.
117. Farquhar, N.; Thornton, S.; Coupland, S.E.; Coulson, J.M.; Sacco, J.J.; Krishna, Y.; Heimann, H.; Taktak, A.; Cebulla, C.M.; Abdel-Rahman, M.H., *et al.* Patterns of *bap1* protein expression provide insights into prognostic significance and the biology of uveal melanoma. *J Pathol Clin Res* **2018**, *4*, 26-38.
118. Kalirai, H.; Dodson, A.; Faqir, S.; Damato, B.E.; Coupland, S.E. Lack of *bap1* protein expression in uveal melanoma is associated with increased metastatic risk and has utility in routine prognostic testing. *Br J Cancer* **2014**, *111*, 1373-1380.
119. Figueiredo, C.R.; Kalirai, H.; Sacco, J.J.; Azevedo, R.A.; Duckworth, A.; Slupsky, J.R.; Coulson, J.M.; Coupland, S.E. Loss of *bap1* expression is associated with an immunosuppressive microenvironment in uveal melanoma, with implications for immunotherapy development. *J Pathol* **2020**, *250*, 420-439.
120. Smit, K.N.; van Poppel, N.M.; Vaarwater, J.; Verdijk, R.; van Marion, R.; Kalirai, H.; Coupland, S.E.; Thornton, S.; Farquhar, N.; Dubbink, H.J., *et al.* Combined mutation and copy-number variation detection by targeted next-generation sequencing in uveal melanoma. *Mod Pathol* **2018**, *31*, 763-771.
121. Thornton, S.; Coupland, S.E.; Olohan, L.; Sibbring, J.S.; Kenny, J.G.; Hertz-Fowler, C.; Liu, X.; Haldenby, S.; Heimann, H.; Hussain, R. Targeted next-generation sequencing of 117 routine clinical samples provides further insights into the molecular landscape of uveal melanoma. *Cancers* **2020**, *12*, 1039.
122. Robertson, A.G.; Shih, J.; Yau, C.; Gibb, E.A.; Oba, J.; Mungall, K.L.; Hess, J.M.; Uzunangelov, V.; Walter, V.; Danilova, L. Integrative analysis identifies four molecular and clinical subsets in uveal melanoma. *Cancer cell* **2017**, *32*, 204-220. e215.
123. Caines, R.; Eleuteri, A.; Kalirai, H.; Fisher, A.C.; Heimann, H.; Damato, B.E.; Coupland, S.E.; Taktak, A.F. Cluster analysis of multiplex ligation-dependent probe amplification data in choroidal melanoma. *Molecular vision* **2015**, *21*, 1.
124. Onken, M.D.; Worley, L.A.; Ehlers, J.P.; Harbour, J.W. Gene expression profiling in uveal melanoma reveals two molecular classes and predicts metastatic death. *Cancer Res* **2004**, *64*, 7205-7209.
125. Harbour, J.W. A prognostic test to predict the risk of metastasis in uveal melanoma based on a 15-gene expression profile. *Methods Mol Biol* **2014**, *1102*, 427-440.
126. Onken, M.D.; Worley, L.A.; Char, D.H.; Augsburger, J.J.; Correa, Z.M.; Nudleman, E.; Aaberg Jr, T.M.; Altaweel, M.M.; Bardenstein, D.S.; Finger, P.T. Collaborative ocular

- oncology group report number 1: Prospective validation of a multi-gene prognostic assay in uveal melanoma. *Ophthalmology* **2012**, *119*, 1596-1603.
127. Singh, A.D.; Damato, B.E. *Clinical ophthalmic oncology: Basic principles*. Springer: 2019.
 128. Tarlan, B.; Kiratli, H. Uveal melanoma: Current trends in diagnosis and management. *Turk J Ophthalmol* **2016**, *46*, 123-137.
 129. Eskelin, S.; Kivela, T. Mode of presentation and time to treatment of uveal melanoma in finland. *Br J Ophthalmol* **2002**, *86*, 333-338.
 130. Diener-West, M.; Earle, J.; Fine, S.; Hawkins, B.; Moy, C.; Reynolds, S.; Schachat, A.; Straatsma, B. The coms randomized trial of iodine 125 brachytherapy for choroidal melanoma, ii: Characteristics of patients enrolled and not enrolled. Coms report no. 17. *Archives of ophthalmology (Chicago, Ill.: 1960)* **2001**, *119*, 951-965.
 131. Bagger, M.; Andersen, M.T.; Andersen, K.K.; Heegaard, S.; Andersen, M.K.; Kiilgaard, J.F. The prognostic effect of american joint committee on cancer staging and genetic status in patients with choroidal and ciliary body melanoma. *Investigative ophthalmology & visual science* **2015**, *56*, 438-444.
 132. Kujala, E.; Makitie, T.; Kivela, T. Very long-term prognosis of patients with malignant uveal melanoma. *Invest Ophthalmol Vis Sci* **2003**, *44*, 4651-4659.
 133. Damato, B.E.; Heimann, H.; Kalirai, H.; Coupland, S.E. Age, survival predictors, and metastatic death in patients with choroidal melanoma: Tentative evidence of a therapeutic effect on survival. *JAMA Ophthalmol* **2014**, *132*, 605-613.
 134. Lommatzsch, P. Treatment of choroidal melanomas with 106ru/106rh beta-ray applicators. *Surv Ophthalmol* **1974**, *19*, 85-100.
 135. Astrahan, M.A.; Luxton, G.; Jozsef, G.; Kampp, T.D.; Liggett, P.E.; Sapozink, M.D.; Petrovich, Z. An interactive treatment planning system for ophthalmic plaque radiotherapy. *International Journal of Radiation Oncology* Biology* Physics* **1990**, *18*, 679-687.
 136. Stannard, C.; Sauerwein, W.; Maree, G.; Lecuona, K. Radiotherapy for ocular tumours. *Eye (Lond)* **2013**, *27*, 119-127.
 137. Brasiuniene, B.; Sokolovas, V.; Brasiunas, V.; Barakauskiene, A.; Strupas, K. Combined treatment of uveal melanoma liver metastases. *Eur J Med Res* **2011**, *16*, 71-75.
 138. Damato, B. Does ocular treatment of uveal melanoma influence survival? *British journal of cancer* **2010**, *103*, 285-290.
 139. Hussain, R.N.; Coupland, S.E.; Kalirai, H.; Taktak, A.F.; Eleuteri, A.; Damato, B.E.; Groenewald, C.; Heimann, H.J.C. Small high-risk uveal melanomas have a lower mortality rate. **2021**, *13*, 2267.
 140. Ardjomand, N.; Komericki, P.; Langmann, G.; Mattes, D.; Moray, M.; Scarpatetti, M.; El-Shabrawi, Y. Lymph node metastases arising from uveal melanoma. *Wiener klinische Wochenschrift* **2005**, *117*, 433-435.

141. Torres, V.; Triozzi, P.; Eng, C.; Tubbs, R.; Schoenfield, L.; Crabb, J.W.; Sauntharajah, Y.; Singh, A.D. Circulating tumor cells in uveal melanoma. *Future Oncology* **2011**, *7*, 101-109.
142. Piris, A.; Mihm, M.C., Jr. Mechanisms of metastasis: Seed and soil. *Cancer Treat Res* **2007**, *135*, 119-127.
143. Diener-West, M.; Reynolds, S.M.; Agugliaro, D.J.; Caldwell, R.; Cumming, K.; Earle, J.D.; Green, D.L.; Hawkins, B.S.; Hayman, J.; Jaiyesimi, I. Screening for metastasis from choroidal melanoma: The collaborative ocular melanoma study group report 23. *Journal of clinical oncology* **2004**, *22*, 2438-2444.
144. Singh, A.D. Uveal melanoma: Implications of tumor doubling time. *Ophthalmology* **2001**, *108*, 829-831.
145. Eskelin, S.; Pyrhonen, S.; Summanen, P.; Hahka-Kemppinen, M.; Kivela, T. Tumor doubling times in metastatic malignant melanoma of the uvea: Tumor progression before and after treatment. *Ophthalmology* **2000**, *107*, 1443-1449.
146. Damato, B.E.; Dukes, J.; Goodall, H.; Carvajal, R.D. Tebentafusp: T cell redirection for the treatment of metastatic uveal melanoma. *Cancers (Basel)* **2019**, *11*.
147. Albert, D.M.; Ryan, L.M.; Borden, E.C. Metastatic ocular and cutaneous melanoma: A comparison of patient characteristics and prognosis. *Arch Ophthalmol* **1996**, *114*, 107-108.
148. Bedikian, A.Y.; Legha, S.S.; Mavligit, G.; Carrasco, C.H.; Khorana, S.; Plager, C.; Papadopoulos, N.; Benjamin, R.S. Treatment of uveal melanoma metastatic to the liver: A review of the m. D. Anderson cancer center experience and prognostic factors. *Cancer* **1995**, *76*, 1665-1670.
149. Rajpal, S.; Moore, R.; Karakousis, C.P. Survival in metastatic ocular melanoma. *Cancer* **1983**, *52*, 334-336.
150. Lorigan, J.G.; Wallace, S.; Mavligit, G.M. The prevalence and location of metastases from ocular melanoma: Imaging study in 110 patients. *AJR Am J Roentgenol* **1991**, *157*, 1279-1281.
151. Coupland, S.E.; Sidiki, S.; Clark, B.J.; McClaren, K.; Kyle, P.; Lee, W.R. Metastatic choroidal melanoma to the contralateral orbit 40 years after enucleation. *Arch Ophthalmol* **1996**, *114*, 751-756.
152. Kivelä, T.; Kujala, E. Prognostication in eye cancer: The latest tumor, node, metastasis classification and beyond. *Eye* **2013**, *27*, 243-252.
153. Callejo, S.A.; Dopierala, J.; Coupland, S.E.; Damato, B. Sudden growth of a choroidal melanoma and multiplex ligation-dependent probe amplification findings suggesting late transformation to monosomy 3 type. *Arch Ophthalmol* **2011**, *129*, 958-960.
154. Mariani, P.; Piperno-Neumann, S.; Servois, V.; Berry, M.; Dorval, T.; Plancher, C.; Couturier, J.; Levy-Gabriel, C.; Lumbroso-Le Rouic, L.; Desjardins, L.J.E.J.o.S.O. Surgical management of liver metastases from uveal melanoma: 16 years' experience at the institut curie. **2009**, *35*, 1192-1197.
155. Fountain, E.; Bassett, R.L.; Cain, S.; Posada, L.; Gombos, D.S.; Hwu, P.; Bedikian, A.; Patel, S.P.J.C. Adjuvant ipilimumab in high-risk uveal melanoma. **2019**, *11*, 152.

156. Nathan, P.; Hassel, J.C.; Rutkowski, P.; Baurain, J.F.; Butler, M.O.; Schlaak, M.; Sullivan, R.J.; Ochsenreither, S.; Dummer, R.; Kirkwood, J.M., *et al.* Overall survival benefit with tebentafusp in metastatic uveal melanoma. *N Engl J Med* **2021**, *385*, 1196-1206.
157. Piulats, J.M.; Espinosa, E.; de la Cruz Merino, L.; Varela, M.; Alonso Carrión, L.; Martín-Algarra, S.; López Castro, R.; Curiel, T.; Rodríguez-Abreu, D.; Redrado, M., *et al.* Nivolumab plus ipilimumab for treatment-naïve metastatic uveal melanoma: An open-label, multicenter, phase ii trial by the spanish multidisciplinary melanoma group (gem-1402). *J Clin Oncol* **2021**, *39*, 586-598.
158. Eskelin, S.; Pyrhonen, S.; Summanen, P.; Prause, J.U.; Kivela, T. Screening for metastatic malignant melanoma of the uvea revisited. *Cancer* **1999**, *85*, 1151-1159.
159. Diener-West, M.; Reynolds, S.M.; Agugliaro, D.J.; Caldwell, R.; Cumming, K.; Earle, J.D.; Green, D.L.; Hawkins, B.S.; Hayman, J.; Jaiyesimi, I., *et al.* Screening for metastasis from choroidal melanoma: The collaborative ocular melanoma study group report 23. *J Clin Oncol* **2004**, *22*, 2438-2444.
160. Mouriaux, F.; Diorio, C.; Bergeron, D.; Berchi, C.; Rousseau, A. Liver function testing is not helpful for early diagnosis of metastatic uveal melanoma. *Ophthalmology* **2012**, *119*, 1590-1595.
161. Gombos, D.S.; Van Quill, K.R.; Uusitalo, M.; O'Brien, J.M. Geographic disparities in diagnostic screening for metastatic uveal melanoma. *Ophthalmology* **2004**, *111*, 2254-2258.
162. Triozzi, P.L.; Singh, A.D. Blood biomarkers for uveal melanoma. *Future Oncol* **2012**, *8*, 205-215.
163. Rietschel, P.; Panageas, K.S.; Hanlon, C.; Patel, A.; Abramson, D.H.; Chapman, P.B. Variates of survival in metastatic uveal melanoma. *J Clin Oncol* **2005**, *23*, 8076-8080.
164. Kim, I.K.; Lane, A.M.; Gragoudas, E.S. Survival in patients with presymptomatic diagnosis of metastatic uveal melanoma. *Arch Ophthalmol* **2010**, *128*, 871-875.
165. Eskelin, S.; Kivela, T. Imaging to detect metastases from malignant uveal melanoma. *Arch Ophthalmol* **2002**, *120*, 676.
166. Choudhary, M.; Gupta, A.; Bena, J.; Singh, A.J.I.O.; Science, V. Systemic surveillance for metastases in patients with uveal melanoma. **2013**, *54*, 4227-4227.
167. Patel, M.; Winston, C.B.; Marr, B.P.; Carvajal, R.D.; Schwartz, G.K.; Wolchok, J.; Busam, K.; Abramson, D.H. Characterization of computed tomography scan abnormalities in patients with biopsy-proven hepatic metastases from uveal melanoma. *Archives of Ophthalmology* **2011**, *129*, 1576-1582.
168. Antoch, G.; Vogt, F.M.; Freudenberg, L.S.; Nazaradeh, F.; Goehde, S.C.; Barkhausen, J.; Dahmen, G.; Bockisch, A.; Debatin, J.F.; Ruehm, S.G.J.J. Whole-body dual-modality pet/ct and whole-body mri for tumor staging in oncology. **2003**, *290*, 3199-3206.

169. Marshall, E.; Romaniuk, C.; Ghaneh, P.; Wong, H.; McKay, M.; Chopra, M.; Coupland, S.E.; Damato, B.E. Mri in the detection of hepatic metastases from high-risk uveal melanoma: A prospective study in 188 patients. *Br J Ophthalmol* **2013**, *97*, 159-163.
170. Balasubramanya, R.; Selvarajan, S.K.; Cox, M.; Joshi, G.; Deshmukh, S.; Mitchell, D.G.; O'Kane, P. Imaging of ocular melanoma metastasis. *Br J Radiol* **2016**, *89*, 20160092.
171. Singh, A.; Shields, C.; Shields, J. Prognostic factors in uveal melanoma. *Melanoma research* **2001**, *11*, 255-263.
172. Kohn, E.C.; Liotta, L.A. Molecular insights into cancer invasion: Strategies for prevention and intervention. *Cancer Res* **1995**, *55*, 1856-1862.
173. Donoso, L.A.; Shields, J.A.; Augsburger, J.J.; Orth, D.H.; Johnson, P. Metastatic uveal melanoma: Diffuse hepatic metastasis in a patient with concurrent normal serum liver enzyme levels and liver scan. *Arch Ophthalmol* **1985**, *103*, 758.
174. Seddon, J.M.; Polivogianis, L.; Hsieh, C.C.; Albert, D.M.; Gamel, J.W.; Gragoudas, E.S. Death from uveal melanoma. Number of epithelioid cells and inverse sd of nucleolar area as prognostic factors. *Arch Ophthalmol* **1987**, *105*, 801-806.
175. Kath, R.; Hayungs, J.; Bornfeld, N.; Sauerwein, W.; Hoffken, K.; Seeber, S. Prognosis and treatment of disseminated uveal melanoma. *Cancer* **1993**, *72*, 2219-2223.
176. Hsueh, E.C.; Essner, R.; Foshag, L.J.; Ye, X.; Wang, H.J.; Morton, D.L. Prolonged survival after complete resection of metastases from intraocular melanoma. *Cancer: Interdisciplinary International Journal of the American Cancer Society* **2004**, *100*, 122-129.
177. Aoyama, T.; Mastrangelo, M.J.; Berd, D.; Nathan, F.E.; Shields, C.L.; Shields, J.A.; Rosato, E.L.; Rosato, F.E.; Sato, T. Protracted survival after resection of metastatic uveal melanoma. *Cancer: Interdisciplinary International Journal of the American Cancer Society* **2000**, *89*, 1561-1568.
178. Ben-Shabat, I.; Belgrano, V.; Ny, L.; Nilsson, J.; Lindnér, P.; Bagge, R.O. Long-term follow-up evaluation of 68 patients with uveal melanoma liver metastases treated with isolated hepatic perfusion. *Annals of surgical oncology* **2016**, *23*, 1327-1334.
179. Karydis, I.; Gangi, A.; Wheeler, M.J.; Choi, J.; Wilson, I.; Thomas, K.; Pearce, N.; Takhar, A.; Gupta, S.; Hardman, D. Percutaneous hepatic perfusion with melphalan in uveal melanoma: A safe and effective treatment modality in an orphan disease. *Journal of surgical oncology* **2018**, *117*, 1170-1178.
180. Valpione, S.; Aliberti, C.; Parrozzani, R.; Bazzi, M.; Pigozzo, J.; Midena, E.; Pilati, P.; Campana, L.G.; Chiarion-Sileni, V. A retrospective analysis of 141 patients with liver metastases from uveal melanoma: A two-cohort study comparing transarterial chemoembolization with cpt-11 charged microbeads and historical treatments. *Melanoma research* **2015**, *25*, 164-168.
181. Zell, J.A.; Cinar, P.; Mobasher, M.; Ziogas, A.; Meyskens Jr, F.L.; Anton-Culver, H. Survival for patients with invasive cutaneous melanoma among ethnic groups: The effects of socioeconomic status and treatment. *Journal of clinical oncology: official journal of the American Society of Clinical Oncology* **2008**, *26*, 66-675.

182. Pyrhönen, S. The treatment of metastatic uveal melanoma. *European Journal of Cancer* **1998**, *34*, 27-30.
183. Rivoire, M.; Kodjikian, L.; Baldo, S.; Kaemmerlen, P.; Négrier, S.; Grange, J.-D. Treatment of liver metastases from uveal melanoma. *Annals of surgical oncology* **2005**, *12*, 422-428.
184. Pyrhonen, S. The treatment of metastatic uveal melanoma. *Eur J Cancer* **1998**, *34 Suppl 3*, S27-30.
185. Kivela, T.; Suciú, S.; Hansson, J.; Kruit, W.H.; Vuoristo, M.S.; Kloke, O.; Gore, M.; Hahka-Kemppinen, M.; Parvinen, L.M.; Kumpulainen, E., *et al.* Bleomycin, vincristine, lomustine and dacarbazine (bold) in combination with recombinant interferon alpha-2b for metastatic uveal melanoma. *Eur J Cancer* **2003**, *39*, 1115-1120.
186. Augsburger, J.J.; Correa, Z.M.; Shaikh, A.H. Effectiveness of treatments for metastatic uveal melanoma. *Am J Ophthalmol* **2009**, *148*, 119-127.
187. Whitehead, J.; Tishkovskaya, S.; O'Connor, J.; Damato, B. Devising two-stage and multistage phase ii studies on systemic adjuvant therapy for uveal melanoma. *Invest Ophthalmol Vis Sci* **2012**, *53*, 4986-4989.
188. Pfohler, C.; Cree, I.A.; Ugurel, S.; Kuwert, C.; Haass, N.; Neuber, K.; Hengge, U.; Corrie, P.G.; Zutt, M.; Tilgen, W., *et al.* Treosulfan and gemcitabine in metastatic uveal melanoma patients: Results of a multicenter feasibility study. *Anticancer Drugs* **2003**, *14*, 337-340.
189. Khalil, D.N.; Smith, E.L.; Brentjens, R.J.; Wolchok, J.D. The future of cancer treatment: Immunomodulation, cars and combination immunotherapy. *Nat Rev Clin Oncol* **2016**, *13*, 273-290.
190. Singh, A.D.; Borden, E.C. Metastatic uveal melanoma. *Ophthalmol Clin North Am* **2005**, *18*, 143-150, ix.
191. Keilholz, U.; Scheibenbogen, C.; Brado, M.; Georgi, P.; Maclachlan, D.; Brado, B.; Hunstein, W. Regional adoptive immunotherapy with interleukin-2 and lymphokine-activated killer (lak) cells for liver metastases. *Eur J Cancer* **1994**, *30A*, 103-105.
192. Hodi, F.S.; O'Day, S.J.; McDermott, D.F.; Weber, R.W.; Sosman, J.A.; Haanen, J.B.; Gonzalez, R.; Robert, C.; Schadendorf, D.; Hassel, J.C., *et al.* Improved survival with ipilimumab in patients with metastatic melanoma. *N Engl J Med* **2010**, *363*, 711-723.
193. Heppt, M.V.; Steeb, T.; Schlager, J.G.; Rosumeck, S.; Dressler, C.; Ruzicka, T.; Nast, A.; Berking, C. Immune checkpoint blockade for unresectable or metastatic uveal melanoma: A systematic review. *Cancer Treat Rev* **2017**, *60*, 44-52.
194. Heppt, M.V.; Amaral, T.; Kähler, K.C.; Heinzerling, L.; Hassel, J.C.; Meissner, M.; Kreuzberg, N.; Loquai, C.; Reinhardt, L.; Utikal, J. Combined immune checkpoint blockade for metastatic uveal melanoma: A retrospective, multi-center study. *Journal for immunotherapy of cancer* **2019**, *7*, 299.
195. Sato, T.; Nathan, P.D.; Hernandez-Aya, L.; Sacco, J.J.; Orloff, M.M.; Visich, J.; Little, N.; Hulstine, A.-M.; Coughlin, C.M.; Carvajal, R.D. Redirected t cell lysis in patients with metastatic uveal melanoma with gp100-directed tcr imcgp100: Overall survival findings. American Society of Clinical Oncology: 2018.

196. Middleton, M.R.; Steven, N.M.; Evans, T.J.; Infante, J.R.; Sznol, M.; Mulatero, C.; Hamid, O.; Shoushtari, A.N.; Shingler, W.; Johnson, A. Safety, pharmacokinetics and efficacy of imcgp100, a first-in-class soluble tcr-antid3 bispecific t cell redirector with solid tumour activity: Results from the fih study in melanoma. *American Society of Clinical Oncology*: 2016.
197. Sacco, J.; Carvajal, R.; Butler, M.; Shoushtari, A.; Hassel, J.; Ikeguchi, A.; Hernandez-Aya, L.; Nathan, P.; Hamid, O.; Rodriguez, J.P.J.A.o.O. 64mo a phase (ph) ii, multi-center study of the safety and efficacy of tebentafusp (tebe)(imcgp100) in patients (pts) with metastatic uveal melanoma (mum). **2020**, *31*, S1442-S1443.
198. Chandran, S.S.; Somerville, R.P.T.; Yang, J.C.; Sherry, R.M.; Klebanoff, C.A.; Goff, S.L.; Wunderlich, J.R.; Danforth, D.N.; Zlott, D.; Paria, B.C., *et al.* Treatment of metastatic uveal melanoma with adoptive transfer of tumour-infiltrating lymphocytes: A single-centre, two-stage, single-arm, phase 2 study. *Lancet Oncol* **2017**, *18*, 792-802.
199. Bosch, J.J.; Iheagwara, U.K.; Reid, S.; Srivastava, M.K.; Wolf, J.; Lotem, M.; Ksander, B.R.; Ostrand-Rosenberg, S. Uveal melanoma cell-based vaccines express mhc ii molecules that traffic via the endocytic and secretory pathways and activate cd8+ cytotoxic, tumor-specific t cells. *Cancer Immunol Immunother* **2010**, *59*, 103-112.
200. Brovkina, A.F.; Keshelava, V.V.; Sologub, V.K.; Koromyslova, I.K.; Severin, S.E.; Barannikova, T.V. [live xenogenic vaccine in the prevention of metastases of uveal melanoma]. *Vestn Oftalmol* **2009**, *125*, 46-50.
201. Triozzi, P.L.; Eng, C.; Singh, A.D. Targeted therapy for uveal melanoma. *Cancer Treat Rev* **2008**, *34*, 247-258.
202. Mariani, P.; Servois, V.; Piperno-Neumann, S. Therapeutic options in metastatic uveal melanoma. *Dev Ophthalmol* **2012**, *49*, 166-181.
203. Fournier, G.A.; Albert, D.M.; Arrigg, C.A.; Cohen, A.M.; Lamping, K.A.; Seddon, J.M. Resection of solitary metastasis. Approach to palliative treatment of hepatic involvement with choroidal melanoma. *Arch Ophthalmol* **1984**, *102*, 80-82.
204. Frenkel, S.; Nir, I.; Hendler, K.; Lotem, M.; Eid, A.; Jurim, O.; Pe'er, J. Long-term survival of uveal melanoma patients after surgery for liver metastases. *Br J Ophthalmol* **2009**, *93*, 1042-1046.
205. Salmon, R.; Levy, C.; Plancher, C.; Dorval, T.; Desjardins, L.; Leyvrazi, S.; Pouillart, P.; Schlienger, P.; Servois, V.; Asselain, B.J.E.J.o.S.O. Treatment of liver metastases from uveal melanoma by combined surgery—chemotherapy. **1998**, *24*, 127-130.
206. Lieberman, S.; Goldin, E.; Lotem, M.; Bloom, A.I. Irrigation of the bile ducts with chilled saline during percutaneous radiofrequency ablation of a hepatic ocular melanoma metastasis. *AJR Am J Roentgenol* **2004**, *183*, 596-598.
207. Sato, T.; Eschelman, D.J.; Gonsalves, C.F.; Terai, M.; Chervoneva, I.; McCue, P.A.; Shields, J.A.; Shields, C.L.; Yamamoto, A.; Berd, D., *et al.* Immunoembolization of malignant liver tumors, including uveal melanoma, using granulocyte-macrophage colony-stimulating factor. *J Clin Oncol* **2008**, *26*, 5436-5442.

208. Yamamoto, A.; Chervoneva, I.; Sullivan, K.L.; Eschelmann, D.J.; Gonsalves, C.F.; Mastrangelo, M.J.; Berd, D.; Shields, J.A.; Shields, C.L.; Terai, M., *et al.* High-dose immunoembolization: Survival benefit in patients with hepatic metastases from uveal melanoma. *Radiology* **2009**, *252*, 290-298.
209. Varghese, S.; Xu, H.; Bartlett, D.; Hughes, M.; Pingpank, J.F.; Beresnev, T.; Alexander, H.R. Isolated hepatic perfusion with high-dose melphalan results in immediate alterations in tumor gene expression in patients with metastatic ocular melanoma. *Annals of surgical oncology* **2010**, *17*, 1870-1877.
210. Alexander, H.R.; Libutti, S.K.; Pingpank, J.F.; Steinberg, S.M.; Bartlett, D.L.; Helsabeck, C.; Beresneva, T. Hyperthermic isolated hepatic perfusion using melphalan for patients with ocular melanoma metastatic to liver. *Clinical cancer research* **2003**, *9*, 6343-6349.
211. van Iersel, L.B.; Hoekman, E.J.; Gelderblom, H.; Vahrmeijer, A.L.; van Persijn van Meerten, E.L.; Tijl, F.G.; Hartgrink, H.H.; Kuppen, P.J.; Nortier, J.W.; Tollenaar, R.A., *et al.* Isolated hepatic perfusion with 200 mg melphalan for advanced noncolorectal liver metastases. *Ann Surg Oncol* **2008**, *15*, 1891-1898.
212. Braat, A.J.; Smits, M.L.; Braat, M.N.; van den Hoven, A.F.; Prince, J.F.; de Jong, H.W.; van den Bosch, M.A.; Lam, M.G. (9)(0)y hepatic radioembolization: An update on current practice and recent developments. *J Nucl Med* **2015**, *56*, 1079-1087.
213. Sato, T. Locoregional management of hepatic metastasis from primary uveal melanoma. *Semin Oncol* **2010**, *37*, 127-138.
214. Singh, A.D.; Topham, A. Survival rates with uveal melanoma in the united states: 1973-1997. *Ophthalmology* **2003**, *110*, 962-965.
215. Singh, A.D.; Turell, M.E.; Topham, A.K. Uveal melanoma: Trends in incidence, treatment, and survival. *Ophthalmology* **2011**, *118*, 1881-1885.
216. Harbour, J.W. Molecular prognostic testing in uveal melanoma: Has it finally come of age? *Arch Ophthalmol* **2007**, *125*, 1122-1123.
217. Lane, A.M.; Kim, I.K.; Gragoudas, E.S. Survival rates in patients after treatment for metastasis from uveal melanoma. *JAMA Ophthalmol* **2018**, *136*, 981-986.
218. Damato, B.; Heimann, H. Personalized treatment of uveal melanoma. *Eye (Lond)* **2013**, *27*, 172-179.
219. Damato, B.; Eleuteri, A.; Taktak, A.F.; Coupland, S.E. Estimating prognosis for survival after treatment of choroidal melanoma. *Progress in retinal and eye research* **2011**, *30*, 285-295.
220. Damato, B.; Eleuteri, A.; Fisher, A.C.; Coupland, S.E.; Taktak, A.F. Artificial neural networks estimating survival probability after treatment of choroidal melanoma. *Ophthalmology* **2008**, *115*, 1598-1607.
221. Augsburger, J.J.; Gamel, J.W. Clinical prognostic factors in patients with posterior uveal malignant melanoma. *Cancer* **1990**, *66*, 1596-1600.
222. Paul, E.V.; Parnell, B.L.; Fraker, M.J.I.O.C. Prognosis of malignant melanomas of the choroid and ciliary body. **1962**, *2*, 387-402.

223. Pogrzebielski, A.; Orłowska-Heitzman, J.; Romanowska-Dixon, B.J.G.s.A.f.C.; Ophthalmology, E. Uveal melanoma in young patients. **2006**, *244*, 1646-1649.
224. Diener-West, M.; Hawkins, B.S.; Markowitz, J.A.; Schachat, A.P.J.A.o.o. A review of mortality from choroidal melanoma: II. A meta-analysis of 5-year mortality rates following enucleation, 1966 through 1988. **1992**, *110*, 245-250.
225. Affeldt, J.C.; Minckler, D.S.; Azen, S.P.; Yeh, L.J.A.o.O. Prognosis in uveal melanoma with extrascleral extension. **1980**, *98*, 1975-1979.
226. Pach, J.M.; Robertson, D.M.; Taney, B.S.; Martin, J.A.; Campbell, R.J.; O'Brien, P.C.J.A.j.o.o. Prognostic factors in choroidal and ciliary body melanomas with extrascleral extension. **1986**, *101*, 325-331.
227. Gündüz, K.; Shields, C.L.; Shields, J.A.; Cater, J.; Brady, L.J.A.j.o.o. Plaque radiotherapy for management of ciliary body and choroidal melanoma with extraocular extension. **2000**, *130*, 97-102.
228. Mooy, C.M.; Luyten, G.; De Jong, P.; Luider, T.M.; Stijnen, T.; van de Ham, F.; Van Vroonhoven, C.; Bosman, F.T.J.T.A.j.o.p. Immunohistochemical and prognostic analysis of apoptosis and proliferation in uveal melanoma. **1995**, *147*, 1097.
229. Sisley, K.; Rennie, I.G.; Parsons, M.A.; Jacques, R.; Hammond, D.W.; Bell, S.M.; Potter, A.M.; Rees, R.C. Abnormalities of chromosomes 3 and 8 in posterior uveal melanoma correlate with prognosis. *Genes Chromosomes Cancer* **1997**, *19*, 22-28.
230. Jones, A.S.; Taktak, A.G.; Helliwell, T.R.; Fenton, J.E.; Birchall, M.A.; Husband, D.J.; Fisher, A.C. An artificial neural network improves prediction of observed survival in patients with laryngeal squamous carcinoma. *Eur Arch Otorhinolaryngol* **2006**, *263*, 541-547.
231. Jeffery, M.; Hickey, B.E.; Hider, P.N. Follow-up strategies for patients treated for non-metastatic colorectal cancer. *Cochrane Database of Systematic Reviews* **2019**.
232. Taktak, A.; Fisher, A.; Jones, A.; Damato, B. In *The role and efficacy of non-linear models in decision making and prognostication*, The 26th Annual International Conference of the IEEE Engineering in Medicine and Biology Society, 2004; IEEE: pp 411-414.
233. Taktak, A.F.; Fisher, A.C.; Damato, B.E. Modelling survival after treatment of intraocular melanoma using artificial neural networks and bayes theorem. *Physics in Medicine & Biology* **2003**, *49*, 87.
234. Kaiserman, I.; Rosner, M.; Pe'er, J. Forecasting the prognosis of choroidal melanoma with an artificial neural network. *Ophthalmology* **2005**, *112*, 1608. e1601-1608. e1606.
235. Vaquero-Garcia, J.; Lalonde, E.; Ewens, K.G.; Ebrahimzadeh, J.; Richard-Yutz, J.; Shields, C.L.; Barrera, A.; Green, C.J.; Barash, Y.; Ganguly, A. Primeum: A model for predicting risk of metastasis in uveal melanoma. *Investigative ophthalmology & visual science* **2017**, *58*, 4096-4105.
236. Eleuteri, A.; Damato, B.; Coupland, S.E.; Taktak, A.F. Enhancing survival prognostication in patients with choroidal melanoma by integrating pathologic, clinical and genetic predictors of metastasis. *International Journal of Biomedical Engineering and Technology* **2012**, *8*, 18-35.

237. Taktak, A.; Antolini, L.; Aung, M.; Boracchi, P.; Campbell, I.; Damato, B.; Ifeachor, E.; Lama, N.; Lisboa, P.; Setzkorn, C. Double-blind evaluation and benchmarking of survival models in a multi-centre study. *Computers in biology and medicine* **2007**, *37*, 1108-1120.
238. Coupland, S.E.; Taktak, A.; Damato, B. Incorporating clinical, histological, and genetic parameters for choroidal melanoma prognostication. *JAMA Ophthalmol* **2017**, *135*, 818-819.
239. Rospond-Kubiak, I.; Wroblewska-Zierhoffer, M.; Twardosz-Pawlik, H.; Kociecki, J. The liverpool uveal melanoma prognosticator online (lumpo) for prognosing metastasis free survival in the absence of cytogenetic data after ruthenium brachytherapy for uveal melanoma. *Acta Ophthalmologica* **2015**, *93*, n/a-n/a.
240. DeParis, S.W.; Taktak, A.; Eleuteri, A.; Enanoria, W.; Heimann, H.; Coupland, S.E.; Damato, B. External validation of the liverpool uveal melanoma prognosticator online. *Invest Ophthalmol Vis Sci* **2016**, *57*, 6116-6122.
241. Eleuteri, A.; Taktak, A.F.; Coupland, S.E.; Heimann, H.; Kalirai, H.; Damato, B. Prognostication of metastatic death in uveal melanoma patients: A markov multi-state model. *Computers in biology and medicine* **2018**.
242. Steyerberg, E.W. *Clinical prediction models*. Springer: 2019.
243. Shields, J.A.; Augsburger, J.J.; Donoso, L.A.; Bernardino, V.B., Jr.; Portenar, M. Hepatic metastasis and orbital recurrence of uveal melanoma after 42 years. *Am J Ophthalmol* **1985**, *100*, 666-668.
244. Rantala, E.S.; Hernberg, M.; Kivelä, T.T. Overall survival after treatment for metastatic uveal melanoma: A systematic review and meta-analysis. *Melanoma Res* **2019**, *29*, 561-568.
245. Gomez, D.; Wetherill, C.; Cheong, J.; Jones, L.; Marshall, E.; Damato, B.; Coupland, S.; Ghaneh, P.; Poston, G.; Malik, H. The liverpool uveal melanoma liver metastases pathway: Outcome following liver resection. *Journal of Surgical Oncology* **2014**, *109*, 542-547.
246. Dall'Era, M.A. Patient and disease factors affecting the choice and adherence to active surveillance. *Curr Opin Urol* **2015**, *25*, 272-276.
247. Carpentier, M.Y.; Vernon, S.W.; Bartholomew, L.K.; Murphy, C.C.; Bluethmann, S.M. Receipt of recommended surveillance among colorectal cancer survivors: A systematic review. *J Cancer Surviv* **2013**, *7*, 464-483.
248. Wen, J.C.; Sai, V.; Straatsma, B.R.; McCannel, T.A. Radiation-related cancer risk associated with surveillance imaging for metastasis from choroidal melanoma. *JAMA Ophthalmol* **2013**, *131*, 56-61.
249. Aaberg, T.M., Jr.; Cook, R.W.; Oelschlager, K.; Maetzold, D.; Rao, P.K.; Mason, J.O., 3rd. Current clinical practice: Differential management of uveal melanoma in the era of molecular tumor analyses. *Clin Ophthalmol* **2014**, *8*, 2449-2460.
250. Amin, M.B.; Greene, F.L.; Edge, S.B.; Compton, C.C.; Gershenwald, J.E.; Brookland, R.K.; Meyer, L.; Gress, D.M.; Byrd, D.R.; Winchester, D.P. The eighth edition ajcc

- cancer staging manual: Continuing to build a bridge from a population-based to a more "personalized" approach to cancer staging. *CA Cancer J Clin* **2017**, *67*, 93-99.
251. Shields, C.L.; Dalvin, L.A.; Vichitvejpaisal, P.; Mazloumi, M.; Ganguly, A.; Shields, J.A. Prognostication of uveal melanoma is simple and highly predictive using the cancer genome atlas (tcga) classification: A review. *Indian J Ophthalmol* **2019**, *67*, 1959-1963.
 252. Nathan, P.; Cohen, V.; Coupland, S.; Curtis, K.; Damato, B.; Evans, J.; Fenwick, S.; Kirkpatrick, L.; Li, O.; Marshall, E., *et al.* Uveal melanoma uk national guidelines. *Eur J Cancer* **2015**, *51*, 2404-2412.
 253. Servois, V.; Mariani, P.; Malhaire, C.; Petras, S.; Piperno-Neumann, S.; Plancher, C.; Levy-Gabriel, C.; Lumbroso-le Rouic, L.; Desjardins, L.; Salmon, R.J. Preoperative staging of liver metastases from uveal melanoma by magnetic resonance imaging (mri) and fluorodeoxyglucose-positron emission tomography (fdg-pet). *Eur J Surg Oncol* **2010**, *36*, 189-194.
 254. Chadha, V.; Cauchi, P.; Kincaid, W.; Schipani, S.; Waterston, A.; Cram, O.; Ritchie, D.; Salvi, S.; Nathan, P.; Blair, R. Consensus statement on metastatic surveillance for uveal melanoma in scotland. **2019**.
 255. Mathis, T.; Cassoux, N.; Tardy, M.; Piperno, S.; Gastaud, L.; Dendale, R.; Maschi, C.; Nguyen, A.-m.; Meyer, L.; Bonnin, N. Prise en charge des mélanomes oculaires, le minimum pour les oncologues. *Bulletin du Cancer* **2018**, *105*, 967-980.
 256. Barker, C.A.; Salama, A.K. New nccn guidelines for uveal melanoma and treatment of recurrent or progressive distant metastatic melanoma. *Journal of the National Comprehensive Cancer Network* **2018**, *16*, 646-650.
 257. Weis, E.; Salopek, T.; McKinnon, J.; Larocque, M.; Temple-Oberle, C.; Cheng, T.; McWhae, J.; Sloboda, R.; Shea-Budgell, M. Management of uveal melanoma: A consensus-based provincial clinical practice guideline. *Current oncology* **2016**, *23*, e57.
 258. Einhorn, L.H.; Burgess, M.A.; Gottlieb, J.A. Metastatic patterns of choroidal melanoma. *Cancer* **1974**, *34*, 1001-1004.
 259. Gragoudas, E.S.; Egan, K.M.; Seddon, J.M.; Glynn, R.J.; Walsh, S.M.; Finn, S.M.; Munzenrider, J.E.; Spar, M.D. Survival of patents with metastases from uveal melanoma. *Ophthalmology* **1991**, *98*, 383-390.
 260. Leyvraz, S.; Spataro, V.; Bauer, J.; Pampallona, S.; Salmon, R.; Dorval, T.; Meuli, R.; Gillet, M.; Lejeune, F.; Zografos, L. Treatment of ocular melanoma metastatic to the liver by hepatic arterial chemotherapy. *Journal of clinical oncology* **1997**, *15*, 2589-2595.
 261. Choudhary, M.M.; Gupta, A.; Bena, J.; Emch, T.; Singh, A.D. Hepatic ultrasonography for surveillance in patients with uveal melanoma. *JAMA Ophthalmol* **2016**, *134*, 174-180.
 262. Floriani, I.; Torri, V.; Rulli, E.; Garavaglia, D.; Compagnoni, A.; Salvolini, L.; Giovagnoni, A. Performance of imaging modalities in diagnosis of liver metastases from colorectal cancer: A systematic review and meta-analysis. *Journal of magnetic resonance imaging : JMRI* **2010**, *31*, 19-31.

263. Wang, G.; Zhu, S.; Li, X. Comparison of values of ct and mri imaging in the diagnosis of hepatocellular carcinoma and analysis of prognostic factors. *Oncology letters* **2019**, *17*, 1184-1188.
264. Simpson, P. Does active surveillance lead to anxiety and stress? *Br J Nurs* **2014**, *23 Suppl 18*, S4-s12.
265. Smith, T.E.; Steven, A.; Bagert, B.A. Gadolinium deposition in neurology clinical practice. *Ochsner J* **2019**, *19*, 17-25.
266. Amin, M.B.; Edge, S.B. *Ajcc cancer staging manual*. springer: 2017.
267. Thornton, S.; Kalirai, H.; Aughton, K.; Coupland, S.E. Unpacking the genetic etiology of uveal melanoma. *Expert Review of Ophthalmology* **2020**, *15*, 211-220.
268. Rantala, E.S.; Hernberg, M.M.; Lundin, M.; Lundin, J.; Kivelä, T.T. Metastatic uveal melanoma managed with best supportive care. *Acta Oncol* **2021**, *60*, 135-139.
269. Rantala, E.S.; Peltola, E.; Helminen, H.; Hernberg, M.; Kivelä, T.T. Hepatic ultrasonography compared with computed tomography and magnetic resonance imaging at diagnosis of metastatic uveal melanoma. *Am J Ophthalmol* **2020**, *216*, 156-164.
270. Khoja, L.; Atenafu, E.G.; Suci, S.; Leyvraz, S.; Sato, T.; Marshall, E.; Keilholz, U.; Zimmer, L.; Patel, S.P.; Piperno-Neumann, S., *et al.* Meta-analysis in metastatic uveal melanoma to determine progression free and overall survival benchmarks: An international rare cancers initiative (irci) ocular melanoma study. *Ann Oncol* **2019**, *30*, 1370-1380.
271. Damato, B.; Eleuteri, A.; Hussain, R.; Kalirai, H.; Thornton, S.; Taktak, A.; Heimann, H.; Coupland, S.E. Parsimonious models for predicting mortality from choroidal melanoma. *Invest Ophthalmol Vis Sci* **2020**, *61*, 35.
272. Feinstein, E.G.; Marr, B.P.; Winston, C.B.; Abramson, D.H. Hepatic abnormalities identified on abdominal computed tomography at diagnosis of uveal melanoma. *Arch Ophthalmol* **2010**, *128*, 319-323.
273. Bellerive, C.; Ouellet, E.; Kamaya, A.; Singh, A.D. Liver imaging techniques: Recognition of uveal melanoma metastases. *Ocul Oncol Pathol* **2018**, *4*, 254-260.
274. Shields, C.L.; Furuta, M.; Thangappan, A.; Nagori, S.; Mashayekhi, A.; Lally, D.R.; Kelly, C.C.; Rudich, D.S.; Nagori, A.V.; Wakade, O.A., *et al.* Metastasis of uveal melanoma millimeter-by-millimeter in 8033 consecutive eyes. *Arch Ophthalmol* **2009**, *127*, 989-998.
275. Shields, C.L.; Sioufi, K.; Robbins, J.S.; Barna, L.E.; Harley, M.R.; Lally, S.E.; Say, E.A.T.; Mashayekhi, A.; Shields, J.A. Large uveal melanoma (≥ 10 mm thickness): Clinical features and millimeter-by-millimeter risk of metastasis in 1311 cases. The 2018 albert e. Finley lecture. *Retina* **2018**, *38*, 2010-2022.
276. International validation of the american joint committee on cancer's 7th edition classification of uveal melanoma. *JAMA Ophthalmol* **2015**, *133*, 376-383.
277. Kujala, E.; Mäkitie, T.; Kivelä, T. Very long-term prognosis of patients with malignant uveal melanoma. *Investigative ophthalmology & visual science* **2003**, *44*, 4651-4659.

278. Kujala, E.; Damato, B.; Coupland, S.E.; Desjardins, L.; Bechrakis, N.E.; Grange, J.D.; Kivela, T. Staging of ciliary body and choroidal melanomas based on anatomic extent. *J Clin Oncol* **2013**, *31*, 2825-2831.
279. Kivelä, T.T.; Piperno-Neumann, S.; Desjardins, L.; Schmittel, A.; Bechrakis, N.; Midena, E.; Leyvraz, S.; Zografos, L.; Grange, J.D.; Ract-Madoux, G., *et al.* Validation of a prognostic staging for metastatic uveal melanoma: A collaborative study of the european ophthalmic oncology group. *Am J Ophthalmol* **2016**, *168*, 217-226.
280. Shields, C.L.; Say, E.A.T.; Hasanreisoglu, M.; Saktanasate, J.; Lawson, B.M.; Landy, J.E.; Badami, A.U.; Sivalingam, M.D.; Mashayekhi, A.; Shields, J.A., *et al.* Cytogenetic abnormalities in uveal melanoma based on tumor features and size in 1059 patients: The 2016 w. Richard green lecture. *Ophthalmology* **2017**, *124*, 609-618.
281. Shields, C.L.; Kaliki, S.; Furuta, M.; Fulco, E.; Alarcon, C.; Shields, J.A. American joint committee on cancer classification of posterior uveal melanoma (tumor size category) predicts prognosis in 7731 patients. *Ophthalmology* **2013**, *120*, 2066-2071.
282. Freton, A.; Chin, K.J.; Raut, R.; Tena, L.B.; Kivelä, T.; Finger, P.T. Initial pet/ct staging for choroidal melanoma: Ajcc correlation and second nonocular primaries in 333 patients. *Eur J Ophthalmol* **2012**, *22*, 236-243.
283. Garg, G.; Finger, P.T.; Kivelä, T.T.; Simpson, E.R.; Gallie, B.L.; Saakyan, S.; Amiryan, A.G.; Valskiy, V.; Chin, K.J.; Semenova, E., *et al.* Patients presenting with metastases: Stage iv uveal melanoma, an international study. *Br J Ophthalmol* **2021**.
284. Coupland, S.E.; Campbell, I.; Damato, B. Routes of extraocular extension of uveal melanoma: Risk factors and influence on survival probability. *Ophthalmology* **2008**, *115*, 1778-1785.
285. White, V.A.; Chambers, J.D.; Courtright, P.D.; Chang, W.Y.; Horsman, D.E. Correlation of cytogenetic abnormalities with the outcome of patients with uveal melanoma. *Cancer* **1998**, *83*, 354-359.
286. Kilic, E.; Naus, N.C.; van Gils, W.; Klaver, C.C.; van Til, M.E.; Verbiest, M.M.; Stijnen, T.; Mooy, C.M.; Paridaens, D.; Beverloo, H.B., *et al.* Concurrent loss of chromosome arm 1p and chromosome 3 predicts a decreased disease-free survival in uveal melanoma patients. *Invest Ophthalmol Vis Sci* **2005**, *46*, 2253-2257.
287. Finger, P.T.; Kurli, M.; Reddy, S.; Tena, L.B.; Pavlick, A.C. Whole body pet/ct for initial staging of choroidal melanoma. *Br J Ophthalmol* **2005**, *89*, 1270-1274.
288. Zimmerman, L.E.; McLean, I.W. Metastatic disease from untreated uveal melanomas. *Am J Ophthalmol* **1979**, *88*, 524-534.
289. Albert, D.M.; Wagoner, M.D.; Smith, M.E. Are metastatic evaluations indicated before enucleation of ocular melanoma? *Am J Ophthalmol* **1980**, *90*, 429-432.
290. Cassoux, N.; Rodrigues, M.J.; Plancher, C.; Asselain, B.; Levy-Gabriel, C.; Lumbroso-Le Rouic, L.; Piperno-Neumann, S.; Dendale, R.; Sastre, X.; Desjardins, L. Genome-wide profiling is a clinically relevant and affordable prognostic test in posterior uveal melanoma. *British Journal of Ophthalmology* **2014**, *98*, 769-774.

291. Mazloumi, M.; Vichitvejpaisal, P.; Dalvin, L.A.; Yaghy, A.; Ewens, K.G.; Ganguly, A.; Shields, C.L. Accuracy of the cancer genome atlas classification vs american joint committee on cancer classification for prediction of metastasis in patients with uveal melanoma. *JAMA ophthalmology* **2020**, *138*, 260-267.
292. Davanzo, J.M.; Binkley, E.M.; Bena, J.F.; Singh, A.D. Risk-stratified systemic surveillance in uveal melanoma. *Br J Ophthalmol* **2019**, *103*, 1868-1871.
293. Carvajal, R.D.; Schwartz, G.K.; Tezel, T.; Marr, B.; Francis, J.H.; Nathan, P.D. Metastatic disease from uveal melanoma: Treatment options and future prospects. *Br J Ophthalmol* **2017**, *101*, 38-44.
294. Triozzi, P.L.; Singh, A.D. Adjuvant therapy of uveal melanoma: Current status. *Ocul Oncol Pathol* **2014**, *1*, 54-62.
295. Shildkrot, Y.; Thomas, F.; Al-Hariri, A.; Fry, C.L.; Haik, B.G.; Wilson, M.W. Socioeconomic factors and diagnosis of uveal melanoma in the mid-southern united states. *Curr Eye Res* **2011**, *36*, 824-830.
296. Plasseraud, K.M.; Cook, R.W.; Tsai, T.; Shildkrot, Y.; Middlebrook, B.; Maetzold, D.; Wilkinson, J.; Stone, J.; Johnson, C.; Oelschlager, K. Clinical performance and management outcomes with the decisiondx-um gene expression profile test in a prospective multicenter study. *Journal of oncology* **2016**, *2016*.
297. Singh, A.D.; Zabor, E.C.; Radivoyevitch, T. Estimating cured fractions of uveal melanoma. *JAMA Ophthalmol* **2020**.
298. Khalili, K.; Menezes, R.; Kim, T.K.; Kochak Yazdi, L.; Jang, H.J.; Sharma, S.; Feld, J.; Sherman, M. The effectiveness of ultrasound surveillance for hepatocellular carcinoma in a canadian centre and determinants of its success. *Can J Gastroenterol Hepatol* **2015**, *29*, 267-273.
299. Kwon, J.W.; Tchoe, H.J.; Lee, J.; Suh, J.K.; Lee, J.H.; Shin, S. The impact of national surveillance for liver cancer: Results from real-world setting in korea. *Gut Liver* **2020**, *14*, 108-116.
300. Mitchell, J.; Callaghan, P.; Street, J.; Neuhaus, S.; Bessen, T. The experience of melanoma follow-up care: An online survey of patients in australia. *J Skin Cancer* **2014**, *2014*, 429149.
301. Corral, J.E.; Das, A.; Bruno, M.J.; Wallace, M.B. Cost-effectiveness of pancreatic cancer surveillance in high-risk individuals: An economic analysis. *Pancreas* **2019**, *48*, 526-536.
302. Lima, P.H.; Fan, B.; Bérubé, J.; Cerny, M.; Olivié, D.; Giard, J.M.; Beauchemin, C.; Tang, A. Cost-utility analysis of imaging for surveillance and diagnosis of hepatocellular carcinoma. *AJR Am J Roentgenol* **2019**, *213*, 17-25.
303. Fazel, R.; Krumholz, H.M.; Wang, Y.; Ross, J.S.; Chen, J.; Ting, H.H.; Shah, N.D.; Nasir, K.; Einstein, A.J.; Nallamothu, B.K. Exposure to low-dose ionizing radiation from medical imaging procedures. *N Engl J Med* **2009**, *361*, 849-857.
304. Booth, T.C.; Jackson, A.; Wardlaw, J.M.; Taylor, S.A.; Waldman, A.D. Incidental findings found in "healthy" volunteers during imaging performed for research: Current legal and ethical implications. *Br J Radiol* **2010**, *83*, 456-465.

305. Chen, J.; Fazel, R.; Ross, J.S.; McNamara, R.L.; Einstein, A.J.; Al-Mallah, M.; Krumholz, H.M.; Nallamothu, B.K. Do imaging studies performed in physician offices increase downstream utilization?: An empiric analysis of cardiac stress testing with imaging. *JACC Cardiovasc Imaging* **2011**, *4*, 630-637.
306. Dieng, M.; Khanna, N.; Nguyen, M.T.H.; Turner, R.; Lord, S.J.; Menzies, A.M.; Allen, J.; Saw, R.; Nieweg, O.E.; Thompson, J. Cost-effectiveness analysis of pet/ct surveillance imaging to detect systemic recurrence in resected stage iii melanoma: Study protocol. *BMJ open* **2020**, *10*, e037857.
307. Kowada, A. Cost-effectiveness of abdominal ultrasound versus magnetic resonance imaging for pancreatic cancer screening in familial high-risk individuals in japan. *Pancreas* **2020**, *49*, 1052-1056.
308. Kivelä, T.; Eskelin, S.; Kujala, E. Metastatic uveal melanoma. *International ophthalmology clinics* **2006**, *46*, 133-149.
309. Afshar, A.R.; Deiner, M.; Allen, G.; Damato, B.E. The patient's experience of ocular melanoma in the us: A survey of the ocular melanoma foundation. *Ocul Oncol Pathol* **2018**, *4*, 280-290.
310. Cunha Rola, A.; Taktak, A.; Eleuteri, A.; Kalirai, H.; Heimann, H.; Hussain, R.; Bonnett, L.J.; Hill, C.J.; Traynor, M.; Jager, M.J. Multicenter external validation of the liverpool uveal melanoma prognosticator online: An oog collaborative study. *Cancers* **2020**, *12*, 477.
311. Counsell, C.; Dennis, M. Systematic review of prognostic models in patients with acute stroke. *Cerebrovascular diseases* **2001**, *12*, 159-170.
312. Minne, L.; Ludikhuizen, J.; De Jonge, E.; De Rooij, S.; Abu-Hanna, A. Prognostic models for predicting mortality in elderly icu patients: A systematic review. *Intensive care medicine* **2011**, *37*, 1258-1268.
313. Altman, D.G.; Vergouwe, Y.; Royston, P.; Moons, K.G. Prognosis and prognostic research: Validating a prognostic model. *Bmj* **2009**, *338*, b605.
314. Vergouwe, Y.; Steyerberg, E.W.; Eijkemans, M.J.; Habbema, J.D.F. Substantial effective sample sizes were required for external validation studies of predictive logistic regression models. *Journal of clinical epidemiology* **2005**, *58*, 475-483.
315. Eleuteri, A.; Rola, A.C.; Kalirai, H.; Hussain, R.; Sacco, J.; Damato, B.E.; Heimann, H.; Coupland, S.E.; Taktak, A.F.G. Cost-utility analysis of a decade of liver screening for metastases using the liverpool uveal melanoma prognosticator online (lumpo). *Comput Biol Med* **2021**, *130*, 104221.
316. National Institute for Health and Care Excellence. Liver cancers., <https://www.nice.org.uk/guidance/conditions-and-diseases/liver-conditions/liver-cancers>.
317. Harrell Jr, F.E. *Regression modeling strategies: With applications to linear models, logistic and ordinal regression, and survival analysis*. Springer: 2015.

318. Pencina, M.J.; D'Agostino, R.B., Sr.; D'Agostino, R.B., Jr.; Vasan, R.S. Evaluating the added predictive ability of a new marker: From area under the roc curve to reclassification and beyond. *Stat Med* **2008**, *27*, 157-172; discussion 207-112.
319. Delgado-Ramos, G.M.; Thomas, F.; VanderWalde, A.; King, B.; Wilson, M.; Pallera, A.M. Risk factors, clinical outcomes, and natural history of uveal melanoma: A single-institution analysis. *Med Oncol* **2019**, *36*, 17.
320. Gray, E.; Marti, J.; Brewster, D.H.; Wyatt, J.C.; Hall, P.S. Independent validation of the predict breast cancer prognosis prediction tool in 45,789 patients using scottish cancer registry data. *Br J Cancer* **2018**, *119*, 808-814.
321. Hyder, O.; Dodson, R.M.; Mayo, S.C.; Schneider, E.B.; Weiss, M.J.; Herman, J.M.; Wolfgang, C.L.; Pawlik, T.M. Post-treatment surveillance of patients with colorectal cancer with surgically treated liver metastases. *Surgery* **2013**, *154*, 256-265.
322. Hess, V. [adjuvant!Online--an internet-based decision tool for adjuvant chemotherapy in early breast cancer]. *Ther Umsch* **2008**, *65*, 201-205.
323. Burke, H.B.; Goodman, P.H.; Rosen, D.B.; Henson, D.E.; Weinstein, J.N.; Harrell, F.E., Jr.; Marks, J.R.; Winchester, D.P.; Bostwick, D.G. Artificial neural networks improve the accuracy of cancer survival prediction. *Cancer* **1997**, *79*, 857-862.
324. Wishart, G.C.; Bajdik, C.D.; Azzato, E.M.; Dicks, E.; Greenberg, D.C.; Rashbass, J.; Caldas, C.; Pharoah, P.D. A population-based validation of the prognostic model predict for early breast cancer. *Eur J Surg Oncol* **2011**, *37*, 411-417.
325. O'Dell, W.; Takita, C.; Casey-Sawicki, K.; Daily, K.; Heldermon, C.D.; Okunieff, P. Projected clinical benefit of surveillance imaging for early detection and treatment of breast cancer metastases. *Breast J* **2019**, *25*, 75-79.
326. Kim, I.K.; Lane, A.M.; Gragoudas, E.S. Survival in patients with presymptomatic diagnosis of metastatic uveal melanoma. *Archives of Ophthalmology* **2010**, *128*, 871-875.
327. Eskelin, S.; Pyrhönen, S.; Hahka-Kemppinen, M.; Tuomaala, S.; Kivelä, T. A prognostic model and staging for metastatic uveal melanoma. *Cancer* **2003**, *97*, 465-475.
328. Piperno-Neumann, S.; Servois, V.; Mariani, P.; Plancher, C.; Lévy-Gabriel, C.; Lumbroso-Le Rouic, L.; Couturier, J.; Asselain, B.; Desjardins, L.; Cassoux, N. Prospective study of surveillance testing for metastasis in 100 high-risk uveal melanoma patients. *J Fr Ophtalmol* **2015**, *38*, 526-534.
329. Gomez, D.; Sangha, V.K.; Morris-Stiff, G.; Malik, H.Z.; Guthrie, A.J.; Toogood, G.J.; Lodge, J.P.; Prasad, K.R. Outcomes of intensive surveillance after resection of hepatic colorectal metastases. *Br J Surg* **2010**, *97*, 1552-1560.
330. Maeda, T.; Tateishi, U.; Suzuki, S.; Arai, Y.; Kim, E.E.; Sugimura, K. Magnetic resonance screening trial for hepatic metastasis in patients with locally controlled choroidal melanoma. *Jpn J Clin Oncol* **2007**, *37*, 282-286.
331. Merrill, S.A.; Stevens, P.; Verschraegen, C.; Wood, M.E. Utility and costs of routine staging scans in early stage breast cancer| per. *American Journal of Hematology/Oncology* **2016**, *12*.

332. Podlipnik, S.; Moreno-Ramírez, D.; Carrera, C.; Barreiro, A.; Manubens, E.; Ferrandiz-Pulido, L.; Sánchez, M.; Vidal-Sicart, S.; Malvey, J.; Puig, S. Cost-effectiveness analysis of imaging strategy for an intensive follow-up of patients with american joint committee on cancer stage iib, iic and iii malignant melanoma. *British Journal of Dermatology* **2019**, *180*, 1190-1197.
333. Armitage, J.O. Who benefits from surveillance imaging? *J Clin Oncol* **2012**, *30*, 2579-2580.
334. Voss, S.D.; Chen, L.; Constine, L.S.; Chauvenet, A.; Fitzgerald, T.J.; Kaste, S.C.; Slovis, T.; Schwartz, C.L. Surveillance computed tomography imaging and detection of relapse in intermediate- and advanced-stage pediatric hodgkin's lymphoma: A report from the children's oncology group. *J Clin Oncol* **2012**, *30*, 2635-2640.
335. Schnipper, L.E.; Smith, T.J.; Raghavan, D.; Blayney, D.W.; Ganz, P.A.; Mulvey, T.M.; Wollins, D.S. American society of clinical oncology identifies five key opportunities to improve care and reduce costs: The top five list for oncology. *J Clin Oncol* **2012**, *30*, 1715-1724.
336. Kodjikian, L.; Grange, J.D.; Baldo, S.; Baillif, S.; Garweg, J.G.; Rivoire, M. Prognostic factors of liver metastases from uveal melanoma. *Graefes Arch Clin Exp Ophthalmol* **2005**, *243*, 985-993.
337. Valpione, S.; Moser, J.C.; Parrozzani, R.; Bazzi, M.; Mansfield, A.S.; Mocellin, S.; Pigozzo, J.; Midena, E.; Markovic, S.N.; Aliberti, C., *et al.* Development and external validation of a prognostic nomogram for metastatic uveal melanoma. *PLoS One* **2015**, *10*, e0120181.
338. Lorenzo, D.; Ochoa, M.; Piulats, J.M.; Gutiérrez, C.; Arias, L.; Català, J.; Grau, M.; Peñafiel, J.; Cobos, E.; Garcia-Bru, P., *et al.* Prognostic factors and decision tree for long-term survival in metastatic uveal melanoma. *Cancer Res Treat* **2018**, *50*, 1130-1139.
339. Mariani, P.; Dureau, S.; Savignoni, A.; Rouic, L.L.; Levy-Gabriel, C.; Piperno-Neumann, S.; Rodrigues, M.J.; Desjardins, L.; Cassoux, N.; Servois, V. Development of a prognostic nomogram for liver metastasis of uveal melanoma patients selected by liver mri. *Cancers (Basel)* **2019**, *11*.
340. Excellence, N.-N.I.f.H.a.C. Who performance status classification. [https://www.nice.org.uk/guidance/ta121/chapter/appendix-c-who-performance-status-classification\(13-05-21\)](https://www.nice.org.uk/guidance/ta121/chapter/appendix-c-who-performance-status-classification(13-05-21)),
341. Wishart, G.C.; Azzato, E.M.; Greenberg, D.C.; Rashbass, J.; Kearins, O.; Lawrence, G.; Caldas, C.; Pharoah, P.D. Predict: A new uk prognostic model that predicts survival following surgery for invasive breast cancer. *Breast Cancer Res* **2010**, *12*, R1.
342. Candido Dos Reis, F.J.; Wishart, G.C.; Dicks, E.M.; Greenberg, D.; Rashbass, J.; Schmidt, M.K.; van den Broek, A.J.; Ellis, I.O.; Green, A.; Rakha, E., *et al.* An updated predict breast cancer prognostication and treatment benefit prediction model with independent validation. *Breast Cancer Res* **2017**, *19*, 58.
343. Damato, B.; Hope-Stone, L.; Cooper, B.; Brown, S.; Heimann, H.; Dunn, L. Patient-reported outcomes and quality of life after treatment for choroidal melanoma. *Ocul Oncol Pathol* **2019**, *5*, 402-411.

344. Brown, S.L.; Fisher, P.L.; Hope-Stone, L.; Hussain, R.N.; Heimann, H.; Damato, B.; Cherry, M.G. Predictors of long-term anxiety and depression in uveal melanoma survivors: A cross-lagged five-year analysis. *Psychooncology* **2020**, *29*, 1864-1873.
345. Hope-Stone, L.; Brown, S.L.; Heimann, H.; Damato, B.; Salmon, P. How do patients with uveal melanoma experience and manage uncertainty? A qualitative study. *Psychooncology* **2015**, *24*, 1485-1491.
346. Rahman, M.S.; Ambler, G.; Choodari-Oskooei, B.; Omar, R.Z. Review and evaluation of performance measures for survival prediction models in external validation settings. *BMC Med Res Methodol* **2017**, *17*, 60.
347. Royston, P.; Altman, D.G. External validation of a cox prognostic model: Principles and methods. *BMC Med Res Methodol* **2013**, *13*, 33.
348. Damato, B.; Dopierala, J.A.; Coupland, S.E. Genotypic profiling of 452 choroidal melanomas with multiplex ligation-dependent probe amplification. *Clinical cancer research* **2010**, *16*, 6083-6092.
349. Snell, K.I.; Hua, H.; Debray, T.P.; Ensor, J.; Look, M.P.; Moons, K.G.; Riley, R.D. Multivariate meta-analysis of individual participant data helped externally validate the performance and implementation of a prediction model. *Journal of clinical epidemiology* **2016**, *69*, 40-50.
350. Steyerberg, E.W.; Vickers, A.J.; Cook, N.R.; Gerds, T.; Gonen, M.; Obuchowski, N.; Pencina, M.J.; Kattan, M.W. Assessing the performance of prediction models: A framework for some traditional and novel measures. *Epidemiology (Cambridge, Mass.)* **2010**, *21*, 128.
351. Pencina, M.J.; D'Agostino, R.B. Overall c as a measure of discrimination in survival analysis: Model specific population value and confidence interval estimation. *Statistics in medicine* **2004**, *23*, 2109-2123.
352. Dogrusöz, M.; Bagger, M.; Van Duinen, S.G.; Kroes, W.G.; Ruivenkamp, C.A.; Böhringer, S.; Andersen, K.K.; Luyten, G.P.; Kiilgaard, J.F.; Jager, M.J. The prognostic value of ajcc staging in uveal melanoma is enhanced by adding chromosome 3 and 8q status. *Investigative ophthalmology & visual science* **2017**, *58*, 833-842.
353. Bagger, M.M. Intraocular biopsy of uveal melanoma risk assessment and identification of genetic prognostic markers. *Acta Ophthalmologica* **2018**, *96*, 1-28.